Investigating Neuronal Network Dynamics Supporting Memory in the Human Brain



Adrien A. Causse

New College

University of Oxford

A thesis submitted for the degree of

Doctor of Philosophy (D. Phil.)

Trinity Term 2026

Acknowledgements

"In gratitude and respect for my teachers,
I shall impart to their children the knowledge that I received from their fathers."

Hippocratic Oath (French version)

First and foremost, I would like to express my sincere gratitude to David Dupret, my primary supervisor, who gave me a home away from home in Britain. Throughout my doctorate, he has been a constant source of support, both in moments of excitement and discovery and in moments of uncertainty and doubt. I am deeply grateful to him for offering me the unique opportunity to bring together the two worlds that shaped me: science and medicine.

I am equally grateful to Leila Reddy, who welcomed me into her laboratory with such warmth and generosity and quickly made me feel like a valued member of her team. My sincere thanks also go to Vítor Lopes-dos-Santos for the many discussions, critiques, comments, and suggestions that nourished this project, as well as to all members of David Dupret's and Leila Reddy's laboratories for their constant support.

I would also like to thank Vivienne Collins, Meetali Dayabhai and Ben Micklem for their unwavering administrative and logistical support, and for their seemingly endless patience, without which this cross-border project would never have been possible. My thanks also go to Tim Denison, Masud Husain, Andy Sharott, Huiling Tan and Ashwini Oswal for their insightful feedback and academic guidance, and to Helen Barron for her assistance in developing the behavioural task.

More broadly, I would like to thank the two teams whose collaboration made this work possible and whose members made the experience both scientifically enriching and personally enjoyable: in Toulouse, Jonathan Curot, Emmanuel Barbeau, Luc Valton, Marie Denuelle, Amaury de Barros, Jean-Albert Lotterie, Jean-Christophe Sol and Hélène Mirabeau; in Paris, Katia Lehongre, Sara Fernandez-Vidal, Vincent Navarro and Valerio Frazzini.

My sincere thanks go to all the participants and their families. Their time, trust, and generosity were essential to this project, and I am deeply grateful for their contribution to this research.

I am also deeply grateful to the students who entrusted me with the privilege of passing on what I learned from my own mentors: Raphaël Nunes-da-Silva, Erin Mugnier-Payne, Claire Morat, and Jules Mondoly. Working with them has been a genuine pleasure, and I hope that my supervision lived up to their expectations.

This DPhil project was funded through a UK Medical Research Council (MRC) studentship and two MRC supplementary high-cost training awards. I am also sincerely grateful to New College, the Guarantors of Brain, and the European Brain and Behaviour Society for their generous travel grants, which enabled me to present this work at scientific conferences.

These acknowledgements also offer me an opportunity to express my gratitude to the people who helped me become the young scientist I am today.

As a medical student at the University of Montpellier, I was fortunate to meet generous and attentive mentors whose passion and enthusiasm infected me with an incurable virus: the love of scientific research. Vivien Szabo, Orianne Villard, Badreddine Boussadia and Stefan Matecki first introduced me to the unprecedented, and perhaps slightly crazy, possibility of pursuing scientific training alongside medical studies. Later, Jean-Philippe Pin, Philippe Rondard and Pierre-André Laffon guided me through my first laboratory placement with kindness and warmth, sharing with me the curiosity and delight that lie at the heart of any serious scientific endeavour.

I was then fortunate enough to join the École de l'Inserm Liliane Bettencourt and subsequently the École normale supérieure de Lyon, where I was able to refine and deepen my scientific aspirations under the guidance of individuals who were as inspiring as they were devoted to the transmission of knowledge: Boris Barbour, Eric Clauser, Jean-Claude Chottard, Antoine Corbin and Stéphane Vincent.

A decisive turning point in the development of my scientific project came during my second research placement, in Cyril Herry's laboratory, when I performed my first *in vivo* extracellular recordings in mice. Fortune smiled on me a second time, as I was supervised by Thomas Bienvenu and Pierre Meyrand, who together ignited in me the "fire of experimental science": that profound fascination with the unknown and the mysteries of life, coupled with the patience and determination required to uncover them. In this case, my first hippocampal ripples! Friendship did the rest.

I then embarked on my Master's project with David Dupret at Oxford with great enthusiasm. By placing his trust in me, he gave me the opportunity to undertake this challenging cross-border endeavour. Through a project that would later grow into my doctoral research, I was able to dedicate myself fully to fundamental science while remaining at the interface between basic research and medicine. After two remarkable research placements, I had the immense privilege of working under the supervision of Charlie Clarke-Williams, who, with creativity, kindness, and humility, taught me the analytical foundations that proved indispensable throughout my doctorate.

This journey would not have been nearly as joyful without the support of my friends: Amaury, Mathilde, Maxime and Mehdi, with whom conversations gave rise to some of the most important ideas in this work; Nicole, Demi, Katerina, Rosie, Adrian, Atharva, Matteo, Marcel and Luca, who brought colour and warmth to my days in Oxford; and Adrian, Yann, Aditya, Ulysse, Ram, Vincent and Benoit who made my travels to Toulouse all the more enjoyable.

No words can fully express my gratitude to my family, my father, my mother, my grandmother, and Fabien, who have been unwavering pillars of support throughout these doctoral years. I hope they will be proud to see a "Causse" find a place in the scientific

literature.

Finally, and above all, thank you to the person who placed her trust in me when I embarked on this journey across the Channel, the one who gave me the strength to persevere through the most difficult moments of doubt, the one who put a smile on my face every morning—quite simply: Léa.

At the conclusion of this work, I have come to believe that the greatest mysteries remain beyond what our instruments can measure.

Remerciements

"Respectueux et reconnaissant envers mes maîtres,
je rendrai à leurs enfants l'instruction que j'ai reçue de leurs pères."

Serment d'Hippocrate

Je souhaite tout d'abord adresser mes sincères remerciements à David Dupret, mon directeur de thèse, qui m'a donné un "chez-moi" en terre britannique. Il m'a toujours soutenu pendant le doctorat, dans les moments de joie et d'eurêka, tout comme dans les moments de doute. Je lui suis immensément reconnaissant de m'avoir offert cette occasion unique d'entreprendre la synthèse des deux mondes qui m'ont vu naître: la science et la médecine.

Je remercie également Leila Reddy, qui m'a accueilli avec tant de sympathie et de bienveillance dans son laboratoire et m'a rapidement donné le sentiment d'être un membre à part entière de son équipe. Merci mille fois à Vítor Lopes-dos-Santos pour les nombreuses discussions, critiques, remarques et conseils qui ont accompagné la maturation de ce projet, ainsi qu'à tous les membres des laboratoires de David Dupret et de Leila Reddy pour leur aide constante.

Je souhaite également remercier Vivienne Collins, Meetali Dayabhai et Ben Micklem pour leur soutien administratif et logistique sans faille ainsi que pour leur patience infinie, qui ont rendu possible ce projet transfrontalier. Merci également à Tim Denison, Masud Husain, Andy Sharott, Huiling Tan et Ashwini Oswal pour leurs remarques éclairantes et leur accompagnement académique, ainsi qu'à Helen Barron pour son aide dans l'élaboration de la tâche comportementale.

Je tiens aussi à remercier plus largement les deux équipes dont la collaboration a rendu ce travail possible et qui ont grandement contribué à en faire une expérience aussi enrichissante qu'agréable : à Toulouse, Jonathan Curot, Emmanuel Barbeau, Luc Valton, Marie Denuelle, Amaury de Barros, Jean-Albert Lotterie, Jean-Christophe Sol et Hélène Mirabeau; à Paris, Katia Lehongre, Sara Fernandez-Vidal, Vincent Navarro et Valerio Frazzini.

Je souhaite également exprimer ma gratitude envers tous les participants et participantes, ainsi qu'envers leurs familles. Leur temps, leur confiance et leur générosité ont été essentiels à la réalisation de ce projet, et je leur suis profondément reconnaissant de leur contribution à ce travail.

Merci aussi aux étudiants et étudiantes qui m'ont accordé leur confiance pour leur transmettre ce que j'ai appris de mes maîtres : Raphaël Nunes-da-Silva, Erin Mugnier-

Payne, Claire Morat et Jules Mondoly. Travailler avec eux a été une grande joie, et j'espère que mon encadrement a été à la hauteur de leurs attentes.

Ce projet de doctorat a bénéficié du soutien financier d'une bourse doctorale du Medical Research Council (MRC) du Royaume-Uni, ainsi que de deux MRC supplementary high-cost training awards. Je remercie également chaleureusement New College, the Guarantors of Brain et l'European Brain and Behaviour Society pour leurs généreuses bourses de mobilité, grâce auxquelles j'ai eu l'opportunité de présenter ce travail lors de plusieurs conférences scientifiques.

Ces remerciements sont aussi pour moi l'occasion d'exprimer ma gratitude envers les personnes qui m'ont permis de devenir le jeune scientifique que je suis aujourd'hui.

D'abord étudiant en médecine à la faculté de Montpellier, j'ai eu la chance de rencontrer des mentors bienveillants et attentifs, dont la passion et l'enthousiasme ont été les vecteurs d'un virus incurable : celui de la recherche scientifique. Vivien Szabo, Orianne Villard, Badreddine Boussadia et Stefan Matecki m'ont d'abord fait découvrir la possibilité inédite, et peut-être un peu folle, d'entamer un cursus scientifique parallèlement à mes études médicales. Ensuite, Jean-Philippe Pin, Philippe Rondard et Pierre-André Laffon m'ont accompagné avec douceur et sympathie pendant mon premier stage au laboratoire, me transmettant la joie et la curiosité nécessaires à toute entreprise scientifique sérieuse.

Ayant eu la chance d'intégrer l'École de l'Inserm Liliane Bettencourt, puis l'École normale supérieure de Lyon, j'ai pu poursuivre et préciser mon élan scientifique au contact de personnes aussi inspirantes que dévouées à la transmission de leur savoir: Boris Barbour, Eric Clauser, Jean-Claude Chottard, Antoine Corbin et Stéphane Vincent.

Le tournant décisif dans la maturation de mon projet scientifique a été la réalisation de mes premiers enregistrements extracellulaires *in vivo* chez la souris, à l'occasion de mon second stage, dans le laboratoire de Cyril Herry. La chance me souriant une deuxième fois, j'ai été encadré par Thomas Bienvenu et Pierre Meyrand, qui ont ensemble allumé en moi le "feu de la science expérimentale", cette passion absolue pour l'inconnu et le mystère du vivant, alliée à la patience et à la détermination pour en goûter les fruits. En l'occurrence, mes premiers ripples hippocampiques ! Et puis l'amitié a fait le reste.

C'est ensuite avec un grand enthousiasme que j'ai débuté mon stage de Master avec David Dupret à Oxford, qui m'a accordé sa confiance pour entreprendre ce projet trans-frontalier périlleux. En m'engageant dans ce projet qui est ensuite devenu celui de mon doctorat, j'ai pu me consacrer pleinement à la recherche fondamentale, tout en restant à l'interface avec la clinique. "Jamais deux sans trois" : après deux excellentes expériences de stage, j'ai eu l'immense privilège de travailler sous la supervision de Charlie Clarke-Williams, qui m'a transmis avec créativité, douceur et humilité les fondements analytiques qui se sont révélés indispensables tout au long de mon doctorat.

Cette aventure n'aurait pas été aussi joyeuse sans le soutien de mes amis: Amaury, Mathilde, Maxime et Mehdi, avec qui les discussions ont fait naître certaines des idées les plus importantes de ce travail; Nicole, Demi, Katerina, Rosie, Adrian, Atharva, Matteo, Marcel et Luca, qui ont coloré mes jours à Oxford; et enfin Adrian, Yann, Aditya, Ulysse, Ram, Vincent et Benoît, qui ont adouci mes multiples voyages à Toulouse.

Aucun mot ne saurait pleinement exprimer ma reconnaissance envers ma famille : papa,

maman, mamie et Fabien, qui ont été des piliers tout au long de ces années de doctorat. J'espère qu'ils seront fiers de voir un Causse rejoindre la littérature scientifique.

Enfin, et au-delà de tout, merci à celle qui m'a accordé sa confiance dans cette quête outre-Manche, celle qui m'a donné la force de persévérer dans les moments de doute les plus éprouvants, celle qui m'a donné le sourire tous les matins, tout simplement : Léa.

Au terme de ce travail, j'ai acquis la conviction que les plus grands mystères demeurent au-delà de ce que nos instruments peuvent mesurer.

Abstract

Memory is a fundamental property of living beings. In the brain, memory relies on the coordinated activity of distributed neuronal populations. The two-stage model of memory proposes that during active wakefulness, newly acquired information is coordinated within hippocampal-dependent circuits, and during subsequent rest and sleep, such patterns of neuronal activity are reactivated to support consolidation. This coordinated activity is reflected in rhythmic fluctuations of neural activity, known as brain oscillations, which can be measured using electrophysiological recordings. In rodents, the two stages of memory are associated with distinct oscillatory states: theta oscillations during active wakefulness and sharp-wave ripples during rest and sleep. In humans, however, the oscillatory mechanisms supporting these two stages remain incompletely understood. Human lesion studies have long established the importance of the medial temporal lobe (MTL) for memory, but how MTL structures support encoding, coordination, and consolidation at the level of neuronal activity remains unclear.

In humans, few studies have combined single-neuron and large-scale brain recordings across memory tasks, rest, and sleep. Consequently, the neural mechanisms that coordinate population activity across the different stages of memory remain poorly understood. Although theta-band oscillations have been reported in the human hippocampus, their behavioural relevance, their role in memory processing, and their capacity to coordinate distributed neuronal populations across the MTL remain unresolved. Likewise, it remains unclear whether neuronal coactivity motifs formed during memory acquisition are subsequently reactivated during offline states, as predicted by the two-stage model of memory. This thesis addresses these questions by combining local field potentials (LFPs) and single-neuron recordings from multiple MTL regions in patients with drug-refractory epilepsy during a relational memory task, and during periods of rest and sleep.

First, I established a relational memory task suitable for investigating the two-stage model of memory in humans. Participants with drug-refractory epilepsy successfully learned and recalled associations embedded within a social community structure. By comparing their performance with paired control participants and integrating neuropsychological assessments, I identified the cognitive factors that contributed to individual differences in learning and memory outcomes. Importantly, the task generated substantial variability across participants and associations, allowing neural activity to be related to memory performance.

Second, I identified a prominent hippocampal oscillation centred around 2 Hz during wakefulness, which occurred as transient bursts (or "bouts") evoked by memory-relevant visual cues. These bursts were selectively recruited during learning and retrieval, being more frequent and longer than during passive viewing or rest. Furthermore, their expression

was also associated with higher subsequent memory performance, linking hippocampal 2-Hz activity to mnemonic processing. This oscillation was most prominent in contacts free of interictal epileptiform discharges and was visible in both local field potentials and single-neuron activity, supporting its physiological origin.

Third, I showed that 2-Hz oscillations organized neuronal activity in the hippocampus and across the MTL. Neuronal spiking preferentially locked to the phase of the 2-Hz oscillation, gamma activity was more strongly modulated at 2 Hz than at neighbouring frequencies, and neuronal coactivity increased during 2-Hz bursts. This organization extended beyond the hippocampus, as neuronal and gamma-band activity in other MTL regions synchronized preferentially to hippocampal 2-Hz phase. Moreover, gamma activity across MTL regions became more strongly synchronized during learning and retrieval, a phenomenon that was specific to 2 Hz and not observed at neighbouring frequencies. These findings indicate that transient 2-Hz bursts define temporal windows during which distributed MTL networks are coordinated during memory-guided behaviour.

Fourth, I showed that hippocampal 2-Hz oscillations were re-expressed during rapid eye movement (REM) sleep, whereas hippocampal ripples predominated during rest and slow-wave sleep (SWS), consistent with the behavioural-state dependence reported for theta oscillations and ripples in other mammals. Most importantly, neuronal coactivity motifs formed during waking 2-Hz bursts were preferentially reactivated during hippocampal ripples in post-learning rest relative to pre-learning rest. This reactivation was strongest for coactivity motifs formed during learning and for associations that were later well remembered, providing direct evidence for the reactivation of behaviourally relevant single-neuron activity in humans.

Together, these findings support the existence of a two-stage organization of memory-related activity in the human hippocampal system. During active wakefulness, transient hippocampal 2-Hz oscillations coordinate neuronal activity across the MTL. During offline states, hippocampal ripples reactivate neuronal coactivity motifs formed during these bursts. Although the organizing rhythm is slower than the canonical theta oscillation described in rodents, the functional logic is comparable: a slow oscillatory state supports online coordination of distributed neuronal activity and links it to ripple-mediated offline reactivation in humans. The graphical abstract presented below summarises the main findings of this thesis (Fig. 0.1), which have been published in an open-access format (Causse et al. 2026).

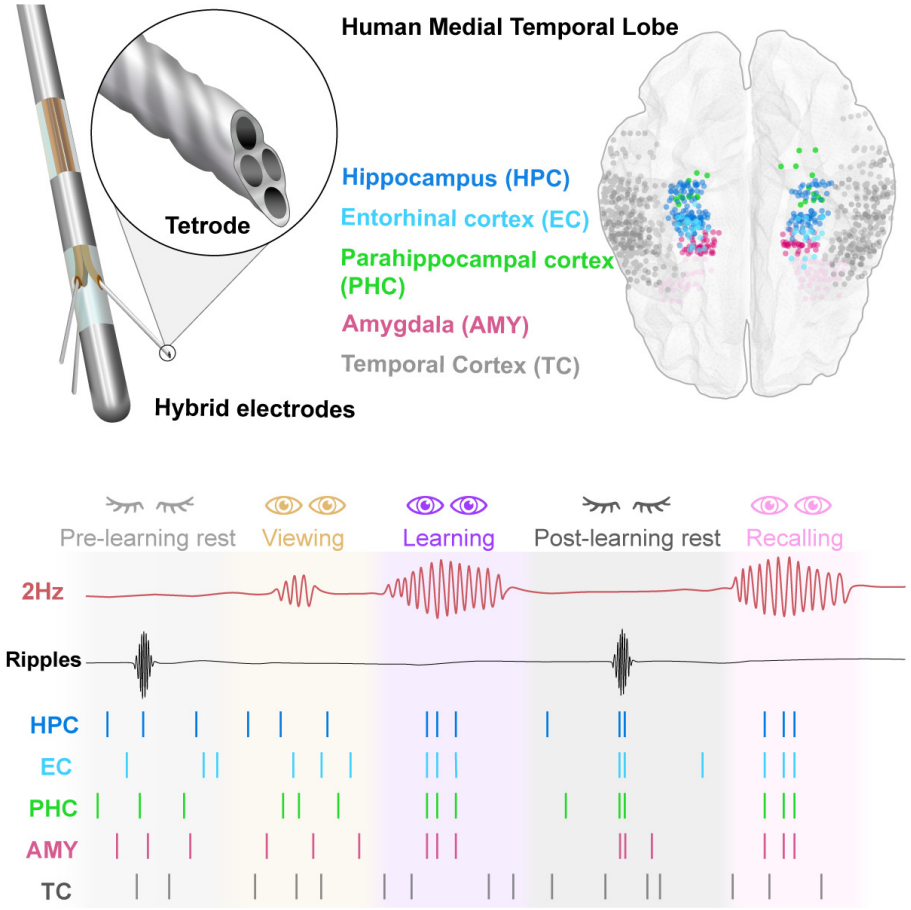


Figure 0.1: **Graphical summary.** Using hybrid micro-macro electrodes containing tetrodes, I showed that hippocampal 2-Hz bursts are recruited during memory-guided behaviour (strongest during learning and recall), coordinate neuronal activity across the medial temporal lobe (MTL), and organize coactivity motifs that are later reactivated during offline hippocampal ripples. These results have been published in Causse et al. (2026).

Contents

List of Abbreviations **20**

1 General introduction **22**

1.I Models of memory 23

1.I.1 The legacy of associationism 23

1.I.2 Beyond mere associationism 24

1.I.2.a Memory is flexible and anticipatory 24

1.I.2.b Schema theory 24

1.I.2.c Cognitive maps and relational memory 25

1.I.2.d Predictive coding 26

1.II Studying memory at the macroscopic level 27

1.II.1 In search of the neural substrate of memory 27

1.II.2 The multiple memory systems theory in the context of amnesia . 29

1.II.2.a The Medial Temporal Lobe (MTL) in memory 29

1.II.2.b The multiple memory systems theory 30

1.II.2.c Animal models of human amnesia 30

1.II.3 Beyond the MTL alone 31

1.III Studying memory at the microscopic level 32

1.III.1 Neuronal "codes" 32

1.III.1.a From the neuron doctrine to population coding in animal models 32

1.III.1.b Human neuronal codes 34

1.III.2 Neural oscillations and coordination mechanisms 35

1.III.2.a The hippocampus: a model to understand the fundamental properties of neural oscillations 35

1.III.2.b Behavioural-state dependence of neural oscillations . . . 38
1.III.2.c Neural oscillations as coordination mechanisms 38
1.III.3 Synthesis 40
1.III.3.a The two-stage model and the role of sleep in memory consolidation 40
1.III.3.b Hippocampal indexing and distributed cell assemblies . . 40
1.IV Insights into memory mechanisms from human depth recordings 42
1.IV.1 Reviewing evidence for theta oscillations in humans 42
1.IV.1.a Theta oscillations during tasks 42
1.IV.1.b Theta oscillations during REM sleep 43
1.IV.1.c Modulation of gamma and spiking activity by hippocampal theta oscillations 43
1.IV.2 Reviewing evidence for ripples and reactivation in humans 44
1.IV.2.a Detecting ripples in humans 44
1.IV.2.b Distinguishing ripples from gamma processes 45
1.IV.2.c Evidence for reactivation and memory consolidation . . . 45
1.V Hypotheses and aims of this work 46

2 Materials and Methods: Experimental procedures 49
2.I Neurophysiological recordings 49
2.I.1 Data acquisition and preprocessing 49
2.I.1.a Participants 50
2.I.1.b Behavioural datasets 50
2.I.1.c Electrode models 52
2.I.1.d Co-registration and anatomical verification of the contacts 52
2.I.1.e Neurophysiological recordings 53
2.I.2 Spike sorting and single-unit analyses 53
2.I.3 Automated pipeline and quality criteria 53
2.I.3.a Identification of putative pyramidal neurons and interneurons 55
2.I.3.b Spike-field relationship 55
2.II Analysis of local field potentials 60
2.II.1 Detection of IEDs 60

2.II.2 Decomposing LFPs into oscillatory components 60
2.II.2.a Tailored Masked Empirical Mode Decomposition 60
2.II.2.b Cycle detection and quality control 61
2.II.2.c Detection of oscillatory bursts 62
2.II.3 Other spectral decompositions 62
2.II.3.a Detection of gamma activity 62
2.II.3.b PSDs estimation and comparison of oscillatory power . . 63
2.II.3.c Wavelet spectrograms and quantification of evoked oscillations 64
2.II.4 Quantification of ERPs 64
2.II.5 Cross-frequency analyses 65
2.II.5.a PAC and phase randomization 65
2.II.5.b Phase synchronization 67
2.II.5.c HHSA 67
2.III Ripples and reactivation 71
2.III.1 Ripple detection and validation 71
2.III.1.a Ripple detection 71
2.III.1.b Characterization of ripple central frequency 73
2.III.1.c Ripple-triggered averages 73
2.III.2 Detection of cross-regional coactivity motifs 75
2.III.3 Reactivation of coactivity motifs in hippocampal ripples 75
2.IV Statistical analyses 76

3 Results: Assessing relational memory in human participants 78

3.I Introduction 78
3.I.1 Relational memory 78
3.I.2 The role of the hippocampal network in relational memory 79
3.II Investigating relational memory in humans using a social community task 80
3.II.1 Behavioural paradigm 80
3.II.2 Variants of the memory task 81
3.II.2.a Simple and complex tasks 81
3.II.2.b Population diversity 81

3.III Quantifying behavioural performance 83
3.III.1 Basic performance metrics 83
3.III.1.a Group-level performance 83
3.III.1.b Across-group comparisons 84
3.III.2 Variability of performance between subjects 89
3.III.2.a Demographic and cognitive contributors 89
3.III.2.b Standardised cognitive testing 93
3.IV Discussion 94

4 Results: A 2-Hz rhythm dominates LFPs in the human hippocampus 96
4.I Introduction 96
4.II Prominent 2-Hz bursts structure hippocampal LFPs 97
4.II.1 Recording hippocampal LFPs with sEEG in humans 97
4.II.2 Hippocampal LFPs are paced by a 2-Hz oscillation 98
4.II.3 Hippocampal 2-Hz oscillations are transient 102
4.II.4 Validation of 2-Hz oscillations 103
4.II.4.a Phase reversal of hippocampal 2-Hz oscillations 103
4.II.4.b Slow-oscillation amplitude and IEDs rate 104
4.II.4.c Local reference impairs the detection of slow oscillations 104
4.III Hippocampal 2-Hz is selectively evoked in the memory task 107
4.III.1 Hippocampal 2-Hz power increase with mnemonic engagement . . 107
4.III.2 Hippocampal 2-Hz bursts are evoked by mnemonic cues 108
4.III.2.a ERPs are modulated by mnemonic engagement 108
4.III.2.b Hippocampal 2-Hz is an evoked oscillation and follows the ERPs 110
4.III.2.c Hippocampal 2-Hz bursts track mnemonic engagement . 112
4.III.3 Hippocampal 2-Hz oscillations are not evoked by motor activity . 112
4.IV Discussion 116

5 Results: Hippocampal 2-Hz organizes neuronal activity in the MTL 118
5.I Introduction 118
5.II Hippocampal neuronal activity is preferentially modulated at 2 Hz 119

5.II.1 Hippocampal neurons are paced at 2-Hz 119
5.II.1.a Basic firing properties of hippocampal neurons reveal 2-Hz rhythmicity 119
5.II.1.b Hippocampal neurons prefer 2-Hz oscillations 120
5.II.2 Hippocampal gamma oscillations are preferentially modulated at 2 Hz 122
5.II.2.a Hippocampal gamma activity is preferentially coupled to 2-Hz phase 122
5.II.2.b Holo-Hilbert amplitude modulation analysis confirms prevailing 2-Hz hippocampal modulation of gamma activity 125
5.III Hippocampal 2-Hz synchronizes neuronal activity across MTL regions . . 127
5.III.1 2-Hz oscillations are preferentially observed in the MTL 127
5.III.1.a 2-Hz power dominates in the MTL and particularly in the hippocampus 127
5.III.1.b Prominent 6–8-Hz oscillations in the non-MTL were detected using tmEMD 131
5.III.1.c 2-Hz oscillations are not directly evoked by mnemonic cues outside the hippocampus 131
5.III.2 MTL local activity is paced by hippocampal 2-Hz 132
5.III.2.a MTL neurons are paced at 2-Hz 132
5.III.2.b Hippocampal 2-Hz synchronizes MTL gamma oscillations 135
5.IV Discussion 138

6 Results: Neural activity in the offline human hippocampus 140
6.I Introduction 140
6.II Hippocampal physiology across sleep stages 141
6.II.1 Hippocampal 2-Hz features REM sleep but not SWS 142
6.II.2 Validation of hippocampal ripples 144
6.II.2.a Hippocampal ripples feature SWS and rest sessions . . . 144
6.II.2.b Ripple modulation of neuronal activity and propagation to the MTL 151
6.II.2.c Temporal constraints in the occurrence of hippocampal ripples 153
6.III Neuronal coactivity motifs in 2-Hz bursts reactivate in post-learning hippocampal ripples 154

6.III.1 Coactivity motifs formed during 2-Hz bursts reactivate in post-learning hippocampal ripples 154
6.III.2 Reactivation is relevant for behavioural performance 155
6.IV Discussion 157

7 General discussion **159**
7.I Summary of the main findings 159
7.II Is human hippocampal 2-Hz a putative homologue of type 2 theta? . . . 161
7.III Why would human hippocampal rhythms be slower? 163
7.IV Why has hippocampal 2-Hz remained elusive? 164
7.V Limitations 166
7.VI Future directions 167

A Appendix: Local referencing **170**

B Appendix: Gamma oscillations **176**
B.I Definition of gamma oscillations 176
B.II Analysis of gamma-band bursts in the human hippocampus 177
B.III Gamma-band responses in the ventral visual stream 180

C Appendix: Analysis of the References used in this thesis **188**

List of Figures

0.1 Graphical summary 9

2.1 Datasets used in this study 51
2.2 Recording setup and conductive fabric 54
2.3 Correlation between gamma envelopes and spiking activity 59
2.4 Detection of oscillatory cycles 61
2.5 Holo-Hilbert spectral analysis of gamma modulation by slow oscillations . 70
2.6 Ripple templates 72
2.7 Ripple detection 74

3.1 Schematic representing the layout of the relational memory task 80
3.2 Schematic representing the social community in the simple and the complex versions of the task 82
3.3 Schematic representing the memory task used for the control cohort . . . 82
3.4 Average accuracy in the relational memory task 83
3.5 Average reaction time in the relational memory task 85
3.6 Comparison of the behavioural performance between the two cohorts . . 86
3.7 Comparison of the behavioural performance between the simple and the complex versions of the task 87
3.8 Definition of best and worst remembered paired associates 88
3.9 Accuracy as a function of age and educational level 90
3.10 Reaction time as a function of age and educational level 91
3.11 Accuracy as a function of age at onset of epilepsy 92
3.12 Neuropsychological factors associated with memory performance 94

4.1 Direct electrophysiological recordings from the human hippocampus . . . 98

4.2 Anatomical localization and distribution of hippocampal electrode contacts 99
4.3 Tailored Masked EMD in the human hippocampus 100
4.4 Example hippocampal LFPs showing a 2-Hz burst 101
4.5 2-Hz oscillations dominate in the human hippocampus 101
4.6 Examples of hippocampal 2-Hz bursts 102
4.7 Detection of hippocampal 2-Hz bursts 103
4.8 Phase reversal of hippocampal 2-Hz oscillations 104
4.9 Examples of interictal epileptiform discharges 105
4.10 Hippocampal slow oscillations are more prominent outside irritative zones 105
4.11 Local reference impairs detection of slow oscillations 106
4.12 Hippocampal 2-Hz power increases with mnemonic engagement 107
4.13 Hippocampal oscillatory dynamics during the memory task — controls . 108
4.14 Hippocampal ERPs across task sessions 109
4.15 Hippocampal ERPs deflections are modulated by mnemonic engagement 109
4.16 Example hippocampal ERPs and evoked 2-Hz burst 110
4.17 Hippocampal 2-Hz is evoked by mnemonic cues 111
4.18 Correlation between hippocampal ERPs deflection and evoked oscillations 111
4.19 Hippocampal 2-Hz bursts across task sessions 113
4.20 Hippocampal 2-Hz bursts and memory performance 114
4.21 Stepping movement does not elicit 2-Hz oscillations in the human hippocampus 115

5.1 Basic properties of hippocampal neurons 120
5.2 2-Hz rhythmicity of hippocampal neurons 121
5.3 Hippocampal single-neurons preferentially lock to the phase of 2-Hz oscillations 122
5.4 Illustration of gamma and neuronal spiking co-modulation at 2-Hz 123
5.5 Gamma activity coupling to hippocampal oscillations 124
5.6 Anatomical gradients of gamma coupling to hippocampal slow oscillations 125
5.7 Holo-Hilbert spectral analysis reveals gamma amplitude modulation by 2-Hz in the human hippocampus 126
5.8 Hippocampal structural connectivity with temporal and occipital regions 129
5.9 Electrode contact localization across temporal lobe regions 129
5.10 Trigger average of MTL LFPs by hippocampal 2-Hz 130

5.11 Slow-frequency oscillations across the temporal lobe 130
5.12 Slow-frequency oscillatory components in the superior temporal cortex . 131
5.13 Event-related potentials in the amygdala 132
5.14 ERP deflection does not correlate with evoked 2-Hz bursts outside the hippocampus 133
5.15 2-Hz rhythmicity of MTL neurons 134
5.16 MTL neurons preferentially couple to the phase of hippocampal 2-Hz oscillations 135
5.17 Gamma coupling to hippocampal slow oscillations in the MTL 136
5.18 Synchronization of MTL gamma patterns by hippocampal 2-Hz phase . . 137
5.19 Synchronization of MTL gamma patterns in oscillatory bursts 138

6.1 Example of sleep staging in one participant 141
6.2 Raw hippocampal LFPs display 2-Hz bursts in human REM sleep but not during SWS 142
6.3 2-Hz bursts can be observed alongside rapid eye movements 143
6.4 2-Hz oscillations feature human hippocampal LFPs during REM sleep . . 144
6.5 Example of detected ripples 145
6.6 Bipolar referencing impairs the delta-waves 146
6.7 Characterization of ripple frequency 147
6.8 Hippocampal ripples share the same properties between macrocontacts and tetrodes 149
6.9 Example hippocampal fast-ripple detected in one participant 150
6.10 Hippocampal ripples are predominant in task rests, N1 and slow-wave sleep 150
6.11 Hippocampal single-neuron activity is modulated by ripples 151
6.12 Hippocampal ripples propagate preferentially to MTL regions 152
6.13 Inter-ripple intervals of hippocampal ripples in mice and humans 153
6.14 Coactivity motifs detected from neuronal activity in the MTL 155
6.15 Preferential reactivation of 2-Hz structured spiking motifs in hippocampal ripples 156
6.16 Reactivation and memory consolidation 156
6.17 Reactivation controls 157

7.1 Human 2-Hz in a putative evolutionary continuum 163

A.1 Bipolar reference with different phase relationships 171
A.2 Example of phase distortions induced by bipolar reference 172
A.3 Correlation between phase difference and 2-Hz amplitude change induced by bipolar referencing 173
A.4 Correlation between phase difference and amplitude changes induced by bipolar referencing across participants 174

B.1 Hippocampal power spectral densities in the gamma band 177
B.2 Gamma-band bursts in the human hippocampus 179
B.3 Gamma-band responses to photographs in the recall session 181
B.4 Gamma-band responses in the amygdala 184
B.5 Gamma-band responses in the fusiform gyrus 186
B.6 Gamma-band responses in regions of the occipital lobe 187

C.1 References: timeline and journals. 189
C.2 References: authors 190

List of Abbreviations

CAR common-average reference

CI confidence interval

CT computed tomography

DW-MRI diffusion-weighted MRI

EEG electroencephalography

EMD empirical mode decomposition

ERP event-related potential

GLM generalized linear model

HHSA Holo-Hilbert Spectral Analysis

IED interictal epileptiform discharge

IMF intrinsic mode function

ISI inter-spike interval

ISOMAP isometric mapping

LFP local field potential

LMEM linear mixed-effects model

mEMD masked EMD

MI modulation index

MNI Montreal Neurological Institute

MRI magnetic resonance imaging

MTL medial temporal lobe

PAC phase-amplitude coupling

PPC pairwise-phase consistency

PSD power spectral density

REM rapid eye movement

sEEG stereoelectroencephalography

SWR sharp-wave ripple

SWS slow-wave sleep

tmEMD tailored-masked EMD

UMAP uniform manifold approximation and projection

1 General introduction

"La connaissance du réel est une lumière qui projette toujours quelque part des ombres."

"Knowledge of reality is a light that always casts shadows somewhere."

— Gaston Bachelard, La Formation de l'esprit scientifique (1938)

Contents

1.I Models of memory 23

1.I.1 The legacy of associationism 23

1.I.2 Beyond mere associationism 24

1.II Studying memory at the macroscopic level 27

1.II.1 In search of the neural substrate of memory 27

1.II.2 The multiple memory systems theory in the context of amnesia 29

1.II.3 Beyond the MTL alone 31

1.III Studying memory at the microscopic level 32

1.III.1 Neuronal "codes" 32

1.III.2 Neural oscillations and coordination mechanisms 35

1.III.3 Synthesis 40

1.IV Insights into memory mechanisms from human depth recordings 42

1.IV.1 Reviewing evidence for theta oscillations in humans 42

1.IV.2 Reviewing evidence for ripples and reactivation in humans . . . 44

1.V Hypotheses and aims of this work 46

Memory is one of the most extensively studied faculties of human beings. Across philosophy, psychology, and neuroscience, great thinkers have embarked in the adventure of defining memory and uncovering its fundamental properties. Yet, many of its core mechanisms remain mysterious, and memory continues to occupy a central place in contemporary research.

The aim of the work presented in this thesis is decidedly more circumscribed. Although memory can be approached from various angles, I adopt here a reductionist and mechanistic perspective, using memory as a means of investigating how the brain works. More specifically, this thesis focuses on everyday memory and on the contribution of the hippocampus to its acquisition, organization, and consolidation. In that sense, the primary

object of this work is not memory in its full complexity, but the neural mechanisms that make a particular form of memory possible.

Inevitably, this approach relies on a number of assumptions that restrict the scope of the study. I do not attempt to provide a general theory of memory. Rather, I examine a set of foundational theories of memory when they generate mechanistic predictions about how the brain functions. In particular, I focus on those predictions which can be tested against neurobiological evidence. For this reason, I aim to be as explicit and transparent as possible about the assumptions adopted throughout the thesis, and about the limits they place on the interpretation of the results. To illustrate this approach and in order to be explicit about the intellectual legacy of this work, in Appendix C I provide a short analysis of the citations employed throughout the thesis.

1.I Models of memory

1.I.1 The legacy of associationism

Associationism has played a major role in the historical development of theories of memory and learning. In its classical form, it proposed that mental life is built from elementary sensations or ideas which become linked through experience. These links were thought to depend on principles such as contiguity, similarity, repetition, and later reinforcement (Hume 1690; Locke 1740; Hartley 1801; Mill 1829; Mill 1843; Bain 1855; Spencer 1855; Maudsley 1877; Ribot 1888; James 1890; Thorndike 1898). In this view, memory can be understood as the capacity to preserve and retrieve relations between elements that were previously experienced together. This idea was progressively extended from the association of ideas to the association between sensations, actions, and consequences, a generalization that explained learning, habit formation, and adaptive behaviour. While the details differed between authors, associationism helped to explain how experience could shape the mind without requiring innate structures or complex internal representations.

This intellectual tradition strongly influenced the development of experimental psychology. Early memory research attempted to isolate elementary laws of learning by studying repetition, retention, forgetting, and recall under controlled conditions (Wundt 1910; Ebbinghaus 1913). This approach was formalized by Ebbinghaus, who used nonsense syllables to reduce the influence of pre-existing knowledge and quantify learning and forgetting experimentally (Ebbinghaus 1913). It was then extended to the study of conditioning and reinforcement, where behaviour was explained through associations between stimuli, responses, and outcomes (Thorndike 1898; Pavlov 1927; Skinner 1938). Even later neurobiological theories preserved this legacy, notably through the idea that repeated co-activation strengthens connections between neurons (Hebb 1949). As a result, many classical paradigms in memory research still reflect an associationist logic, including paired-associate learning, conditioning, stimulus-response learning, recognition memory, and tests of associative memory. Associationism therefore provided a major methodological foundation for the experimental study of memory, encouraging a view of memory as the storage of links between discrete elements.

1.I.2 Beyond mere associationism

1.I.2.a Memory is flexible and anticipatory

Associationism has been a powerful and fruitful approach for understanding memory, but it struggles to capture the full complexity of behaviour. First, not all associations are equally stored or retained, and retrieval does not simply reproduce the conditions of initial learning. These observations suggest that learning and memory are constrained by pre-existing structures that shape how knowledge is constructed and organized over time. This limitation was made explicit in the development of schema theories (Piaget 1923; Piaget 1952; Bartlett 1932), which propose that new knowledge is not stored in isolation but is rather integrated within broader and structured "schemata" that govern how it is subsequently used.

A second limitation of the associationist tradition lies in the fact that the primary function of memory is not to passively store events, but to guide behaviour. From an evolutionary perspective, memory helps select the most appropriate behavioural strategy to adopt in a given context, based on previous experience (Cisek 2019). This capacity requires adapting to novel situations for which no direct associations exist, that is generalizing to novel contexts. As Lashley (1951) argued in his seminal analysis of language, complex behaviour does not follow a strictly ordered sequence, i.e., a simple chain of associations in which one element triggers the next. Instead, it is shaped by hierarchically organized internal structures that represent future actions, goals, or the relation between separate elements (Rosenbaum et al. 2007; Kolodny and Edelman 2015). A similar criticism was raised by Chomsky (1959) who argued that language acquisition cannot be explained by stimulus-response-reinforcement loops alone. In particular, children can generalize and produce new sentences despite limited and irregular reinforcement, suggesting that they rely on internal representations of linguistic structure rather than on stored associations. This capacity for abstraction and generalization indicates that memory supports structured and flexible representations that extend beyond past experience.

Consequently, to account for the flexible and anticipatory nature of memory, we need to go beyond associationism.

1.I.2.b Schema theory

The idea of a pre-existing structure that constrains the acquisition of new information was developed by Immanuel Kant, who introduced the notion of "schemas" as general procedural rules mediating between abstract concepts and sensory experience (Kant 1781). Jean Piaget later developed the concept of "schèmes" in the context of child development, to explain how knowledge is actively constructed through interaction with the environment. In this account, knowledge is not passively stored; rather, new information is either "assimilated" into existing structures or leads to their modification through "accommodation" (Piaget 1923). Even though these two theories of schemas accounted for some aspects of learning and memory, they were not formulated as explicit theories of memory. By focusing directly on remembering, Bartlett showed that memory recall is not a simple retrieval of isolated traces, but instead operates as an “organized mass”, indicating the existence of a reconstructive process at play during retrieval (Bartlett 1932).

This perspective implies that memories are not fixed but are continuously re-organized over time.

Schema theory was further developed in cognitive psychology and early computational approaches as a way to explain how knowledge is organized and how prior experience shapes memory (van Kesteren et al. 2012; Ghosh and Gilboa 2014). In particular, studies focussed on how prior knowledge supports comprehension and recall (Alba and Hasher 1983; Anderson et al. 1983; Anderson and Pearson 1988). According to this view, prior knowledge facilitates memory formation, and schema-congruent information is acquired and remembered more efficiently (Schulman 1974; Craik and Tulving 1975; Brewer and Treyens 1981; Anderson et al. 1983; Staresina et al. 2009), but see (van Kesteren et al. 2012) who propose an interpretation accounting for novelty. Importantly, schema theory has played a significant role in shifting the study of memory beyond simple associative rules toward a more structured, model-based view of memory. However, schema theory was initially formulated to account for behavioural observations rather than to describe the neural processes underlying memory (van Kesteren et al. 2012; Ghosh and Gilboa 2014), but see more recent accounts (Gilboa and Marlatte 2017). Consequently, despite a renewed interest in schemas in contemporary neurosciences (Tse et al. 2007; Tse et al. 2011; McKenzie et al. 2014; Baldassano et al. 2018; Zhou et al. 2021; Samborska et al. 2022; El-Gaby et al. 2024), their neural implementation remains loosely defined. Instead, current accounts rely on other theories, such as the complementary learning theory (Chapter 1.III.3), to provide a mechanistic basis for schema formation and development (van Kesteren et al. 2012).

1.I.2.c Cognitive maps and relational memory

Another attempt to develop a theory of memory that goes beyond associationism was made in parallel by Tolman (1948) who proposed that learning consists not in the gradual strengthening of mere stimulus-response associations by repetition or reinforcement, but in constructing internal "cognitive maps". These cognitive maps do not represent space as an absolute variable, but instead capture the relative or "relational" structure of the environment, which can be flexibly used to guide behaviour. Crucially, they vary in their degree of abstraction, with broader and more flexible maps supporting adaptation to novel situations, whereas narrow, over-specific ones lead to rigid behaviour. This framework was later formalized by O'Keefe and Nadel (1978), who distinguished simpler forms of conditioning (stimulus-response associations, cue-guided strategies) from map-based navigation, situating cognitive maps as a distinct memory system supporting flexible, context-dependent behaviour. In contrast to the schema theory, cognitive map theory was initially linked more directly to hippocampal physiology, motivated both by the discovery of place-cells in rodents (O'Keefe 1976) (Chapter 1.III.1) and by cognitive studies in amnesic patients (Scoville and Milner 1957) (Chapter 1.II.2). Although the authors acknowledged the influence of Bartlett's schemas (Bartlett 1932), they argue that the cognitive map theory is primarily based on the study of navigation in physical space. Interestingly, in recent experimental work involving cognitive maps, as the spatial structure of the task becomes less explicit and the focus shifts toward more abstract forms of knowledge, there is an increasing use of schema-like concepts (Baram et al. 2021; El-Gaby et al. 2024; Qu et al. 2026). Here, schemas are combined with cognitive maps to explain how structured knowledge supports behaviour beyond physical navigation.

One important aspect of the cognitive map is that it emphasizes the role of relationships between elements rather than the particularities of the elements themselves (O'Keefe and Nadel 1978). This idea naturally extends beyond physical space and led to the formulation of relational memory theory, in which arbitrary relationships between items, contexts and events are stored and later reorganized during sleep (D. Marr 1971; Eichenbaum et al. 1988; Eichenbaum et al. 1989; Eichenbaum and Cohen 1993; Eichenbaum and Cohen 2001). In this view, spatial navigation represents a specific instance of a more general principle whereby knowledge is represented in a relational format to support generalization across domains and flexible behaviour (Konkel and Cohen 2009). Akin to cognitive map theory, relational memory was initially grounded in observations of hippocampal function and dysfunction, revealing its role in organizing relationships between elements (Bunsey and Eichenbaum 1996; Konkel et al. 2008; Zeithamova et al. 2012). However, more recent studies suggest that such relational knowledge is integrated across broader cortical networks, in particular the neocortex (Preston and Eichenbaum 2013; Zong et al. 2025). Again, schema-like concepts have re-emerged in this framework, suggesting continuity between cognitive maps and schemas, with cognitive maps primarily linked to hippocampal function and schemas involving neocortical regions (Ghosh and Gilboa 2014; Gilboa and Marlatte 2017; Lisman et al. 2017).

A central consequence of relational organization is inferential behaviour, which allows organisms to establish connections between elements that have not been directly experienced together (Zeithamova et al. 2012; de Sousa et al. 2021). Inference is a fundamental property of living beings (Friston 2010) and is observed across many species (Müller and Wehner 1988; Wehner and Wehner 1990; Bunsey and Eichenbaum 1996), reviewed in (Vasconcelos 2008) and to a certain extent in (Zentall et al. 2008). From this perspective, memory is not limited to the storage of past experiences, but also enables the flexible recombination of learned relationships to generate predictions about novel or future situations. This view emphasizes that the hippocampal system does not simply retrieve stored representations, but actively supports the construction of new knowledge and adaptive behaviour from previously acquired relationships.

1.I.2.d Predictive coding

In contrast to schema theory, which emphasizes the facilitated integration of congruent information, i.e., consistent with pre-existing knowledge, predictive coding frameworks highlight the role of prediction error, whereby incongruent (unexpected) information drives stronger learning and results in the update of internal representations (Friston 2005; Friston and Kiebel 2009). Originally developed in the context of sensory processing (Rao and Ballard 1999), predictive coding is grounded in the mathematical principles of Bayesian inference, according to which the brain is assumed to maintain probabilistic models of the environment that are continuously updated based on incoming information (Dayan et al. 1995; Doya 2007; Griffiths et al. 2008). Conceptually, this idea can be traced back to Craik's analogy of the brain as a "calculating machine", in which cognition relies on internal representations capable of simulating and anticipating future states (Craik 1967).

Predictive coding proposes that memory can be understood as the maintenance and updating of such internal models: memory acquisition corresponds to the incorporation

of new information through prediction error, while memory retrieval reflects the use of these models to generate predictions about future states. In this sense, predictive coding provides a unifying account that integrates schemas and relational representations, framing both as instances of prediction based on prior knowledge (Barron et al. 2020a). In addition, predictive coding emphasizes the anticipatory nature of memory, consistent with evolutionary accounts of behaviour (Murray et al. 2017; Cisek 2019). Notably, related ideas were already present in the cognitive map theory of O'Keefe and Nadel, who suggested the existence of a "misplace" system for detecting mismatches between expected and actual spatial inputs, suggesting an early link between hippocampal function and prediction error (O'Keefe and Nadel 1978). Nevertheless, the precise brain networks involved in the generation and interpretation of prediction error signals during learning remain under investigation (Barron et al. 2020a; Gueguen et al. 2021; Miller et al. 2023).

Overall, theories of memory seem to face a trade-off: psychological approaches capture complex behaviour but often lack clear neural mechanisms, whereas accounts based on neural physiology provide mechanistic details but may not always generalize across different forms of behaviour, and therefore require ongoing refinement as new evidence emerges. This perspective raises the question of which neural mechanisms support the acquisition, maintenance, and updating of memory representations.

1.II Studying memory at the macroscopic level

1.II.1 In search of the neural substrate of memory

Early attempts to understand psychological processes such as memory were shaped by a methodological constraint: psychological phenomena are subjective and cannot be accessed directly by an external observer. This raises a fundamental problem, namely how to study mental processes objectively.

A solution emerged in the 19th century, based on the idea that psychological states can be inferred from behaviour (Mill 1843; Sechenov 1863; Bain 1855). As Skinner defined it in the middle of the 20th century: "Behavior is what an organism is doing—or more accurately what it is observed by another organism to be doing" (Skinner 1938). In this view, behaviour becomes the primary empirical access point to psychology.

A complementary solution was introduced by evolutionists, who proposed that psychological processes can be understood by studying their gradual development across species. This perspective builds on the continuity between animals, such that mental functions emerge progressively with the evolution of the nervous system (Spencer 1855). Darwin supported this view by showing that similarities in behaviour (in particular emotions) across species reflect common ancestry (Darwin 1872). Moreover, the observation that simple organisms can learn from experience and adapt their behaviour accordingly (Morgan 1843) reveals that memory is a fundamental property of living beings (George John Romanes 1882).

Building on this evolutionary perspective, comparative psychology emerged as a controlled experimental system to study behaviour across species. While evolutionary approaches emphasized behavioural adaptation to environmental constraints, comparative

psychology aimed at revealing general laws of learning and memory. Indeed, rather than comparing behaviours in their natural context, Thorndike (1898) introduced standardized experimental paradigms applied to different species to investigate how they solve the same problem. Pavlov (1927) further argued that, since higher nervous activity relies on similar mechanisms across species, experiments in animals can provide general insights into brain function, including humans. Comparative psychology culminated in behaviourism, which aimed to establish a science of behaviour based on observable and measurable actions using controlled experiments (Watson 1919; Skinner 1938). This approach is grounded in methodological reductionism, which assumes that complex psychological phenomena can be explained from the basic interactions between these simpler elements (Bain 1855; Sechenov 1863; Hering 1895; Semon 1921).

Comparative psychology established objective and reproducible behavioural paradigms which could be applied in several animal species, but it also drastically reduced the diversity of species under investigation. In a famously provocative article, Beach (1950) noted that in hunting for "animal behaviour," psychologists had effectively rediscovered a single species (the laboratory rat), suggesting that comparative psychology had quietly turned into the study of rat learning rather than a truly comparative science. Given the predominance of mouse models in contemporary neuroscience, this standpoint remains largely valid, despite recent efforts to study natural behaviour (Ulanovsky and Moss 2007; Hong et al. 2015; Wiltschko et al. 2015; Mathis et al. 2018; Marshall et al. 2021; Cisek and Green 2024), to perform cross-species investigations (Barron et al. 2020b; Barron et al. 2021) and to broaden the range of species studied (Ulanovsky and Moss 2007; Muir et al. 2009; Laurent 2020; Payne et al. 2021; Bergel et al. 2025).

At the conceptual level, recent work has revived evolutionary approaches to the study of behaviour and memory (Murray et al. 2017; Cisek 2019), reinforcing their value as a model for understanding how brain mechanisms support adaptive behaviour. Early investigations emphasized the importance of examining the anatomy, histology and connectivity of the hippocampus across species in order to identify conserved principles of brain organization and function (Cadilhac 1954). Although this approach became less prominent with the rise of species-specific experimental paradigms, it continued to be defended by authors such as C.H. Vanderwolf, who argued that understanding memory requires placing neural mechanisms within their evolutionary and behavioural context (Vanderwolf and Cain 1994). Drawing on this perspective, in Chapter 1.III.2, I examine how comparing behaviour and brain networks across species could reveal shared neural mechanisms of learning, with a focus on the conserved role of theta oscillations during sensory acquisition and exploratory behaviour.

Comparative psychology and evolution were instrumental in establishing memory as a fundamental and phylogenetically conserved cognitive function, whose neural substrates can be revealed by cross-species comparison. Another influential methodological solution to investigate memory was the study of pathological states. Influenced by Bernard (1865), who established medicine as an experimental science, Ribot systematically analysed clinical cases of retrograde amnesia to elaborate a functional and hierarchical organization of memory within the nervous system (Ribot 1888). While he did not identify a precise neural substrate for memory, his account anticipated the view that memory relies on distributed neural systems, a principle that remains central to contemporary neuroscience (Chapter 1.III.3). This approach was later transformed by lesion-based neuropsychology,

which suggested the existence of a direct mapping between brain structures and cognitive functions, and will form the focus of the next section (Chapter 1.II.2).

1.II.2 The multiple memory systems theory in the context of amnesia

1.II.2.a The Medial Temporal Lobe (MTL) in memory

A major turning point in memory research came from the study conducted by Scoville and Milner (1957). Among the ten patients who underwent surgical resection of the MTL, seven patients with psychiatric disorders (mostly schizophrenia) and one with intractable epilepsy (patient H.M.) developed subsequent anterograde amnesia, associated with retrograde amnesia of variable extent. Earlier studies had reported memory deficits following lesions to the MTL and/or temporal neocortex in humans (Glees and Griffith 1952; Petit-Dutaillis et al. 1954; Milner and Penfield 1955–1956; Terzian and Ore 1955). Nonetheless, the systematic psychological assessment of memory before and after surgery in this study was a critical methodological advance. While the clinical rationale for these procedures, rooted in earlier psychosurgical practices such as lobotomy (Miller 1967), reflects a historical medical context very different from current standards, they provided an opportunity to relate memory deficits to brain lesions, and set the ground for several decades of research on memory in humans (Spiers et al. 2001). In particular, patient H.M. was further involved in memory studies for almost five decades (Milner et al. 1968; Corkin 1984; Corkin 2002). These studies yielded extensive evidence for the role of the MTL in memory.

Even though these initial studies involved patients with broad MTL lesions, further studies of patients with more circumscribed hippocampal lesions were instrumental in refining the understanding of memory systems (Milner and Penfield 1955–1956). An important step was the report of patient R.B., who developed marked anterograde amnesia after an ischemic episode; post-mortem analysis showed a bilateral lesion largely limited to the CA1 field of the hippocampus, with little evidence of retrograde amnesia or other cognitive impairment (Zola-Morgan et al. 1986). This case supported the view that hippocampal damage alone can be sufficient to produce a deficit in memory acquisition. A later clinicopathological case confirmed that bilateral hippocampal lesions after status epilepticus could produce severe, persistent amnesia (Victor and Agamanolis 1990). Then, work on transient global amnesia linked small, mostly CA1 lesions to acute but reversible memory deficits, suggesting a temporary disturbance of hippocampal memory circuits rather than permanent damage (Bartsch et al. 2006). Studies of patient K.C., who had extensive bilateral hippocampal damage, showed that retrograde amnesia is not uniform: general knowledge about familiar environments, routes, and large spatial layouts were preserved, whereas detailed landmarks, houses, and autobiographical episodes were severely impaired (Rosenbaum et al. 2000; Rosenbaum et al. 2005). More recent work on LGI1-antibody limbic encephalitis identified focal CA3 atrophy associated with impaired autobiographical episodic memory, affecting both recent and remote memories, while semantic information was relatively preserved (Miller et al. 2017; Miller et al. 2020). Together, these studies show that hippocampal lesions are especially disruptive for new learning and detailed episodic recollection, while the severity and profile of amnesia depend

on lesion extent, subfield involvement, and the kind of memory tested.

1.II.2.b The multiple memory systems theory

An important observation from studies of amnesic patients is that their memory deficits are not uniform. An important piece of evidence in support of this idea is their preserved ability to acquire unconscious, perceptual-motor skills, referred to as non-declarative memory (Milner et al. 1968; Brooks and Baddeley 1976; Cohen and Squire 1980). This capacity contrasts with their profound impairment in learning and recalling consciously accessible facts and events, known as declarative memory (Squire 1987; Squire 2004; Squire 2009). This dissociation provided some of the earliest empirical evidence for the multiple memory systems theory (Tulving 1972; Squire 1992b; Schacter and Tulving 1994), which posits that memory is composed of distinct domains supported by different brain systems.

Within declarative memory, a further distinction was proposed between episodic memory, referring to the recollection of events, and semantic memory, referring to general knowledge. This distinction was raised following the observation that amnesic patients retain access to semantic knowledge despite severe episodic impairments (Tulving 1972; Tulving and Thomson 1973; Craik and Tulving 1975; Tulving 1983; Tulving 1985). Additional support comes from studies of patients with semantic dementia, a syndrome characterized by a deficit in semantic memory with relatively preserved episodic memory functions (Snowden et al. 1989; Hodges et al. 1992; Hodges and Graham 2001; Piolino et al. 2003). This disease was associated with lesions in the anterior part of the temporal lobe (Hodges et al. 1992; Hodges and Graham 2001; Barbeau et al. 2011; Busigny et al. 2015), a pattern distinct from episodic amnesia, further supporting the multiple memory systems theory.

1.II.2.c Animal models of human amnesia

Initial reports of memory deficits in human patients with specific lesions to the temporal lobe were followed by attempts to replicate these findings in animal models (Squire 1992a), particularly in non-human primates. Although early studies had described behavioural changes, including memory impairments, following temporal lobe lesions in monkeys (Brown and Sharpey-Schafer 1888; Klüver and Bucy 1937; Klüver and Bucy 1938), it was only after the seminal work with human amnesic patients that primate research began to focus systematically on memory (Mishkin 1978). By performing selective lesions to different parts of the MTL, either in isolation or in combination, and by using tasks analogous to those employed in humans, some of these studies demonstrated the role of the MTL and in particular the hippocampus in declarative memory (Mishkin 1978; Zola-Morgan et al. 1989; Zola-Morgan et al. 1992). Importantly, lesioned animals showed preserved acquisition of motor skills (Salmon et al. 1987), mirroring findings in humans and supporting the distinction between declarative and non-declarative memory systems. These studies with non-human primates made it possible to establish a causal link between MTL lesions and behavioural deficits (Zola-Morgan et al. 1989; Zola-Morgan and Squire 1990; Squire and Zola-Morgan 1991; Zola-Morgan et al. 1992; Buckmaster et al. 2004), which was not possible in patients whose disease could be interpreted as a confounding factor.

A third, complementary line of research was conducted in parallel and involved the study of memory in rodents. By performing lesions to the hippocampus in rodents, it was shown that the hippocampus is necessary for some forms of memory, but not all (Squire 1992a). Because conscious recollection cannot be directly assessed in rodents, episodic-like memory is instead studied using behavioural tasks that test whether animals remember information about what happened, where and when it happened, or in which context it occurred. Using these methods, early studies reported changes in activity, inhibition, and avoidance after hippocampal lesions, even though these effects were not easily interpreted as selective memory deficits (Isaacson and Wickelgren 1962; Kimble 1963; Teitelbaum and Milner 1963). Later work suggested that hippocampal damage particularly impairs memory when behaviour depends on contextual, spatial, or relational information rather than simple stimulus-response associations, supporting the cognitive map theory (O'Keefe and Nadel 1978; Hirsh 1974; Hirsh 1980). This view was supported by experiments with the Morris water maze, where rats with hippocampal lesions were impaired in finding a hidden platform using distal spatial cues, despite preserved sensory, motor, and motivational abilities (Morris et al. 1982). Subsequent studies showed that hippocampal lesions spare simple recognition or discrimination learning, but impair cross-modal associations, contextual conditioning, topographical memory, and flexible use of odour associations through symmetry or transitive inference (Sutherland and McDonald 1990; Bunsey and Eichenbaum 1996; Dusek and Eichenbaum 1997). Together, these findings indicate that the rodent hippocampus supports relational and episodic-like memory, but not simpler associative, procedural, or habit-based learning (Squire 1992a), in support of the multiple memory systems theory.

1.II.3 Beyond the MTL alone

Despite this evidence, most studies involving discrete lesions restricted to subregions of the MTL in non-human primates and rodents failed to reproduce the severity of the memory impairment (dense amnesia) described in the original work of Scoville and Milner (Scoville and Milner 1957; Horel 1978). This was partly due to the fact that these original resections were quite extensive, as revealed by the anatomical magnetic resonance imaging (MRI) performed with patient H.M. (Corkin et al. 1997). While the multiple memory systems theory has been useful in accounting for dissociable memory deficits in patients, it does not fully capture the extent to which memory depends on interactions within distributed neural circuits (Horel 1978; Vanderwolf and Cain 1994; Gaffan 2001; Gaffan 2002). This idea was implied in a seminal paper published by Lashley (1950), who wrote that "it is not possible to demonstrate the isolated localization of a memory trace anywhere within the nervous system". Despite this early conceptual intuition, it was formally addressed only after studies on "disconnection syndromes" had demonstrated that lesions of white matter pathways can produce cognitive deficits, including memory impairments, by disrupting communication between otherwise intact regions (Geschwind 1965).

These early findings led to the proposal that cognitive functions like memory are supported by large-scale networks rather than the MTL alone, such that damage to white matter tracts, like the fornix, the temporal stem and the amygdalofugal pathway, results in amnesic syndromes comparable to those observed following MTL lesions (Horel and

Misantone 1976; Olton et al. 1978; Bachevalier et al. 1985; Gaffan and Gaffan 1991; Gaffan 1994). The proposal of an integrated network supporting normal memory was also supported by evidence of amnesia after lesions to diencephalic regions that are part of the Papez circuit (Papez 1937), and in particular the anterior thalamus which connects the limbic system with the neocortex (Squire and Moore 1979; Warrington and Weiskrantz 1982; Aggleton and Mishkin 1983; von Cramon et al. 1985; Graff-Radford et al. 1990; Parkin et al. 1994; Parker and Gaffan 1997). This perspective was formalised in the influential model of Aggleton and Brown (1999), which reflects a paradigm shift from a localisationist view of amnesia to a network-based account, implying that both memory impairment and normal memory function depend on the integrity of distributed cortico-subcortical circuits.

While lesion studies have been essential for identifying the macroscopic networks involved in memory, they provide a rather static and indirect view of memory mechanisms. This work revealed which brain regions and pathways are necessary for memory, but not how information is dynamically acquired, stored, and retrieved within these circuits. To address this, a complementary line of research has focused on the activity of single neurons and populations, in vivo, while subjects engaged in memory tasks. This work has led to the discovery of specialised cells, such as place cells and concept cells, and to the idea that memories are supported by coordinated activity within neuronal populations, referred to as cell assemblies. This approach shifts the focus from brain structures to neural circuits, revealing a dynamic view of memory based on how information is represented and processed in the brain.

1.III Studying memory at the microscopic level

1.III.1 Neuronal "codes"

1.III.1.a From the neuron doctrine to population coding in animal models

The idea that experience leaves lasting traces in the nervous system, termed "engrams" by Semon (1921), long preceded direct experimental access to neural activity (Ribot 1888). With the development of in vivo extracellular recordings (Hubel 1957), it first became possible to record the response of individual neurons to the presentation of sensory stimuli, revealing highly selective neurons in the cortex across mammals (Mountcastle 1957; Hubel and Wiesel 1959; Gross et al. 1972). This early work on receptive fields, a term coined by Sherrington (1906), gave single neurons a central explanatory role in sensory perception (Barlow 1972), forming the basis of a “neuron doctrine” centred on single-cell coding (Yuste 2015).

The extension of these approaches to freely moving animals led to the discovery of place cells (O’Keefe and Dostrovsky 1971; O’Keefe 1976), providing the first direct link between single-neuron activity and memory-related processes. This finding shifted attention toward neuronal mechanisms of memory and spatial representation (O’Keefe and Nadel 1978; Eichenbaum and Cohen 1988). This discovery was followed by the description of several other navigation-specific neurons in the hippocampus and entorhinal cortex, including

head-direction, grid, and boundary cells (Quirk et al. 1992; Taube et al. 1990; Frank et al. 2000; Fyhn et al. 2004; Hafting et al. 2005; Ulanovsky and Moss 2007), which reinforced the theory of cognitive maps (Behrens et al. 2018). Early in the development of this theory, it was postulated that memory is not supported by isolated neurons, but by the coordinated activity (co-activity) of neuronal ensembles (Gerstein and Aertsen 1985; Traub et al. 1989; Ahissar et al. 1992) in line with Hebb's hypothesis (Hebb 1949). Experimental evidence for such synchrony in the hippocampus was later obtained by using recordings of neuronal populations (Buzsaki et al. 1992; Wilson and McNaughton 1993), a development made possible by advances in recording techniques, notably tetrodes which allow the identification of multiple neurons simultaneously (McNaughton et al. 1983; Gray et al. 1995; Buzsáki 2004).

In parallel, a complementary line of work used immediate early genes as markers of neuronal activation in rodents, after early studies showed that c-fos expression is rapidly induced in neurons following neuronal activity (following seizures (Morgan et al. 1987) and electrical stimulation (Sagar et al. 1988)). This approach was extended to memory with genes such as Arc (Lyford et al. 1995), whose expression can reveal hippocampal neurons which were hyper-active following a spatial experience (Guzowski et al. 1999), identifying molecular "traces" of neuronal ensembles. Activity-dependent genetic tagging then made it possible to label neurons recruited during learning and to show that these neurons are preferentially active during memory retrieval (Reijmers et al. 2007). Subsequent studies combining this approach with optogenetics showed that artificial activation of hippocampal neurons recruited during learning is sufficient to reinstate behaviour associated with a fear memory, while manipulation of these ensembles can modify memory expression (Liu et al. 2012; Ramirez et al. 2013; Ryan et al. 2015). Although early work suggested that such engrams form relatively stable neuronal ensembles, more recent studies have revealed that their composition and properties can change over time, reflecting their dynamic and flexible organization (Redondo et al. 2014; Trouche et al. 2016; Tomé et al. 2024).

Building on these findings, the dominant paradigm has shifted from a neuron-centred perspective toward a population-level view, in which information is encoded by distributed and dynamic patterns of activity across neuronal populations (Harris et al. 2003; Ikegaya et al. 2004; Buzsáki 2010; Dupret et al. 2013; Yuste 2015; van de Ven et al. 2016; Lopes-dos-Santos et al. 2018; El-Gaby et al. 2021; Gava et al. 2021; Yuste et al. 2024). Moreover, converging evidence indicates that stable behavioural representations can be maintained despite ongoing drift in the activity of individual neurons, through the preservation of population-level structure and coordinated ensemble dynamics (Deitch et al. 2021; Sheintuch et al. 2023). Importantly, causal manipulations have demonstrated that such population activity directly contributes to perception and memory (Carrillo-Reid et al. 2016; Gridchyn et al. 2020; Gava et al. 2024; Zaki et al. 2025). These results support the view that cognition emerges from the coordinated dynamics of neural populations rather than the activity of individual neurons (Dupret et al. 2026). Together, these studies provide strong evidence that memories are encoded within sparse and distributed neuronal ensembles.

1.III.1.b Human neuronal codes

The first direct recordings of neuronal activity in humans were acquired during epilepsy surgery (Ward and Thomas 1955), but it was only after the development of stereoelectroencephalography (sEEG) as a diagnostic procedure in patients with drug-resistant epilepsy (developed in parallel by (Spiegel et al. 1947; Leksell 1951; Talairach et al. 1962; Reif et al. 2016; Zanello et al. 2022)) and the introduction of hybrid electrodes containing microwires (Babb et al. 1973) that semi-chronic neuronal recordings from deep structures like the MTL were possible (Cash and Hochberg 2015; Quian Quiroga 2019). As in animal models (Mountcastle 1957; Hubel and Wiesel 1959; Gross et al. 1972), the first basic science questions addressed with these recordings in humans were related to receptive fields (Wilson et al. 1983) and neuronal tuning to visual stimuli (Heit et al. 1988). Interestingly, because epilepsy often involves MTL regions (Barba et al. 2021), and there was a strong interest in the role of MTL regions in declarative memory (Chapter 1.II.2), studies of neuronal activity in humans soon focussed on memory mechanisms (Fried et al. 1997; Cameron et al. 2001).

The first studies on single-neuron dynamics investigated episodic memory (Fried et al. 1997; Cameron et al. 2001). However, one of the most influential outcomes of this research was related to semantic memory, with the identification of single-neurons exhibiting selective and invariant responses to specific concepts in the human MTL, known as "concept cells" (Quiroga et al. 2005). This discovery was a logical continuation of the early work on receptive fields, as it was previously reported that neurons located along the ventral visual stream respond to progressively more abstract features of the images presented (Gross et al. 1972) and the inferior temporal cortex is connected with the MTL (Nauta and Whitlock 1956; Jones and Powell 1970; Van Hoesen and Pandya 1975). For more than 20 years, concept cells have shaped virtually all subsequent single-neuron studies and are now viewed as one of the building blocks of declarative memory (Quiroga 2012; Quian Quiroga 2019; Quian Quiroga 2026). The legacy of the multiple memory systems theory (Chapter 1.II.2) continues to shape this line of research (Rutishauser et al. 2021), with reports of neurons tuned to episodic features (Rutishauser et al. 2006; Rutishauser et al. 2008; Rutishauser et al. 2015; Reber et al. 2017; Staresina et al. 2019; Kolibius et al. 2023; Daume et al. 2024b; Daume et al. 2024a) or semantic features (Kreiman et al. 2000; Quiroga et al. 2009; Reber et al. 2019; Jamali et al. 2024).

Although human microwire recordings provide access to single-neuron activity, they sample only a small subset of the underlying population, and hippocampal representations appear particularly sparse (Waydo et al. 2006; Wixted et al. 2014; Urgolites et al. 2022; Tallman et al. 2025). Concept cells and "memory-selective" cells are therefore assumed to participate in larger, distributed cell assemblies, implying that in vivo recordings capture only a limited fraction of the full representation (Quiroga 2012; Quian Quiroga 2019; Quian Quiroga 2026). Despite these technical limitations, recent studies have begun to reveal population-level properties in human recordings (Courellis et al. 2024; Tacikowski et al. 2024; Cao et al. 2025), supporting the idea that memory relies on coordinated activity across neuronal populations. Consistent with this view, recent work in non-human primates has identified cell assemblies encoding memory content, with ensemble representations dynamically reorganized as a function of experience (novel versus familiar; (Abbaspoor et al. 2025), further suggesting that similar population-level mechanisms could operate in the human brain.

However, these findings also raise a fundamental problem: if memory representations are sparse (Chapter 1.III.1), and distributed across multiple brain regions within the MTL (Chapter 1.II.2) and beyond it (Chapter 1.II.3), how are they coordinated into coherent activity? Given the fast timescale of synaptic transmission and the delays imposed by long-range conduction, one influential proposal is that distributed neuronal ensembles are organized and coordinated by neural oscillations.

1.III.2 Neural oscillations and coordination mechanisms

1.III.2.a The hippocampus: a model to understand the fundamental properties of neural oscillations

Definitions: Neural oscillations are rhythmic fluctuations of neural activity that arise from the coordinated synaptic activity of neuronal populations and reflect the summed postsynaptic currents and subthreshold potentials generated by groups of neurons (Buzsáki et al. 2012). They were first described using scalp electroencephalography (EEG) recordings in humans (Berger 1929) and can now be measured across multiple spatial scales, from intracellular recordings of subthreshold membrane potentials (Harvey et al. 2009; Villette et al. 2019; Adam et al. 2019; Liao et al. 2024; Gonzalez et al. 2026) to indirect techniques such as magnetoencephalography (MEG). However, the method providing the highest combined spatial and temporal resolution for studying neural oscillations is extracellular recording of voltage fluctuations in the surrounding tissue, commonly referred to as local field potentials (LFPs). These signals are represented as time series reflecting the difference in electrical potential between a recording electrode in the region of interest and a reference electrode, and are described analytically in terms of their amplitude, frequency and phase. Several factors influence the signals that can be measured, including the anatomical organization of the neurons in the surrounding tissue (e.g., columnar, layered, nuclear; (Buzsáki et al. 2012; Lindén et al. 2011; Einevoll et al. 2013)), the spatial and temporal scale of the recorded activity (Katzner et al. 2009; Łęski et al. 2013), the types of neurons and local microcircuits involved (Reimann et al. 2013), the geometry and properties of the recording electrode (Einevoll et al. 2013), and the conductive properties of the extracellular medium (Bédard et al. 2004; Bédard and Destexhe 2011).

Gamma oscillations: A particularly clear demonstration of the fact that neural oscillations report the activity of different microcircuits comes from the study of gamma oscillations recorded from the mouse dorsal CA1 region. Gamma oscillations are fast rhythmic fluctuations of the LFPs, spanning frequencies between 30 and 150 Hz. While they were extensively described in the cat visual cortex, where synchronized gamma activity can be induced by specific visual stimuli (Gray et al. 1989; Fries et al. 1997), the dense recurrent connectivity of cortical circuits, combined with converging feedforward and feedback inputs across multiple visual areas, made it difficult to identify the precise pathways and microcircuits contributing to gamma generation. In contrast, gamma oscillations were also recorded in the dorsal CA1 region of the rodent hippocampus (Bragin et al. 1995a; Csicsvari et al. 2003; Colgin et al. 2009), whose anatomy and connectivity are well characterized. In the dorsal CA1, the main inputs project to distinct layers, making it possible to relate different gamma oscillations to specific neuronal pathways and local circuits (Lasztóczi and Klausberger 2014; Lasztóczi and Klausberger

2016; Fernández-Ruiz et al. 2021; Lopes-Dos-Santos et al. 2025). In this model, different microcircuits give rise to different gamma oscillations, which can be measured from various depths of the CA1: in the pyramidal layer, local recurrent interactions between pyramidal cells and perisomatic-targeting fast-spiking interneurons generate "fast-gamma" oscillations (100–150 Hz); in the lacunosum-moleculare, projections from the layer 3 entorhinal cortex neurons generate "mid-gamma" (60–100 Hz) oscillations; in the stratum radiatum, axonal projections from the hippocampal CA3 region generate "slow-gamma" (30–50 Hz) oscillations (Lopes-dos-Santos et al. 2018; Lopes-Dos-Santos et al. 2025). Even though they are separated by only a few hundred micrometers, these three hippocampal gamma oscillations are thought to reflect the activity of different networks and thus report different computations (Fernandez-Ruiz et al. 2023).

Theta oscillations: Another illustration of the importance of describing oscillations not only by their frequency content (Fernandez-Ruiz et al. 2023), but also by the behaviour and the networks from which they emerge, comes from the study of theta oscillations. Theta-band oscillations (5–12 Hz) were first described in the hippocampus of mammals as an "arousal reaction", primarily based on observations made in rabbits and cats (Green and Arduini 1954; Winson 1974). Other studies identified theta oscillations across a range of mammalian species, including rabbits (Jung and Kornmüller 1938; Klemm 1971; Harper 1971), cats (Maclean et al. 1955; Grastyan et al. 1959; Adey et al. 1960; Brown 1968; Sakai et al. 1973; Whishaw and Vanderwolf 1973; Kemp and Kaada 1975), guinea pigs (Liberson and Cadilhac 1953; Liberson and Akert 1955; Sainsbury and Montoya 1984), dogs (Shimazono et al. 1960; Arnolds et al. 1979a; Arnolds et al. 1979b) and rats (Buzsáki et al. 1983; Winson 1974; Kramis et al. 1975).

These findings refined the original concept of theta as a unitary “arousal reaction” by distinguishing two forms of theta activity. “Type 1” theta typically had a frequency of 7–12 Hz and was associated primarily with voluntary movement (Klemm 1971; Arnolds et al. 1979a; Arnolds et al. 1979b) whereas “type 2” theta had a frequency of 4–7 Hz and correlated more strongly with attentional and arousal-related states (Green and Arduini 1954). Species differences were also observed: dogs and guinea pigs more readily exhibited type 1 theta, whereas rabbits and cats more commonly displayed type 2 theta (Robinson 1980). Pharmacological studies further supported this distinction, demonstrating that type 1 theta is resistant to anticholinergic drugs, while type 2 theta is abolished by anticholinergic manipulation (Vanderwolf 1975; Sainsbury and Montoya 1984). These early results were complemented more recently with reports of theta oscillations in bats during echolocation but not voluntary movement (Ulanovsky and Moss 2007), in sheep during locomotion (Perentos et al. 2022) and in non-human primates during visual exploration (eye saccades) and spatial navigation (Jutras et al. 2013; Courellis et al. 2019; Mao et al. 2021). Theta oscillations were later linked to memory functions after influential studies in rats showed that theta disruption was associated with impaired memory performance (Winson 1978; Givens and Olton 1990; Mizumori et al. 1990).

One influential reinterpretation of these findings was proposed by Las and Ulanovsky, who argued that theta oscillations are not specifically linked to movement or arousal per se, but more generally to periods of active sensory acquisition (Derdikman and Knierim 2014). According to this view, theta emerges whenever an animal actively samples behaviourally relevant information from its environment, regardless of the sensory modality involved. This theory explains why theta accompanies olfaction and locomotion

in mice, echolocation in bats, locomotion in sheep and dogs, and visual exploration in primates and cats. More broadly, it suggests that understanding the function of theta oscillations requires considering how different species interact with their ecological niche. From this evolutionary perspective, cross-species comparisons provide a powerful approach for identifying conserved functions of neural oscillations, and in particular theta rhythms (Chapter 1.II.1). Consequently, a careful analysis of behaviour becomes essential for the characterization and interpretation of neural oscillations. This view also helps explain why theta oscillations are conserved during rapid eye movement (REM) sleep across species (Jouvet et al. 1959; Shimazono et al. 1960; Brown 1968; Jouvet 1969; Vanderwolf 1969; Sakai et al. 1973; Winson 1972; Buzsáki 2002), as this brain state shares several electrophysiological properties with exploratory behaviour, while relying predominantly on internally generated activity.

Moreover, these early studies set the ground for a brain-level, network investigation of neural oscillations, by investigating the brain regions connected with the hippocampus (Green and Arduini 1954) and involved in the generation of theta. Using electrical stimulation, lesions or pharmacological manipulations, these works showed that the medial septum (Petsche et al. 1962; Winson 1978; Freund and Antal 1988; Givens and Olton 1990; Mizumori et al. 1990; Vinogradova et al. 1993), the entorhinal cortex (Mitchell and Ranck 1980; Brankack et al. 1993; Bragin et al. 1995a), and brainstem nuclei (Macadar et al. 1974; Assaf and Miller 1978; Vertes 1982) (reviewed in (Vertes and Kocsis 1997)) are involved in the regulation of theta oscillations in the hippocampus. Together, these findings progressively shifted the field away from a localized view of theta generation toward the idea that theta emerges from distributed and state-dependent interactions across multiple interconnected brain regions (Buzsáki 2002). Because most of these studies were conducted in rodents, and theta oscillations are conserved across mammals, an important remaining question is whether similar networks regulate theta across the mammalian clade (Cisek 2019).

Sharp-wave ripples: A third important property of neural oscillations is that they can also emerge from internally generated network dynamics, independently of direct interactions with the external environment. This property is particularly well illustrated by sharp-wave ripples, which consist of large-amplitude deflections (sharp waves) coupled to fast oscillations (ripples) (Buzsáki et al. 1983; Buzsaki et al. 1992; Ylinen et al. 1995). We already encountered this principle in the context of REM sleep, during which theta oscillations can be recorded in the hippocampal LFPs despite the absence of external sensory cues. However, sharp-wave ripples provide an even clearer example of internally generated activity because they are predominant during slow-wave sleep, the behavioural state most strongly associated with sensory disconnection and with the highest arousal thresholds (Rechtschaffen et al. 1966; Bonnet et al. 1978; Neckelmann and Ursin 1993; Andrillon and Kouider 2020). During these events, neuronal assemblies active during previous experience are spontaneously reactivated, promoting memory consolidation (Wilson and McNaughton 1994) (Chapter 1.III.3).

Although sharp-wave ripples were classically described as a homogeneous network phenomenon resulting from synchronized CA3-to-CA1 inputs and local pyramidal-interneuron interaction (Buzsáki 2015), recent work revealed the existence of distinct ripple subtypes with different laminar current profiles (across the CA1-DG axis) and neuronal recruitment patterns (Castelli et al. 2025). In particular, ripples associated with current

sinks in the stratum radiatum differ from those associated with sinks in the stratum lacunosum-moleculare, likely reflecting different contributions from CA3 and entorhinal inputs (Lasztóczi and Klausberger 2014; Sebastian et al. 2023; Aleman-Zapata et al. 2025). This finding further illustrates that different oscillations reflect distinct microcircuits and network dynamics.

1.III.2.b Behavioural-state dependence of neural oscillations

Within a given brain region, the dominant oscillatory regime depends on the behavioural state of the subject. In the dorsal CA1 region of the rodent hippocampus, theta oscillations dominate the LFPs during exploratory behaviour (Brown 1968; Vanderwolf 1969; Sainsbury and Montoya 1984; Buzsáki 2002) and REM sleep (Jouvet 1969; Winson 1972; Buzsáki 2002), whereas during quiet wakefulness and non-REM sleep they are replaced by non-oscillatory, large irregular activity (LIA) associated with delta-frequency components (Buzsáki et al. 1983; Sainsbury et al. 1987; Buzsáki 1986; Ylinen et al. 1995). This state is characterized by the occurrence of sharp-wave ripples in CA1 and dentate spikes in the dentate gyrus (Bragin et al. 1995b), which are largely suppressed during wake and REM sleep. In contrast, gamma oscillations are more prominent during wake than during REM sleep (Montgomery et al. 2008).

These states are controlled in large part by septo-hippocampal inputs (Petsche et al. 1962; Freund and Antal 1988; Hangya et al. 2009; Fuhrmann et al. 2015; Király et al. 2023) and neuromodulators like acetylcholine (Vanderwolf 1975; Kramis et al. 1975; Sainsbury and Montoya 1984; Lee et al. 1994; Hasselmo 2006; Vandecasteele et al. 2014). During active states and REM sleep, septal inputs promote theta activity (type 2), with GABAergic septal neurons providing a rhythmic drive that organizes hippocampal theta, while cholinergic inputs increase network excitability and push the system toward theta and gamma rhythms. By contrast, during quiet wakefulness and non-REM sleep, lower cholinergic tone promotes large irregular activity and the emergence of sharp-wave ripples.

1.III.2.c Neural oscillations as coordination mechanisms

Microelectrodes allow the recording of neuronal action potentials, which appear as fast deflections in the LFPs and can be attributed to individual neurons using spike-sorting algorithms (Rey et al. 2015). Importantly, neuronal firing is not random but is temporally structured, occurring at specific phases of ongoing neural oscillations (Buzsáki et al. 1983; O'Keefe and Recce 1993). This phase-locking of spikes to oscillatory activity is particularly prominent in the rodent hippocampus, and provides strong evidence that the oscillations observed in LFPs recordings reflect genuine neural processes rather than recording artifacts (Fernandez-Ruiz et al. 2023). By defining alternating periods of high and low excitability, neural oscillations therefore regulate the timing of neuronal firing. For example, distinct interneuron classes and pyramidal neurons fire preferentially at different phases of theta oscillations (Klausberger et al. 2004; Klausberger and Somogyi 2008; Mizuseki et al. 2011; Masurkar et al. 2017; Navas-Olive et al. 2020; Masurkar et al. 2020), but also ripples (Valero and de la Prida 2018; Valero et al. 2015; Lopes-Dos-Santos et al. 2025), reflecting differences in their intrinsic properties, synaptic inputs, and connectivity. On one hand, oscillations increase the likelihood of coordinated firing between neurons,

thereby facilitating information transfer within neuronal assemblies (Markram et al. 1997; Singer and Gray 1995; Akam and Kullmann 2010; Buzsáki 2010). On the other hand, they constrain which neuronal populations can interact at a given time. In this way, oscillatory synchrony both facilitates communication between assemblies that are phase-aligned and functionally segregates those that are out of phase (Fries 2005; Akam and Kullmann 2010; Bastos et al. 2015), providing a temporal structure, or "neural syntax", for the coordination of neuronal activity (Buzsáki 2010).

However, this coordination is constrained by the biophysics of inter-neuronal communication. Conduction delays (propagation of action potentials) and synaptic integration are shorter within local circuits than across distant brain regions, placing limits on how quickly distributed neurons can interact (Buzsáki et al. 2013; Bastos et al. 2015). In addition, oscillations define temporal windows for synchronisation: fast oscillations provide narrow windows (on the order of 20 ms for gamma), whereas slower rhythms offer broader windows (around 100 ms for theta). This trade-off between conduction delays (space) and oscillatory timescales (time) leads to a functional organization in which fast oscillations preferentially synchronise local neuronal assemblies, while slower oscillations facilitate coordination across distributed brain networks (Kopell et al. 2000; Buzsaki 2004; Fries 2005; Łęski et al. 2013).

This multiscale organization can be revealed analytically by phase-amplitude coupling, which shows that short bursts of fast oscillations occur at specific phases of slower oscillations (Bragin et al. 1995a). In this configuration, slow oscillations define broad windows of excitability, within which fast oscillations promote precise spike synchrony within local neuronal populations. This hierarchical nesting allows local neuronal assemblies synchronized at fast timescales to be organized within slower oscillatory cycles, providing a temporal structure for the coordination of neuronal activity across multiple spatial and temporal scales (Buzsáki 2010; Lisman and Jensen 2013; Lopes-dos-Santos et al. 2018). By aligning these windows across regions, slow rhythms coordinate the timing of activity in distributed neuronal populations, linking separate assemblies into a coherent functional network (Fries 2005; Fell and Axmacher 2011). In this sense, communication between neuronal groups depends on their relative phase alignment, such that information is most efficiently "exchanged" when their activity is synchronised within shared periods of high excitability (communication through coherence, (Fries 2005; Fries 2009; Mizuseki et al. 2009; Bastos et al. 2015)). More generally, this nested oscillatory architecture provides a mechanism for temporal multiplexing, enabling multiple neuronal representations to be segregated, selectively routed, or sequentially organized within shared neural circuits (McLelland and VanRullen 2016).

These observations suggest that neural oscillations provide an efficient mechanism to link memory processes across scales. At the microscopic level, neuronal representations are supported by coordinated activity within cell assemblies, locally synchronized by fast oscillations, of which highly selective neurons such as place cells or concept cells likely represent a partial readout. At the macroscopic level, lesion and neuropsychological studies show that memory depends on distributed networks, particularly within the MTL, whose interactions must be dynamically coordinated. Oscillatory dynamics reconcile these levels by integrating local assemblies within larger, recurrent networks through slower oscillations that coordinate neuronal activity across brain regions. In the following section, I extend this mechanistic paradigm to demonstrate how memory relies on complementary

learning systems: "online" memory acquisition and retrieval during wake are supported by theta-gamma interactions, and "offline" reactivation during rest is mediated by sharp-wave ripples (Buzsáki 1989; Colgin 2016). This two-stage model enables the gradual integration of hippocampal and cortical representations, supported by memory consolidation.

1.III.3 Synthesis

1.III.3.a The two-stage model and the role of sleep in memory consolidation

One of the central questions in psychology and neuroscience is how memories can remain stable over long periods of time, even when they are formed after a single experience (Scoville and Milner 1957; D. Marr 1971; Squire and Alvarez 1995). This problem is closely related to how experiences are selected for long-term storage and how memories transition from short-term to long-term representations (Dudai 2004; Dudai et al. 2015). Repetition has long been proposed as one possible mechanism supporting memory stabilization (Chapter 1.I.1) (Ebbinghaus 1885). However, outside controlled laboratory settings, the same event is rarely experienced twice. Long-term memory formation therefore also requires the extraction of regularities across related experiences and the gradual generalization of knowledge (Chapter 1.I.1) (McClelland et al. 1995).

A major advance in understanding this process came from the study of offline states such as rest and sleep, which are known to play a critical role in memory consolidation (Jenkins and Dallenbach 1924; Karni et al. 1994; Plihal and Born 1997; Stickgold et al. 2000). The early two-stage model proposed by Buzsáki suggested that memories are initially encoded during active exploration and subsequently reactivated during offline states such as sleep (Buzsáki 1989). Building on this logic, the Complementary Learning Systems theory proposed that newly formed memories are initially encoded rapidly by the hippocampus and gradually integrated into distributed cortical networks through repeated reinstatement (during wake) and reactivation (during sleep) (McClelland et al. 1995; O'Reilly et al. 2014). Indeed, it was shown that patterns of neuronal activity formed in the mouse hippocampus during waking experience is reactivated during sleep (Wilson and McNaughton 1994) (actually published in the same journal issue as (Karni et al. 1994), (Girardeau and Lopes-dos-Santos 2021)), especially during sharp-wave ripples which support memory consolidation (O'Neill et al. 2008; Girardeau et al. 2009; Ego-Stengel and Wilson 2009; Dupret et al. 2010; Roux et al. 2017).

1.III.3.b Hippocampal indexing and distributed cell assemblies

A possible mechanistic implementation of the two-stage model (and the Complementary Learning Systems theory) is provided by hippocampal index theory, which proposes that the hippocampus stores sparse "indices" linking the distributed cortical representations of an experience (Teyler and DiScenna 1986; Teyler and Rudy 2007). Partial sensory or contextual cues then replay these hippocampal indices, leading to the reinstatement of the cortical representations specifically associated with a particular experience through pattern completion and pattern separation (D. Marr 1971; O'Reilly and McClelland 1994; Rolls 2013). A plausible biological substrate for these indices may be the distributed hippocampo-

cortical neuronal assemblies which have been described experimentally (Rothschild et al. 2017; Todorova and Zugaro 2019). According to this view, the hierarchical coordination of slow (global) and fast (local) oscillations during wake (theta-gamma (Lisman and Jensen 2013), or 4Hz-beta (Clarke-Williams et al. 2024)) provides a mechanism for the dynamic formation and reinstatement of these distributed assemblies (Chapter 1.III.2.c) (Jones and Wilson 2005; Siapas et al. 2005). The selection of specific assemblies further depends on neuromodulatory signals associated with salience, novelty, and increased arousal states during wake (Lisman and Grace 2005; Sara 2009; McNamara et al. 2014; Kempadoo et al. 2016; Takeuchi et al. 2016; Tsetsenis et al. 2023; Tsetsenis et al. 2021).

Reactivation of these distributed ensembles during sleep, particularly during hippocampal sharp-wave ripples but also during dentate gyrus spikes (Farrell et al. 2024; McHugh et al. 2024), therefore contributes to the selective strengthening (or weakening), updating, and long-term stabilization of distributed neuronal assemblies (Ji and Wilson 2007; Peyrache et al. 2009; Wierzynski et al. 2009; Maingret et al. 2016; Rothschild et al. 2017; Todorova and Zugaro 2019; Liu et al. 2021; Miyawaki and Mizuseki 2022; Harvey et al. 2023). Interestingly, recent evidence showed that different ripple-associated coactivity motifs support complementary operations during consolidation, with stable low-dimensional "core" motifs preserving pre-existing representations while denser "composite" motifs preferentially integrate recent waking experience into these pre-existing structures (Castelli et al. 2025). Such an organization may provide a mechanism for balancing the integration of new experiences with the preservation and gradual refinement of pre-existing schemas (Chapter 1.I.2.b). It could also account for the predictive and inferential properties of hippocampal reactivation, as ripple-associated activity can support inference beyond direct experience (Dragoi and Tonegawa 2011; Barron et al. 2020b; Igata et al. 2021) (Chapter 1.I.2.c). Mechanistically, this could occur by the binding of discrete elements of an experience during ripple-mediated reactivation (Barron et al. 2020b). According to this perspective, reactivation would not simply reproduce past events, but it would progressively refine internal representations by integrating recent experience into pre-existing structures (Chapter 1.I.2.d).

Taken together, these studies show that neural oscillations can be understood as a useful mechanism to link the large-scale brain networks identified by lesion and neuropsychological studies and the neuronal representations supported by coordinated cell assemblies. With a particular focus on the rodent hippocampus, I showed that oscillations are not defined solely by their frequency content or spectral characteristics, but should instead be understood as the readout of specific neuronal pathways and microcircuits, whose expression depends on behavioural state, neuromodulatory context, and ongoing computations (Fernandez-Ruiz et al. 2023). Their functional significance lies in their ability to coordinate neuronal activity across multiple spatial and temporal scales, from local cell assemblies to distributed brain networks.

In the next section, I will evaluate how these principles translate to the human brain by examining evidence from direct recordings of brain activity in human patients implanted with sEEG electrodes for diagnostic purposes. I will focus primarily on this method because it provides direct access to deep brain structures like the MTL, and is most comparable with studies of hippocampal physiology performed in rodents and other mammals. First, I will review evidence for theta oscillations in the human hippocampus (Chapter 1.IV.1), and then I will focus on ripples and neuronal reactivation (Chapter 1.IV.2).

1.IV Insights into memory mechanisms from human depth recordings

1.IV.1 Reviewing evidence for theta oscillations in humans

1.IV.1.a Theta oscillations during tasks

The first recordings from the human hippocampus during wakefulness were reported by Brazier et al., who described hippocampal LFP activity as being "almost entirely dominated by delta activity" in patients with epilepsy and schizophrenia (Brazier 1968; Brazier 1970). A few years later, however, Halgren et al. failed to identify hippocampal rhythmic slow activity (RSA) and instead reported desynchronized LFPs activity during voluntary movement and attentive states (Halgren et al. 1978). In parallel, Arnolds et al. observed slow-frequency activity around 3 Hz during "high-intensity" behaviours and verbal memory retrieval in a single participant (Arnolds et al. 1980). Similar findings were later reported by Huh et al. and Meador et al., who found increased delta-band power (1–3.75 Hz) together with decreased theta-band power (4–7.75 Hz) during visuospatial and verbal tasks compared to resting states (Huh et al. 1990; Meador et al. 1991). Together, these early studies suggested that slow-frequency activity predominates in human hippocampal LFP recordings.

The discovery of theta oscillations (5–12 Hz) in animal models strongly influenced subsequent efforts to identify a homologous rhythm in humans, often by focusing on frequency range. Theta-band oscillations were therefore reported in the human temporal neocortex during virtual navigation and working memory tasks (Kahana et al. 1999; Caplan et al. 2001; Raghavachari et al. 2001; Caplan et al. 2003; Rizzuto et al. 2003; Sederberg et al. 2003), and were proposed to correspond to rodent hippocampal theta (Kahana et al. 2001). While these studies played an important role in the development of human sEEG research and standardized cognitive paradigms (Kahana et al. 1999) (reviewed in (Kahana et al. 2001)), most were not based on recordings from the hippocampus or the MTL.

When focusing specifically on the hippocampus, several studies instead reported either no change or decreases in theta-band power during memory and navigation tasks (Fell et al. 2003; Axmacher et al. 2007; Sederberg et al. 2007; Burke et al. 2013; Long et al. 2014), or broader non-specific spectral changes (Jacobs et al. 2010). The influence of this frequency-band approach remained apparent in later studies, which continued to focus on the theta range despite often reporting stronger effects at slower frequencies (Ekstrom et al. 2005; Babiloni et al. 2009). Nevertheless, task-related modulation of slow-frequency oscillations during navigation and memory paradigms was replicated in several subsequent studies (van Vugt et al. 2010; Watrous et al. 2011; Lega et al. 2012; Clemens et al. 2013; Watrous et al. 2013), leading to the influential proposal that human theta oscillations may occur at slower frequencies than in rodents and other mammals studied so far (Jacobs 2014).

Despite these findings, subsequent studies reported highly heterogeneous associations between hippocampal slow oscillations and memory or navigation performance. Some studies reported increases in both "slow theta" (1–4 Hz) and "fast theta" power (5–12 Hz)

(Bohbot et al. 2017; Bush et al. 2017; Goyal et al. 2020; Stangl et al. 2021; Vivekananda et al. 2021; Li et al. 2022; Joensen et al. 2023; Seger et al. 2023), others reported increases only in "slow theta" power (Lin et al. 2017; Miller et al. 2018; Kota et al. 2020; Rudoler et al. 2023) or only in "fast theta" power (Solomon et al. 2019a; Gattas et al. 2023; Maoz et al. 2023; Seeber et al. 2025). In contrast, other studies found decreases in "slow theta" power (Crespo-García et al. 2016), decreases in "fast theta" power (Aghajan et al. 2017; Solomon et al. 2019b), or no significant task-related changes at all (Vass et al. 2016; Chen et al. 2018; Maidenbaum et al. 2018; Kragel et al. 2020; Costa et al. 2022; Saint Amour di Chanaz et al. 2023; Zheng et al. 2024). Overall, these results remain difficult to reconcile and currently provide no clear consensus on whether memory and navigation processes in humans are preferentially associated with "slow theta", "fast theta", or both, nor on the functional significance of these oscillatory changes.

1.IV.1.b Theta oscillations during REM sleep

Because epileptic seizures occur preferentially during sleep (Shouse et al. 1996; Herman et al. 2001; Ng and Pavlova 2013), the physiology and pathophysiology of sleep constitute a major part of the early sEEG literature. As theta oscillations are consistently observed during REM sleep across other mammals (Chapter 1.III.2), the presence of theta activity during human REM sleep represents an important criterion for identifying homologous oscillatory dynamics. Importantly, both epileptic seizures and interictal epileptiform discharges (IEDs) are strongly reduced during REM sleep, making this behavioural state relatively less confounded by epileptic activity.

The first studies reported the presence of slow oscillations between 2 and 5 Hz during REM sleep in patients with epilepsy and schizophrenia (Freemon and Walter 1970; Giaquinto 1973). Similar findings were reported nearly thirty years later by Bodizs et al., who described prominent 2 Hz oscillations recorded from foramen ovale electrodes during REM sleep, disappearing with bipolar referencing (Bódizs et al. 2001; Clemens et al. 2009). Consistent with these observations, Moroni et al. later reported increased delta-band power during REM sleep using sEEG recordings (Moroni et al. 2007). In contrast, Cantero et al. described a theta-band (4–8 Hz) oscillation in the human hippocampus during REM sleep (Cantero et al. 2003), leaving unresolved whether human REM sleep is primarily characterized by delta-range ("slow theta") or faster-frequency theta oscillations.

1.IV.1.c Modulation of gamma and spiking activity by hippocampal theta oscillations

In rodents, a defining property of hippocampal theta oscillations is the modulation of gamma activity and neuronal firing during navigation and memory tasks (Chapter 1.III.2.c). Similar mechanisms were also investigated in humans using sEEG recordings from the hippocampus and broader MTL.

The first studies reported transient rhinal-hippocampal synchronization during declarative memory formation (Fell et al. 2001; Fell et al. 2003), together with evidence that hippocampal gamma activity is modulated by the phase of slow-frequency oscillations (Mormann et al. 2005). However, the frequency ranges associated with these interactions

varied substantially across studies. Some described theta-gamma coupling in the "fast theta" range (Axmacher et al. 2010; Solomon et al. 2019b; Costa et al. 2022), whereas others identified coupling predominantly in slower frequencies around 2–5 Hz (Lega et al. 2016; Gattas et al. 2023). In some cases, both "slow" and "fast" theta bands were associated with gamma modulation (Vivekananda et al. 2021). Similar discrepancies were observed for inter-regional synchronization (Babiloni et al. 2009; Foster et al. 2013).

Single-neuron studies also reported heterogeneous results concerning the frequencies at which neuronal firing is coordinated. Jacobs et al. initially found that hippocampal neurons preferentially phase-lock to delta (1–4 Hz) oscillations rather than classical theta (Jacobs et al. 2007). Subsequent studies, however, described spike phase-locking to both "slow theta" and "fast theta" oscillations in the hippocampus and MTL (Rutishauser et al. 2010; Watrous et al. 2018; Schonhaut et al. 2024; Guth et al. 2024). Other studies reported phase coding within "slow theta" frequencies (Kunz et al. 2019), while others reported it in the "fast theta" range (Reddy et al. 2021; Saint Amour di Chanaz et al. 2023; Daume et al. 2024b). Overall, it remains unclear whether the coordination of gamma activity and neuronal firing in the human MTL is primarily related to "slow theta", "fast theta", or to multiple overlapping slow-frequency oscillations.

1.IV.2 Reviewing evidence for ripples and reactivation in humans

1.IV.2.a Detecting ripples in humans

The first observation of ripples in the human hippocampus described oscillatory events around 80 Hz that synchronized local neuronal firing during slow wave sleep or rest with eyes closed but not during active states (Bragin et al. 1999a). Given the matched behavioural-state dependence and coupling of local neuronal activity, these events were proposed to represent physiological oscillations homologous to those previously described in rodents, despite a reported slower central frequency (Buzsáki 1986; Buzsáki et al. 2013).

Interestingly, these events were recorded alongside faster oscillations termed "fast-ripples" (250–500 Hz), which were hypothesized to arise from the epileptic network (Bragin et al. 1999b). This distinction laid the foundation for an important field of research on fast-ripples (Bragin et al. 2002; Staba et al. 2002; Foffani et al. 2007; Valero et al. 2017), now considered as a potential biomarker of epilepsy (Liu et al. 2022). Epileptic networks also generate IEDs, which are prominent transient non-oscillatory events characteristic of irritative zones and can be recorded using sEEG as well as scalp EEG (Gotman and Gloor 1976; Henin et al. 2021; Maslarova et al. 2025). Because IEDs are high-amplitude transient events, they can generate spurious ripple-like detections when using linear filtering approaches if recordings are not carefully reviewed during preprocessing (Fig. 4.9) (Liu et al. 2022). Hence, because most direct recordings of hippocampal activity are obtained in patients with epilepsy, particular caution is required when detecting and interpreting ripple events.

1.IV.2.b Distinguishing ripples from gamma processes

Despite the initial description of ripples occurring specifically during offline states, further studies reported ripples during active states like encoding (Kunz et al. 2024) or recall (Norman et al. 2019; Vaz et al. 2019; Norman et al. 2021; Sakon and Kahana 2022), sometimes with identical (Dickey et al. 2022b; Dickey et al. 2022a) or higher rates than during rest or sleep (Axmacher et al. 2008). These findings differ markedly from observations in other mammals (Buzsáki et al. 2013). Ripples have also been reported during wake states in rodents (Foster and Wilson 2006; Karlsson and Frank 2009). Nonetheless, they occur mainly during disengaged states such as immobility or grooming, and remain less prevalent than during slow-wave sleep (Buzsáki 1986). In contrast, active exploration and memory-guided behaviour in rodents are typically associated with theta-gamma states (Bragin et al. 1995a; Colgin 2015), and gamma oscillations have been implicated in memory encoding and retrieval (Lopes-dos-Santos et al. 2018).

Several human studies similarly emphasized the role of gamma activity during memory tasks (Fell et al. 2001; Axmacher et al. 2007; Burke et al. 2013; Stevenson et al. 2018; Henin et al. 2019; Lin et al. 2019; Daume et al. 2024b). Importantly, the frequency ranges and analytical methods used to identify ripples and gamma activity substantially overlap, typically between 60 and 200 Hz. The main distinction is methodological: ripples are generally treated as discrete transient events, whereas gamma activity is analysed as a continuous process, often referred to as "broadband gamma" or "fast-frequency broadband". This conceptual overlap was highlighted by Tong et al., who reported that transient 80–120 Hz ripple events contribute to broadband fast-frequency activity and are associated with synchronized neuronal spiking in the human temporal cortex (Tong et al. 2021). Consequently, the distinction between ripples and gamma processes during active wake states remains unclear in the current human literature (Liu et al. 2022).

Interestingly, a recent study comparing ripples during wake and sleep reported that slow-wave sleep ripples occur more frequently, last longer, and have larger amplitude than wake ripples (Chen et al. 2021). Moreover, slow-wave sleep ripples, but not wake ripples, were nested within slower deflections resembling the sharp-waves described in rodents (Buzsáki 1986). Given the absence of a clear physiological distinction between ripples and gamma activity during active wake states in humans, the present thesis will follow the consensus established in rodents, distinguishing theta-gamma processes during active wake states from ripples during rest and sleep (Chapter 1.III.2.b).

1.IV.2.c Evidence for reactivation and memory consolidation

Direct human evidence for memory-related "reactivation" came mainly from active wake states. Single-neuron recordings showed that neurons activated during encoding could become active again during memory retrieval, suggesting content-specific reinstatement of memory traces (Gelbard-Sagiv et al. 2008; Jang et al. 2017; Vaz et al. 2020). In parallel, LFP-based studies showed that successful retrieval is accompanied by reinstatement of distributed oscillatory patterns present during encoding (Manning et al. 2011; Yaffe et al. 2014; Staresina et al. 2016; Pacheco Estefan et al. 2019). These studies therefore provide strong evidence that memory retrieval involves the reinstatement of encoding-related

neural activity patterns. However, according to current consensus terminology, such retrieval-related reinstatement represents an online, wake-state phenomenon and should be distinguished from offline memory reactivation, which occurs outside the context of overt retrieval and is thought to contribute to memory consolidation processes (Genzel et al. 2020).

A second line of work investigated reactivation during rest and sleep using sEEG. Jiang et al. identified large-scale cortical gamma motifs during waking and showed that similar motifs occurred more often during subsequent slow wave sleep than during preceding sleep (Jiang et al. 2017). Zhang et al. later used representational similarity analysis to track stimulus-specific gamma patterns during rest and sleep, showing that spontaneous reactivation occurred in both states, whereas ripple-triggered reactivation during slow wave sleep was specifically linked to later remembered items (Zhang et al. 2018b). More recent targeted memory reactivation studies similarly reported sleep reactivation associated with hippocampal ripples, cortical spindles, fast-frequency activity, and hippocampo-cortical coupling (Schreiner et al. 2024; Duan et al. 2025).

Importantly, this interpretation is supported by physiological studies showing that the sleep rhythms proposed to mediate hippocampo-cortical dialogue in rodents are also synchronised in humans. Direct hippocampal recordings demonstrated that ripples during sleep are nested within spindles and slow oscillations (Staresina et al. 2015). Subsequent studies further showed that hippocampal ripples are associated with increased hippocampo-neocortical spindle coupling, and that coupling between ripples, slow waves, and spindles engages distributed cortical and MTL activity during slow wave sleep (Helfrich et al. 2019; Ngo et al. 2020; Skelin et al. 2021; Staresina et al. 2023; Geva-Sagiv et al. 2023). These studies do not directly demonstrate content-specific reactivation, but they show that physiological processes required for a hippocampo-cortical consolidation dialogue are present in humans (reviewed in (Staresina 2024)). This provides confidence that rest/sleep reactivation may be mediated by analogous mechanisms to those described in rodents.

However, an important gap remains between single-neuron and LFP-based evidence. Studies of active wake states have shown single-neuron reinstatement during retrieval, whereas sleep and rest studies have mainly relied on LFP measures such as representational similarity analyses using gamma processes. Consequently, it remains unclear whether hippocampal ripples during offline states support the reactivation of behaviourally relevant single-neuron activity following a memory task in humans. The present thesis therefore aims to bridge this gap by examining the relationship between ripples and single-neuron reactivation during offline rest following memory-guided behaviour.

1.V Hypotheses and aims of this work

The previous introductory sections proposed a mechanistic account of memory that attempts to link observations obtained across multiple levels of investigation and research fields. Psychological theories emphasized the flexible and inferential nature of memory (Chapter 1.I), neuropsychological and lesion studies identified distributed brain systems supporting memory function (Chapter 1.II), while electrophysiological work in animal models revealed coordinated neuronal activity underlying memory representations (Chapter 1.III). Neural oscillations and the two-stage model of memory help unify these

experimental evidence into a coherent account grounded in neurobiology (Chapter 1.III.2). In this view, distributed neuronal assemblies are dynamically coordinated by oscillations across brain networks, generating experimentally testable hypotheses about how memory is acquired, consolidated and retrieved.

Current models of memory therefore propose a two-stage organization of learning and consolidation (Chapter 1.III.3). During wakefulness, memory acquisition and retrieval are associated with theta-gamma states, which support the online coordination of neuronal assemblies. During rest and sleep, these representations are reactivated in hippocampal sharp-wave ripples, promoting offline consolidation and the long-term integration of memory traces across distributed networks. Importantly, animal studies have shown that these oscillations cannot be defined solely by their frequency band, but must also be characterized by the behavioural states in which they occur and the neuronal networks and microcircuits from which they emerge (Chapter 1.III.2).

While this model is strongly supported in rodents, evidence for an equivalent two-stage organization in humans remains incomplete. In particular, the nature of human hippocampal theta oscillations remains unclear, including their frequency range, behavioural correlates, and physiological properties (Chapter 1.IV.1). Similarly, although indirect evidence suggests that memory reactivation could occur during human sleep and rest, direct evidence linking hippocampal ripples to the reactivation of behaviourally relevant single-neuron activity is still lacking (Chapter 1.IV.2).

To address these questions, the present thesis first investigates whether a putative homologue of theta oscillations can be identified in the human hippocampus. Based on observations in animal models, such an oscillation should satisfy several criteria: it should be present during wakefulness and associated with active, engaged states like memory acquisition and retrieval, organize local neuronal and gamma activity in the hippocampus, coordinate activity across connected MTL regions and be re-expressed during REM sleep. To test these predictions, we recorded hippocampal and MTL activity in human participants performing a relational memory task and during subsequent overnight sleep sessions.

After a brief methodological chapter describing the experimental procedures employed in this study (Chapter 2), in the first results chapter I will begin by analysing the behavioural performance of participants with epilepsy and paired controls in the relational memory task (Chapter 3). Then, I will characterize slow oscillations occurring in the human hippocampus during memory-guided behaviour by describing their physiological properties and behavioural correlates (Chapter 4). Next, I will quantify the interaction of these slow oscillations with neuronal firing and gamma oscillations locally and across the MTL (Chapter 5). Finally, I will evaluate whether these oscillations identified during wake are re-expressed during REM sleep (Chapter 6 and in particular Chapter 6.II.1).

The second objective of this work is to test whether hippocampal ripples support the reactivation of learning-related neuronal activity in humans. To address this question, in the last chapter I will begin with the characterization of hippocampal ripples during rest and sleep, and compare their physiological properties across behavioural states (Chapter 6.II.2). Then, I will examine whether neuronal coactivity motifs expressed during online active states reappear during subsequent offline ripples, and whether this reactivation is related to behavioural performance (Chapter 6.III).

Together, these experiments aim to test whether the principles of the two-stage model described in animal studies extend to the human hippocampal system.

2 Materials and Methods: Experimental procedures

"Les faits et les artefacts ne correspondent pas respectivement à des énoncés vrais et faux.
Les énoncés se situent plutôt le long d'un continuum,
selon le degré auquel ils renvoient aux conditions de leur construction."

"Facts and artefacts do not correspond respectively to true and false statements.
Rather, statements lie along a continuum
according to the extent to which they refer to the conditions of their construction."

— Bruno Latour and Steve Woolgar, Laboratory Life (1979)

Contents

2.I Neurophysiological recordings 49
2.I.1 Data acquisition and preprocessing 49
2.I.2 Spike sorting and single-unit analyses 53
2.I.3 Automated pipeline and quality criteria 53
2.II Analysis of local field potentials 60
2.II.1 Detection of IEDs 60
2.II.2 Decomposing LFPs into oscillatory components 60
2.II.3 Other spectral decompositions 62
2.II.4 Quantification of ERPs 64
2.II.5 Cross-frequency analyses 65
2.III Ripples and reactivation 71
2.III.1 Ripple detection and validation 71
2.III.2 Detection of cross-regional coactivity motifs 75
2.III.3 Reactivation of coactivity motifs in hippocampal ripples 75
2.IV Statistical analyses 76

2.I Neurophysiological recordings

2.I.1 Data acquisition and preprocessing

2.I.1.a Participants

This study included forty-three adult participants [mean age (interquartile range): 35 (25–42) years; 20 males, 23 females; 34 right-handed] undergoing sEEG monitoring for pharmacologically intractable epilepsy. Participants were recruited from the Epilepsy and Sleep Unit of the Neurology Department at Toulouse University Hospital (Toulouse, France; n = 29) and from the Epilepsy and EEG Units at Pitié-Salpêtrière Hospital (Paris, France; n = 14). These patients underwent sEEG with multi-contact depth electrodes over 7–10 days to localize seizure foci. Electrode placement followed clinical requirements and pre-surgical trajectories determined from individual structural MRI scans.

Moreover, twenty-nine additional participants completed the relational memory task (Chapter 3.II.2.b), and formed the control cohort for behavioural analyses (Dataset 2, Fig. 2.1). Inclusion criteria for this cohort were: age between 18 and 63 years, fluency in French, absence of neurological history likely to affect memory, and normal or corrected-to-normal vision. The primary aim in recruitment was achieving matching with the epilepsy cohort in terms of age and educational level. A matched study design was therefore employed. Control participants were selected based on age and level of education to closely correspond to those of the epilepsy cohort. To facilitate recruitment, a limited age tolerance was allowed. On average, control participants were approximately nine months older than the epilepsy cohort.

All participants provided informed consent in accordance with procedures approved by the relevant institutional review boards.

2.I.1.b Behavioural datasets

Thirty-five participants (n = 21 in Toulouse; n = 14 in Paris) performed the computer-based relational memory task. For behavioural analyses, we selected the twenty-nine participants who matched the control cohort in terms of age and educational level, by using the Hungarian optimization algorithm (Kuhn 1955) (Dataset 1, Fig. 2.1). For neurophysiological analyses, we selected twenty-seven participants with electrode contacts in the hippocampus and who engaged in the same version of the memory task (Dataset 4, Fig. 2.1). Indeed, among the thirty-five original participants, six subjects did not have electrodes targeting the hippocampus, and two subjects performed a task which did not include the 2-second delay between cue and question onsets (see Fig. 3.1 and Chapter 3.II.1 for details on the task). A schematic summarizing the five datasets used in this study is provided in Fig. 2.1.

We further validated the network physiology identified in the awake human hippocampus during the relational memory task by examining data from eight additional awake participants who were watching a sitcom series (Friends), and were instructed to maintain attention throughout each episode (Dataset 3, Fig. 2.1; 25 minutes per episode). A member of the team continuously monitored participants' vigilance to ensure sustained attention.

To further validate our ripple detection algorithm used during rest sessions of the relational memory task, we also characterized oscillatory patterns expressed during overnight sleep in seven of the participants recruited to do the memory task in Paris and

who had electrodes targeting the hippocampus (Dataset 5, Fig. 2.1). These participants were recorded continuously for 24 hours including overnight sleep. Sleep staging was performed according to American Academy of Sleep Medicine guidelines (Troester et al. 2023). N2 and N3 stages were merged and referred to as slow-wave sleep (SWS) throughout the manuscript.

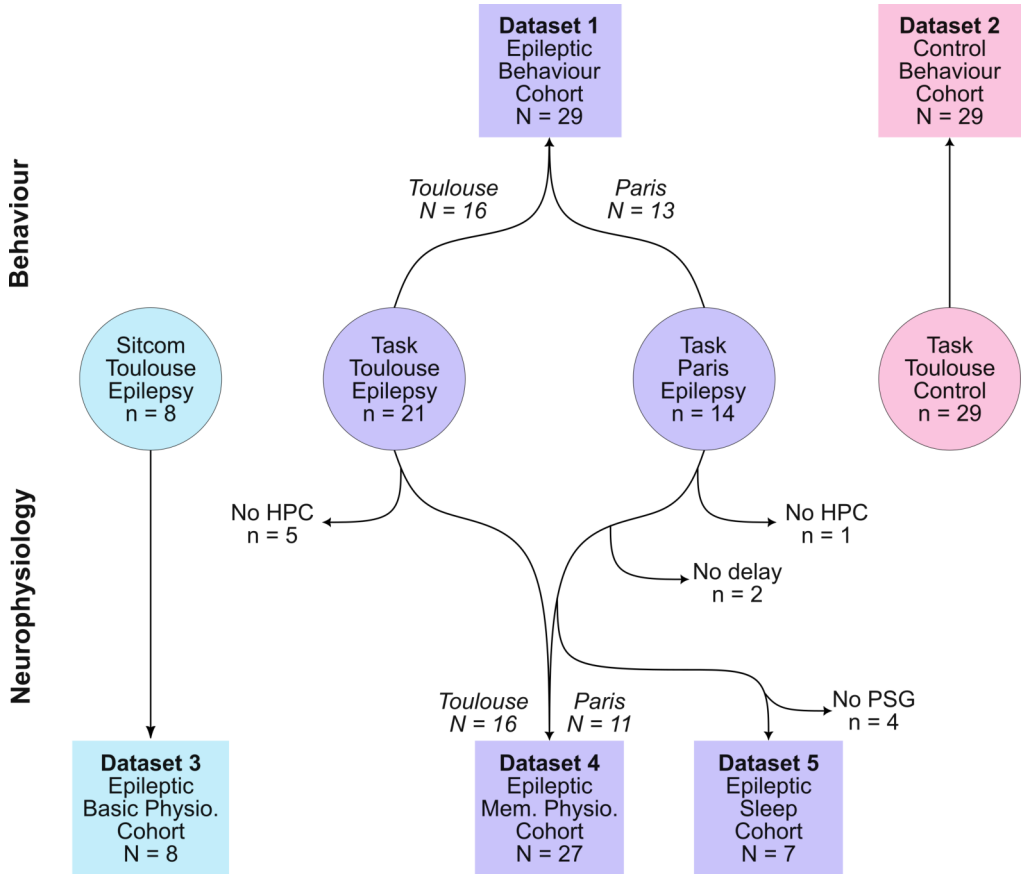


Figure 2.1: **Datasets used in this study.** coloured circles indicate original data sources, and coloured squares indicate the five final datasets included in this study. Datasets 1 and 2 comprised participants with epilepsy and paired-controls, respectively, matched for age and educational level, and were used for behavioural analyses (Chapter 3). Dataset 3 included participants with epilepsy who viewed the sitcom series and was used for basic physiological analyses (Chapter 5). Dataset 4 constituted the core dataset for physiological analyses and included participants with epilepsy who performed the relational memory task (Chapter 4, Chapter 5 and Chapter 6). Dataset 5 included participants with epilepsy who completed the relational memory task in Paris and additionally underwent full-night polysomnography for sleep physiology analyses (Chapter 6). "No HPC" denotes participants without electrodes targeting the hippocampus. "No delay" denotes participants who performed the relational memory task without the imposed delay between the cue and type 2 memory questions (Chapter 3.II.1 for details on the task); this delay was required for the analysis of evoked oscillations. "No PSG" denotes participants from the Paris dataset for whom overnight polysomnography data were unavailable. "Physio." refers to physiology, and "Mem." refers to the memory task.

2.I.1.c Electrode models

Participants were implanted with standard and hybrid depth electrodes. In Toulouse, hybrid electrodes (DIXI Medical ®; maximum of six electrodes per subject; platinium/iridium, 2 mm in length, 0.8 mm in diameter) comprised 5–18 macrocontacts and were equipped with two or three tetrodes (tungsten wires, 20 γm in diameter), as described in (Despouy et al. 2020). Tetrodes typically protruded between the two deepest macrocontacts on each electrode (Fig. 4.1B). However, in few hybrid electrodes, they extended between the eighth and the ninth macrocontacts to sample more superficial regions. These particular electrode models were occasionally employed to record neurons in the temporal cortices (Fig. 5.15, bottom row). The exact model of all electrodes employed in this study is presented in Table 2.1 below. The reference for both tetrodes and macrocontacts was a macrocontact located in white matter. In Paris, hybrid electrodes contained 9 macrocontacts (3 mm spacing between contact 1 and 2, and 4.5 mm for the others) and eight microwires (Behnke-Fried electrodes, Ad-Tech Medical; maximum of two electrodes per subject), with one additional microwire used as a reference. Standard electrodes had 5 mm spacing between contacts.

Electrode type	**Manufacturer**	**Models**
DIXI electrodes / Microdeep® Micro-macro electrodes (Toulouse)	DIXI Medical®	MM08-09A33D08; MM08-09A40D08; MM08-09A51D08; MM08-06B33D12; MM08-06B40D12; MM08-06B51D12; MM08-06B40P12 (superficial tetrodes); MM08-06B33P12 (superficial tetrodes)
Behnke-Fried electrodes / Macro electrodes (Paris)	Ad-Tech® Medical	SD04R-SP05X-000; SD06R-SP05X-000; SD08R-SP05X-000; SD10R-SP05X-000; SD12R-SP05X-000; BF09R-SP61X-0BB; WB09R-SP00X-014

Table 2.1: Electrode models used in the Toulouse and Paris cohorts.

2.I.1.d Co-registration and anatomical verification of the contacts

The anatomical location of each macrocontact was determined by co-registering post-operative computed tomography (CT) scans with preoperative 3D T1-weighted MRI data. Preoperative T1 3T MRI images were automatically segmented in the native space (using FreeSurfer, $https://surfer.nmr.mgh.harvard.edu/$), and the anatomical location of each electrode macrocontact was then detected on the CT scans and positioned in the Desikan-Killiani atlas (Desikan et al. 2006). The location of all gray matter contacts and Behnke-Fried microwire bundles were further verified by an expert clinician. Each tetrode was assigned the anatomical label of the nearest macrocontact. To localize macrocontacts within the hippocampal volume, each macrocontact was assigned a standardized anatomical position based on individual hippocampal geometry. Hippocampal volumes were segmented from native T1-weighted MRI scans, and segmentation quality was manually verified. For each validated volume, anterior-posterior and medial-lateral axes were defined

and normalized (-1 to +1, see Fig. 4.2B), allowing macrocontacts to be projected onto these axes and expressed as standardized two-dimensional hippocampal coordinates. All contact coordinates were then normalized in the Montreal Neurological Institute (MNI) space for group-level analyses and visualizations. Hippocampal macrocontacts with y-axis coordinates < -22 in the MNI space were considered posterior.

2.I.1.e Neurophysiological recordings

Electrophysiological signals were recorded continuously for approximately one hour while participants performed the behavioural task, using an ATLAS 16SX 256-channel Neuralynx system (Toulouse) and ATLAS 16SX 256-channel Neuralynx system (Paris) (Datasets 1, 3 and 4, Fig. 2.1). For overnight sleep recordings (Dataset 5, Fig. 2.1), additional surface electrodes were also used according to the 10–20 system alongside electrooculography and electromyography electrodes for polysomnography (Troester et al. 2023). The signal was primarily acquired using a distal white matter contact as the reference (monopolar referencing), and a skull contact as the ground (Fig. 2.2A). To minimize contamination from 50 Hz line noise during data acquisition, we shielded the electrode cables with a conductive fabric (YSHIELD® SILVER-ELASTIC) connected via a skin electrode (Fig. 2.2B-E) and which proved very efficient in improving data quality (Lehongre et al. 2022). Data were filtered between 0.1 and 8,000 Hz and sampled at 32,768 Hz, then downsampled to 20,000 Hz and 1,250 Hz for subsequent analyses of ensemble spiking and neural oscillations, respectively. Macrocontact and microelectrode signals were visually inspected to exclude artifactual channels. In total, 2,667 macrocontacts were retained (99 ± 24 per subject). A common-average referencing was next applied to macrocontact data (using the median to minimize the potential influence of large-amplitude events including IEDs) but not to microelectrode recordings. Where mentioned in the manuscript, bipolar referencing was occasionally used for control analyses and is referred to as "local referencing" (e.g., Fig. 4.11 and Fig. 2.3). Line noise at 50 Hz was minimal under the recording conditions; consequently, notch filtering was never applied. Synchronization between stimulus events (e.g., photographic presentations) and neural recordings was achieved via TTL pulses, with each event type assigned a unique TTL identification code. Throughout the manuscript, LFPs refer to sEEG signals recorded from macrocontacts, except in Fig. 4.4, Fig. 4.11, Fig. 6.8 and Fig. 2.5 where tetrode LFPs were used. LFPs from microwires (Behnke-Fried electrodes) are not used in this study be cause local referencing was employed for initial acquisition of the signal. Consequently, Behnke-Fried electrodes are not displayed in the figures of this thesis.

2.I.2 Spike sorting and single-unit analyses

2.I.3 Automated pipeline and quality criteria

Spike sorting and unit isolation were performed with an automated clustering pipeline using Kilosort ($https://github.com/cortex-lab/KiloSort$) via the SpikeForest and SpikeInterface frameworks ($https://github.com/flatironinstitute/spikeforest$) (Magland et al. 2020; Buccino et al. 2020), as previously used in rodent studies (Gava et al. 2024; Lopes-Dos-Santos et al. 2025). For this, the algorithm restricted templates to channels

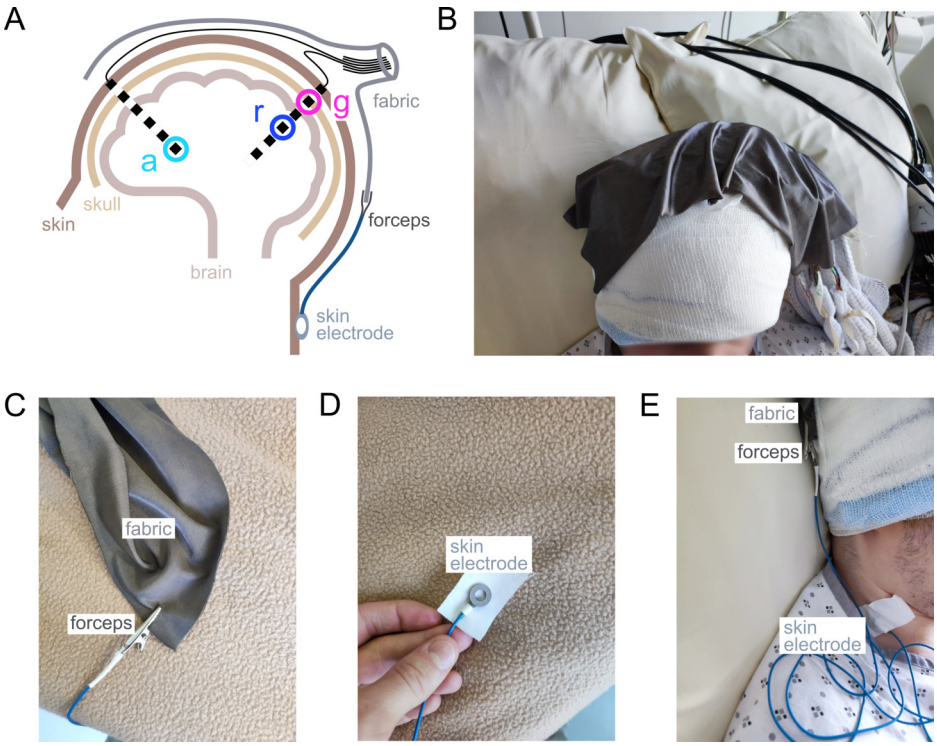


Figure 2.2: **Recording setup and conductive fabric.** (**A**) Schematic of the monopolar recording used for initial acquisition of the data. The acquisition electrode (a, light blue, macrocontact or tetrode) was referenced to a distal white matter macrocontact (r, dark blue), and grounded using a contact located in the skull (g, pink). To improve signal quality by minimizing line noise contamination, a conductive fabric was used to cover the electrode cables, which was connected via a forceps and a skin electrode. (**B**–**E**) Photographs representing the shielding scheme using the conductive fabric, forceps and skin electrode.

within a given microelectrode while masking all other recording channels. All sessions recorded contiguously on a given day were concatenated and cluster cut together to monitor cells throughout the experiment. The resulting clusters were verified by the operator using cross-channel spike waveforms, auto-correlation histograms, and cross-correlation histograms. Each unit used for analyses showed throughout the entire recording day stable spike waveforms, clear refractory period in their auto-correlation histogram, and absence of refractory period in its cross-correlation histograms with the other units. All analyses were performed on these single units. In total, 257 single units were identified in the MTL, of which 211 in the hippocampus (Fig. 5.1). All hippocampal single-units analysed in this manuscript were detected using tetrodes (from n = 18 human participants out of the 24 recruited in Toulouse). This decision was made to ensure that hippocampal neurons were located close to the macrocontacts used for LFPs extraction (e.g., to detect the phase of local oscillations, see the model of the hybrid electrode in Fig. 4.1B). In the extra-hippocampal MTL, 39 single units were detected with tetrodes, and 7 using microwires (Behnke-Fried electrodes).

2.I.3.a Identification of putative pyramidal neurons and interneurons

Putative pyramidal neurons (pPYR) and interneurons (pINT) were distinguished based on spike waveform features extracted from individual hippocampal units. To improve resolution, the 32 waveform points sampled at 20 kHz were upsampled by a factor of 100 using quadratic interpolation (via the interpolate function from scipy). For each neuron, trough-to-peak latency and peak amplitude asymmetry were computed from the average normalized spike waveform. Trough-to-peak latency was defined as the time interval between the negative trough and the subsequent positive peak of the waveform. Peak amplitude asymmetry was quantified as (b-a)/(b+a), where a and b correspond to the amplitudes of the pre- and post-trough positive peaks (also named "shoulders" of the spike waveform), respectively (Fig. 5.3E). Clustering was performed using a Gaussian mixture model (two components) applied to the joint distribution of trough-to-peak latency and peak amplitude asymmetry. Clusters were interpreted as putative pyramidal neurons (pPYR; broad spikes) and putative interneurons (pINT; narrow spikes).

2.I.3.b Spike-field relationship

PPC and phase randomization: To assess the relationship between spike timing and the phase of slower oscillations, we computed the pairwise-phase consistency (PPC) as in (Vinck et al. 2010). Spike trains were either taken from neurons located in the same region as the phase (local PPC, nearest macrocontact; Fig. 5.3) or from a distal region (distal PPC, across structures; Fig. 5.16). For each neuron, we extracted the instantaneous phase of the IMF (e.g., 2-Hz) at the time of spike occurrence. Given a set of N spike times, each associated with a phase value $\phi_n \in [0, 2\pi]$ the PPC is computed as:

$$\mathrm{PPC}_0 = \frac{2}{N(N-1)} \sum_{i=1}^{N} \sum_{j=i+1}^{N} \cos(\phi_i - \phi_j) \tag{2.1}$$

This expression corresponds to the average cosine of the phase differences between

all unique spike pairs. It can also be reformulated for computational efficiency using trigonometric identities:

$$\mathrm{PPC}_0 = \frac{2}{N(N-1)} \sum_{i=1}^{N} \sum_{j=i+1}^{N} \Big[\cos(\phi_i)\cos(\phi_j) + \sin(\phi_i)\sin(\phi_j)\Big] \tag{2.2}$$

The PPC value ranges from -1/(N-1) to 1; it is centred around 0 for uniformly distributed phases; 1 indicates perfect phase locking; and can take negative values due to finite-sample variability or phase configurations dominated by large pairwise phase differences. To determine whether the observed spike-phase coupling was statistically significant, we used the same phase randomization followed by z-scoring procedure described in 2.II.5 for PAC. Specifically, we generated 300 surrogate phase signals by shuffling the phase time series and recomputed the PPC between each surrogate phase and the spike times. This yielded a null distribution, against which the PPC computed from the original phase signal was z-scored. This z-scored PPC reflects the likelihood of spike-phase locking beyond chance and was used for statistical testing across IMFs and neuronal units (Fig. 5.3A,B and Fig. 5.16A,B). A z-score threshold of 2 or 5 (when mentioned) was used to identify significant coupling (Fig. 5.3C). Preference was then measured by comparing, for each neuron, which of the three oscillations (1-, 2-, or 6-Hz) had the highest z-scored PPC value, only considering neurons with at least one significant locking in these frequency bands (Fig. 5.3D and Fig. 5.16C). PPC was measured on epochs clear from interictal discharges.

Example phase preference at 2 Hz between pPYR and pINT recorded from the same tetrode are represented in Fig. 5.3F. For each tetrode containing both pPYR and pINT units, PPC at 2 Hz was averaged within each class (pPYR or pINT), and these values were compared between classes using paired statistics (Fig. 5.3G).

Spike-gamma relationship: Single-neuron spiking activity is tightly locked to gamma oscillations in rodents (Fernandez-Ruiz et al. 2023). Likewise, studies in humans also reported that gamma-band activity correlated with single-neuron spike trains (Manning et al. 2009; Miller 2010; Watson et al. 2018). To verify that this was also the case in our dataset, we leveraged the unique shape of our hybrid electrodes with tetrodes protruding between the two deepest macrocontacts (Fig. 4.1B). This electrode model allowed us to investigate the relationship between single-neuron activity and either median- or bipolar-referenced gamma activity (Fig. 2.3A). To assess the temporal coupling between local neuronal firing and gamma activity, we computed time-lagged cross-correlations between population rate and gamma activity. For each recording session, we retained hybrid electrodes with at least five recorded neurons. Population rate was obtained by summing spike trains from all single-units recorded within the same region and temporally smoothing the resulting spike-rate vector with a Gaussian kernel (width = 50 ms, σ = 25 ms). For each region, Pearson correlation coefficients were computed between the population rate and each local gamma trace across contiguous, IED-free epochs. To evaluate specificity, the same population rate signal was correlated with gamma envelopes from distal macrocontacts located on other electrode shafts. Mean correlation coefficients across distal contacts were used as controls (Fig. 2.3B-G). Population firing rate was better correlated with gamma activity patterns recorded on the local macrocontact than the distal ones for median referenced (Fig. 2.3C,D) and bipolar-referenced signals

(Fig. 2.3F,G). Note that neuronal spikes could not be recorded from the macrocontacts (Fig. 2.3H). Interestingly, the correlation with local gamma activity was not different between bipolar-referenced signal and median-referenced signal (Fig. 2.3I,J).

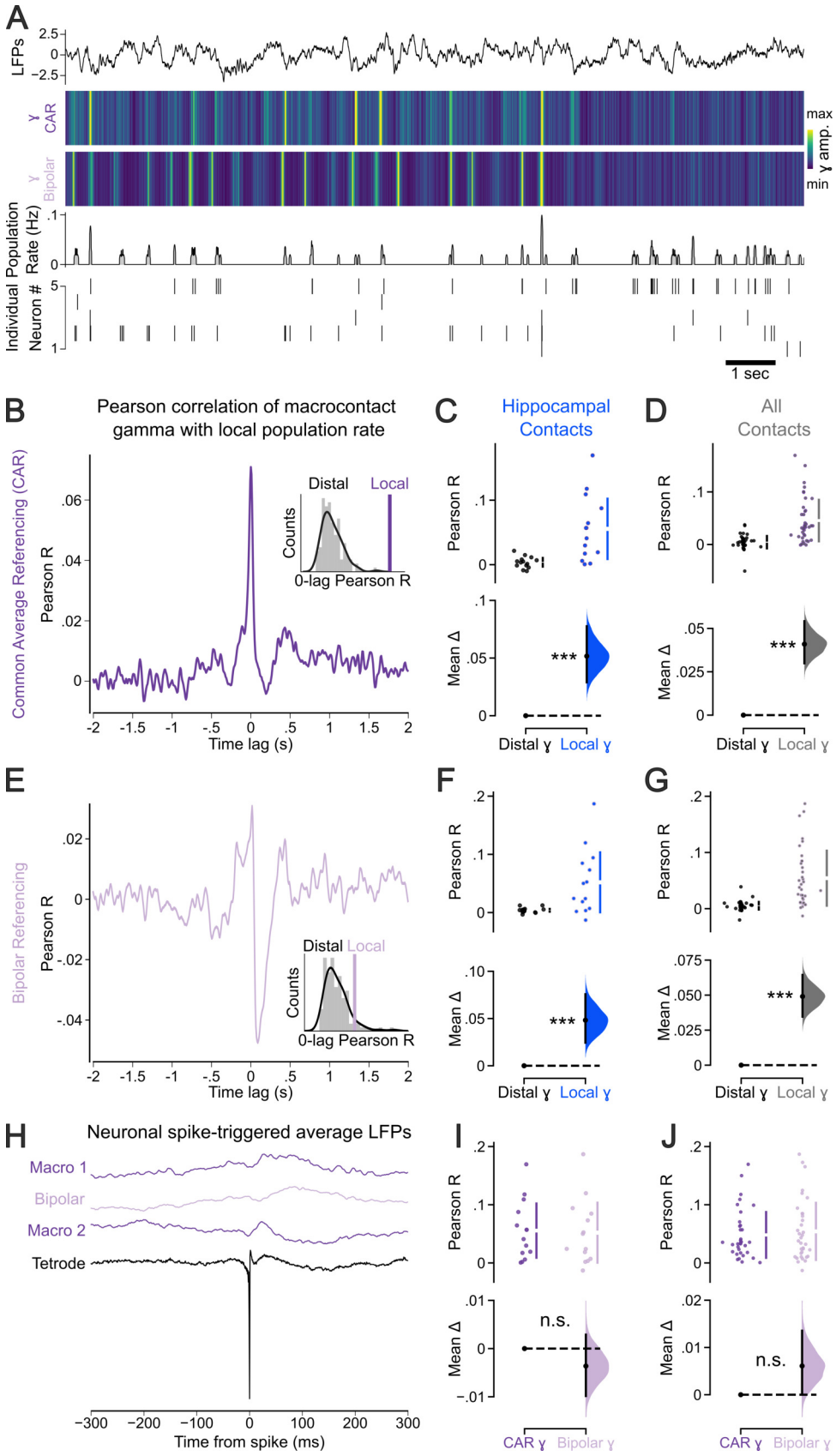

A
LFPs
2.5
0
−2.5
γ CAR
γ Bipolar
max
γ amp.
min
Individual Population Rate (Hz)
.1
0
Neuron #
5
1
1 sec
B
Pearson correlation of macrocontact gamma with local population rate
Common Average Referencing (CAR)
Pearson R
.06
.04
.02
0
Distal
Local
Counts
0-lag Pearson R
-2
-1.5
-1
-.5
0
.5
1
1.5
2
Time lag (s)
C
Hippocampal Contacts
Pearson R
.1
0
Mean Δ
.1
.05
0
***
Distal γ
Local γ
D
All Contacts
Pearson R
.1
0
Mean Δ
.05
.025
0
***
Distal γ
Local γ
E
Bipolar Referencing
Pearson R
.02
0
-.02
-.04
Distal
Local
Counts
0-lag Pearson R
-2
-1.5
-1
-.5
0
.5
1
1.5
2
Time lag (s)
F
Pearson R
.2
.1
0
Mean Δ
.10
.05
0
***
Distal γ
Local γ
G
Pearson R
.2
.1
0
Mean Δ
.075
.050
.025
0
***
Distal γ
Local γ
H
Neuronal spike-triggered average LFPs
Macro 1
Bipolar
Macro 2
Tetrode
−300
−200
−100
0
100
200
300
Time from spike (ms)
I
Pearson R
.2
.1
0
Mean Δ
.01
0
−.01
n.s.
CAR γ
Bipolar γ
J
Pearson R
.2
.1
0
Mean Δ
.02
.01
0
n.s.
CAR γ
Bipolar γ

Figure 2.3: **Correlation between gamma envelopes and spiking activity.** (**A**) Example 10-s recording showing median-referenced LFPs, gamma activity patterns extracted from median- or bipolar-referenced macrocontact signals, and a raster plot of five local neuronal spike trains with the corresponding population firing rate. (**B**) Time-lagged correlation (±2 seconds, 8-ms steps) between population rate and local gamma activity extracted from median-referenced hippocampal signals. Inset: instantaneous (0-lag) correlation between local population rate and gamma activity recorded from distal (gray distribution) or local (purple bar) macrocontacts. (**C** and **D**) Estimation plots showing mean differences in instantaneous correlations between local and distal macrocontacts in the hippocampus (C) and across brain regions (D). (**E** and **F**) Same analyses as in (B–D) for bipolar-referenced signals. (**H**) Average LFPs from median- (purple) or bipolar- (pink) referenced signals aligned to neuronal spikes on the local tetrode, confirming that no neuronal spike or artifact appears on macrocontacts. (**I** and **J**) Estimation plots showing mean differences between correlations of population rate and bipolar- versus median-referenced signals in the hippocampus (I) and across brain regions (J). Only neurons detected from tetrodes were used for these analyses. Data were analysed by two-sided paired permutation tests; ***P < 0.001; n.s., not significant.

2.II Analysis of local field potentials

2.II.1 Detection of IEDs

We detected IEDs recorded in our datasets using an envelope-based, data-driven algorithm adapted from Janca et al. (Janca et al. 2015). The continuous LFP traces were downsampled to 200 Hz and band-pass filtered (Chebyshev type-II high-pass 10 Hz and low-pass 60 Hz, stopband attenuation 30 dB). The analytic envelope (Hilbert) was computed and scanned with overlapping 5-s windows stepped by 1 second. Within each window, the envelope distribution was modeled by a log-normal function, and events were detected when the signal amplitude exceeded three times the typical (mode + median) level estimated from that distribution. This adaptive thresholding identifies transient amplitude outliers that deviate from the typical background activity. Window thresholds were cubic-spline interpolated to sample resolution and boxcar-smoothed, and contiguous supra-threshold samples were grouped into events. Nearby events were merged by extending boundaries by ±120 ms and the envelope peak within each merged window was taken as the IED time. All detections were produced on the downsampled signal and indices were mapped back to the native sampling rate for downstream analyses. Examples of detected events are shown in Fig. 4.9. Macrocontacts showing an average detection rate below one IED per minute during active sessions were considered free of epileptiform activity.

To characterize spectral and LFPs dynamics around IEDs (Fig. 4.9C,D), we computed IED-triggered averages of LFPs and time-frequency spectrograms. For each macrocontact containing at least five IED per minute, ±1 second of signal surrounding each detected IED peak was extracted and averaged across events. The corresponding time-frequency spectrograms were computed using Morlet wavelets (1–150 Hz, logarithmic spacing). To show absolute amplitude changes around IEDs (Fig. 4.9D, left panel), raw spectral amplitude was averaged. Finally, to reveal the relative modulation in oscillatory amplitude associated with IED activity, the amplitude at each frequency was z-scored across time before averaging (Fig. 4.9D, right panel).

2.II.2 Decomposing LFPs into oscillatory components

2.II.2.a Tailored Masked Empirical Mode Decomposition

To decompose the LFPs into their elementary oscillatory components, or intrinsic mode functions (IMFs), we applied tailored-masked EMD (tmEMD) (Clarke-Williams 2022; Clarke-Williams et al. 2024). Empirical mode decomposition (EMD) is an unsupervised, iterative sifting algorithm that extracts signal components based on local time-frequency properties. Masked EMD (mEMD) enhances this process by introducing a mask signal at each sifting step to reduce mode mixing and thus improve the separation of IMFs. The tailored variant of mEMD was developed to minimize mode mixing, increasing consistency across recordings from different subjects and electrode contacts. Using the macrocontacts located in the anatomical region of interest (e.g., hippocampus in Fig. 4.3; superior temporal cortex in Fig. 5.12), we applied the tmEMD procedure to LFPs recordings using

two steps.

The first step allowed us to assess the epochs to be analysed and optimizing the masks. For each signal, we used two 45-second LFPs epochs free of IEDs and with high signal-to-noise ratio. To quantify signal-to-noise ratio for a given epoch, we computed the Welch power spectral density (PSD) and calculated the power ratio between 1–20 Hz and >200 Hz. Mask frequencies were optimized by pooling the identified clean epochs across macrocontacts and applying tmEMD to identify mask parameters that maximize consistency and minimize mode mixing.

The second step performed the full-session decomposition using optimized masks: once optimal masks were identified, we applied mEMD to the full recording session. Instantaneous amplitude, frequency, and phase were then obtained using the Hilbert transform. IMF consistency was assessed by computing the PSDs of each IMF in IED-free epochs (Fig. 4.3B and Fig. 5.12B). To characterize the frequency band of each IMF, we computed its PSD using Welch's method and averaged the resulting spectra across all macrocontacts (Fig. 4.3C and Fig. 5.12C, thick lines). For each IMF, the peak frequency was defined as the frequency of maximum power, and the frequency band was determined as the contiguous band containing 80% of the total spectral power (i.e., 80% power band).

2.II.2.b Cycle detection and quality control

To segment individual oscillatory cycles from each IMF, we identified four key waveform features: troughs (local minima), peaks (local maxima), ascending and descending zero-crossings. Cycles were defined as sequences of six temporally ordered points: two consecutive troughs (or alternatively, two peaks, or two zero-crossings), and four intermediate landmarks corresponding to characteristic inflection points within the waveform (e.g., zero-crossings and extrema) (Fig. 2.4). Each cycle was retained only if all six points followed a strictly increasing temporal order, ensuring well-formed and physiologically plausible waveforms. Additional checks were applied to exclude cycles with overlapping or missing components. This procedure enabled the consistent identification of complete cycles across IMFs (Fig. 4.8, Fig. 5.4 and Fig. 5.10).

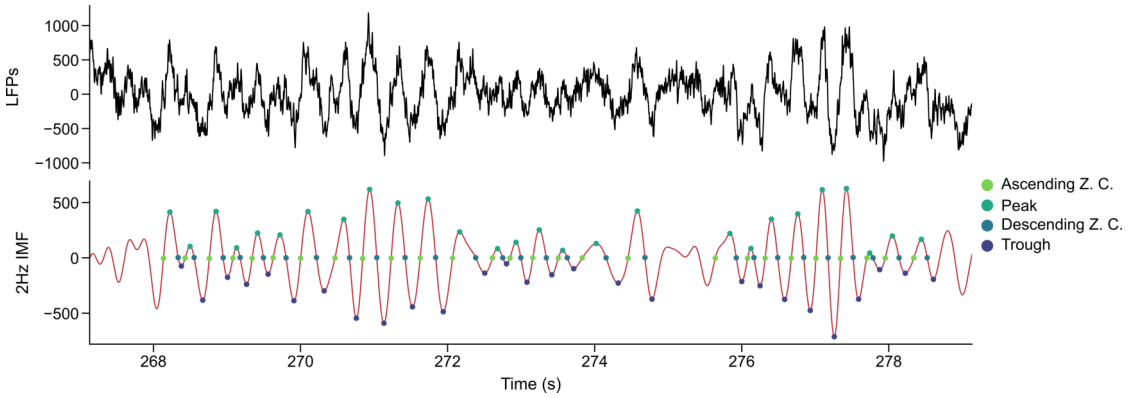


Figure 2.4: **Detection of oscillatory cycles.** Example 12-second LFP (top) and 2Hz IMFs signal with detected points of the oscillatory cycles overlaid (bottom): ascending zero-crossing (Z. C.), peak, descending zero-crossing and trough.

To relate slow oscillatory phase (1-, 2-, and 6-Hz) to gamma activity and population firing rate (Fig. 5.4), we computed cycle-triggered averages aligned to each extracted IMF cycle. Cycles that coincided with IEDs were excluded. For each cycle, we extracted ±1.5, ±2.5 or ±5 seconds around the descending zero-crossing and binned signals at 10, 5, or 3 ms resolution for 1-, 2-, and 6-Hz cycles, respectively. LFPs were z-scored, and spike counts were converted to population rate (Hz) per bin. Cycle-averaged LFPs, gamma, spike-rate traces, and time-frequency spectrograms (>10 Hz) were obtained by averaging across cycles (and across units for the population rate). To visually compare the three frequencies, gamma activity was normalized, and the same y-scales were applied to all graphs.

2.II.2.c Detection of oscillatory bursts

Oscillatory bursts were detected from IMF-derived signals using a spectrogram-based thresholding approach. For each hippocampal recording, the signal reconstructed up to the IMF of interest (1-, 2- or 6-Hz IMF) was converted to a wavelet spectrogram using 30 logarithmically spaced (0.2–20 Hz for 1-Hz bursts, 0.5–25 Hz for 2-Hz bursts, and 1–45 Hz for 6-Hz bursts). The spectrogram was z-scored, and contiguous time-frequency clusters exceeding a z-score of 2 were identified as candidate bursts. Clusters were retained only if at least half of their energy fell within the target frequency band (0.5–1.5, 1–4, 5–12 Hz for 1-, 2- and 6-Hz bursts, respectively) and if their duration corresponded to at least two oscillatory cycles. Adjacent clusters separated by <400 ms (1-Hz), <200 ms (2-Hz) or <50 ms (6-Hz) were merged. Example 2-Hz bursts are shown in Fig. 4.6. Burst onset and offset were then defined from the merged clusters, and each burst's duration was extracted (Fig. 4.7). Out-of-burst epochs used in this manuscript (Fig. 6.15, Fig. 5.19) corresponded to all segments between detected bursts.

Burst rate of occurrence and burst duration were compared between viewing, learning and recall sessions using paired statistics (Fig. 4.19); between best- and worst-recalled associations using paired statistics (Fig. 4.20); and between higher and lower performers using unpaired statistics (Fig. 4.20). To characterize the temporal dynamics of burst rate (Fig. 4.19B,F) and duration (Fig. 4.19D,H) across the task, each session for each participant was divided into 50 equal-duration time bins. Burst rate and duration per bin were then calculated by averaging across hippocampal contacts and participants. This "warped time" was used to compute the Pearson correlation between burst rate or duration and task progression within each session. To estimate burst dynamics across the task (Fig. 4.19B,D,F,H), the mean bin duration for each session was used to rescale the bins. Accordingly, although each session is represented by 50 time bins, the relative temporal proportions of each session are preserved.

2.II.3 Other spectral decompositions

2.II.3.a Detection of gamma activity

In this work, we detected broadband gamma activity by dividing the signal into five contiguous frequency bands between 60 and 160 Hz (20-Hz steps). Although 50 Hz line

noise was minimal under our recording conditions, we voluntarily started the broadband detection from 60 Hz to avoid any confound from this line noise. Each band was bandpass-filtered and transformed into its analytic representation using the Hilbert transform to obtain the instantaneous amplitude. The envelope from each band was normalized by its mean amplitude to equalize their contributions, and the normalized envelopes were averaged across all bands to produce a single broadband gamma envelope representing moment-to-moment fluctuations in gamma activity (Fig. 5.4).

2.II.3.b PSDs estimation and comparison of oscillatory power

PSD estimation: PSD estimates were computed using Welch's method with a Hann window (from the scipy.signal.welch function in the scipy.signal module). PSDs were calculated across contiguous 1-s windows with a frequency-dependent sampling density optimized for slow and fast oscillations (20 points/Hz for 0.5-20 Hz; 4 points/Hz for 20-200 Hz). All LFP signals were z-scored prior to spectral estimation. To account for inter-individual differences in the broadband (aperiodic) component of the power spectrum, we modeled each PSD using the "Fitting Oscillations and One-Over-F" (FOOOF) algorithm (Donoghue et al. 2020). Each PSD was fit within the 0.5-20 Hz range to isolate the aperiodic (1/f) component. The full modeled spectrum and the aperiodic fit were then subtracted to obtain a log-corrected, aperiodic-adjusted PSD, preserving only periodic features (Fig. 4.5, Fig. 4.10, Fig. 4.11, Fig. 4.12B, Fig. 4.13, Fig. 4.21F-H, Fig. 5.11 and Fig. 6.4B). Narrowband oscillations were then quantified by averaging power within the 1-Hz (0.5–1.25 Hz), 2-Hz (1.25–3.5 Hz), and 6-Hz (3.75–8.5 Hz) frequency bands, corresponding to the power distribution of the initially detected IMFs (Fig. 4.3).

In addition, to characterize rhythmicity in single-neuron spiking activity, PSDs were computed on spike-train autocorrelograms. For each unit, the autocorrelogram was calculated over a 2-s window and smoothed with a Gaussian kernel (width = 10 ms, σ = 5 ms) to reduce high-frequency noise while preserving rhythmic structure. The PSD of the resulting autocorrelation signal was then computed (0.9–15 Hz range) to identify oscillatory modulation of firing patterns. Peaks in these autocorrelogram-derived PSDs indicate dominant rhythmic frequencies in the spike timing of individual neurons (Fig. 5.2 and Fig. 5.15).

Comparison of oscillatory power between task sessions: Session-related changes in oscillatory power were quantified across task sessions for the 1-, 2-, and 6-Hz frequency bands. Power values were obtained from log-corrected PSDs computed for each hippocampal macrocontact as described above, excluding those with interictal activity (Fig. 4.12 and Fig. 4.13). Linear mixed-effects models were used to compare power across sessions, with task session treated as a fixed effect and individual subject as a random factor, allowing assessment of frequency-specific modulation of slow oscillations throughout the task, controlling for putative subject-driven effects (Fig. 4.13B).

Comparison of oscillatory power between brain regions: Regional differences in oscillatory power were assessed by comparing log-corrected spectra between hippocampal (HPC), extra-hippocampal medial temporal (MTL; entorhinal, parahippocampal, amygdala), and non-MTL temporal cortical contacts (inferior, middle and superior temporal cortices and fusiform gyrus). For each macrocontact, log-corrected spectra were computed as described above (Fig. 5.11). To better capture the dominance of 6-8-Hz

oscillations over 2-Hz in non-MTL regions, we then used the peak power measured as the maximum of the corrected power spectrum in the designated frequency band (Fig. 5.11B). To quantify the relative predominance of 2-Hz over 6-Hz activity, a normalized ratio $(2Hz - 6Hz)/(2Hz + 6Hz)$ was computed for each macrocontact and compared across regions (Fig. 5.11C).

Comparison of oscillatory power between sleep stages: State-dependent changes in slow oscillatory power were quantified across sleep stages (Fig. 6.1; SWS, N1, REM, and wake) for the 1-, 2-, and 6-Hz frequency bands. Continuous LFPs recordings were divided into 30-s epochs based on manual sleep scoring, and log-corrected PSDs were computed as described above. To ensure comparable sampling across stages, 200 randomly selected windows were analysed per condition. For wakefulness, only daytime segments (8:00 a.m. to 6:00 p.m.) were included, excluding brief night-time arousals (Fig. 6.2, Fig. 6.4 and Fig. 6.10).

2.II.3.c Wavelet spectrograms and quantification of evoked oscillations

Amplitude spectrograms were computed from the raw signal using complex Morlet wavelet convolution for each macrocontact across sessions. This approach provides high temporal precision for fast frequencies and high frequency resolution for slow oscillations, making it well suited to characterize non-stationary neural dynamics. Wavelets were constructed with five cycles per frequency and normalized to unit energy, producing 80 logarithmically spaced frequencies between 1 and 150 Hz. Stimulus-locked spectrograms were then extracted from -1 to +3 seconds (viewing and recalling sessions) or +4 seconds (learning session) relative to stimulus onset, excluding trials containing IEDs or motor responses. To ensure comparability across sessions, trials were subsampled to equalize stimulus counts. For each contact and frequency, post-stimulus amplitudes were normalized to baseline (-1 to 0 second) by z-scoring and next averaged across trials using the amplitude from the baseline only (Fig. 4.17B-D and Fig. 4.18). This baseline normalization was not applied in Fig. 4.17A, where the mean amplitudes in the post-stimulus window were compared to mean amplitudes obtained from the baseline. Mean evoked amplitudes were then quantified within the 1-, 2-, and 6-Hz frequency bands during the post-stimulus window (+1 to +3 seconds for viewing and recalling, +2 to +4 seconds for learning). This ensures that the observed changes in evoked amplitude are not confounded by differences in the magnitude of event-related potential (ERP) deflections between conditions.

2.II.4 Quantification of ERPs

Comparison of event-related potentials between sessions: ERPs were measured by averaging LFPs time-locked to photograph onsets. For each recording, signals were z-scored, and trials contaminated by IEDs or falling outside the recordings were excluded. Epochs extending from 1 second before to 4 seconds after photograph onset were extracted, baseline-corrected using the mean pre-stimulus activity, and averaged across trials for each contact (Fig. 4.14, Fig. 5.13 and Fig. 4.15). To test for session-related differences, the two average ERPs were compared using a nonparametric cluster-based permutation test (1,024 iterations, mne-python package (Gramfort et al. 2013)), which identifies contiguous time intervals showing consistent differences in ERP deflections while controlling for

multiple comparisons. Significant clusters ($p < 0.01$) indicated time windows with reliable modulation of evoked responses across sessions (Fig. 4.15).

Correlation between ERP deflection and evoked oscillatory amplitude: To relate ERP deflection with evoked oscillations in the recalling session, we compared the mean ERP deflection (0.3–0.9 second after stimulus onset in the hippocampus) with the corresponding post-stimulus spectral amplitude averaged within the 1-, 2-, or 6-Hz bands (1–4 second window). Correlations were computed across contacts using Pearson's coefficient, and significance was assessed by two-tailed testing. Scatterplots in Fig. 4.18 and Fig. 5.14 display the linear fit with bootstrapped 95% confidence intervals, showing the relationship between the strength of evoked slow oscillations and the magnitude of the ERP deflection. The mean ERP deflection was taken between 0.3–0.9, 0.15–0.6 and 0.15–0.5 second after stimulus onset for the entorhinal cortex, parahippocampal cortex and amygdala macrocontacts, respectively (Fig. 5.14). These epochs were selected to match the largest ERP deflection visible in the grand averages computed for each region. However, various epochs were tested and none of them showed significant correlation with evoked amplitude.

2.II.5 Cross-frequency analyses

2.II.5.a PAC and phase randomization

Quantification of phase-amplitude coupling (PAC): To quantify the actual phase-amplitude coupling (PAC) between gamma activity and slower oscillations, we computed the modulation index (MI) as in Tort et al. (Tort et al. 2010). Gamma signals were taken either from the same macrocontact signal as the phase (local PAC; Fig. 5.5 and Fig. 5.6) or from a distal macrocontact (distal PAC, across structures; Fig. 5.17). The computation of the MI involved measuring the deviation of the amplitude distribution across phase bins from uniformity using the Kullback-Leibler distance. First, we measured the instantaneous phase of the IMFs using the Hilbert transform. The phase of each IMF (e.g., 2-Hz) was then binned into N (24) equally spaced intervals over $[0, 2\pi]$. For each bin i, we computed the mean amplitude of the gamma activity, and then normalized the amplitude distribution. The Kullback-Leibler distance between this distribution and the uniform distribution was computed as:

$$D_{\mathrm{KL}}(P \parallel U) = \sum_{i=1}^{N} P(i) \log\left(\frac{P(i)}{U(i)}\right) \tag{2.3}$$

We normalized this value to define the MI:

$$\mathrm{MI} = \frac{D_{\mathrm{KL}}(P \parallel U)}{\log(N)} \tag{2.4}$$

This yielded a value between 0 (no coupling; uniform distribution of amplitudes across phase bins) and 1 (maximal concentration in a single phase bin), indicating how strongly the amplitude of the gamma activity depends on the phase of the slow oscillation. Then, we generated 300 surrogate versions of the IMFs while preserving their spectral content by

applying phase randomization in the Fourier domain. This approach destroys temporal structure but retains the power spectrum, making it suitable for surrogate-based statistical testing of the PAC.

The original signal $x[n]$ was transformed using the discrete Fourier transform:

$$X[k] = \sum_{n=0}^{N-1} x[n]\, e^{-2\pi i k n/N} \tag{2.5}$$

where $A[k]$ is the amplitude spectrum and $\phi[k]$ the phase spectrum. This was expressed in polar form as:

$$X[k] = A[k]\, e^{i\phi[k]} \tag{2.6}$$

where $A[k] = |X[k]|$ is the amplitude spectrum, and $\phi[k] = \arg(X[k])$ is the phase spectrum.

We then generated a random permutation $\pi(k)$ over frequency indices and substituted:

$$\tilde{X}[k] = A[k]\, e^{i\phi[\pi(k)]} \tag{2.7}$$

The inverse Fourier transform yielded the phase-randomized surrogate signal:

$$\tilde{x}[n] = \Re\left\{ \frac{1}{N} \sum_{k=0}^{N-1} \tilde{X}[k]\, e^{2\pi i k n/N} \right\} \tag{2.8}$$

We then computed PAC between the unchanged gamma activity and each of the 300 surrogate phase signals. This generated a null distribution of PAC values, which we used to assess statistical significance. The actual PAC value, computed using the original (non-randomized) phase signal, was transformed into a z-score relative to this surrogate distribution. This z-scored PAC reflects the likelihood—rather than the magnitude—of coupling and was used for statistical comparisons across IMFs and electrode contacts (Fig. 5.5A,B and Fig. 5.17B,C). Coupling was considered significant when the z-scored PAC exceeded a threshold of 2 or 5 (where mentioned) (Fig. 5.5C and Fig. 5.17D). Preference was assessed by comparing, for each given contact, which of the three oscillations (1-, 2-, or 6-Hz) had the highest z-scored PAC value, only considering contacts with at least one significant locking in these frequency bands (z-score >5, Fig. 5.5D and Fig. 5.17E). For the leave-one-out controls (Fig. 5.5E and Fig. 5.17F), we omitted the PAC values from each given day and reported the average oscillatory preference based on the remaining data. PAC was measured on epochs clear from interictal discharges.

Anatomical gradients in local phase-amplitude coupling: Anatomical gradients in local PAC were assessed to determine whether the strength of oscillatory coupling varied along hippocampal axes. For each hippocampal contact, coupling values were related to the anteroposterior and mediolateral coordinates of this recording site using a generalized linear model fitted separately for the 1-, 2-, and 6-Hz frequency bands. Coupling values were transformed to match normality of the distributions (Yeo-Johnson):

$$\mathrm{PAC}_i = \beta_0 + \beta_1\,\mathrm{AP}_i + \beta_2\,\mathrm{ML}_i + \varepsilon_i \tag{2.9}$$

where PAC_i is the transformed local PAC value for contact i; AP_i and ML_i are the anteroposterior and mediolateral coordinates of this recording site; β_0 is the intercept; β_1 and β_2 represent the effects of position along the hippocampal axes; and ε_i is the residual error term. Model coefficients were extracted and summarized as a heatmap (Fig. 5.6B).

Mixed-effects models for regional differences in distal phase-amplitude coupling: To test whether distal PAC to HPC differed between MTL and non-MTL contacts and whether that difference depended on frequency, we pooled distal PAC estimates for the 1-, 2- and 6-Hz bands across macrocontacts and subjects and fitted a mixed-effects model with an MTL $*$ frequency interaction and recording day as a random factor. Coupling values were transformed for normality (Yeo-Johnson) and distance between contacts was included as a covariate:

$$\mathrm{PAC}_{ij} = \beta_0 + \beta_1\,\mathrm{MTL}_i + \beta_2\,\mathrm{Frequency} + \beta_3\Big(\mathrm{MTL}_i \times \mathrm{Frequency}\Big) + \beta_4\,\mathrm{Distance}_{ij} + u_{ij} + \varepsilon_{ij} \tag{2.10}$$

where PAC_{ij} is the transformed distal PAC value for the pair of distal macrocontact i and hippocampal contact j; MTL_i is a binary variable indicating whether contact i is in the MTL or not; Frequency represents the categorical frequency factor (1-, 2-, or 6-Hz); $\mathrm{Distance}_{ij}$ is the Euclidean distance between contact i and j and controls for inter-contact spacing; u_ij is the random intercept accounting for subject-level variability; and ϵ_ij is the residual error term. From the fitted model we extracted the MTL - non-MTL simple effect at each frequency (estimated difference ±95% Confidence interval (CI)) and tested difference-of-differences contrasts (2-Hz versus 1-Hz and 6-Hz) using Wald t-tests. This method quantifies whether MTL contacts show selectively greater slow-frequency coupling and whether that regional bias is specific to the 2-Hz band.

2.II.5.b Phase synchronization

Phase synchronization between gamma activity recorded from different macrocontacts was quantified from the dispersion of their preferred hippocampal 1-, 2-, and 6-Hz phases. For each hippocampal macrocontact, the mean preferred phase of gamma activity was determined for all extra-hippocampal sites, and the pairwise circular differences between these phases were computed. The average of these pairwise differences was then inverted ($2\pi - \Delta\phi$) so that higher values reflected stronger phase alignment. Synchronization indices were calculated separately for MTL and non-MTL contacts to compare the spatial organization of phase coupling across regions (Fig. 5.18).

2.II.5.c HHSA

The Holo-Hilbert Spectral Analysis (HHSA) is designed to analyse non-linear and non-stationary signals and capture both carrier frequencies and their amplitude modulations (Huang et al. 2016). This spectral method uses a two-layer EMD followed by Hilbert

transforms to provide a two-dimensional representation of energy across carrier frequencies and modulation frequencies (Fig. 2.5). This allows us to deal with non-linearities and harmonics and reduces the risk of detecting spurious PAC (Huang et al. 1998; Juan et al. 2021) to identify genuine cross-frequency interactions and nested oscillations in LFP signals. To do this, we first selected epochs clear from IEDs and used IMFs extracted using tmEMD on each macrocontact, retaining the first K=9 IMFs capturing slow to fast oscillations. Each IMF was transformed into its analytic signal via the Hilbert transform:

$$z_k(t) = \mathrm{IMF}_k(t) + i\,\mathcal{H}[\mathrm{IMF}_k(t)] \tag{2.11}$$

yielding instantaneous amplitude $A_k(t) = |z_k(t)|$ and carrier frequency:

$$f_k^{(1)}(t) = \frac{1}{2\pi}\frac{d}{dt}\arg(z_k(t)) \tag{2.12}$$

To capture amplitude fluctuations over time, we applied a second-layer EMD to the amplitude envelopes, decomposing each into slower amplitude modulation components:

$$A_k(t) = \sum_{j=1}^{J} a_{k,j}(t) \tag{2.13}$$

Each modulation component was again Hilbert-transformed to extract modulation frequency. The holospectrum represents signal energy jointly as a function of carrier frequency $f^{(1)}$ and amplitude modulation frequency $f^{(2)}$. It was computed across all IMF pairs and projected onto a 2D frequency space:

$$H(f_{\text{carrier}}, f_{\text{AM}}) = \text{Energy at } \left(f^{(1)}, f^{(2)}\right) \tag{2.14}$$

Log-spaced frequency bins were used from 0.1 to 195 Hz for both axes, allowing fine resolution of slow-frequency modulations. The average energy measured on each electrode-contact signals were then z-scored before averaging across contacts. We finally averaged the energy in several frequency bands to compare gamma (60-160 Hz) modulation across slow oscillations (Fig. 5.7A,B,D,E). That is, in humans, 1-Hz (0.5–1.25 Hz), 2-Hz (1.25–3.5 Hz), and 6-Hz (3.75–8.5 Hz); in mice, 3-Hz (1.5–4.5 Hz), 7-Hz (5–10 Hz), and 15-Hz (11–20 Hz). To quantify the gain in amplitude modulation in contacts clear from IEDs, we computed the difference between 2-Hz and 6-Hz energy per macrocontact (Fig. 5.7C) and reported the unpaired difference between contacts clear from IEDs (labelled "No IEDs") and contacts containing IEDs (labelled "With IEDs").

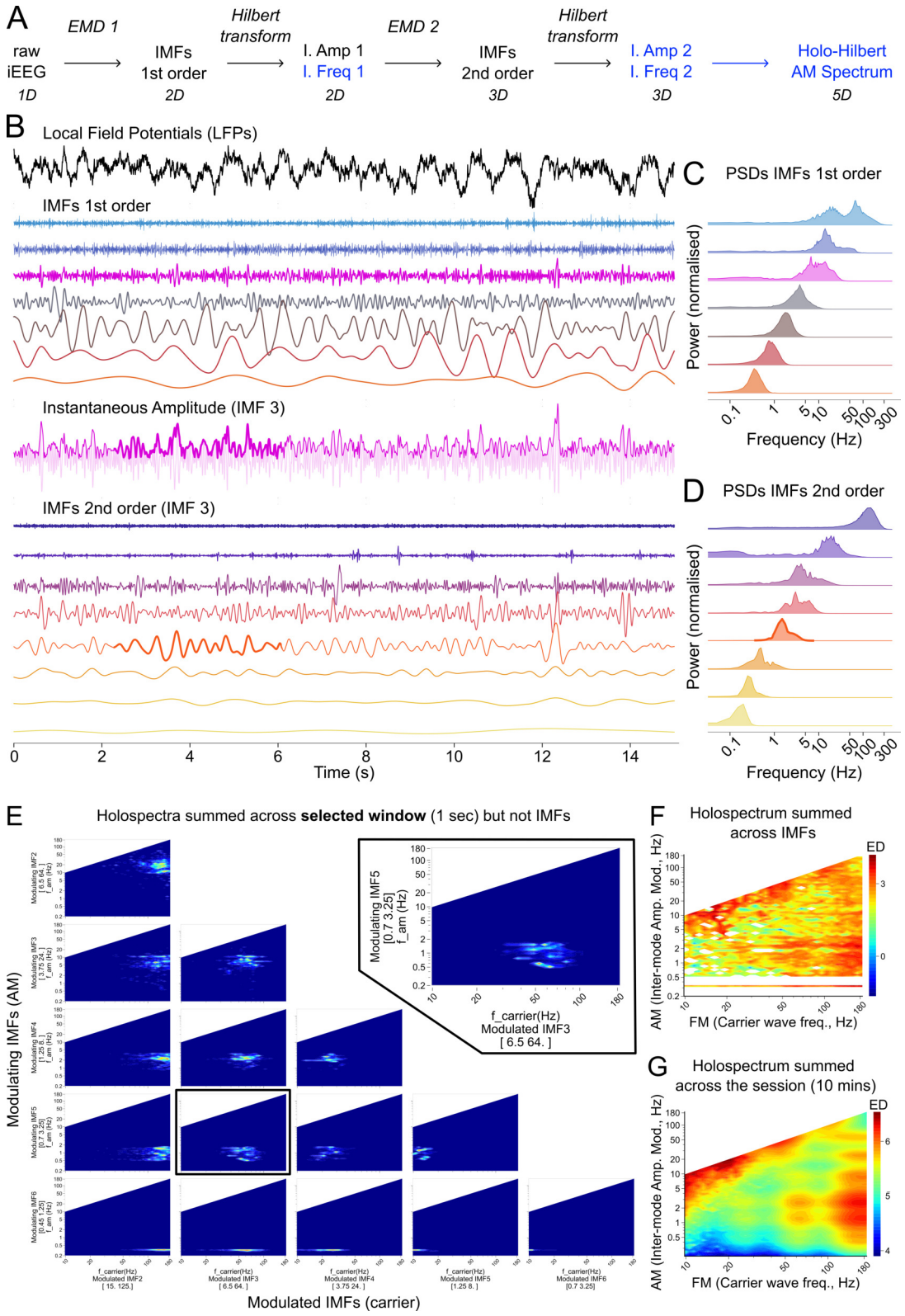

A
raw iEEG
1D
EMD 1
IMFs 1st order
2D
Hilbert transform
I. Amp 1
I. Freq 1
2D
EMD 2
IMFs 2nd order
3D
Hilbert transform
I. Amp 2
I. Freq 2
3D
Holo-Hilbert AM Spectrum
5D
B
Local Field Potentials (LFPs)
IMFs 1st order
Instantaneous Amplitude (IMF 3)
IMFs 2nd order (IMF 3)
Time (s)
C
PSDs IMFs 1st order
Power (normalised)
Frequency (Hz)
D
PSDs IMFs 2nd order
Power (normalised)
Frequency (Hz)
E
Holospectra summed across selected window (1 sec) but not IMFs
Modulating IMFs (AM)
Modulated IMFs (carrier)
F
Holospectrum summed across IMFs
AM (Inter-mode Amp. Mod., Hz)
FM (Carrier wave freq., Hz)
ED
G
Holospectrum summed across the session (10 mins)
AM (Inter-mode Amp. Mod., Hz)
FM (Carrier wave freq., Hz)
ED

Figure 2.5: **Holo-Hilbert spectral analysis reveals gamma amplitude modulation by slow oscillations.** (**A**) Schematic of the HHSA (Huang et al. 2016). LFPs were first decomposed into first-order IMFs. A Hilbert transform was applied to each IMF to extract instantaneous amplitude and frequency (I.Amp1 and Freq1). A second EMD was then applied to instantaneous amplitude signals, yielding second-order IMFs that captured oscillatory structure within amplitude envelopes. Applying a second Hilbert transform produced second-order instantaneous amplitude and frequency (I.Amp2 and Freq2), reflecting the energy and frequency of envelope modulation, respectively. The resulting matrix—the Holo-Hilbert amplitude-modulation spectrum (holospectrum)—represents signal energy across five dimensions: time, carrier IMF, amplitude-modulating (AM) IMF, carrier frequency, and AM frequency. (**B**) Example 15-s hippocampal recording showing raw LFPs, first-order IMFs, the instantaneous amplitude of IMF 3, and its second-order IMFs. The bolded trace highlights alpha-band amplitude modulation at 2 Hz. (**C** and **D**) Power spectral densities of first- (C) and second-order (D) IMFs, normalized to show frequency distribution. (**E**) Example matrix of holospectra, summed over 1 s taken from the window displayed in panel A, but before the summation across IMFs. In rows, AM (modulating) IMFs are organized from fastest to slowest IMFs from top to bottom. In columns, carrier (modulated) IMFs are organized from fastest to slowest IMFs from left to right. This shows that holospectra are sparse matrices before summation across IMFs. (**F**) Holospectrum summed across IMFs and over the second taken from the window displayed in panel A (same as in E). This holospectrum already shows modulation (energy density) of fast oscillations by the 2-Hz IMF during the analysed second, despite this being less intuitive from the raw trace. ED, energy density. (**G**) Holospectrum summed across IMFs and over an entire learning session (10 min) calculated on one hippocampal contact.

2.III Ripples and reactivation

2.III.1 Ripple detection and validation

2.III.1.a Ripple detection

Hippocampal ripple events were identified and validated through a multistage procedure combining automated detection, dimensional embedding, and template-based classification.

Initial ripple detection using overnight sleep recordings: Hippocampal LFPs recorded during slow-wave sleep were bandpass-filtered between 60 and 180 Hz, and ripple candidates were identified by thresholding the ripple-band amplitude and comparing it to the closest white-matter macrocontact (referred to as control). Candidate events were retained when the amplitude in the ripple band exceeded five standard deviations and was at least twice as strong as in the control macrocontact, and the event lasted for at least one oscillatory cycle. The precise peak times of the filtered signal were extracted to provide a first set of putative ripples for each macrocontact during overnight sleep.

Dimensional embedding and template generation: For each recording night, candidate ripple waveforms were then extracted from the ripple-band-filtered signal (60–180 Hz) using 25-ms snippets centred on the ripple peaks. These band-limited segments, capturing the oscillatory component of each event, were normalized and used as input to Isomap (15 neighbors, intrinsic dimensionality estimated per recording night) to embed the high-dimensional waveforms into a low-dimensional space while preserving their temporal structure (Tenenbaum et al. 2000; Maslarova et al. 2025). Events were clustered with k-means, and clusters corresponding to canonical ripple morphologies were manually verified and retained. Then, within each recording night, 200 waveforms from verified clusters were subsampled and averaged to form “super-events”. These "super-events" were pooled across recording nights and clustered again to generate a compact library of representative ripple templates characterized by their average waveform and dominant frequency. Dominant frequency of the templates was estimated from the inverse of the period between two oscillatory peaks in the average ripple-band-filtered signal. Fourteen different templates were retained, with dominant frequencies ranging from 67.6 Hz to 113.6 Hz.

Loose detection of putative ripple events: A permissive detector was then applied to all hippocampal recordings to capture all potential high-frequency bursts in the ripple range (60–180 Hz). The analytic amplitude envelope was smoothed (width = 80 ms, σ = 40 ms) and adaptively thresholded to detect transient events, targeting 20-30 events per minute while constraining event duration ($\geq$ 20 ms) and separation ($\geq$ 150 ms). Periods containing IEDs were excluded to prevent contamination by large, transient high-power deflections and to avoid detecting pathological events. Event peaks were realigned using the instantaneous phase of an 80-Hz narrowband signal to ensure consistent phase definition.

Template matching and white-matter control: These loosely detected events were then compared to each validated ripple template using cosine similarity. For every event, the highest similarity score and corresponding template were obtained both in the

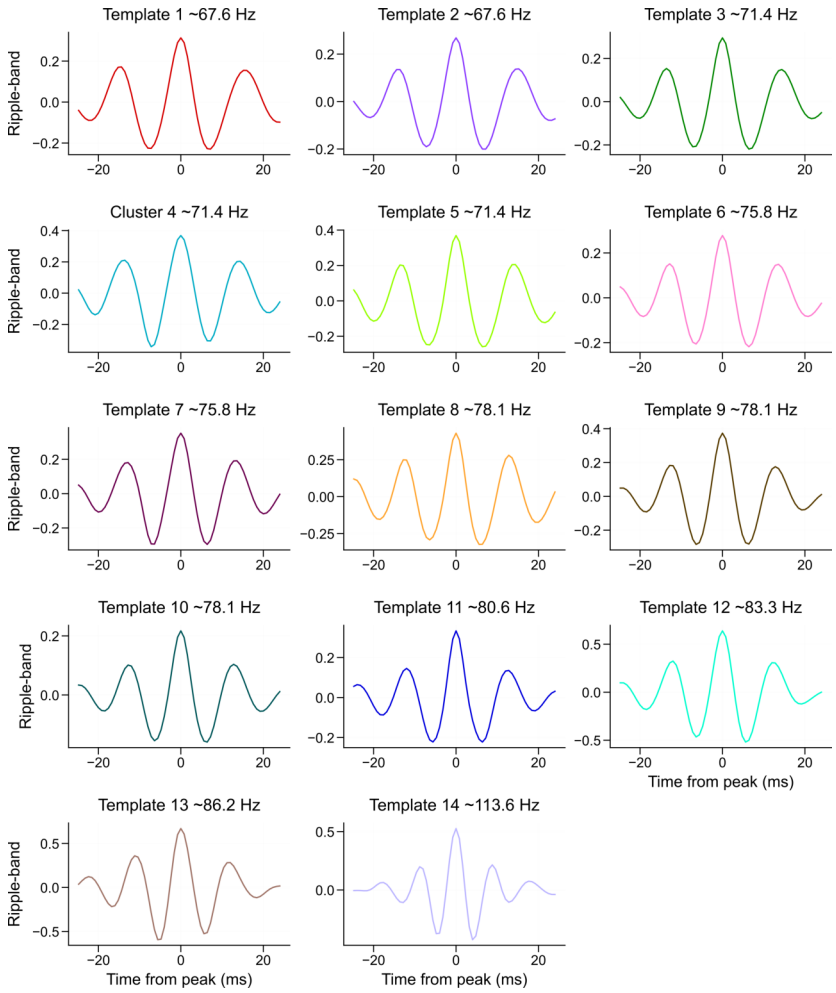


Figure 2.6: **Ripple templates.** Average ripple-band signals triggered by the peak of the detected events, grouped by cluster of ripples. These triggered-averages of the ripple-band formed the 14 templates used for ripple detection in the subsequent algorithmic steps.

hippocampal contact and in its anatomically defined white-matter control by realigning to the local peak in the ripple-band. Events were classified as genuine ripples only when their match score exceeded 0.85 in the hippocampal macrocontact but remained below this threshold in the control macrocontact (Fig. 2.7 B, F and J). This match score of 0.85 corresponded to the 95th percentile of the distribution of all match scores obtained in white matter macrocontacts, representing a meaningful null distribution for transient, non-specific fast-frequency events. This two-stage validation, which required both high morphological similarity to verified sleep ripples and spatial specificity relative to the white-matter reference, ensured that the final set of detected events reflected true, locally generated hippocampal ripples (Fig. 2.7).

2.III.1.b Characterization of ripple central frequency

Hippocampal ripple events were analysed from LFPs band-pass filtered between 55 and 200 Hz (zero-phase fourth-order Butterworth filter). Instantaneous phase and amplitude were obtained using the Hilbert transform. Ripple onset and offset were defined as the first and last time points at which the z-scored amplitude exceeded 2. Within these limits, the unwrapped phase was used to compute the total number of oscillatory cycles as the difference between phase values at offset and onset (in degrees) divided by 360. For instance, an unwrapped phase change of 1800° corresponds to five cycles ($1800/360 = 5$). The ripple central frequency was then calculated by dividing the number of cycles by the event duration in seconds (e.g., $3cycles/400ms = 75Hz$). This analysis was performed separately in sleep (Fig. 6.7G,H) and rest recordings (Fig. 6.7H-J), with sleep events further grouped by sleep stage (wake, N1, SWS, REM).

2.III.1.c Ripple-triggered averages

Ripple-triggered averages were computed to characterize hippocampal LFPs, spike train, and spectral dynamics as well as associated gamma activity from the MTL contacts during rest and sleep sessions. For each hippocampal contact, detected events were realigned to the local peak of the ripple-band signal to ensure consistent phase alignment across ripples. Around each realigned peak, ±250 ms (or ±150 ms) of broadband LFPs and corresponding time-frequency spectrograms (10–200 Hz, logarithmic spacing) were extracted and averaged across events to obtain mean ripple-locked waveforms (Fig. 6.7E,F and Fig. 6.8C). In Fig. 6.7F, ripple-triggered averages were computed on the same example hippocampal macrocontact, from events detected in the task rest or during overnight N1 sleep. In Fig. 6.8, ripples were detected on the macrocontact and realigned to the local peak of the ripple-band signals obtained from the local and the distal tetrodes. In Fig. 6.11, local spike trains were averaged in 24-ms bins, z-scored within neuron, and averaged across ripples. In Fig. 6.12, gamma activity from MTL contacts were z-scored within contact, and averaged across ripples.

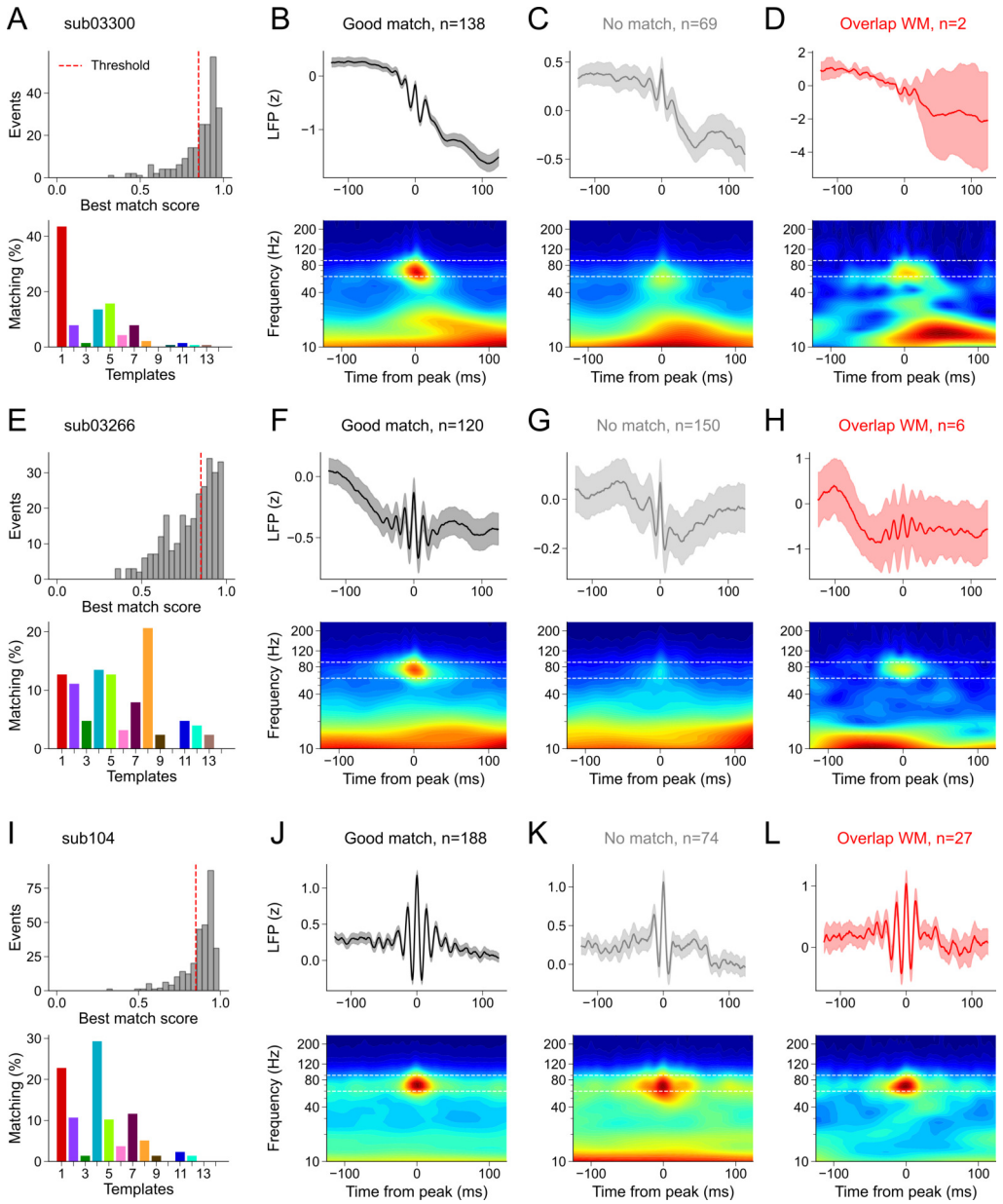


Figure 2.7: **Ripple detection.** Ripple detection on a single hippocampal macrocontact in three different subjects during pre-learning rest (10 minutes): sub03300 (**A**–**D**), sub03266 (**E**–**H**), sub104 (**I**–**L**). (**A, E** and **I**) Top, distribution of the matching scores for all events initially detected; bottom, percentage of the "good" events matching one of the 14 templates used for initial detection. (**B, F** and **J**) Average LFPs and corresponding spectrograms triggered by the peak of all "good match" events (above $threshold = 0.85$ matching score for one of the template on the hippocampal macrocontact but not the white matter macrocontact). (**C, G** and **K**) Same as **B, F** and **J** but for events which did not match any of the templates (below $threshold = 0.85$). (**C, G** and **K**) Same as **B, F** and **J** but for events which matched a template on the hippocampal macrocontact and the reference white matter macrocontact (likely reflecting noise).

2.III.2 Detection of cross-regional coactivity motifs

Pairwise coactivity motifs were derived from simultaneously recorded single-unit activity during in-burst versus out-of-burst periods (Fig. 6.14 and Fig. 6.15), task epochs (Fig. 6.16 and Fig. 6.17) and hippocampal ripples. Bursts were detected as described above (see section Chapter 2.II.2.c) for 1-, 2- and 6-Hz IMFs. For each recording day, units from the MTL were included when at least five well-isolated neurons were available. Spike trains were converted into binned firing-rate matrices using 25-ms bins. We then selected bins overlapping with oscillatory bursts (Fig. 6.15, viewing and learning sessions concatenated), photograph presentation and its subsequent inter-stimulus intervals in task (viewing versus learning, best versus worst conditions, Fig. 6.16 and Fig. 6.17) or ripple events (±200 ms). Control bins were drawn from out-of-burst epochs (Fig. 6.15A) or out-of-ripple intervals of matched duration and distance from ripple events (Fig. 6.17C). Firing rates were z-scored for each neuron, and the influence of overall population activity was removed by regressing out the instantaneous population rate (P). Pairwise coactivity between neurons i and j was defined as the Pearson correlation between their residual binned firing rate (Fig. 5.19C), producing one coactivity matrix per condition. To assess the specificity of these patterns, neuron identities were randomly permuted within each time bin, preserving the instantaneous population profile but disrupting pairwise structure. Coactivity matrices computed from the permuted data provided null distributions (Fig. 6.17D).

2.III.3 Reactivation of coactivity motifs in hippocampal ripples

Reactivation was quantified by relating neuronal coactivity motifs expressed during wake (evoked by photographs or during oscillatory bursts) to those measured during pre- and post-learning ripples. For each recording day, the neuron-by-neuron coactivity matrices were vectorized and concatenated across participants to form predictor and response variables (n = 603 coactivity motifs from 6 participants and 8 recording days with at least 5 simultaneously recorded MTL neurons). Group-level relationships were estimated using GLMs.

For each waking condition, the following model (Model 1):

$$Y = \beta_0 + \beta_{\text{wake}}\, X_{\text{wake}} + \beta_{\text{cond}}\, C_{\text{rest}} + \varepsilon \tag{2.15}$$

was fitted to quantify the correspondence between waking and rest motifs, where Y is the vector of ripple coactivity coefficients, X_{wake} the corresponding waking coefficients (in-burst or out-of-burst, viewing or learning, best or worst recalled associations), and C_{rest} is a categorical factor indicating pre- or post-learning rest. Parameter estimates, 95% confidence intervals, and p-values were obtained from Wald t-tests on fitted generalized linear model (GLM) coefficients. Model 1 provided β coefficients (β_{cond}) and their 95% confidence intervals reported in Fig. 6.15A,B (left panels) and Fig. 6.17C (left panel) and are referred to as "Waking vs rest coactivity (β)".

Reactivation strength was then defined as the change in the slope linking waking and ripple motifs across rest sessions, estimated from the interaction term in the following model (Model 2):

$$Y = \beta_0 + \beta_{\text{wake}} X_{\text{wake}} + \beta_{\text{cond}} C_{\text{rest}} + \beta_{\text{int}}(X_{\text{wake}} \times C_{\text{rest}}) + \varepsilon \tag{2.16}$$

The interaction coefficients (β_{int}) and their 95% confidence intervals extracted from Model 2 represent the difference between post- and pre-learning wake-rest slopes and are referred to as "Reactivation ($\Delta Post - Pre$)" in Fig. 6.15A,B (right panels), Fig. 6.16 and Fig. 6.17C (right panel). The p-value of these interaction coefficients (β_{int}) was used to assess significance of the reactivation in Fig. 6.15A,B (left panels) and Fig. 6.16A.

Differences in reactivation between waking conditions (in-burst vs out-of-burst, viewing vs learning, best vs worst recalled associations) were tested with a combined model (Model 3) including a three-way interaction term $X_{wake} * C_{rest} * C_{cond}$ where C_{cond} indexes the waking condition. The p-value of this three-way interaction coefficient was used to assess significance in Fig. 6.15A,B (right panels), Fig. 6.16B and Fig. 6.17C (right panel).

At the subject level (Fig. 6.17A), reactivation was assessed as the partial correlation between waking and ripple coactivity vectors computed separately for each recording day, controlling for the alternate rest session (pre-learning rest controlled by post-learning rest and vice versa).

In Fig.6.17C, reactivation was measured using out-of-ripple epochs, which were defined as windows distant from ripple events. We matched the number and duration of these control epochs with those of actual ripples so that all conditions were comparable.

2.IV Statistical analyses

Data analyses were conducted using Python version 3.10, using the following packages: DABEST v2023.2.14 (Ho et al. 2019), scikit-learn v1.2.2 and nilearn v0.10.1 (Pedregosa et al. 2011), NumPy v1.24.3 (Harris et al. 2020), SciPy v1.10.1 (Virtanen et al. 2020), Stats-Models v0.14.0 (Seabold and Perktold 2010), Matplotlib v3.7.1 (Hunter 2007), Pandas v1.5.3 (McKinney 2010), and Seaborn v0.11.0 (Waskom 2021), MNE-Python v1.5.1 (Gramfort et al. 2013).

Symmetric distribution assumptions underpinned the two-sided statistical tests, visualized using Gardner-Altman and Cumming plots from the DABEST Framework. These plots illustrate effect sizes by comparing mean or median differences across groups. Each plot consists of two panels: the top (or left) shows raw data distributions with group means ± SEM (unless stated otherwise), and the bottom (or right) shows differences relative to a reference group, calculated from 5,000 bootstrapped samples. Black dots represent the mean (or median), black ticks indicate 95% confidence intervals, and bootstrapped error distribution curves are included.

To compare two conditions, bootstrap tests were employed. These tests, which accommodated both paired and unpaired comparisons, estimated the bootstrapped mean difference (either absolute or as a percentage relative to one of the two variables) by resampling the data 100,000 times (unless stated otherwise) with replacement. For paired comparisons, indices were resampled to preserve the relationship between pairs, whereas for unpaired comparisons, each condition was resampled independently. P values for these tests were computed numerically, under the null hypothesis of zero difference. The p value

was determined by multiplying the smaller proportion of bootstraps below or above zero by two.

Median differences were preferred over mean differences when the original distributions were skewed (visual inspection). In some instances, we visualized the bootstrapped mean (or median) differences using histograms or boxplots, from which the corresponding p values were derived. These histograms do not depict the distribution of raw data points but rather represent empirical estimations of the sampling distribution of the mean difference, obtained by the resampling approach described above. All confidence intervals (95% CI) were calculated via bootstrapping with 100,000 resamples (unless stated otherwise). For each interval, data were resampled randomly with replacement, and the 2.5th and 97.5th percentiles of the bootstrapped distributions determined the lower and upper bounds of the CI.

Two-sided t-tests or Wilcoxon signed-rank tests were also used to compare conditions, depending on whether normality (assessed by the Shapiro-Wilk test) was met. Significance of model coefficients was evaluated using two-sided Wald tests.

3 Results: Assessing relational memory in human participants

"Les désordres et les maladies de cette faculté [...] nous apparaissent comme soumis à certaines lois qui constituent le fond même de la mémoire et en mettent à nu le mécanisme."

"The disorders and diseases of this faculty [...] appear to us as governed by certain laws that constitute the very foundation of memory and lay bare its mechanism."

— *Théodule Ribot, Les maladies de la mémoire (1888)*

Contents

3.I Introduction 78

3.I.1 Relational memory 78

3.I.2 The role of the hippocampal network in relational memory . . 79

3.II Investigating relational memory in humans using a social community task 80

3.II.1 Behavioural paradigm 80

3.II.2 Variants of the memory task 81

3.III Quantifying behavioural performance 83

3.III.1 Basic performance metrics 83

3.III.2 Variability of performance between subjects 89

3.IV Discussion 94

3.I Introduction

3.I.1 Relational memory

Relational memory refers to the ability to encode and retrieve the relationships between separate elements of an experience, such as objects, places, people, or events. Rather than storing isolated items independently, relational memory supports the flexible binding of information into structured representations that can later be used to guide behaviour and inference (Eichenbaum and Cohen 1993; Konkel and Cohen 2009). This form of memory is thought to be a fundamental property of the hippocampal system and has been described across mammals using behavioural paradigms based on paired-associate

learning, contextual memory, or inferential reasoning (Bunsey and Eichenbaum 1996; Dusek and Eichenbaum 1997; Konkel and Cohen 2009).

One of the simplest and most widely used paradigms to investigate relational memory is paired-associate learning, in which two items are repeatedly associated so that presentation of one element later allows retrieval of the other (Calkins 1896). In contrast to simpler forms of recognition memory, successful performance in these tasks requires the formation of associations between distinct elements beyond memory for the items themselves. Importantly, relational memory supports inferential behaviour, enabling the establishment of links between items that were not directly experienced together, but that share overlapping associations (Dusek and Eichenbaum 1997; Zeithamova et al. 2012). Lesion studies showed that the hippocampus is necessary for this form of memory, especially when it depends on flexible retrieval of relationships between elements (Bunsey and Eichenbaum 1996; Konkel and Cohen 2009).

3.I.2 The role of the hippocampal network in relational memory

The study of relational memory has therefore played an important role in linking behavioural observations with hippocampal physiology. In animal models, hippocampal lesions impair the acquisition and retrieval of contextual, spatial, and relational associations while sparing simpler stimulus-response learning (O'Keefe and Nadel 1978; Bunsey and Eichenbaum 1996; Dusek and Eichenbaum 1997). In humans, lesion studies similarly demonstrated that damage to the hippocampus and broader medial temporal lobe disrupts associative and episodic memory (Scoville and Milner 1957; Squire 1992a; Konkel et al. 2008). Consistent with these observations, direct brain recordings in humans revealed coordinated neuronal and oscillatory activity within the hippocampus and medial temporal lobe during declarative memory tasks (Fell et al. 2001; Rutishauser et al. 2010).

Importantly, relational memory paradigms also provide a useful behavioural context to investigate the two-stage model of memory described in the general introduction. During active wakefulness, learning and retrieval are expected to engage hippocampal theta-related states coordinating neuronal activity across the medial temporal lobe. During subsequent rest and sleep, recently formed representations are expected to reactivate during hippocampal ripples, contributing to memory consolidation (Buzsáki 1989; McClelland et al. 1995; Girardeau and Lopes-dos-Santos 2021). Consequently, a behavioural paradigm suitable for investigating this model must engage hippocampal-dependent memory processes during wakefulness while also allowing the study of offline neural activity after learning.

In the present work, I therefore used a relational memory task in which participants learned associations between members of a social community. This task was designed to promote hippocampal-dependent associative learning while providing well-controlled visual and behavioural events for further electrophysiological analyses (Chapter 4). Importantly, the task generated substantial variability in memory performance across participants and across individual associations, providing a useful basis for examining the neural correlates of successful learning, retrieval, and subsequent offline reactivation (Chapters 4, 5, 6).

3.II Investigating relational memory in humans using a social community task

3.II.1 Behavioural paradigm

Participants with drug-refractory epilepsy (Dataset 1, Fig. 2.1) performed a computer-based relational memory task implemented in MATLAB using Psychophysics Toolbox 3 (PTB-3). The task involved learning associations among individuals forming a community, in which each person was represented by a photograph and a name. Each recording day consisted of five consecutive sessions: pre-learning rest, viewing, learning, post-learning rest, and recall (total duration: approximately 1 hour, Fig 3.1).

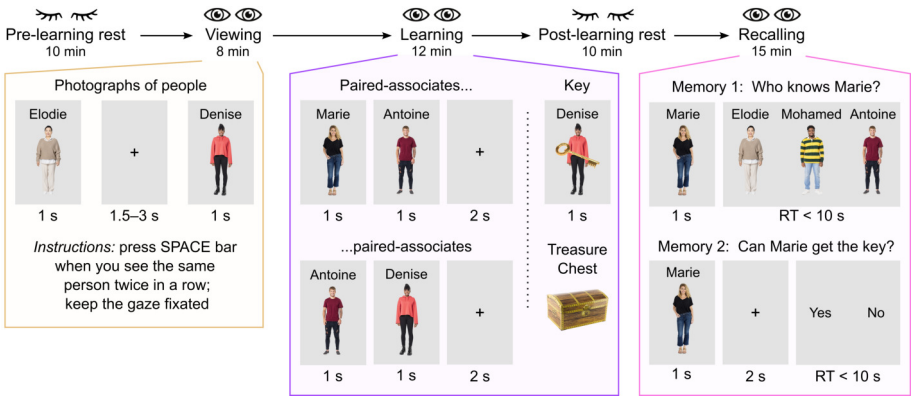


Figure 3.1: **Schematic representing the layout of the relational memory task.**

During the two rest sessions, participants sat still with eyes closed (10 minutes each session). In the viewing session (8 minutes), they were familiarized with 144 photographs of community members displayed for 1 second each and in random order, separated by 1.5-3 second inter-stimulus intervals sampled from a gamma distribution, during which a central fixation dot was shown. This timing distribution allowed the task to remain relatively brief while introducing occasional longer delays to help maintain attention of the participants. Participants were instructed to maintain fixation on the central dot during the inter-stimulus intervals. To ensure compliance, we asked them to press the space bar whenever they detected that the same photograph was presented consecutively, a repetition that we introduced at random intervals.

We then briefly familiarized participants to the structure of the learning session (1-2 minutes). During the learning session (10 minutes), participants viewed pairs of individuals presented consecutively, one person after the next, with each pair described as "friends" to facilitate the formation of associative memories (i.e., "paired associates"). Between each pair, participants were instructed to maintain fixation on the displayed central dot. Learning progress was assessed through intermittent multiple-choice questions: a cue photograph appeared for 1 second, followed by a screen displaying three possible associates. Participants had up to 10 seconds to identify the correct associate and respond using the left, down, or right arrow keys. Learning questions appeared after the presentation of four paired associates. In this community, one individual was intermittently shown holding a key to a treasure chest and participants were asked to remember it. In total, participants

were exposed 96 times to the paired associates, and answered 24 learning questions.

After the post-learning rest session, participants performed the recall session (15 minutes) to test retention of the learned associations. During recall, participants answered two types of memory questions. The first type consisted of multiple-choice questions identical to those used during learning, in which participants identified the correct associate among three photographs (direct memory questions). The second type presented a single photograph for 1 second, after which participants judged whether the depicted person could help obtain the key based on the associations they had learned (indirect memory questions). During these indirect memory questions, responses were permitted after a 2-second delay, creating a fixed 3-second interval between cue onset and the earliest possible motor response. This delay ensured that the visual display was directly comparable to the viewing and learning photographs for analysis of event-related potentials and evoked oscillations (Chapter 4.III). In total, participants answered 24 type 1 memory questions and 72 type 2 memory questions. The recording day finished with a post-recall viewing session, which we used as a second control session.

3.II.2 Variants of the memory task

3.II.2.a Simple and complex tasks

Participants with drug-refractory epilepsy stayed at the hospital for several days, and some participants were included in the study two or three days consecutively. Therefore, to make sure the memory task was adapted to each recording session, we used two difficulty levels. The simple version of the task contained six different people, producing four paired associates to learn (Fig. 3.2A), while the complex one had eight people and six paired associates (Fig. 3.2B). If the participants had a good performance on the first day (Chapter 3.III) and they were willing to continue, we offered them to take the complex task on the next days. Otherwise, we used the simple task on the second day. In both cases, we used new photographs and names of the people forming the community on subsequent days to ensure reproducibility across days.

3.II.2.b Population diversity

Subjects with epilepsy suffer from various cognitive deficits (Black et al. 2010; Dinkelacker et al. 2016; Wang et al. 2020; Phuong et al. 2021), which can affect their performance on relational memory tasks. Therefore, it was essential to evaluate the extent of the cognitive deficit in the population with epilepsy included in this study. To do this, we recruited healthy participants to perform a shortened version of the relational memory task, which featured the simple and the complex versions of the task in the same session (Fig. 3.3). This control cohort was matched to the cohort with epilepsy in age and educational level using the Hungarian optimization algorithm (Kuhn 1955) (Table 3.1, age, $P = 0.051$; paired t-test; education, $P = 0.785$, Wilcoxon test). This cohort allowed us to compare the behavioural performance (accuracy, reaction time) of the controls with the participants with epilepsy (Chapter 3.III.1.b) and to investigate the effect of the age and the educational level on memory performance in this task (Chapter 3.III.2.a).

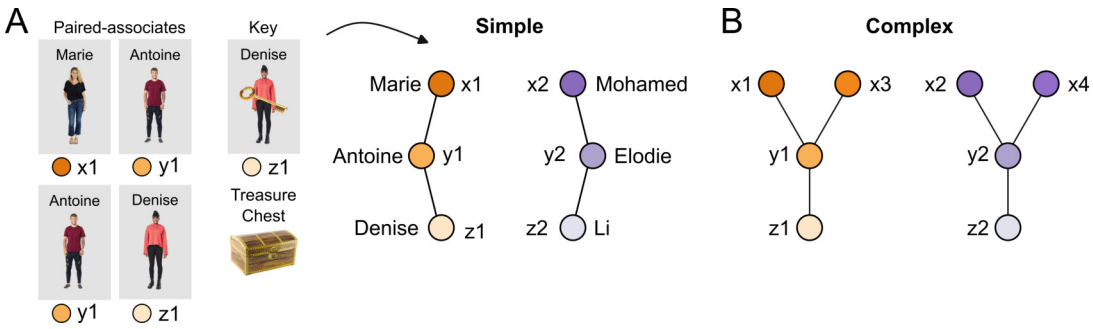


Figure 3.2: **Schematic representing the social community in the simple (A) and the complex (B) versions of the task.** Members are represented with a letter and a number to indicate their position in the social community: "Z1" has the key to the treasure chest, while "Z2" is in the community without a treasure chest. "Y1" is the direct friend of the key owner, while "Y2" is the direct friend of "Z2". "X1" and "X3" are the indirect friends of the key owner, while "X2" and "X3" are the indirect friends of "Z2".

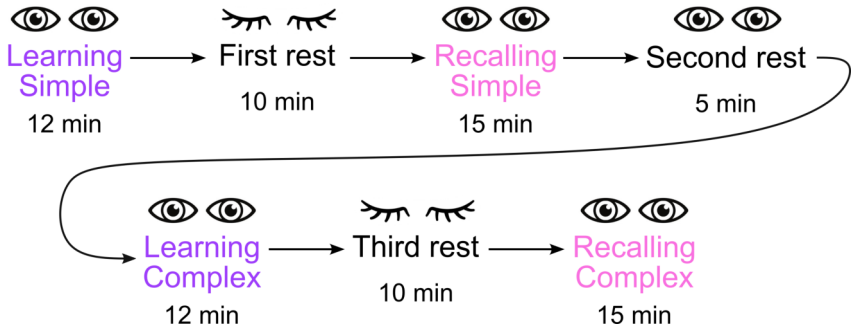


Figure 3.3: **Schematic representing the memory task used for the control cohort.**

Demographics	Epilepsy	Controls	p-value
Age (mean [95% CI])	34.1[30.02, 38.19]	35.58[30.87, 39.88]	0.051
Education (mean [95% CI])	12.14[11.43, 12.85]	12.17[11.47, 12.88]	0.785

Table 3.1: Demographic characteristics of paired cohorts

3.III Quantifying behavioural performance

3.III.1 Basic performance metrics

3.III.1.a Group-level performance

Participants with epilepsy were able to learn the community structure (Fig. 3.4A, left), with a clear improvement in accuracy (percentage correct responses) throughout the learning session and significant retention of the paired associates after the 10-min rest session (Fig. 3.4A, right, $P = 0.00125$; Wilcoxon test compared to chance). Participants in the control cohort also showed learning and retention of the community structure (Fig. 3.4B, $P < 0.001$; Wilcoxon test compared to chance). In addition, both participants with epilepsy and paired controls performed above chance on the type 2 memory questions ($P = 0.038$ and $P < 0.001$, respectively), confirming correct understanding of the relational memory task. Differences in memory accuracy between the two cohorts will be discussed in Chapter 3.III.1.b.

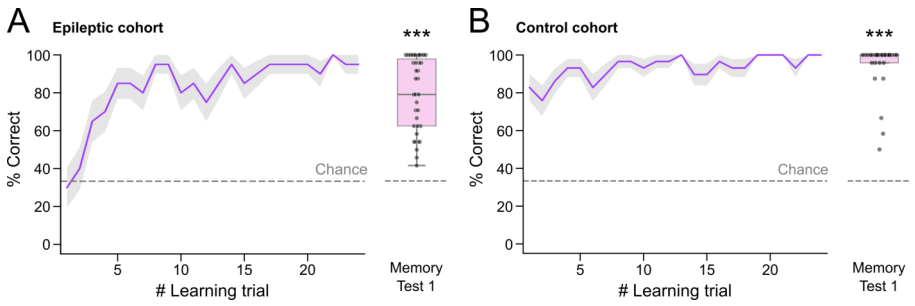


Figure 3.4: **Average accuracy in the relational memory task.** (**A**) Learning accuracy (percentage correct trials, left) and average recall accuracy to type 1 memory questions (percentage correct responses, right) in the cohort with epilepsy. (**B**) Same as in (A) but for the control cohort. Data were analysed using Wilcoxon tests; ***$P < 0.001$.

By design, participants were allowed to respond immediately following the onset of the multiple-choice questions at their own pace, making this paradigm well-suited for quantifying reaction time during both the learning phase and the type 1 memory questions (Fig. 3.5). Reaction time progressively decreased across the learning session in both the epileptic and control cohorts (Fig. 3.5A-D). This reduction in reaction time over successive questions may reflect improved confidence, motor execution (e.g. familiarity with keyboard response), or a better understanding of the task structure (flexibility). To further characterize this effect, we exploited a specific feature of the task design in the control cohort, in which the complex version of the task was administered immediately

after the simple version on the same day (Fig. 3.3). By comparing the reaction time within and between these versions of the task (simple versus complex), we could differentiate procedural (motor) from cognitive effects on learning. If this effect was purely driven by motor learning, the reaction time at the end of the simple version should be identical to the reaction time at the beginning of the complex version of the task. Conversely, if this effect was purely cognitive, the reaction time at the beginning of the learning in the complex version should be higher than that at the beginning of the learning in the simple version, because the participants have more associations to learn.

Reaction time decreased across both the simple and complex versions of the task during learning and memory questions (Fig. 3.5E,F, [a, d and e]). Notably, despite the first eight questions of the complex task being more demanding (six paired associates to remember compared with four in the simple task), reaction time for these questions was lower than in the corresponding simple condition (Fig. 3.5F, [b]). This result rules out a purely cognitive effect on reaction time. In addition, the reaction time at the end of the simple version was lower than that at the beginning of the complex version, also ruling out a purely motor effect on reaction time (Fig. 3.5F, [c]). Moreover, reaction times for the last eight questions did not differ between the simple and complex versions of the task (Fig. 3.5F, [f]), suggesting the presence of a ceiling effect, with reaction times converging to approximately one second.

Taken together, these observations indicate that reaction time varied systematically across the session and across task versions, but did not scale monotonically with task difficulty in this paradigm. This effect likely reflects a combination of cognitive and procedural (motor) factors rather than memory demands alone.

3.III.1.b Across-group comparisons

Next, to estimate the extent of the cognitive deficit in the epileptic cohort, we compared the behavioural performance of participants with epilepsy with their paired control subjects in the simple version of the relational memory task. Participants with epilepsy showed lower accuracy (Fig 3.5A-C) and higher reaction times (Fig 3.5D,E) than control participants on learning and memory questions. The most pronounced differences were observed for memory questions, reaching a 20% deficit in memory accuracy and up to a 1.8-second delay in reaction time (Fig 3.5B,E). These results confirm that participants with epilepsy included in this study perform worse than their paired controls, replicating the deficits previously reported in this population (Black et al. 2010; Dinkelacker et al. 2016; Wang et al. 2020; Phuong et al. 2021).

We next examined whether the control and epileptic cohorts were similarly affected by increased task difficulty, i.e., six instead of four paired associates to remember. In the epileptic cohort, average memory performance declined in the complex condition relative to the simple condition, whereas no such decrease was observed in the control cohort (Fig. 3.7).

In this task, participants learned and later recalled discrete paired associates, allowing us to determine which individual associations were retained or forgotten following the 10-min rest period. Memory performance was quantified as the mean accuracy across all questions probing knowledge of each paired associate. Based on this measure, paired

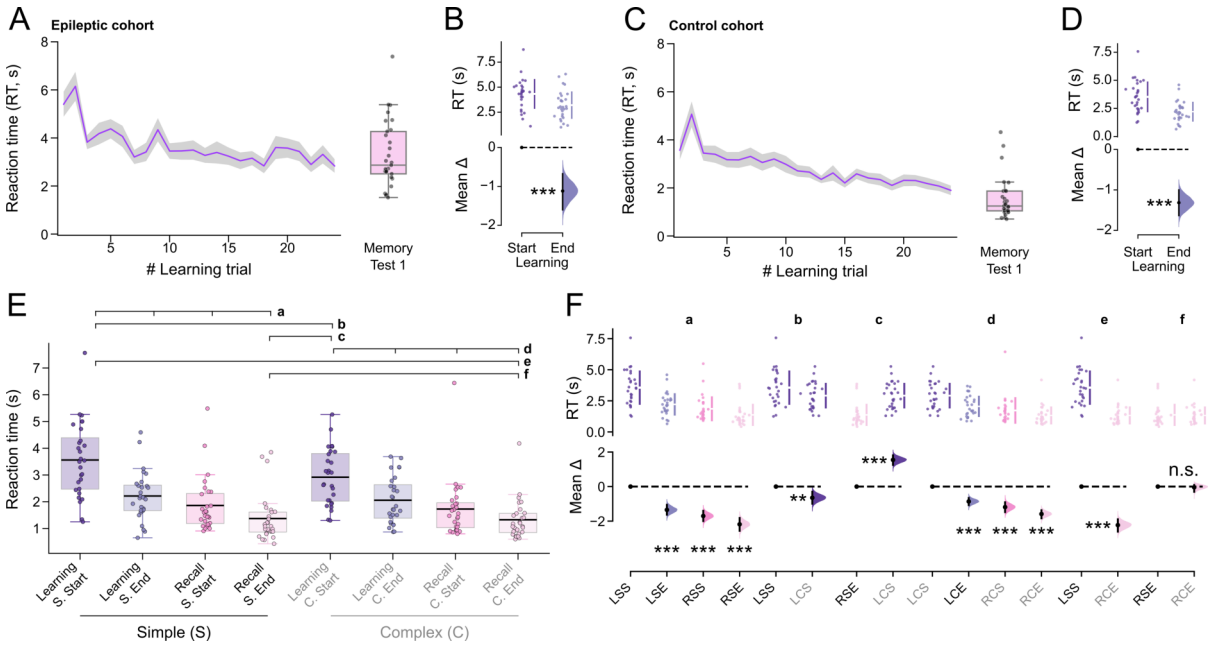


Figure 3.5: **Average reaction time in the relational memory task.** (**A**) Learning reaction time (in seconds, left) and average recall reaction time to type 1 memory questions (in seconds, right) in the cohort with epilepsy. (**B**) Estimation of the difference in learning reaction time between the average eight first (Start) or last (End) questions, in the cohort with epilepsy. (**C** and **D**) Same as in (A and B) but for the control cohort in the simple version of the task. (**E**) Box-and-whisker plot representing the reaction time to multiple-choice questions in learning and memory sessions, from the simple (S) and the complex (C) versions of the task, averaged across the eight first (Start) or last (End) questions, in the control cohort. Specific comparisons (a-f) used in F are displayed on this panel to improve clarity. (**F**) Estimation of the difference in reaction time between task stages presented in E. Data were analysed by two-sided paired permutation tests; ***P $<$ 0.001, **P $<$ 0.01, n.s., not significant.

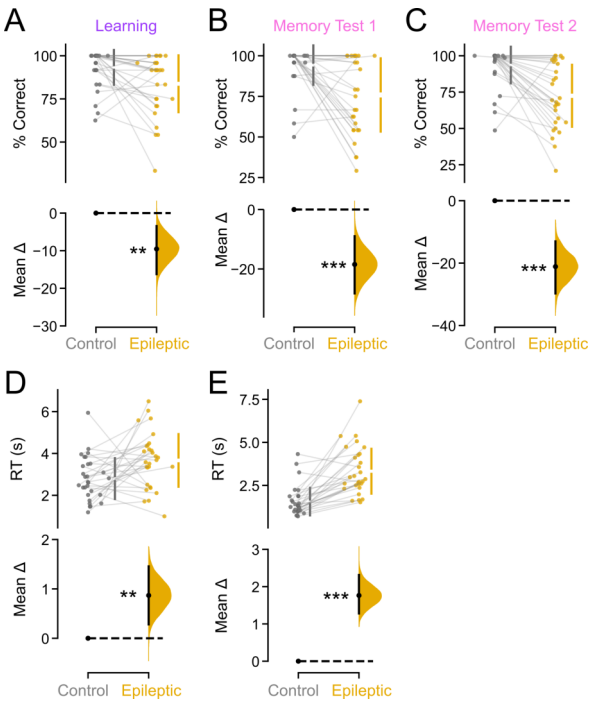


Figure 3.6: **Comparison of the behavioural performance between the two cohorts.** (**A**–**C**) Estimation of the difference in average accuracy (% correct responses) to the learning (A), direct memory (B) and indirect memory (C) questions between the epileptic and the control cohorts. (**D**–**E**) Estimation of the difference in average reaction time (in seconds) to the learning (D), direct memory (E) and indirect memory (F) questions between the epileptic and the control cohorts. Data were analysed by two-sided paired permutation tests; ***P $<$ 0.001, **P $<$ 0.01.

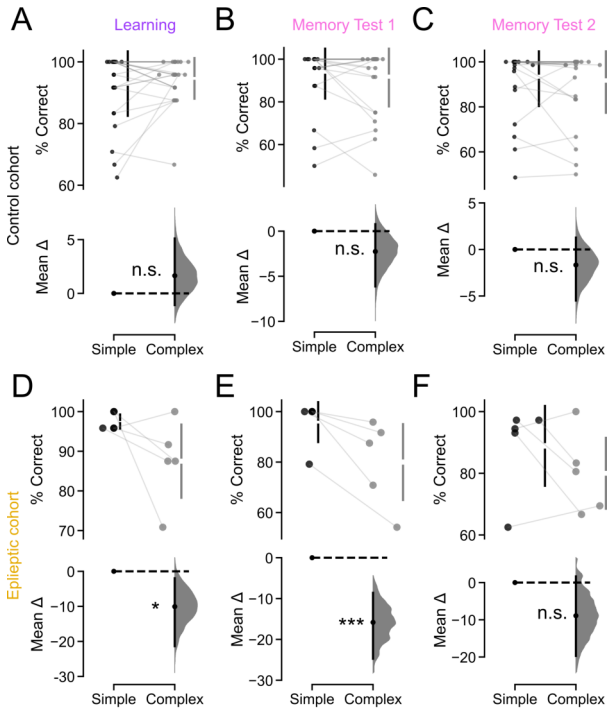


Figure 3.7: **Comparison of the behavioural performance between the simple and the complex versions of the task.** (**A**–**C**) Estimation of the difference in average accuracy (% correct responses) to the learning (A), direct memory (B) and indirect memory (C) questions between the simple and the complex versions of the task, in the control cohort. (**D**–**E**) Estimation of the difference in average accuracy (% correct responses) to the learning (D), direct memory (E) and indirect memory (F) questions between the simple and the complex versions of the task, in the epileptic cohort. Data were analysed by two-sided paired permutation tests; ***P $<$ 0.001, *P $<$ 0.05, n.s., not significant.

associates were ranked and divided into two categories: those with the highest and lowest subsequent memory accuracy (Fig. 3.8A-C).

Participants in the control cohort performed near ceiling on this relational memory task, with most individuals exhibiting ceiling-level accuracy for both simple and complex memory questions (Fig. 3.7B,C). Consequently, controls showed a reduced performance contrast between the best- and worst-remembered paired associates (Fig. 3.8D). These results confirm that the behavioural task was sufficiently sensitive to track changes in memory strength from acquisition through consolidation to recall in the epileptic cohort, while the performance of the control subjects was constrained by ceiling effects.

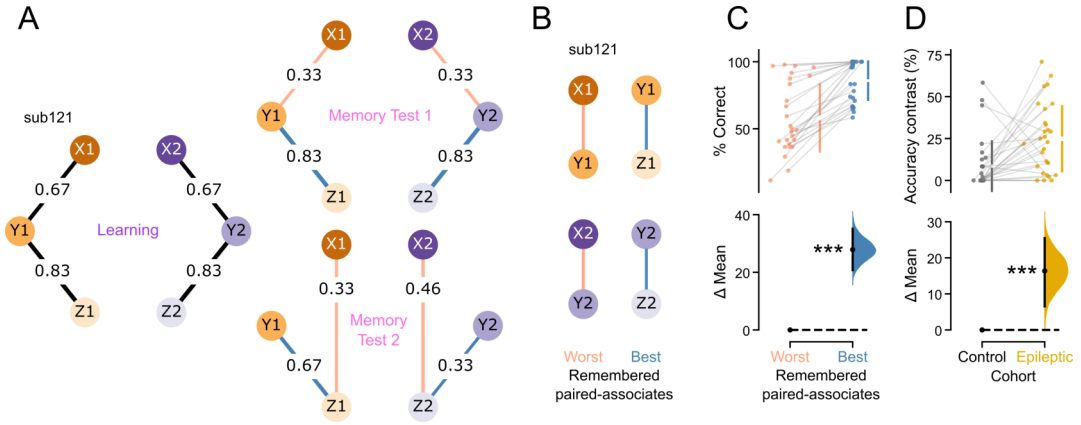


Figure 3.8: **Definition of best and worst remembered paired associates.** (**A**) Example graph showing the average performance for all learning and memory questions separated by paired associates (e.g., X1-Y1), in an example subject (sub121). As a reminder, the position of each member of the community is marked using a letter and a number (e.g., "X1"), and the structure of the community is described in Fig. 3.2. (**B**) In the example subject shown in A, Y1-Z1 and Y2-Z2 were the paired associates giving the highest average accuracy in the memory tests (best remembered), while X1-Y1 and X2-Y2 were the worst remembered. (**C**) Estimation of the difference in average memory performance for the best versus the worst remembered pairs, showing a 25% contrast on average. (**D**) Estimation of the difference in best versus worst contrast (% correct) between participants in the epileptic or the control cohort. Data were analysed by two-sided paired permutation tests; ***P $<$ 0.001.

Altogether, these findings suggest that the relational memory task was well calibrated to probe memory acquisition and delayed recall over a 10-minute interval in participants with epilepsy. Although performance was lower than in matched control subjects, participants successfully learned and retained the paired associates, with substantial variability across individual associations and levels of task difficulty. This within-subject variability will be leveraged in subsequent analyses examining the neural correlates of learning and memory in the epilepsy cohort (Chapter 4).

Moreover, we also observed a substantial variability in performance between subjects, with some participants exhibiting ceiling accuracy while others performed near chance-level, in particular for memory questions (Fig. 3.7). In the next section, we examine the factors contributing to this between-subject variability.

3.III.2 Variability of performance between subjects

3.III.2.a Demographic and cognitive contributors

Behavioural performance showed substantial variability across subjects, in particular in the epilepsy cohort (Chapter 3.III.1.a). To better characterize this diversity of responses, we first evaluated the relationship between task performance and the two main demographic measures: age and educational level.

To do this, we modelled both task accuracy and reaction time as functions of age and educational level. Because accuracy values are bounded between 0 and 1, accuracy was analysed using beta regression with a logit link function, which is appropriate for proportion data. Prior to model fitting, accuracy values equal to 0 or 1 were adjusted using the Smithson-Verkuijlen correction to map them to the open interval (0,1). Educational level was mean-centred before inclusion in the models. Reaction times, which are strictly positive and right-skewed, were analysed using a GLM assuming a Gamma distribution with a logarithmic link function. This modelling approach ensures positive fitted values and captures the multiplicative structure of reaction time variability. Models were fitted using raw reaction time values, with the log link accounting for the positive, right-skewed nature of the response.

For both accuracy and reaction time, separate models were fitted including age and educational level as predictors. Model fit was assessed using Cox-Snell pseudo-R^2, and predictive performance was quantified using the Pearson correlation between observed and model-predicted values on the response scale. Cox-Snell pseudo-R^2 is a likelihood-based measure of model fit for generalized linear models, where larger values indicate that the model explains the data better relative to a null model with no predictors. For example, values near 0 indicate little improvement over the null model, values around 0.2–0.4 suggest moderate explanatory power, and values above 0.5 indicate relatively strong model fit.

In both the epileptic and control cohorts, learning accuracy showed a modest association with educational level, whereas no reliable relationship with age was observed (Fig. 3.9A,D). In the epileptic cohort, educational level was a significant positive predictor of accuracy for both types of memory questions (Fig. 3.9B,C), while age did not significantly influence performance. In contrast, in the control cohort, accuracy on the memory questions was not significantly related to either age or educational level (Fig. 3.9E,F). Importantly, this apparent absence of demographic effects in controls must be interpreted with caution, as accuracy values in this population were strongly clustered near ceiling, thereby limiting variability and reducing statistical power to detect such relationships (Fig. 3.7B,C).

In both the epileptic and control cohorts, reaction time showed systematic associations with demographic variables, although the strength and consistency of these relationships differed between groups (Fig. 3.10). In the control cohort, both age and educational level reliably predicted reaction time across learning and memory phases, with older age associated with slower responses and higher educational level associated with faster responses (Fig. 3.10C,D). In contrast, in the epileptic cohort, demographic effects on reaction time were weaker and less consistent. During learning, reaction time was not reliably predicted by either age or educational level (Fig. 3.10A), whereas during the memory phase, educational level, but not age, showed a modest association with faster

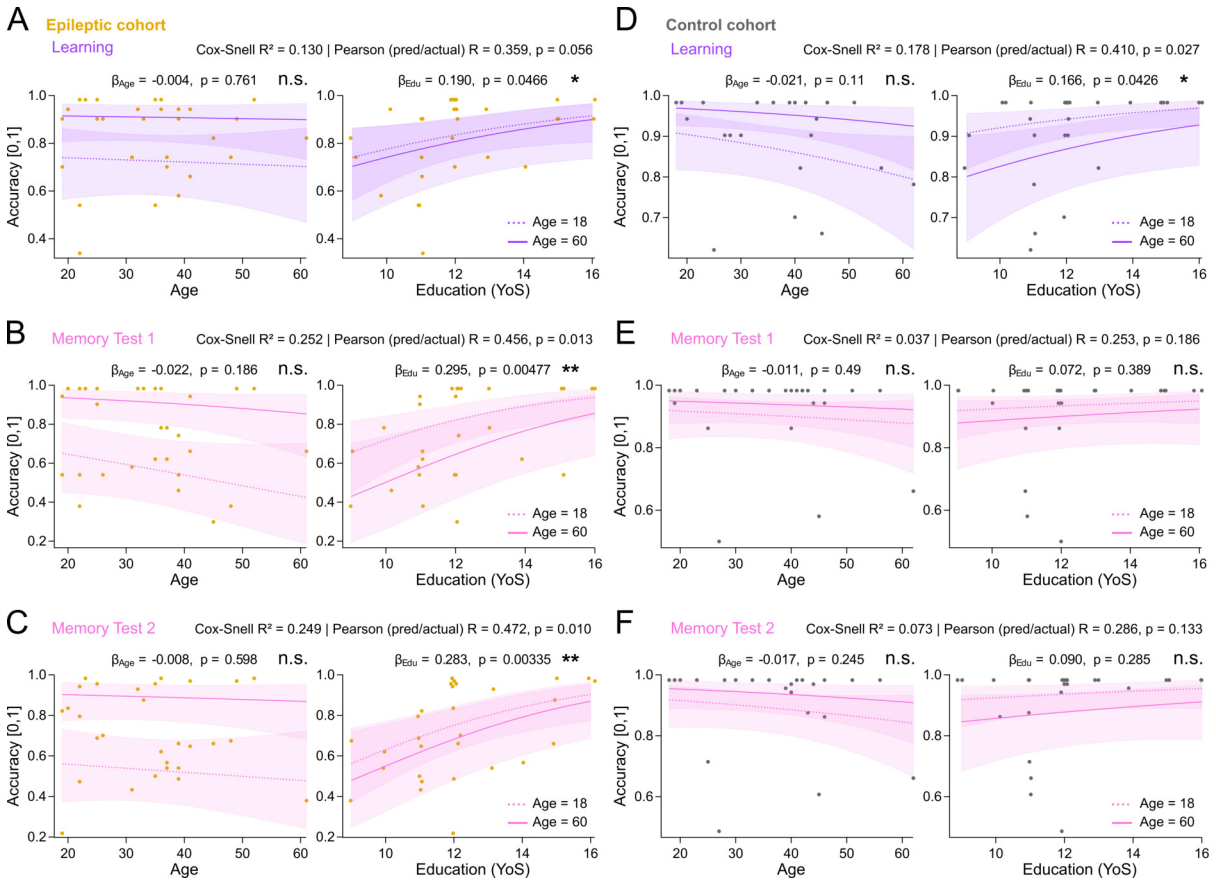


Figure 3.9: **Accuracy as a function of age and educational level.** Accuracy was modelled using beta regression with a logit link, including age and educational level (years of schooling, YoS) as predictors. (**A**–**C**) Epileptic cohort and (**D**–**F**) control cohort. For each cohort, panels show results for the learning phase (**A**, **D**), memory test 1 (**B**, **E**), and memory test 2 (**C**, **F**). In each panel, the left subpanel depicts predicted accuracy as a function of age at two extreme levels of education (YoS = 9 and 16), while the right subpanel depicts predicted accuracy as a function of educational level at two extreme ages (18 and 60 years). Solid and dotted lines represent model-predicted marginal effects, computed while holding the non-plotted covariate constant. Shaded areas indicate 95% confidence intervals for the estimated mean accuracy. Dots represent individual participant data. Model fit is summarized above each panel using Cox–Snell pseudo-R^2 and the Pearson correlation between observed and predicted accuracy values. Regression coefficients (β) and associated p-values are reported for age and education. **P < 0.01, *P < 0.05, n.s., not significant.

responses (Fig. 3.10B).

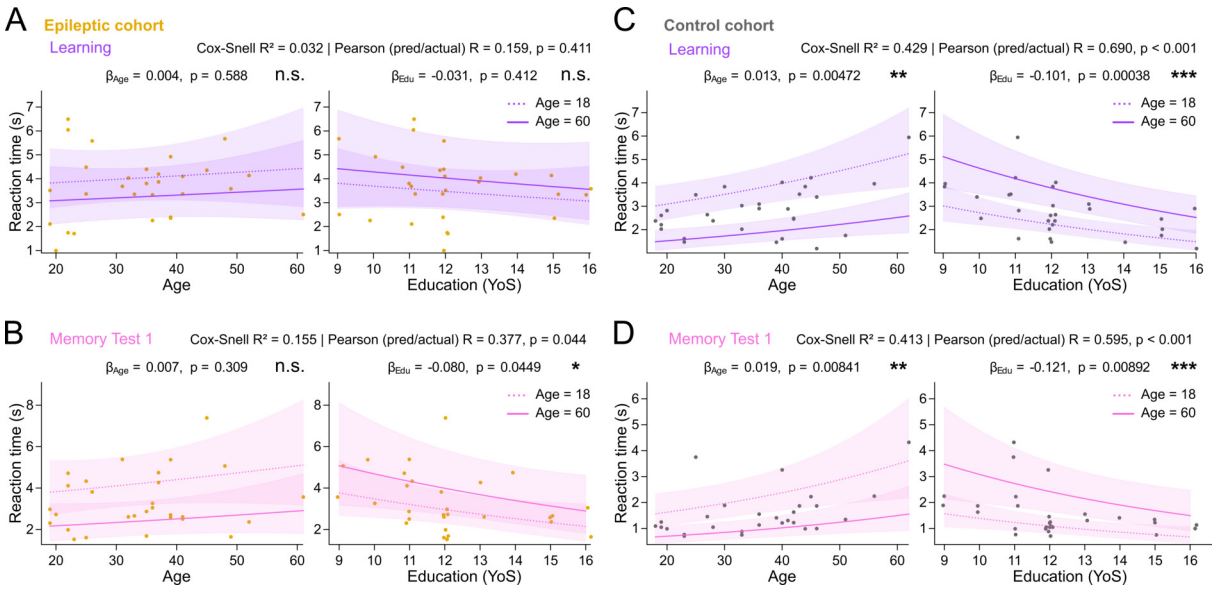


Figure 3.10: **Reaction time as a function of age and educational level.** Reaction times were modelled using GLMs with a Gamma distribution and a logarithmic link function, including age and educational level (years of schooling, YoS) as predictors. (**A**–**B**) Epileptic cohort and (**C**–**D**) control cohort. For each cohort, panels show results for the learning phase (**A**, **C**) and memory test 1 (**B**, **D**). In each panel, the left subpanel depicts predicted reaction time as a function of age at two extreme levels of education (YoS = 9 and 16), while the right subpanel depicts predicted reaction time as a function of educational level at two extreme ages (18 and 60 years). Solid and dotted lines represent model-predicted marginal effects, computed while holding the non-plotted covariate constant. Shaded areas indicate 95% confidence intervals for the estimated mean reaction time. Dots represent individual participant data. Model fit is summarized above each panel using Cox–Snell pseudo-R^2 and the Pearson correlation between observed and model-predicted reaction times. Regression coefficients (β) and associated p-values are reported for age and education. ***P < 0.001, **P < 0.01, *P < 0.05, n.s., not significant.

These results can be interpreted in two different ways. First, education could be a protective factor against the cognitive decline in participants with epilepsy. Alternatively, epilepsy occurring early in life may disrupt schooling, making education more difficult to complete and thereby indirectly affecting cognitive performance later in life. In order to distinguish between these explanations, we examined the relationship between age at epilepsy onset and accuracy in the memory task while controlling for age at inclusion in the study (Fig. 3.11). Age at onset was a positive predictor of accuracy on memory questions (Fig. 3.11B), indicating that earlier epilepsy onset was associated with lower cognitive performance. This finding supports the interpretation that early-onset epilepsy may contribute to later cognitive deficits, potentially through its impact on education and schooling.

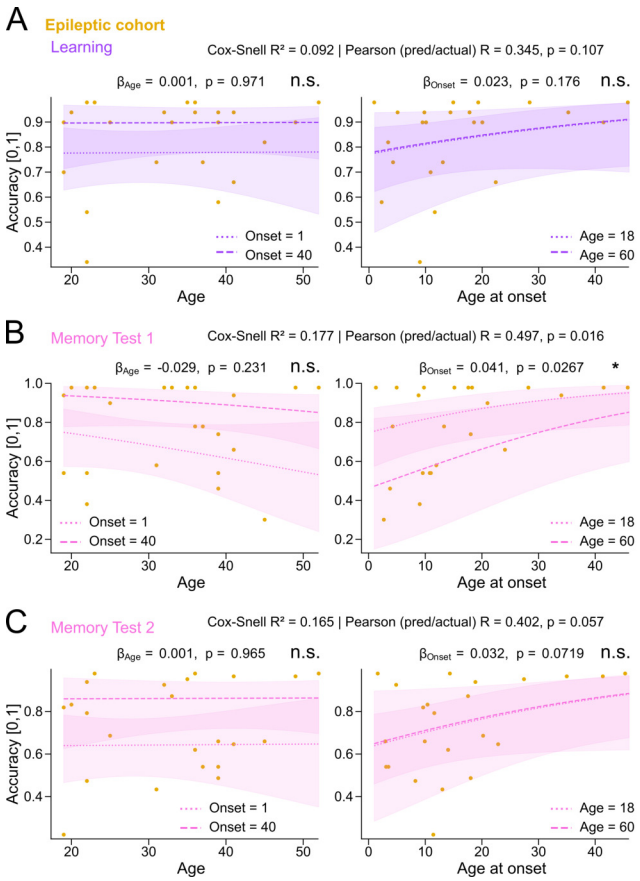


Figure 3.11: **Accuracy as a function of age at onset of epilepsy.** Accuracy was modelled using beta regression with a logit link, including age at inclusion in the protocol and age at onset of epilepsy as predictors. Panels show results for the learning phase (**A**), memory test 1 (**B**), and memory test 2 (**C**). In each panel, the left subpanel depicts predicted accuracy as a function of age at two extreme ages at onset (Onset = 1 and 40), while the right subpanel depicts predicted accuracy as a function of age at onset at two extreme ages at inclusion (18 and 60 years). Solid and dotted lines represent model-predicted marginal effects, computed while holding the non-plotted covariate constant. Shaded areas indicate 95% confidence intervals for the estimated mean accuracy. Dots represent individual participant data. Model fit is summarized above each panel using Cox–Snell pseudo-R^2 and the Pearson correlation between observed and predicted accuracy values. Regression coefficients (β) and associated p-values are reported for age at inclusion in the study and age of onset of epilepsy. *P < 0.05, n.s., not significant.

3.III.2.b Standardised cognitive testing

Before their stay at the hospital for the diagnosis of the epileptic focus, patients with epilepsy performed a battery of cognitive tests which help quantify the extent of their cognitive deficit. These tests were run by a trained clinical psychologist, and helped refine diagnosis and patient care. To further characterize the cognitive profile of the participants with epilepsy included in this study, we collected these metrics from the Toulouse cohort and compared the average scores between the high and low memory performers in our memory task. High and low performers had >75% and <75% performance on both types of memory questions, respectively.

Verbal memory was assessed using immediate recall of the Story Test from the Signoret Memory Efficiency Battery, evaluating episodic verbal memory. Visual memory was evaluated with the Rey-Osterrieth Complex Figure Test, assessing visuospatial memory through delayed reproduction. Language was assessed using the DO80 Oral Picture Naming Test, measuring lexical retrieval, and animal semantic fluency, assessing semantic access and verbal production. Attention was evaluated with Trail Making Test Part A (TMT-A), measuring visual scanning and processing speed, and the Zazzo Double Cancellation Test, assessing selective and sustained attention. Working memory was measured using the Backward Digit Span Test, evaluating short-term retention and information manipulation. Executive functions were assessed using the Stroop Color and Word Test, measuring inhibitory control, the TMT B-A completion time difference, reflecting cognitive flexibility, and phonemic verbal fluency for the letter "P", assessing strategic retrieval and executive search processes. Tests with insufficient participant completion were excluded.

All participants with epilepsy showed impaired performance relative to normative data, in line with previous literature (Fig. 3.12A) (Black et al. 2010; Dinkelacker et al. 2016; Wang et al. 2020; Phuong et al. 2021). We then examined differences between higher and lower performers in the relational memory task to determine whether one group exhibited greater cognitive deficits. No significant differences were observed between higher and lower performers for verbal memory, visual memory, language, or attention. In contrast, significant group differences were observed for working memory and were highly significant for executive functions, with lower normative scores in the lower-performers group (Fig. 3.12B).

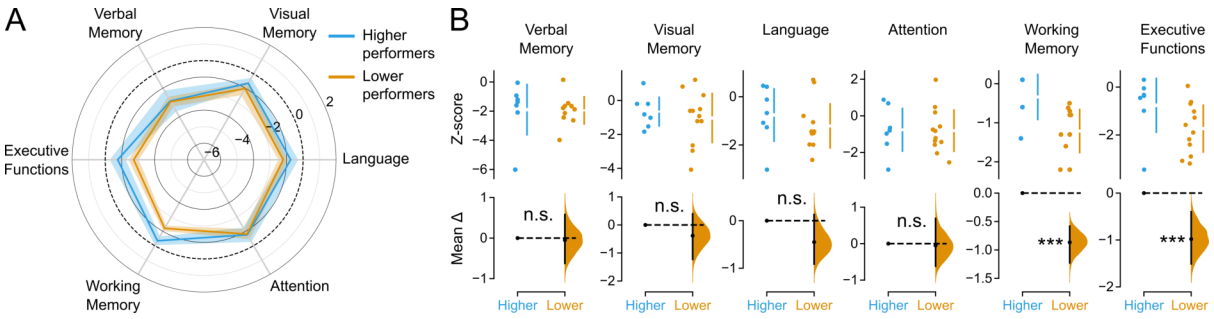


Figure 3.12: **Neuropsychological factors associated with memory performance.** (**A**) Polar plot showing the average neuropsychological metrics (z-score) obtained by higher and lower task performers during the pre-implantation screening. Dashed black circle indicates z-score = 0, corresponding to the average score in the reference population. Shaded areas indicate SEM. (**B**) Estimation of the difference in z-scores between the higher and lower performers for the six neuropsychological metrics displayed in (A): verbal memory, visual memory, language, attention, working memory, executive functions. Data were analysed by two-sided unpaired permutation tests, ***P < 0.001, n.s., not significant.

3.IV Discussion

This chapter describes the behavioural task employed to investigate the neural mechanisms of the two-stage model of memory in human participants. Using a relational memory task based on paired associates embedded within a social community, I showed that participants with epilepsy were able to learn and retain relational associations across wake and post-learning rest periods. Behavioural performance progressively improved during learning and remained significantly above chance during recall, indicating successful acquisition and retrieval of the community structure. Importantly, the task generated substantial variability across paired associates, across task difficulty levels and across participants. Compared with paired control participants, participants with epilepsy showed lower accuracy and slower reaction times, particularly during memory retrieval, consistent with previously described cognitive deficits associated with epilepsy (Black et al. 2010; Dinkelacker et al. 2016; Wang et al. 2020; Phuong et al. 2021). Nevertheless, the task remained sufficiently sensitive to distinguish best- and worst-remembered associations within subjects and best and worst performers, providing a useful contrast for subsequent neural analyses (Chapter 4.III.2.c).

The near-ceiling performance of the control cohort is an important feature of the task. It indicates that the paradigm was sufficiently sensitive to reveal cognitive deficits in the epileptic cohort, but it also suggests that it had limited range for detecting fine-grained variability among control participants. In other words, the task was well calibrated to the cognitive capacities of the participants with drug-refractory epilepsy, but less informative for probing inter-individual differences in a standard population. Adapting this paradigm to healthy participants would likely require increasing task difficulty, for example by reducing the number of repetitions or increasing the complexity of the social community. This ceiling effect should therefore be kept in mind when interpreting the absence of strong demographic effects in controls.

Reaction time in this task should also be interpreted with caution and not be treated as a pure measure of memory strength. Reaction times progressively decreased across learning in both cohorts, but did not scale monotonically with task difficulty. Comparisons between the simple and complex versions of the task further suggested that this effect could not be simply explained by memory load or motor learning. Rather, reaction time likely reflected a combination of mnemonic, cognitive, and procedural factors, including confidence, familiarity with the task structure, and motor execution. Hence, in the following chapters I will focus on accuracy as a readout of memory performance, within and between participants, in order to identify neural processes more closely linked with mnemonic processing.

I further showed that behavioural variability was partially associated with demographic and neuropsychological factors. Educational level was positively associated with memory performance in the epileptic cohort, while earlier onset of epilepsy predicted lower memory accuracy. These results suggest that education should not be interpreted solely as a protective factor. Rather, education may partly reflect the cumulative impact of epilepsy on development, schooling, and cognitive opportunity, particularly when seizures begin early in life. In addition, lower performers exhibited more pronounced impairments in working memory and executive functions compared with higher performers. This association suggests that successful performance in this relational memory task depended on more than associative memory alone. Participants had to maintain recently learned associations, update the structure of the social community, and select the correct response among distractors. These data suggest that relational memory performance in epilepsy may reflect interactions between hippocampal memory processes and broader cognitive functions supporting attentional control, maintenance of information, and flexible response selection.

Together, these findings indicate that the relational memory task was well suited to this patient population while producing substantial within- and between-subject variability. By alternating periods of active wakefulness (learning and recall) with eyes-closed rest periods before and after learning, the task also enables us to investigate the dynamics of MTL electrophysiological activity within the two-stage model of memory processing. In the following chapters, I describe the neural signatures of MTL, and particularly hippocampal, activity during wakefulness (Chapters 4 and 5) and rest (Chapter 6).

4 Results: A 2-Hz rhythm dominates LFPs in the human hippocampus

"La mémoire est, par essence, un fait biologique ; par accident, un fait psychologique."
"Memory is, in essence, a biological phenomenon; only incidentally is it a psychological one."
— Théodule Ribot, Les maladies de la mémoire (1888)

Contents

4.I Introduction 96
4.II Prominent 2-Hz bursts structure hippocampal LFPs 97
4.II.1 Recording hippocampal LFPs with sEEG in humans 97
4.II.2 Hippocampal LFPs are paced by a 2-Hz oscillation 98
4.II.3 Hippocampal 2-Hz oscillations are transient 102
4.II.4 Validation of 2-Hz oscillations 103
4.III Hippocampal 2-Hz is selectively evoked in the memory task 107
4.III.1 Hippocampal 2-Hz power increase with mnemonic engagement 107
4.III.2 Hippocampal 2-Hz bursts are evoked by mnemonic cues 108
4.III.3 Hippocampal 2-Hz oscillations are not evoked by motor activity 112
4.IV Discussion 116

4.I Introduction

In the general introduction, I argued that oscillatory activity provides a useful mechanism for linking memory representations across scales, from local neuronal assemblies to distributed brain networks (Chapter 1.III.2). According to this view, theta oscillations occupy a special place because they are associated in animal models with active behavioural states, including exploration, sensory acquisition, and memory-guided behaviour (Vanderwolf 1969; Winson 1972; Winson 1978; Buzsáki 2002; Derdikman and Knierim 2014). During these states, theta rhythms are thought to organize neuronal firing and to structure communication within the hippocampal system, thereby supporting online memory processing (O'Keefe and Recce 1993; Buzsáki 2010; Lisman and Jensen 2013; Colgin 2016).

Whether the human hippocampus expresses a comparable slow-oscillatory rhythm remains an open question. As discussed in the general introduction, human sEEG studies have reported heterogeneous slow-frequency oscillations during memory and navigation tasks, with variations across tasks and frequency ranges (Chapter 1.IV.1). Hence, the first step in identifying a putative human homologue of hippocampal theta requires determining not only whether a slow rhythm is present, but also whether it exhibits the behavioural-state dependence characteristic of theta in animal models, namely increased expression during mnemonic engagement and reduced expression during resting states.

The relational memory task introduced in the previous chapter is suitable for addressing this question (Chapter 3). Because it engages associative learning and retrieval, it allows us to examine how hippocampal oscillatory components vary across periods of rest, viewing, learning, and recall. Importantly, the task includes both eyes-closed resting sessions and viewing periods in which participants process visual stimuli without explicit mnemonic demands, providing two control conditions for dissociating memory-related oscillations from spontaneous resting dynamics or passive sensory processing. Hence, this design is appropriate to test whether any dominant slow oscillation in the human hippocampus is selectively linked to mnemonic engagement, rather than reflecting visual stimulation alone.

In this chapter, I therefore use direct hippocampal recordings from human participants performing the relational memory task to test the existence of a dominant slow oscillatory regime expressed during wakefulness. I first identify the principal slow-frequency components in hippocampal LFPs using an unsupervised decomposition approach. I then ask whether any of these rhythms is enhanced during mnemonic engagement and associated with behavioural performance. Finally, because recordings obtained in patients with drug-refractory epilepsy require particular caution, I evaluate whether the detected rhythms are compatible with physiological signals rather than pathological or artifactual phenomena secondary to our recording method.

Together, these analyses aim to determine whether the human hippocampus expresses one or more dominant slow rhythms during memory-guided behaviour, and whether its (or their) behavioural correlates resemble those expected from theta-like oscillations.

4.II Prominent 2-Hz bursts structure hippocampal LFPs

4.II.1 Recording hippocampal LFPs with sEEG in humans

To characterize hippocampal network activity in humans, we recorded LFPs directly from the hippocampus using sEEG. Thirty-five participants undergoing clinical monitoring for pharmacoresistant epilepsy in two centers (Toulouse and Paris) were included in this study. Electrode implantation followed clinical requirements only. Because the MTL is commonly involved in seizure networks (Barba et al. 2021), electrodes were often implanted in the hippocampus (Fig. 4.1A). In this manuscript, we focussed on participants with at least one electrode implanted in the hippocampus. Participants were implanted with standard and hybrid micro-macro depth electrodes (DIXI Medical® in

Toulouse or Ad-Tech® Behnke-Fried in Paris). Hybrid electrodes incorporated both macrocontacts and microelectrodes (tetrodes for DIXI Medical® electrodes or microwires for Ad-Tech® electrodes). For consistency across the two centers, macrocontacts were used to obtain LFPs and common average referencing was applied. Tetrodes were used to identify single-neuron activity next to the macrocontact (Fig. 4.1B) and are used from chapter 5.II.1 onward. Anatomical localization of each macrocontact was obtained by co-registering postoperative CT with preoperative MRI and mapping contacts to individual hippocampal volumes (Fig. 4.1C,D). For additional methodological details, see Chapter 2.I.1.

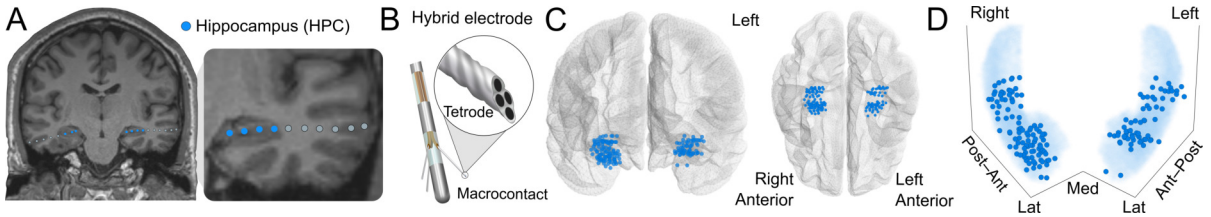


Figure 4.1: **Direct electrophysiological recordings from the human hippocampus.** (**A**) T1-weighted MRI showing contact locations from two representative depth electrodes targeting the hippocampus. (**B**) Each hybrid electrode incorporated tetrodes extending from the macrocontact shaft. (**C** and **D**) MNI template brain and 3D projection showing hippocampal electrode contact locations across participants (axes: Post-Ant; Med-Lat; Sup-Inf).

We further verified the location of hippocampal contacts along the antero-posterior and medio-lateral axes of each participant's hippocampus using their native three-dimensional segmentation (Fig. 4.2A,B). Coverage was denser in the head of the hippocampus than in the body, and virtually no contacts were located in the hippocampal tail (Fig. 4.2C,D).

4.II.2 Hippocampal LFPs are paced by a 2-Hz oscillation

Analysing brain oscillations often involves assuming that a given biological signal lies within a strict frequency range. This approach is efficient when this biological phenomenon is well established such as theta oscillations in mice, but it constrains the analysis to prior knowledge. An alternative is to use unsupervised signal decomposition methods such as empirical mode decomposition (EMD). EMD decomposes LFPs into their constituent oscillatory components (referred to as intrinsic mode function (IMF)) without assuming fixed frequency bands (Huang et al. 1998). However, several factors can influence the spectral structure of LFPs across macrocontacts and subjects. As a result, the extracted IMFs may overlap in frequency (mode mixing, (Huang et al. 1999)) or may not be detected in a consistent manner across macrocontacts or participants (low consistency, (Clarke-Williams et al. 2024)) . These issues make it challenging to ensure that IMFs are reliably identified across subjects. To address these limitations, we used a recently introduced version of masked EMD, referred to as tailored-masked EMD (tmEMD) (Clarke-Williams 2022; Clarke-Williams et al. 2024). This approach introduces controlled masking signals during decomposition to reduce mode mixing and to improve the separation of oscillatory components. In addition, mask parameters are optimized across subjects, which increases the consistency of the detected components at the group level. tmEMD therefore provides

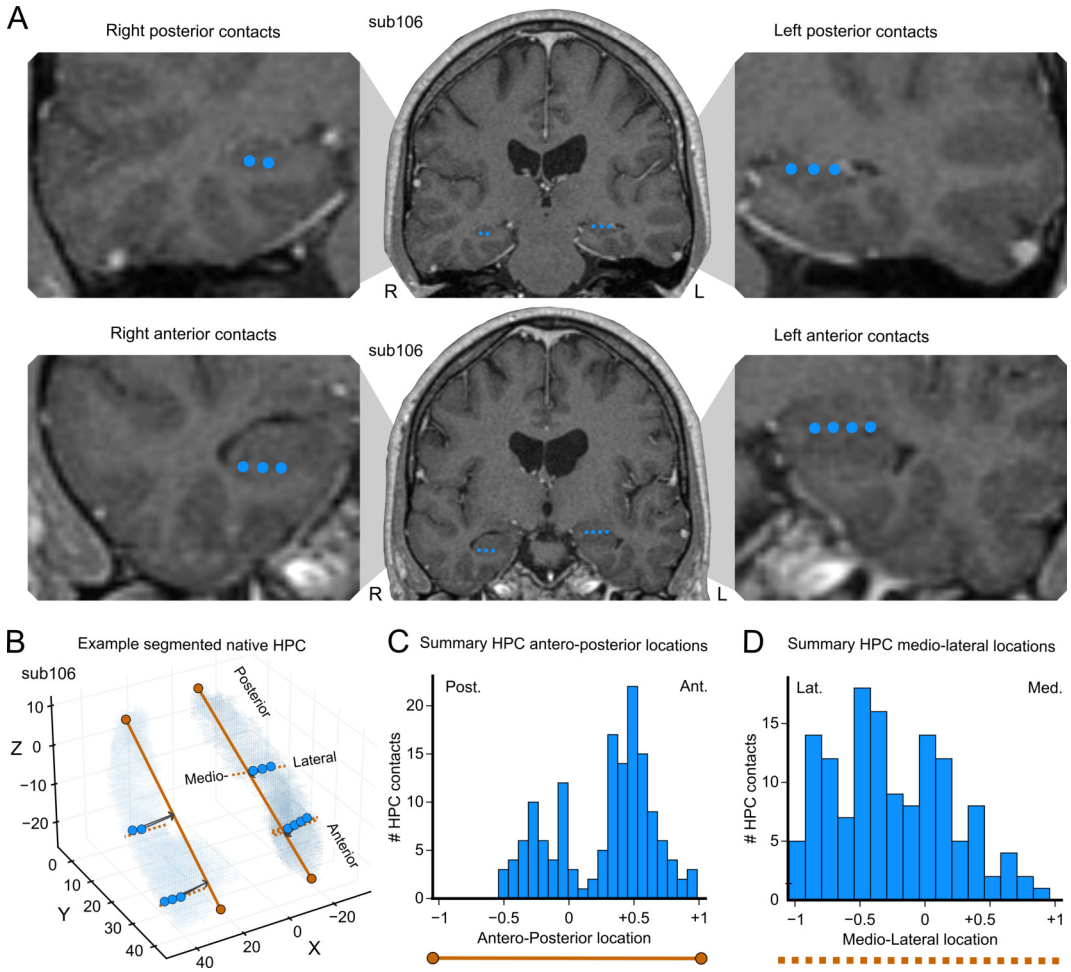


Figure 4.2: **Anatomical localization and distribution of hippocampal electrode contacts.** (**A**) T1-weighted MRI showing posterior (top) and anterior (bottom) hippocampal electrode contacts. Insets display higher magnifications of the right and left hemispheres. (**B**) 3D hippocampal volumes segmented from the same subject's MRI with contact locations (blue dots) overlaid. Solid and dotted brown lines mark the detected antero-posterior and medio-lateral axes, respectively. (**C** and **D**) Distribution of hippocampal contacts along the antero-posterior (C) and medio-lateral (D) axes across all participants. Of 170 contacts, 105 were located in the right hemisphere.

a more stable and interpretable decomposition of hippocampal LFPs than standard EMD, particularly in datasets with substantial inter-individual variability. Full methodological details are provided in Chapter 2.I.1.

In participants who were awake and watching screen displays, we detected one oscillation in the human hippocampus with a peak frequency around 6 Hz (peak [80% power band (PB)]: 6.15 [3.75–8.50] Hz). In addition, we identified two slower rhythms centred near 2 Hz [peak (80% PB): 2.38 (1.25–3.50) Hz] and 1 Hz [peak (80% PB): 1.08 (0.65–1.50) Hz] (Fig. 4.3).

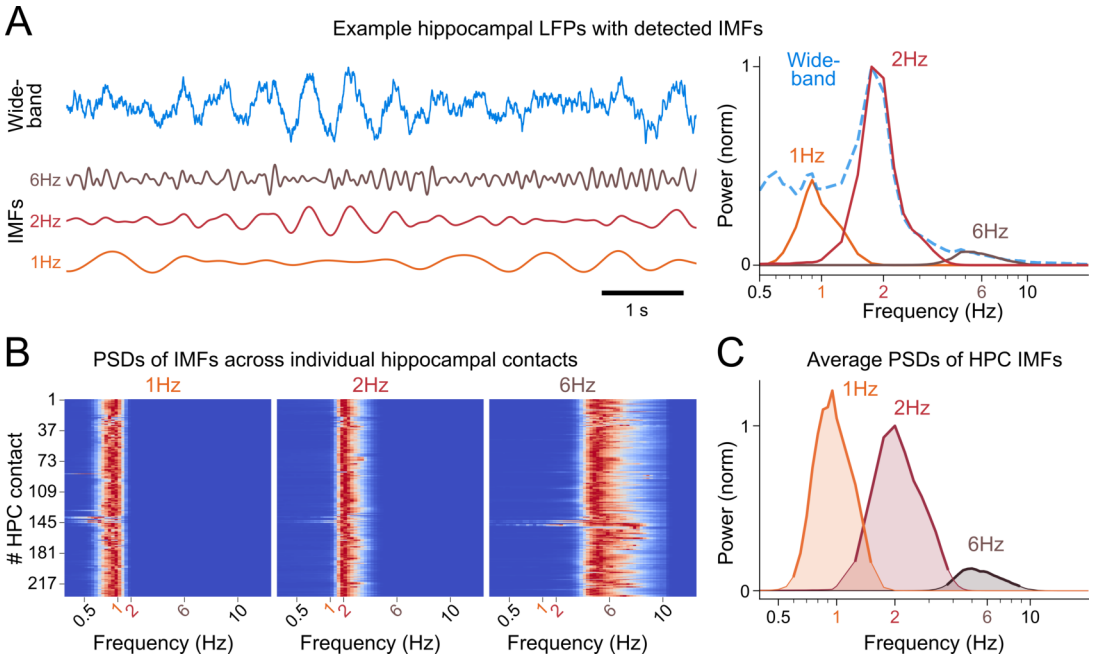


Figure 4.3: **Tailored Masked Empirical Mode Decomposition in the human hippocampus.** (**A**) Left: Example hippocampal wide-band LFP traces with IMFs. Right: Power spectral density (PSD) of the wide-band signal (dashed line) obtained from macrocontact recording and the corresponding 1-, 2-, and 6-Hz IMFs. Note that the 2-Hz component showed a prominent peak whose amplitude was well above what could be expected from the power law. (**B**) Heatmaps showing power distributions of 1-, 2-, and 6-Hz IMFs across all hippocampal contacts, illustrating that IMFs were consistently detected across participants. (**C**) Average power spectral densities across hippocampal contacts, normalized to the maximal 2-Hz power, showing that IMFs exhibited low mode mixing (thick lines indicate 80% power bands).

Alhough we detected 6-Hz oscillations in the human hippocampus, the most prominent oscillation visible in the raw LFPs traces were at 2 Hz (Fig. 4.3A). These 2-Hz oscillations were visible on both macrocontacts and tetrodes (Fig. 4.4).

We confirmed this observation by applying spectral parameterization (Donoghue et al. 2020); Chapter 2.II.3, which separates the periodic components of the PSDs from the broadband, aperiodic structure of the spectrum. This procedure allowed us to quantify narrow-band oscillatory peaks independently of differences in overall spectral slope across contacts or participants. After removing the aperiodic component, the periodic residuals showed components in the 2-Hz and the 6-Hz frequency bands in the hippocampus, but the

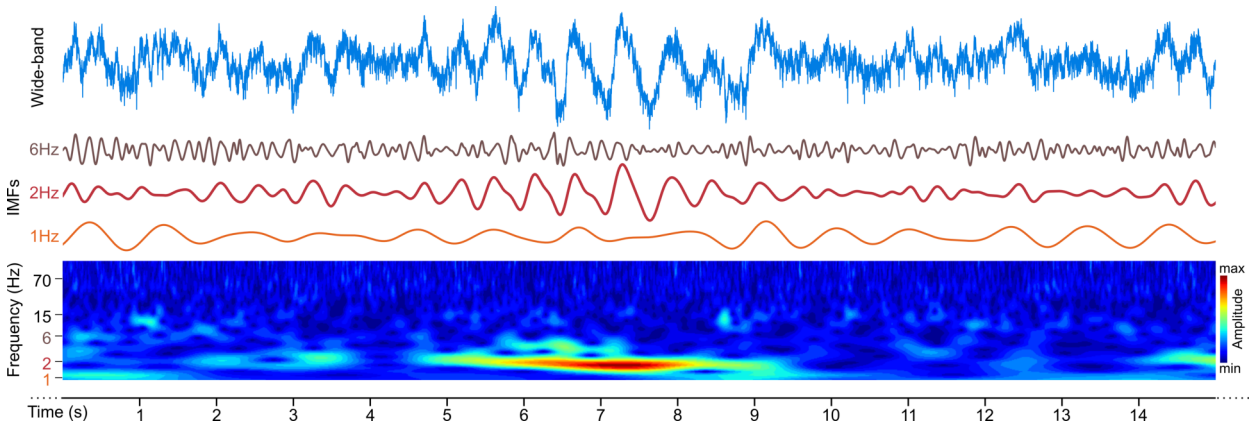


Figure 4.4: **Example hippocampal LFPs showing a 2-Hz burst.** Example 15-s hippocampal tetrode recording showing a prominent 2-Hz burst. From top to bottom: wide-band LFPs trace obtained from tetrode recording, IMFs, and the corresponding wavelet spectrogram. Note that the cycles were markedly non-linear (asymmetric), with the ascending phase being faster than the descending phase. This asymmetry was reported in a previous study (Penner et al. 2022), and reveals the need to use signal processing methods that are sensitive to non-linear signals, like the . This applies in particular to the analysis of 2-Hz to gamma phase-amplitude coupling (PAC), because linear filters are prone to non-specific interactions (Juan et al. 2021). This will be extensively discussed in Chapter 5.

predominant peak was clearly the 2-Hz component (Fig. 4.5A). Specifically, the corrected spectra yielded higher power at 2 Hz than at 1 Hz or 6 Hz (Fig. 4.5B), and the computed 2-Hz/6-Hz peak power ratio was consistently positive across hippocampal contacts (mean ratio [95% CI]: 0.21 [0.15-0.27]; Fig. 4.5C). These results suggest that hippocampal activity is dominated by a 2-Hz rhythm.

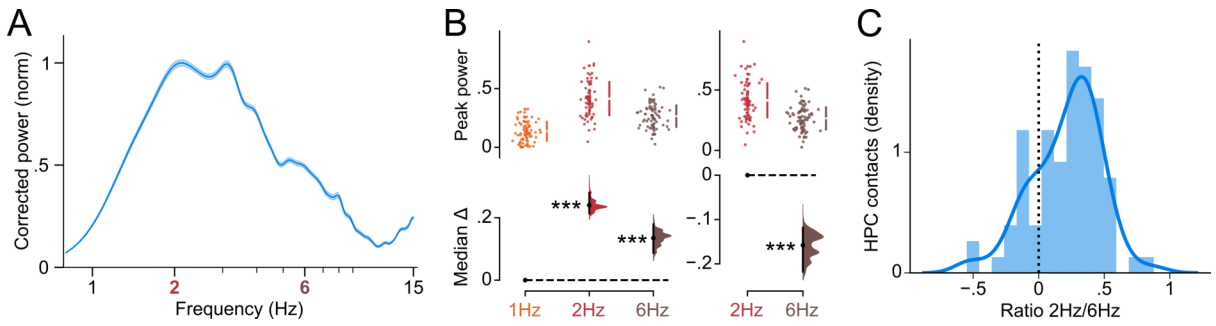


Figure 4.5: **2-Hz oscillations dominate in the human hippocampus.** (**A**) PSDs corrected for the power law and averaged across hippocampal macrocontacts free of IEDs. The dominant peak lies in the 2-Hz frequency band, while some activity is also visible in the 6-Hz band, consistent with our detection of this oscillatory component using EMD in Fig. 4.3. Shaded areas indicate mean ± SEM. (**B**) Estimation plots showing median differences between corrected 1-, 2-, and 6-Hz peak power (left), and between 2-Hz and 6-Hz peak power (right). (**C**) Distribution showing positive 2-Hz/6-Hz peak power ratios in hippocampal contacts. Data were analysed by two-sided paired permutation tests; ***P < 0.001.

4.II.3 Hippocampal 2-Hz oscillations are transient

Hippocampal 2-Hz activity appeared as transient oscillatory bursts and was observable across subjects and along the hippocampal formation (Fig. 4.6).

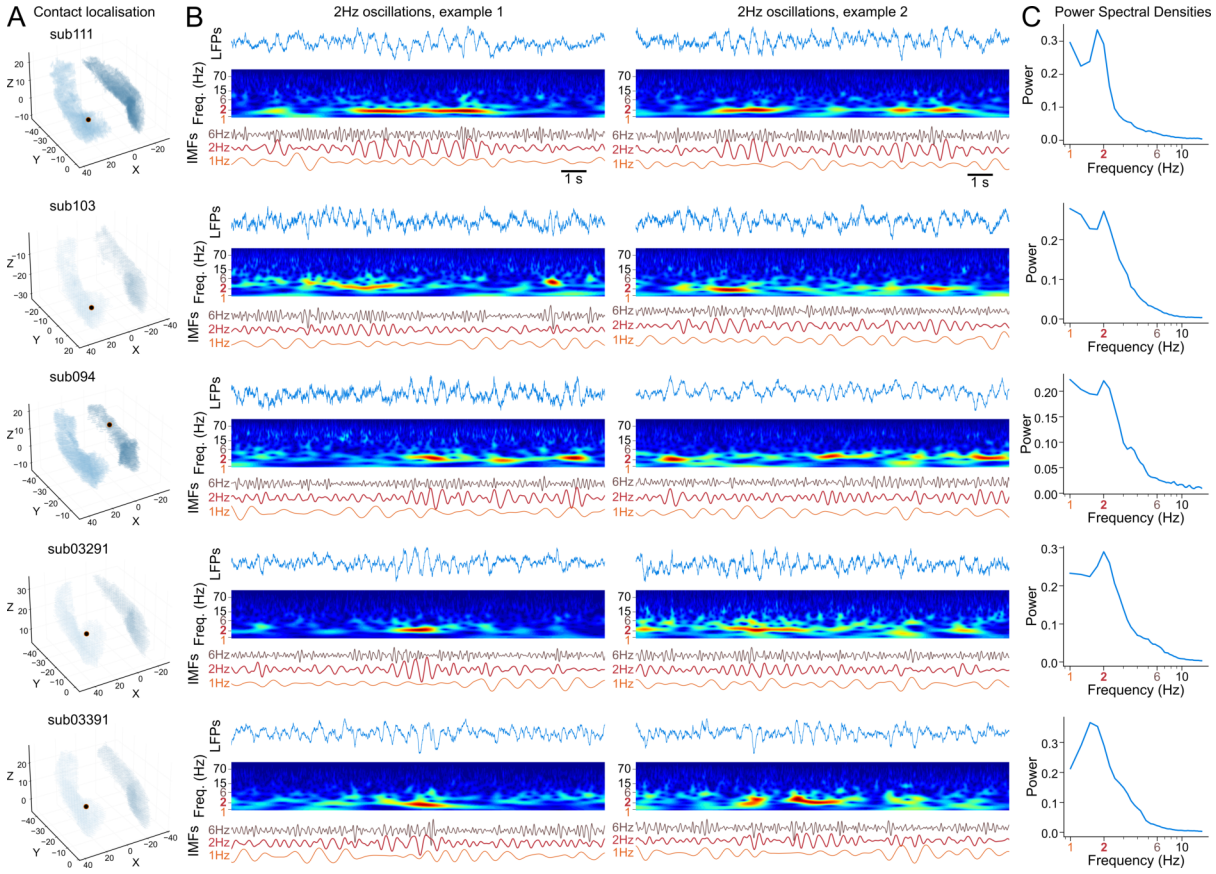


Figure 4.6: **Examples of hippocampal 2-Hz bursts.** (**A**) 3D hippocampal volumes showing electrode contact locations used in panels B and C. (**B**) Example 15-s hippocampal macrocontact recordings showing 2-Hz oscillations with corresponding spectrograms and (IMFs) from five participants (one row per participant). (**C**) PSDs averaged over the 10-min active sessions corresponding to the recordings shown in panel B. All contacts were free of IEDs (from top to bottom: 0, 0.34, 0.79, 0.33, and 0.24 discharges detected per minute).

To quantify these events, we used wavelet spectrograms to detect bursts defined as periods of increased power within the 1-4 Hz range, retaining only events lasting at least two oscillatory cycles (Fig. 4.7A). For each burst, we then measured onset, offset, and duration, expressed both in seconds and in number of cycles (Fig. 4.7B). Full methodological details are provided in Chapter 2.II.2. Across subjects, the maximal burst duration showed substantial variability (Fig. 4.7C), consistent with the transient expression of these 2-Hz events (mean maximal number [95% confidence interval (CI)]: 19.6 [15.8–23.4] cycles per burst).

Before interpreting this 2-Hz activity as a candidate hippocampal oscillation, it was important to verify that it reflected a genuine local signal rather than an artefact of recording, referencing, or epileptiform activity. This is particularly relevant in sEEG

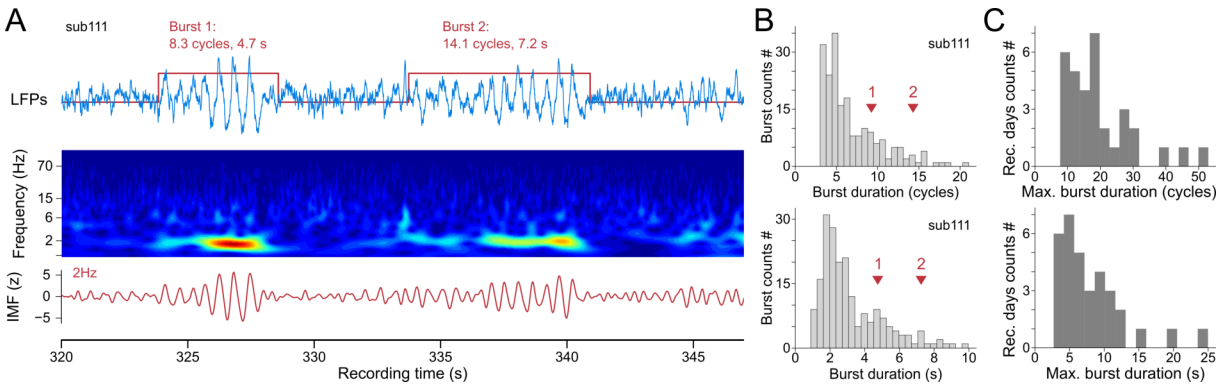


Figure 4.7: **Detection of hippocampal 2-Hz bursts.** (**A**) Example 27-s hippocampal LFP showing 2-Hz oscillatory bursts with corresponding spectrogram and 2-Hz IMF. (**B**) Distributions of burst durations measured in cycles (top) and seconds (bottom) for the hippocampal macrocontact shown in panel A. A total of 174 bursts lasting at least two cycles were detected in this recall session. Arrowheads indicate the durations of the two bursts visible in panel A. (**C**) Distributions of maximal burst duration in cycles (top) and seconds (bottom) per recording day across participants.

obtained from patients with drug-resistant epilepsy, where pathological activity and methodological choices can shape the spectral content of the LFPs. We therefore next evaluated several complementary features of the signal to assess whether the observed 2-Hz oscillations were consistent with a physiological hippocampal oscillation.

4.II.4 Validation of 2-Hz oscillations

4.II.4.a Phase reversal of hippocampal 2-Hz oscillations

Hippocampal pyramidal cells are arranged in a well-defined laminar structure, which creates a consistent somato-dendritic axis that allows oscillations to be detected in LFPs (Buzsáki et al. 2012). When large groups of these neurons receive synchronized post-synaptic currents, the resulting transmembrane currents sum in space and form a macroscopic current dipole. This dipole generates extracellular voltage gradients that can be measured by depth electrodes as LFPs. Because this dipole is aligned across the pyramidal layer, LFPs recorded on linearly arranged contacts, i.e., spanning the somato-dendritic axis, would show a phase reversal: a same oscillatory cycle will have opposed phase on contacts located on opposite sides of the dipole. In the human hippocampus, layers are organized along the para-sagittal axis thus the dipole lies predominantly along the medio-lateral axis. The trajectories of the electrode shafts in our recordings positioned adjacent macrocontacts along this medio-lateral axis (Fig. 4.2A, left anterior contacts and Fig. 4.8A). By taking the average LFPs from three neighboring macrocontacts aligned to the positive peaks of 2-Hz cycles detected on the deepest contact ("Hpc 1a" in Fig. 4.8A), we observed a clear 2-Hz phase reversal (Fig. 4.8B). We next quantified this reversal by extracting the 2-Hz instantaneous phase from IMFs on each macrocontact using the Hilbert transform, and applying circular statistics to determine the mean phase difference between all contact pairs (Fig. 4.8C). This reversal is consistent with a locally generated

oscillation rather than a volume-conducted signal from a distal source (see Chapter 5.II.1 for further evidence).

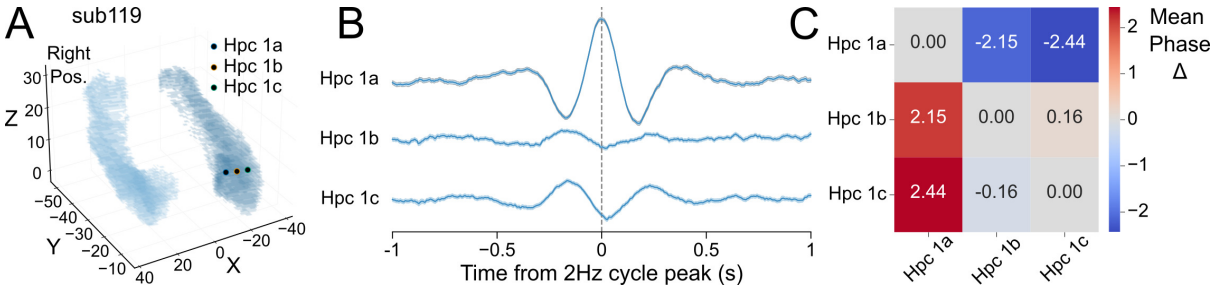


Figure 4.8: **Phase reversal of hippocampal 2-Hz oscillations.** (**A**) 3D hippocampal volumes showing three linearly arranged recording contacts from the same electrode shaft ("Hpc 1a, 1b, and 1c"). (**B**) Average LFP traces aligned to hippocampal 2-Hz oscillatory peaks, showing polarity reversal across adjacent contacts. Shaded areas indicate mean ± SEM. (**C**) Heatmap of average phase differences between the three contacts.

4.II.4.b Slow-oscillation amplitude and IEDs rate

Given that these recordings were obtained from participants with drug-resistant epilepsy we next verified that hippocampal 2-Hz was not a by-product of the underlying pathology. IEDs are a common feature of epilepsy (Dinkelacker et al. 2016) and can be reliably detected (Janca et al. 2015), Fig. 4.9 from sEEG (for further details on IEDs see Chapter 2.I.1). IEDs rate provides an objective measure of how strongly a given tissue is affected by epileptiform activity.

In these recordings, hippocampal macrocontacts with lower IEDs rates showed more prominent slow oscillations (Fig. 4.10). Consistently, 2-Hz power was negatively correlated with IEDs rate (Spearman $r = -0.25 P < 0.001$), whereas 6-Hz power showed no significant relationship (Spearman $r = 0.06, P = 0.336$). These results suggest that hippocampal 2-Hz rhythm is physiological and is not driven by epileptiform processes.

4.II.4.c Local reference impairs the detection of slow oscillations

Referencing has been shown to have an influence on the spectral content of the LFPs, and in particular local referencing methods such as bipolar or local reference can impair the detection of slow oscillations (Bódizs et al. 2001; Parish et al. 2023). To investigate whether this was the case in our recordings, we compared two re-referencing montages commonly used with macrocontacts (common-average reference (CAR) versus bipolar reference), and with microelectrodes (monopolar versus local reference). Bipolar and local reference involve subtracting signal from adjacent macrocontacts or tetrodes, respectively. Raw signals and in particular slow oscillatory bursts were dramatically affected by bipolar and local reference (Fig. 4.11A): they became either invisible or they showed inconsistent phase distortions (Appendix A). Across all hippocampal macrocontacts, bipolar/local reference impaired detectability of these slower oscillations (Fig. 4.11B–D). For this reason, all analyses in this manuscript use the CAR, which better preserves slow oscillatory

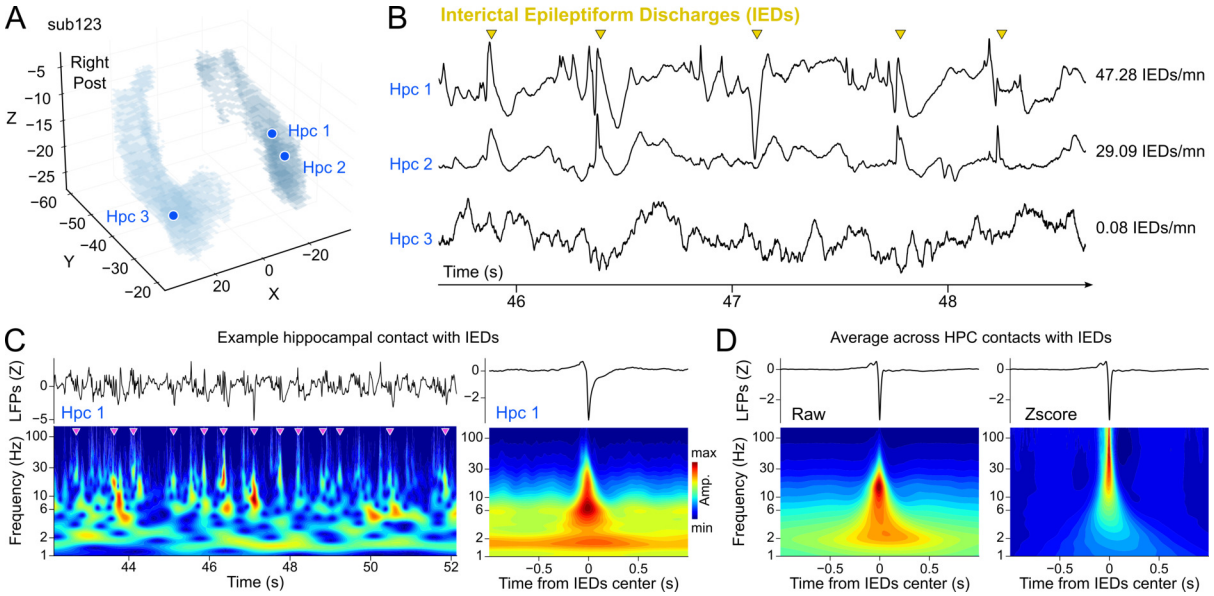


Figure 4.9: **Detection of interictal epileptiform discharges.** (**A**) 3D hippocampal volumes showing the three recording sites used in panel B. (**B**) Example simultaneous 3-s recording from three hippocampal contacts, with IEDs detected on "Hpc 1" (yellow arrowheads). (**C**) Example 10-s LFP trace and spectrogram from "Hpc 1" (left) and corresponding averages triggered by IEDs (right). (**D**) LFP and spectrogram averages triggered by IEDs across all hippocampal contacts before (left) and after z-scoring (right), showing a broadband power increase above 6 Hz.

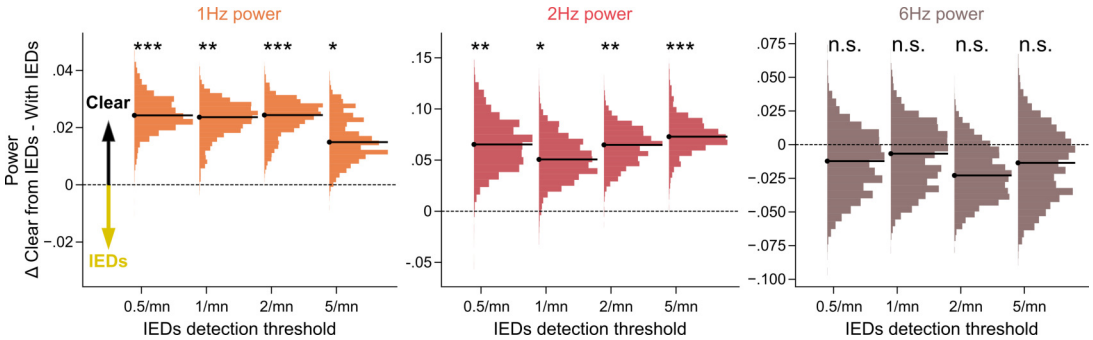


Figure 4.10: **Hippocampal slow oscillations are more prominent outside irritative zones.** Estimation plots showing median differences in 1-, 2-, and 6-Hz power between hippocampal contacts free of IEDs and those containing IEDs, as a function of the IED-rate threshold (0.5, 1, 2, and 5 min^{-1}). Data were analysed using two-sided paired permutation tests; ***P $<$ 0.001, **P $<$ 0.01, *P $<$ 0.05; n.s., not significant.

components. Further analyses related to the impact of local referencing on the detection of slow oscillations are presented in Appendix A.

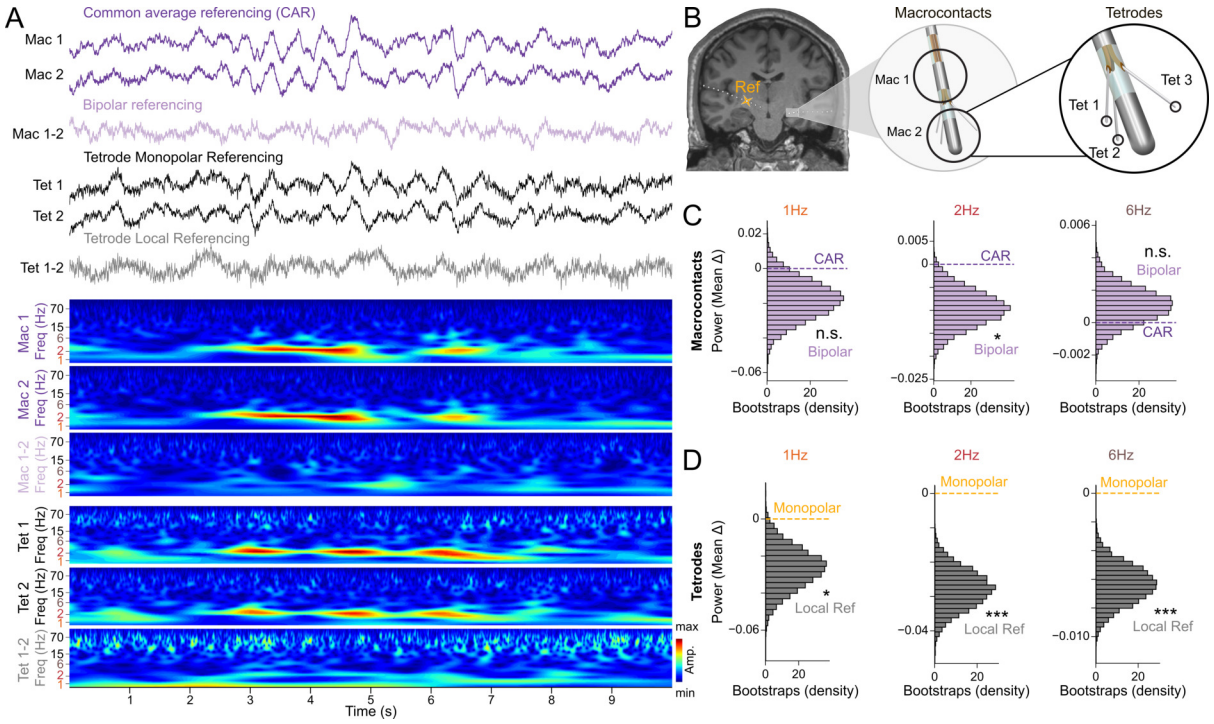


Figure 4.11: **Local reference impairs detection of slow oscillations.** (**A**) Example 10-s recording from a hybrid hippocampal electrode showing macrocontact LFPs traces re-referenced using a common average (CAR, purple) or a bipolar (pink) montage, and tetrode LFPs traces before (black) and after (gray) local reference, with corresponding spectrograms. (**B**) Schematic illustrating local reference: monopolar signals were initially acquired from a distal white-matter contact used as reference and then re-referenced either to the median computed across all macrocontacts (common average reference, CAR) or by subtracting adjacent macrocontacts (e.g., Mac 1 – Mac 2) or tetrodes (e.g., Tet 1 – Tet 2) from the same hybrid electrode. (**C** and **D**) Estimation plots showing mean differences in hippocampal 1-, 2-, and 6-Hz power after applying bipolar reference to macrocontacts (relative to CAR, panel C) and local reference to tetrodes (relative to monopolar, panel D). Data were analysed using two-sided paired permutation tests; ***P $<$ 0.001, *P $<$ 0.05; n.s., not significant.

Having established that the observed 2-Hz activity is consistent with a genuine hippocampal oscillation, the next question is when this rhythm is expressed during the task. Is it simply present during wakefulness in general, or is it specifically enhanced when participants are engaged in mnemonic processing? Does its expression follow changes in arousal, visual stimulation, or active memory demands? In the next section, we address these questions by examining how hippocampal 2-Hz activity varies across viewing, learning, recall, and rest.

4.III Hippocampal 2-Hz is selectively evoked in the memory task

Hippocampal theta oscillations in rodents increase during exploratory behaviour and during memory encoding and recall (Chapter 1.III.2.b). In rabbits, bats, and cats, they are also tightly linked with sensory acquisition and are therefore considered a key mechanism of active sensing (Chapter 1.III.2). If hippocampal 2-Hz oscillations constitute a comparable functional state in humans, they should similarly be enhanced during states of higher arousal, like mnemonic engagement, and evoked by memory-relevant visual cues. We therefore next examined how hippocampal 2-Hz bursts varied across the different stages of the relational memory task, and whether their expression tracked memory processing and behavioural performance.

4.III.1 Hippocampal 2-Hz power increase with mnemonic engagement

To address this question we compared the changes in oscillatory power while participants were engaged in the relational memory task presented in Chapter 3. Focussing on hippocampal macrocontacts free of IEDs, we observed that mnemonic engagement - here defined as task periods involving active acquisition or retrieval of associations rather than passive viewing - was associated with enhanced expression of the slow oscillatory component in the hippocampus. Indeed, 2-Hz oscillations exhibited significantly greater power during both learning and recall than during resting or viewing sessions (Fig. 4.13; learning, $P < 0.001$; recalling, $P = 0.006$; paired permutation tests compared to pre-learning rest).

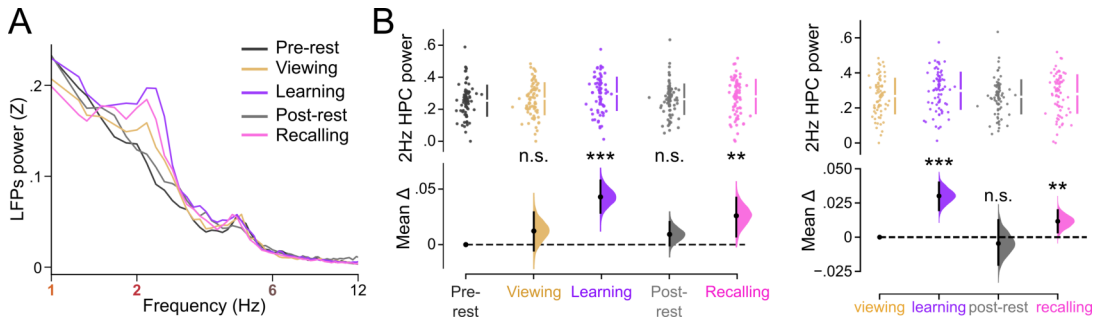


Figure 4.12: **Hippocampal 2-Hz power increases with mnemonic engagement.** (**A**) PSDs from an example hippocampal electrode contact across task stages. (**B**) Group-level estimation plot showing mean hippocampal 2-Hz power across task stages relative to pre-learning rest (left) or viewing (right). Data were analysed by two-sided paired permutation tests; ***$P < 0.001$, **$P < 0.01$; n.s., not significant.

No comparable modulation was seen for the 1-Hz or 6-Hz bands (Fig. 4.13A). Linear mixed-effects models (LMEMs) which included subjects as a random effect confirmed that this enhancement was specific to 2-Hz and did not extend to adjacent frequencies (Fig. 4.13B; learning, $P < 0.001$; recalling, $P = 0.040$; Wald tests). The recording day finished with a post-recall viewing session, which we used to confirm that the changes in oscillation power during the memory recall session were not merely reflecting passage of

time. Indeed, 2-Hz power in this post-recall viewing session was not different than in the pre-learning viewing session (P = 0.095, paired permutation tests; P = 0.464, Wald tests).

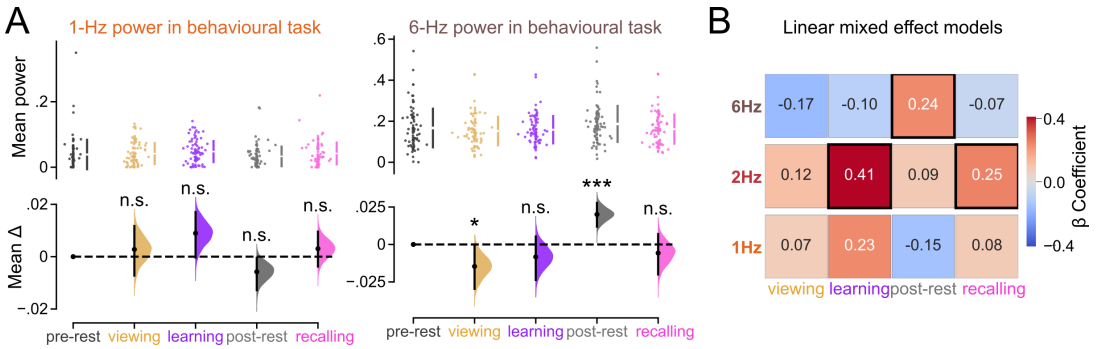


Figure 4.13: **Hippocampal oscillatory dynamics during the memory task — controls.** (**A**) Group-level estimation plot showing mean hippocampal 1-Hz (left) and 6-Hz (right) power differences relative to pre-learning rest. Data were analysed by two-sided paired permutation tests; ***P $<$ 0.001, *P $<$ 0.05; n.s., not significant. (**B**) Heatmap of β coefficients from a LMEM predicting hippocampal 1-, 2-, or 6-Hz power as a function of task stage (pre-learning rest as the reference level), with subject treated as a random effect. Data were analysed by two-sided paired permutation tests in A; in B, black squares indicate significant coefficients (Wald test, P $<$ 0.05). ***P $<$ 0.001, *P $<$ 0.05; n.s., not significant.

4.III.2 Hippocampal 2-Hz bursts are evoked by mnemonic cues

While hippocampal 2-Hz activity varies with overall mnemonic engagement of the participants, it remains unclear when these oscillatory bursts occur during the task. Because visual stimuli evoke strong ERPs in the hippocampus, which manifest as broadband, non-oscillatory deflections in the LFPs, it is essential to separate these evoked responses from genuine oscillatory activity. Thus, to tease apart 2-Hz bursts from these evoked responses, we next analyse LFPs dynamics at different times relative to stimulus onset.

4.III.2.a ERPs are modulated by mnemonic engagement

Hippocampal ERPs have been extensively studied in the early days of sEEG investigations (Halgren et al. 1980; Grunwald et al. 1998; Fernández et al. 1999; Trautner et al. 2004; Axmacher et al. 2010). This body of work has shown that the late ERPs deflection occurring at 600 ms post stimulus onset (hP600) was more pronounced for familiar as opposed to novel stimuli (Trautner et al. 2004; Barbeau et al. 2017), and it was modulated by memory (Fernández et al. 1999). Hence, we first aimed at replicating these results in our behavioural task. For this, we measured average LFPs after the onset of photographs in the viewing, learning and recalling phases of the memory task (Fig. 4.14).

Consistently with earlier reports, the magnitude of the ERP deflection (hP600) was greater after the onset of learning and recalling photographs than after viewing photographs (Fig. 4.15A). This effect could simply be due to the habituation of the visual system to

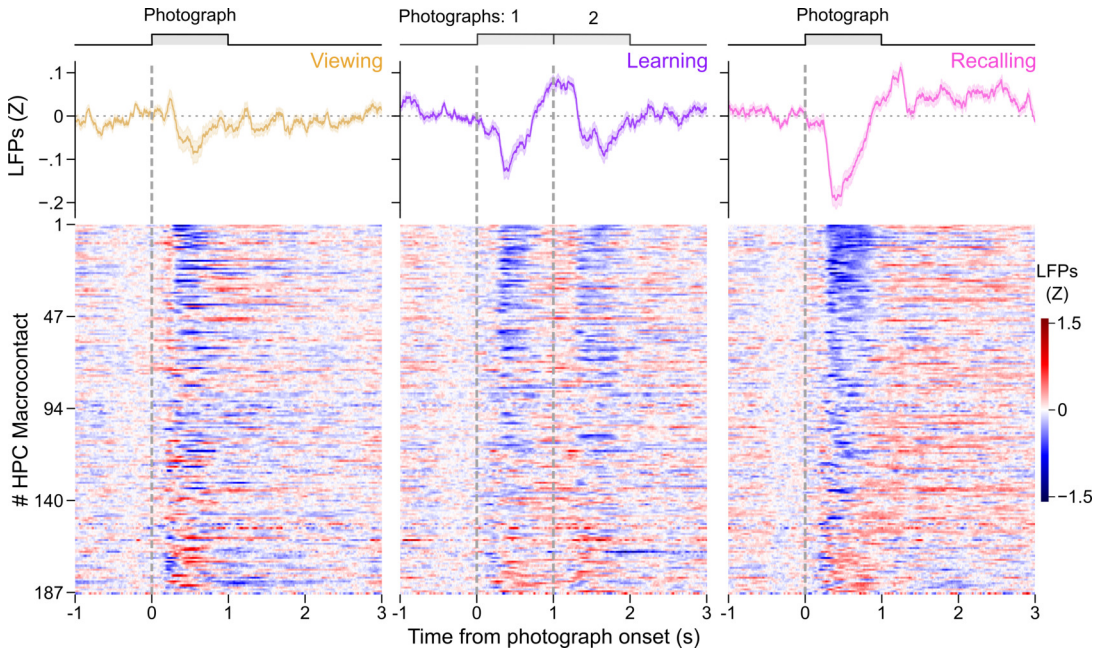


Figure 4.14: **Hippocampal ERP across task sessions.** Group-level average hippocampal LFPs aligned to the onset of viewing (left), learning (middle), or recall (right) photographic cues, with corresponding contact-level averages shown as a heatmap below. Contacts are sorted by the mean negative deflection in the recall condition for clarity. "Photograph 1" and "Photograph 2" denote the first and second paired associates presented during learning, respectively. Shaded areas indicate mean ± SEM.

the stimuli. In order to test this hypothesis, we also compared ERP deflections evoked by paired associates with the best recall performance with those worst remembered, and presented during the recall session. Interestingly, the hippocampal ERP deflections were more pronounced for best than worst remembered stimuli (Fig. 4.15B), confirming that hippocampal LFP responses to visual stimuli are modulated by the mnemonic content of the photographs presented.

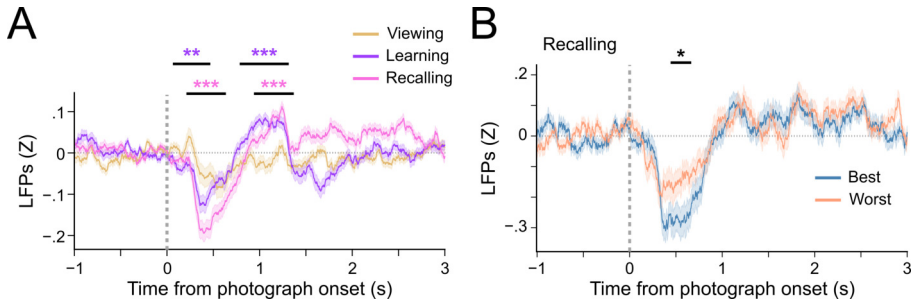


Figure 4.15: **Hippocampal ERP deflections are modulated by mnemonic engagement.** (**A**) Group-level average hippocampal LFPs showing contrasts between viewing and learning or recall sessions. ERP have a greater deflection after the onset of learning and recalling photographs than after viewing photographs. (**B**) Group-level average hippocampal LFPs showing contrasts between best and worst recalled associations during memory recall. Shaded areas indicate mean ± SEM. Data were analysed with cluster-based permutation tests; ***P $<$ 0.001, **P $<$ 0.01, *P $<$ 0.05; n.s., not significant.

4.III.2.b Hippocampal 2-Hz is an evoked oscillation and follows the ERPs

Should 2-Hz oscillations be important for mnemonic processing, they should occur after the onset of memory-relevant cues. Having characterized the early hippocampal response, we next asked whether 2-Hz oscillations appear once the hP600 ERP has resolved, i.e., during the inter-stimulus interval (Fig. 4.16).

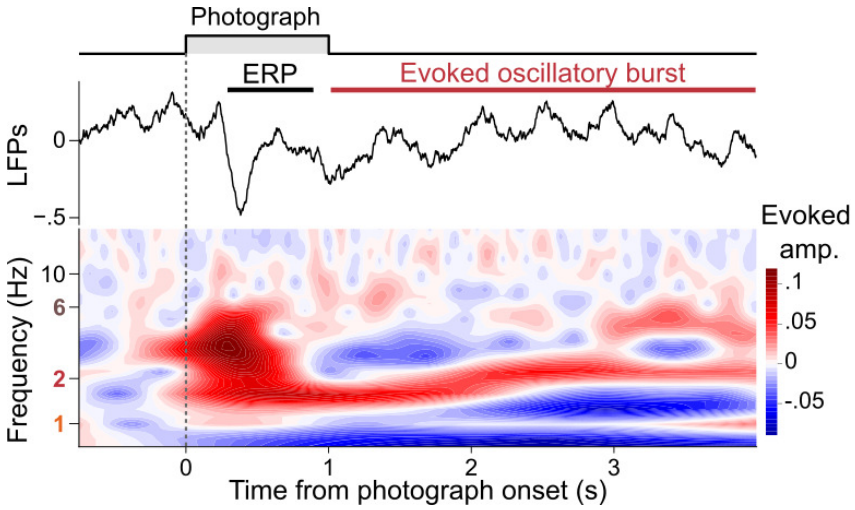


Figure 4.16: **Example hippocampal ERP and evoked 2-Hz burst.** Peri-stimulus average of hippocampal LFPs recorded from an example macrocontact with corresponding spectrogram, showing an ERPs followed by a transient 2-Hz oscillation burst occurring during the inter-stimulus interval period.

To assess whether 2-Hz was evoked by photograph onset, we measured wavelet spectrograms after each stimulus in the three active phases of the memory task, and compared the mean amplitude after stimulus onset to the baseline, pre-stimulus period. Hippocampal 2-Hz amplitude was higher after the onset of learning and recalling photographs, but not viewing photographs (Fig. 4.17A). Moreover, the 2-Hz evoked (baseline-corrected) amplitude was higher in learning and recalling than in viewing (Fig. 4.17B), a difference not observed for the 1- and 6-Hz oscillations (Fig. 4.17D). Finally, during the presentation of learning photographs, the evoked 2-Hz amplitude for paired associates that were subsequently best remembered was greater than that for those subsequently worst remembered (Fig. 4.17C), a phenomenon known as the subsequent-memory effect (Wagner et al. 1998; Brewer et al. 1998).

Taken together, these results show that mnemonic cues trigger an early evoked response that evolves into a slower, sustained 2-Hz oscillation in the human hippocampus. To better link these two processes, we next measured the correlation between the magnitude of the ERP deflection and the amplitude of the evoked oscillations at 1, 2 and 6 Hz in the recall session. Interestingly, hippocampal macrocontacts with the most pronounced ERP deflections also had the highest evoked 2-Hz amplitude, but not the highest 1- or 6-Hz amplitude (Fig. 4.18).

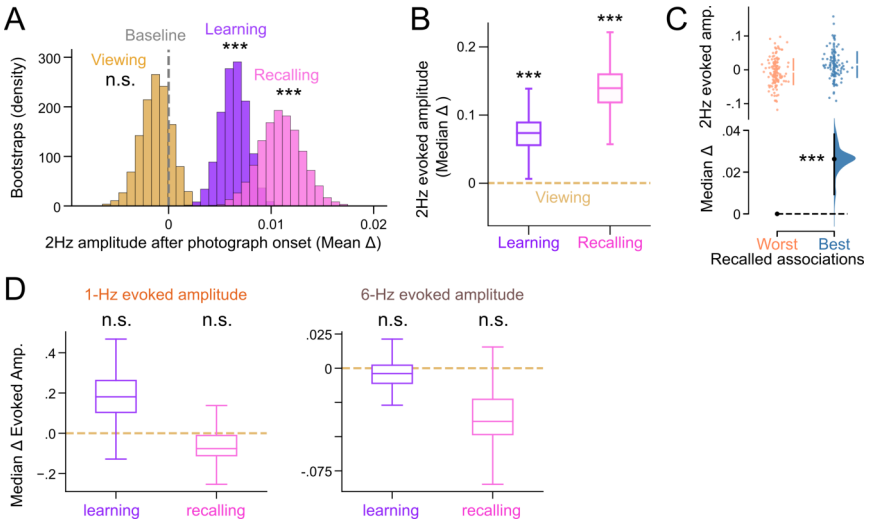


Figure 4.17: **Hippocampal 2-Hz is evoked by mnemonic cues.** (**A**) Mean post-ERPs 2-Hz amplitude (>1 s after photograph onset) relative to the pre-stimulus baseline in viewing, learning, and recall sessions (before baseline correction). (**B**) Median differences in evoked 2-Hz amplitude during learning or recall relative to viewing, computed over post-ERPs epochs (after baseline correction). Note that the two photographs presented during learning were contiguous (directly linked as paired associates), which may have interrupted evoked 2-Hz oscillations (e.g., through phase reset (Gedankien et al. 2023)). This was not the case during the recall session. (**C**) Estimation plot showing 2-Hz evoked amplitude during learning trials that subsequently produced best versus worst memory recall. (**D**) Median differences in evoked 1-Hz (left) and 6-Hz (right) amplitudes as in (B). Data were analysed using two-sided paired permutation tests; ***P $<$ 0.001, **P $<$ 0.01, *P $<$ 0.05; n.s., not significant.

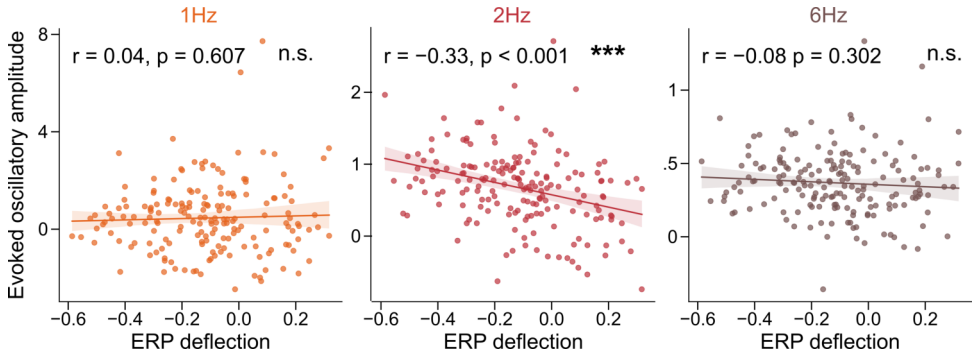


Figure 4.18: **Correlation between hippocampal ERP deflection and evoked oscillations.** Correlation between hippocampal ERP deflection and evoked oscillatory amplitudes at 1, 2, and 6 Hz during recall.

4.III.2.c Hippocampal 2-Hz bursts track mnemonic engagement

Having characterized how 2 Hz amplitude relates to visual stimulus presentation, we next asked whether burst rate and duration of 2-Hz oscillations also track mnemonic engagement across the different task sessions. We observed that hippocampal 2-Hz bursts were more frequent and longer during learning and recall than during viewing sessions (Fig. 4.19A-D). Moreover, burst rate and duration were negatively correlated with time as learning progressed, but not in other task sessions (rate: learning, Pearson r = -0.48, P < 0.001; other task sessions, r > -0.20, P > 0.161; duration: learning, r = -0.33, P = 0.020; other task sessions, r > -0.120, P > 0.399, Fig. 4.19B,D). In contrast, no increase in burst rate or duration was observed for 6-Hz bursts in learning and recall sessions relative to viewing (Fig. 4.19E,G). Moreover, we observed positive correlations between time and 6-Hz rate and duration in the viewing session (Fig. 4.19F,H) suggesting a general effect of task disengagement on 6-Hz dynamics (rate: viewing, Pearson r = 0.58, P < 0.001; duration: viewing, r = 0.52, P < 0.001).

The previous analyses showed that hippocampal 2-Hz bursts tracked mnemonic engagement across task sessions. We next asked whether these oscillatory events were also associated with successful memory formation by relating burst dynamics to subsequent recall performance. First, leveraging within-subject variability across paired associates, we found that photographs that were best remembered during recall were associated with higher 2-Hz burst occurrence during learning (Fig. 4.20A). Next, leveraging between-subject variability, we compared hippocampal 2-Hz bursts between participants who correctly remembered at least three quarters of the associations ("higher performers") and the remaining participants ("lower performers"). Critically, higher performers showed greater 2-Hz burst rate and longer burst duration than lower performers (Fig. 4.20B,C). Together, these findings indicate that mnemonic engagement was associated with a slow oscillatory response in the human hippocampus expressed as stimulus-locked 2-Hz bursts. This transient activity was most prominent during acquisition of new associations, decreased as learning progressed, and was associated with better subsequent recall performance.

4.III.3 Hippocampal 2-Hz oscillations are not evoked by motor activity

One remaining question is whether hippocampal 2-Hz oscillations reflect mnemonic processing specifically, or whether they can also be elicited by repetitive motor behaviour alone. Indeed, in rodents, theta power increases with locomotion, reflecting the acquisition of new sensory information during exploratory behaviour. Although locomotion is not a confounding factor in our relational memory task, we examined whether movement alone could elicit 2-Hz oscillations in humans. To do so, participants remained seated and performed repetitive foot movements ("stepping") for 10 minutes, following a 10-minute eyes-closed rest period (Fig. 4.21A). Interestingly, stepping provides a relevant control because the interval between consecutive foot movements is approximately 500 milliseconds (Fig. 4.21B). Across the three participants who showed clear 2-Hz activity during learning, stepping did not significantly elicit 2-Hz oscillations (Fig. 4.21C-H).

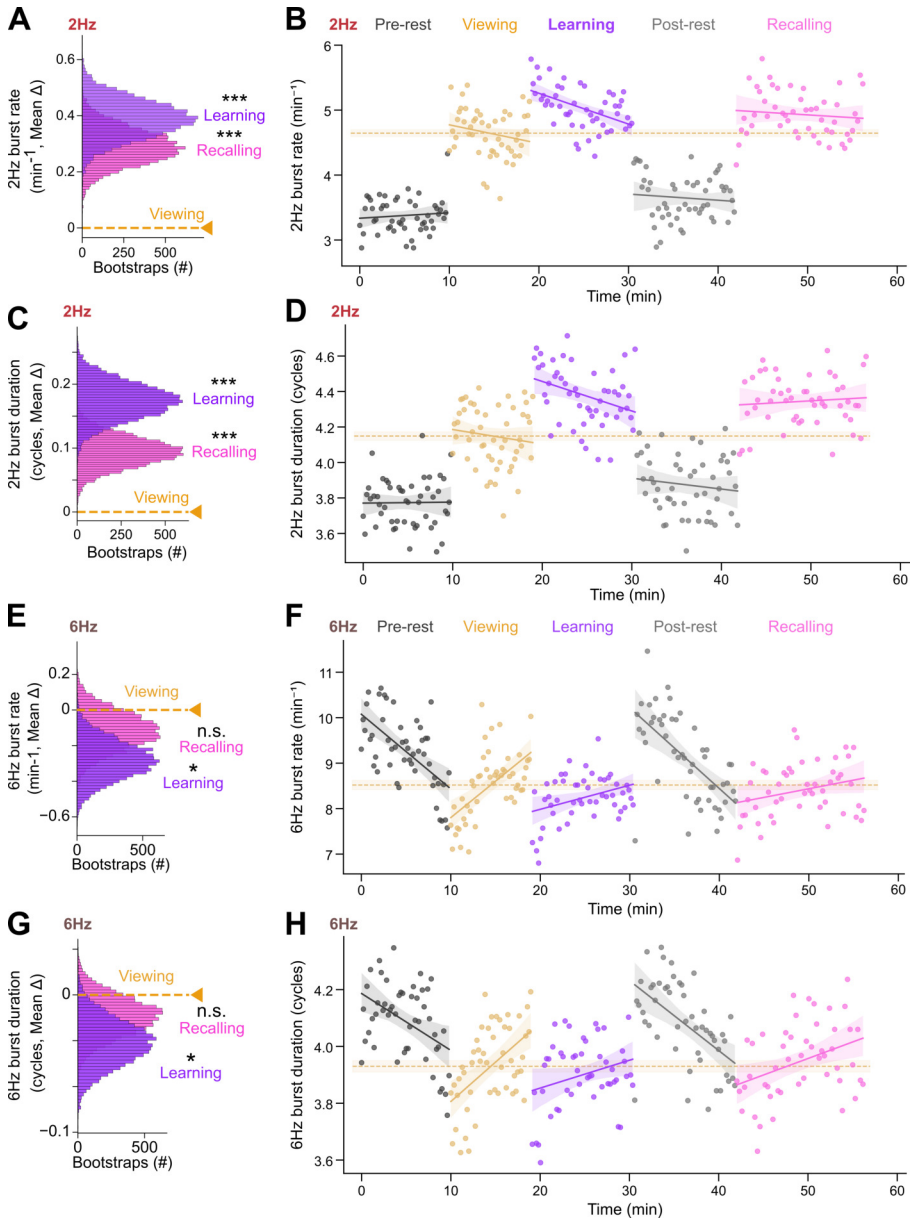


Figure 4.19: **Hippocampal 2-Hz bursts across task sessions.** (**A**–**D**) Hippocampal 2-Hz bursts were more frequent (A, B) and longer (C, D) during learning and recall than during viewing sessions. **A, C** Estimation plots showing the median difference in 2-Hz burst rate during learning and recall relative to viewing. **B, D** Time course showing expression dynamics of hippocampal 2-Hz burst rate (B) and duration (D) in the relational memory task, averaged across participants and contacts. Burst rate and duration were negatively correlated with time as learning progressed (rate: learning, Pearson r = -0.48, P $<$ 0.001; other task sessions, r $>$ -0.20, P $>$ 0.161; duration: learning, r = -0.33, P = 0.020; other task sessions, r $>$ -0.120, P $>$ 0.399). (**E**–**H**) Same as A-D for 6-Hz bursts, showing no increase in burst rate or duration in learning and recall sessions relative to viewing (E, G), and the positive correlations with time in the viewing session (F, H), suggesting a general effect of task disengagement on 6-Hz dynamics. Burst rate and duration were positively correlated with time in the viewing session (rate: viewing, Pearson r = 0.58, P $<$ 0.001; duration: viewing, r = 0.52, P $<$ 0.001). Data were analysed using two-sided paired permutation tests in A, C, E and G; ***P $<$ 0.001, *P $<$ 0.05; n.s., not significant.

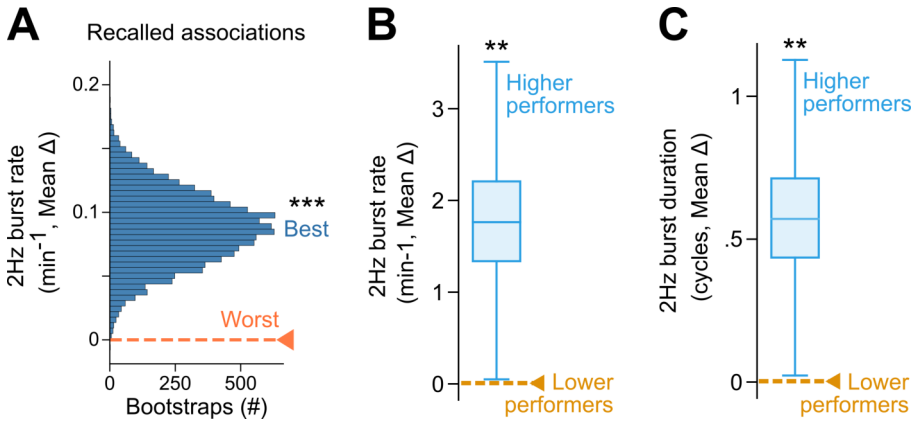


Figure 4.20: **Hippocampal 2-Hz bursts and memory performance.** (**A**) Estimation plot showing the difference in 2-Hz burst rate during learning trials associated with best versus worst subsequent memory recall. (**B and C**) Estimation plots showing the difference in 2-Hz burst rate (B) and duration (C) in the learning session between higher and lower task performers. Data were analysed using two-sided paired permutation tests in A and unpaired permutation tests in B and C; ***P $<$ 0.001, **P $<$ 0.01.

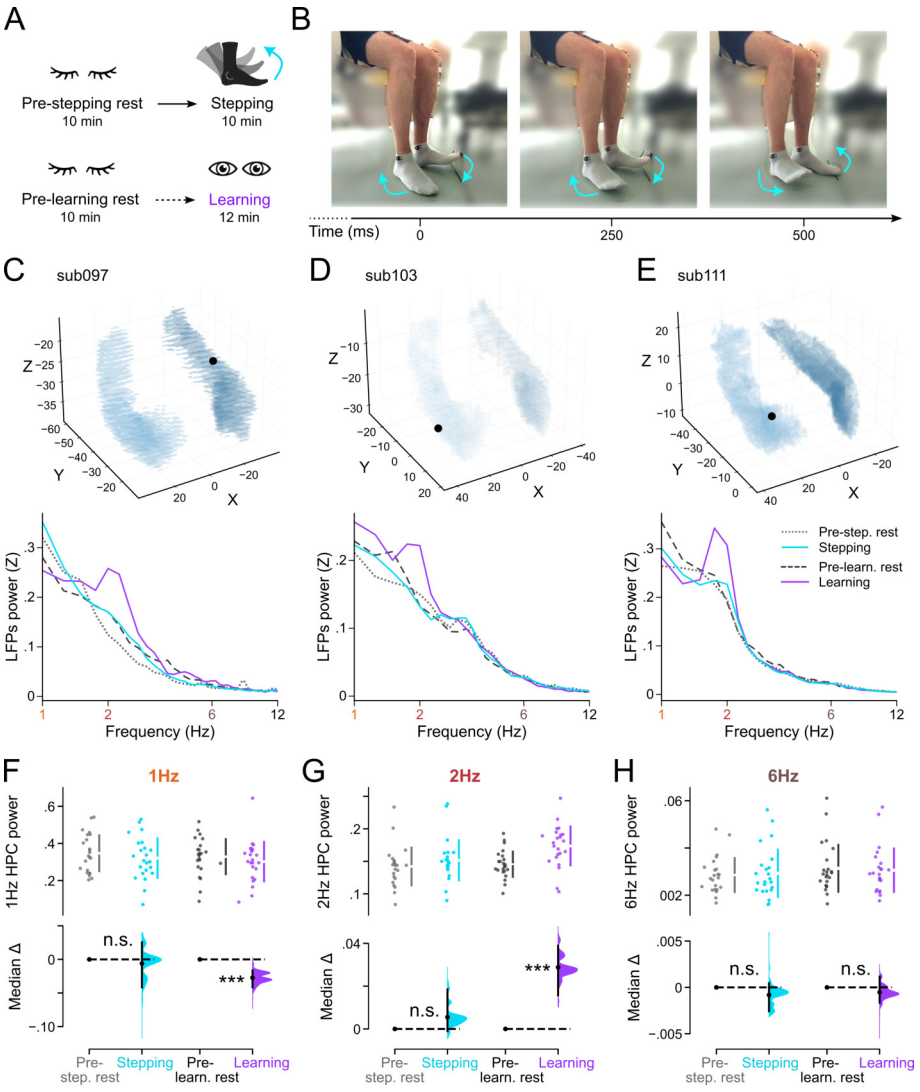


Figure 4.21: **Stepping movement does not elicit 2-Hz oscillations in the human hippocampus.** (**A**–**B**) After a 10-minute rest session, participants performed repetitive stepping movements with their feet while seated (A). Note the 500-millisecond period between two movement onsets (B). (**C**–**E**) 3D hippocampal volumes showing electrode contact locations (top) and corresponding PSDs (bottom) from three example participants. (**F**–**H**) Estimation plots showing the median difference in 1-Hz (F), 2-Hz (G), and 6-Hz (H) oscillatory power during stepping and learning relative to their associated baseline rest sessions. Despite a modest trend, 2-Hz power was not significantly increased during stepping.

4.IV Discussion

Using direct recordings from the human hippocampus during a relational memory task, I identified a prominent slow oscillation centered around 2 Hz that dominated hippocampal LFPs during wakefulness. This rhythm was detected consistently across participants using an unsupervised decomposition approach and appeared as transient oscillatory bursts visible in the raw signal. Rather than forming a continuous oscillation, hippocampal 2-Hz activity occurred in transient bursts, suggesting that slow oscillatory states in the human hippocampus may be recruited on-demand during specific behavioural epochs.

Moreover, several observations support the view that this activity reflects a physiological hippocampal rhythm rather than an artifact of epileptiform activity or signal processing. In particular, 2-Hz oscillations sometimes exhibited a clear laminar phase reversal across adjacent hippocampal contacts and were most prominent in contacts free of IEDs. Additional results supporting this claim will be presented in the next chapter, with modulation of single-neuron activity by the 2-Hz oscillation.

Importantly, hippocampal 2-Hz activity showed behavioural correlates expected from a theta-like state in animal models. Its power and burst dynamics (rate and duration) increased selectively during mnemonic engagement, were evoked by memory-relevant cues, and were associated with subsequently higher memory performance. More precisely, memory-relevant cues first elicited a hippocampal evoked response (Fernández et al. 1999), followed by a sustained 2-Hz oscillatory burst whose amplitude correlated with the ERP deflection, suggesting a functional link between these two processes. In contrast, passive viewing and repetitive motor activity did not produce comparable increases in 2-Hz expression. It is important to note that even though the spectral decomposition methods employed here were sensitive to neighbouring 1- and 6-Hz components, these frequency bands did not show comparable relationships with mnemonic engagement or behavioural performance. Together, these findings suggest that the dominant slow oscillation observed in the human hippocampus at 2 Hz is linked specifically to memory-guided behaviour rather than to visual stimulation or movement alone.

The stepping experiment should nevertheless be interpreted with caution, as it was performed in a limited number of participants and involved a simplified form of movement compared with natural locomotion. Previous human sEEG studies investigating hippocampal oscillations during movement and navigation have reported heterogeneous results (Halgren et al. 1978; Bohbot et al. 2017; Aghajan et al. 2017; Seeber et al. 2025). Further work will therefore be required to determine how hippocampal 2-Hz oscillations relate to locomotion and ambulatory exploratory behaviours in humans. Importantly, such studies should also carefully consider referencing methods, as local bipolar referencing may strongly attenuate slow oscillations and thereby bias the detection of slow-frequency hippocampal rhythms.

Although crucial in defining the properties of a neural oscillation, behavioural correlates alone are not sufficient to establish whether hippocampal 2-Hz constitutes a putative functional homologue of theta oscillations, as described in other mammals. In rodents, one of the defining properties of theta is its ability to organize neuronal firing and gamma activity within hippocampal circuits (O'Keefe and Recce 1993; Bragin et al. 1995a; Csicsvari et al. 1999; Klausberger and Somogyi 2008). If the human 2-Hz rhythm plays a

comparable role, it should similarly coordinate neuronal dynamics locally and in partner structures. Hence, in the next chapter I investigate whether hippocampal 2-Hz oscillations modulate neuronal firing and gamma activity locally (Chapter 5.II) and across the MTL (Chapter 5.III).

5 Results: Hippocampal 2-Hz organizes neuronal activity in the MTL

"Gamma oscillations can be uniquely identified by the rhythm-generating circuit from which they emerge and the current circuit from which they are recorded."

"Les oscillations gamma peuvent être identifiées de manière unique par le circuit qui génère le rythme dont elles émergent et par le circuit neuronal dans lequel elles sont enregistrées."

— Antonio Fernandez-Ruiz et al.,
Over and above frequency: Gamma oscillations as units of neural circuit operations (2023)

Contents

5.I Introduction 118

5.II Hippocampal neuronal activity is preferentially modulated at 2 Hz 119

5.II.1 Hippocampal neurons are paced at 2-Hz 119

5.II.2 Hippocampal gamma oscillations are preferentially modulated at 2 Hz 122

5.III Hippocampal 2-Hz synchronizes neuronal activity across MTL regions 127

5.III.1 2-Hz oscillations are preferentially observed in the MTL 127

5.III.2 MTL local activity is paced by hippocampal 2-Hz 132

5.IV Discussion 138

5.I Introduction

In the previous chapter, I identified a dominant 2-Hz oscillation in the human hippocampus. This rhythm was transient, appeared as bursts, and was selectively enhanced during mnemonic engagement. It also showed a clear relation with memory performance, suggesting that it is not a passive feature of the recorded signal but a meaningful component of hippocampal activity during behaviour. The next question is whether this rhythm does more than track memory demands. If it is a theta-like rhythm, it should also organize local neural activity, as theta does in animal models.

In rodents, theta is not only associated with active wake states, but it also coordinates neuronal firing and local network dynamics. At the cellular level, spikes are phase-locked to ongoing theta, and gamma activity is modulated by theta phase, indicating that this rhythm structures both spike timing and cross-frequency coupling within the hippocampal circuit (O'Keefe and Recce 1993; Bragin et al. 1995a; Csicsvari et al. 1999; Klausberger and Somogyi 2008). More broadly, theta provides a temporal structure for coordinating neuronal activity in the hippocampus and connected brain regions, by creating recurring periods of increased excitability and synchrony (Fries 2005; Buzsáki 2010). This makes theta a plausible mechanism for organizing the neuronal dynamics that support memory processing.

This chapter asks whether the human hippocampal 2-Hz rhythm passes these additional criteria. I first test whether hippocampal neurons are preferentially locked to the phase of 2-Hz oscillations, and whether this coupling is stronger than for other slow rhythms. I then examine whether gamma activity is also modulated by 2-Hz phase, both within the hippocampus and across the MTL. Finally, I ask whether this coordination is especially prominent during mnemonic engagement, when the 2-Hz rhythm was most visible in the previous chapter.

Taken together, these analyses are meant to determine whether the human hippocampal 2-Hz rhythm is not only behaviourally relevant, but also capable of organizing local and distributed neural activity in a way that is consistent with a theta-like function.

5.II Hippocampal neuronal activity is preferentially modulated at 2 Hz

Oscillations at 2 Hz can be observed in the hippocampal LFPs. These oscillations are transient, and selectively evoked by mnemonic cues. However, a 2-Hz oscillation is a particularly slow rhythm in comparison to the timescale of the cellular (ensemble spiking activity) and local network (gamma oscillations) processes at play in the hippocampus. To solve this apparent paradox, we next investigated whether 2-Hz oscillations modulate ensemble spiking and gamma activity locally within the hippocampus.

5.II.1 Hippocampal neurons are paced at 2-Hz

5.II.1.a Basic firing properties of hippocampal neurons reveal 2-Hz rhythmicity

Using tetrode LFP recordings, we isolated single-neuron activity from the human hippocampus while participants were engaged in the relational memory task as well as watching a sitcom series (see Chapter 2.I.1 for details on the datasets and Chapter 2.I.2 for isolation of single-units). In the hippocampus, 211 neurons were identified from 18 participants who had tetrodes in this structure. Because tetrodes protruded between the two deepest macrocontacts, neurons were mostly sampled from the medial parts of the hippocampus (Fig. 5.1A). The majority of neurons detected had a low firing rate, below 5

Hz (Fig. 5.1B) and broad spiking waveforms (Fig. 5.1C-E), consistent with the proportion of pyramidal neurons observed in the rodent hippocampus (Csicsvari et al. 1998; Csicsvari et al. 1999). Thus, broad-spiking units were considered as putative pyramidal neurons (pPYR), while those with narrow spikes were considered as putative interneurons (pINT).

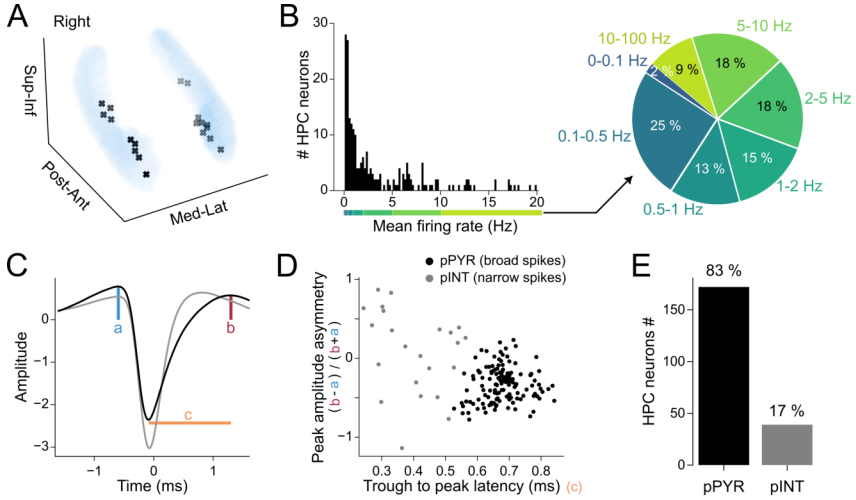


Figure 5.1: **Basic properties of hippocampal neurons.** (**A**) 3D hippocampal volumes showing tetrode locations (black crosshairs). (**B**) Mean firing rates of hippocampal neurons follow a log distribution, with most (73%) firing below 5 Hz. (**C**–**D**) Using peak amplitude asymmetry (b - a / b + a) and trough-to-peak latency (c) measured on the spike waveforms of individual neurons (**C**), pPYR (broad spikes) and pINT (narrow spikes) were separated (**D**). (**E**) Proportion of pPYR and pINT neurons showing that the majority (83%) of hippocampal neurons were classified as pPYR.

Next, we examined the rhythmic structure in spike trains by computing single-neuron autocorrelograms and inter-spike intervals (ISIs) at slow timescales. Several hippocampal neurons recorded from different subjects displayed clear rhythmicity at 2 Hz (Fig. 5.2A-C), indicating that the hippocampal 2-Hz rhythm can also be detected directly at the level of single-neuron activity. These neurons showed typical properties of pyramidal cells: broad spikes and low firing rates (<5 Hz). One neuron exhibited 6-Hz rhythmicity (Fig. 5.2D), confirming that our experimental setup was capable of detecting higher-frequency rhythmic firing, although such cases were less common.

5.II.1.b Hippocampal neurons prefer 2-Hz oscillations

If hippocampal neurons are entrained by the 2-Hz oscillation, their spike trains should lock more strongly to the 2-Hz phase than to the phase of other slow-frequency oscillations. We assessed this coupling by measuring PPC at 1-, 2- and 6-Hz using the IMFs detected from the macrocontact adjacent to the tetrodes. The observed pairwise-phase consistency (PPC) values were then compared with a null distribution obtained by randomly permuting the phase of each IMF in the Fourier domain (see Chapter 2.I.3.b for methodological details). This measure allowed us to compare coupling across frequencies while controlling for potential power-law confounds. Single-neuron locking was higher for 2-Hz than 1- or 6-Hz oscillations in the hippocampus (Fig. 5.3A-D). Phase-coupling to 2-Hz oscillations was comparable between putative pyramidal neurons (pPYR) and interneurons (pINT)

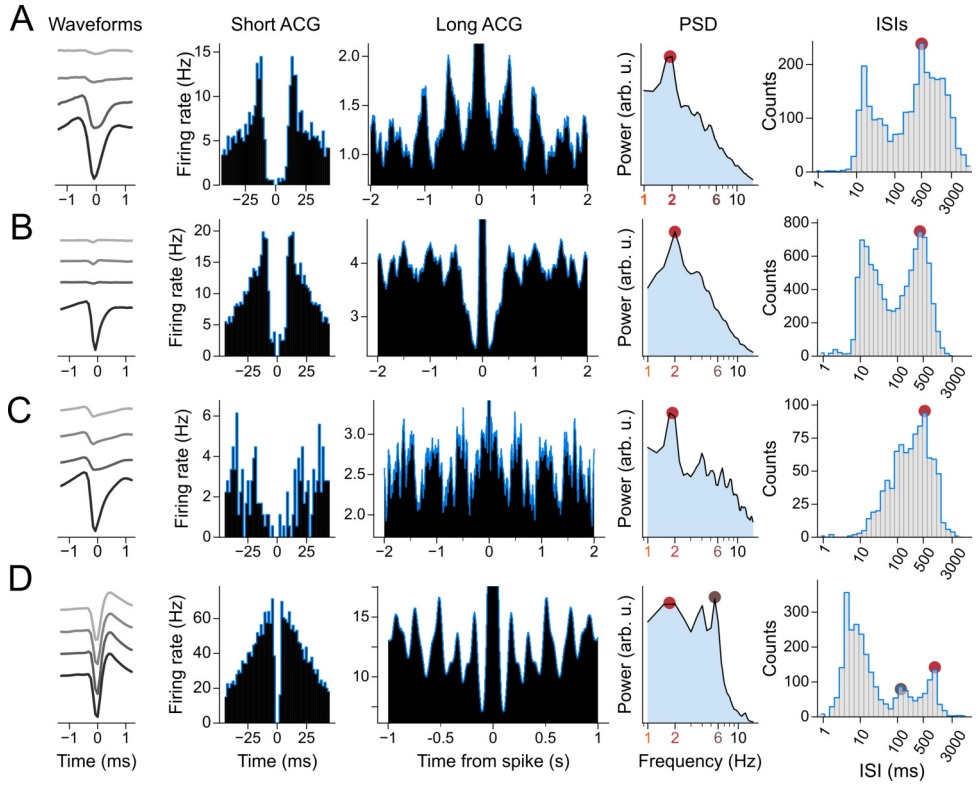


Figure 5.2: **2-Hz rhythmicity of hippocampal neurons.** (**A-D**) Example hippocampal neurons exhibiting 2-Hz (A-C) and 6-Hz (D) rhythmicity. From left to right: mean spike waveform across tetrode channels; short- (millisecond) and long- (second) timescale spike autocorrelograms (ACGs); PSDs; and ISI distributions. Long ACGs were cropped at t=0 for clarity. Note that both hippocampal neurons with broad and narrow spike waveforms could exhibit 2-Hz rhythmicity.

(Fig. 5.3E-G). Hence, this result confirms that the 2-Hz rhythm organizes single-neuron and population activity locally in the hippocampus.

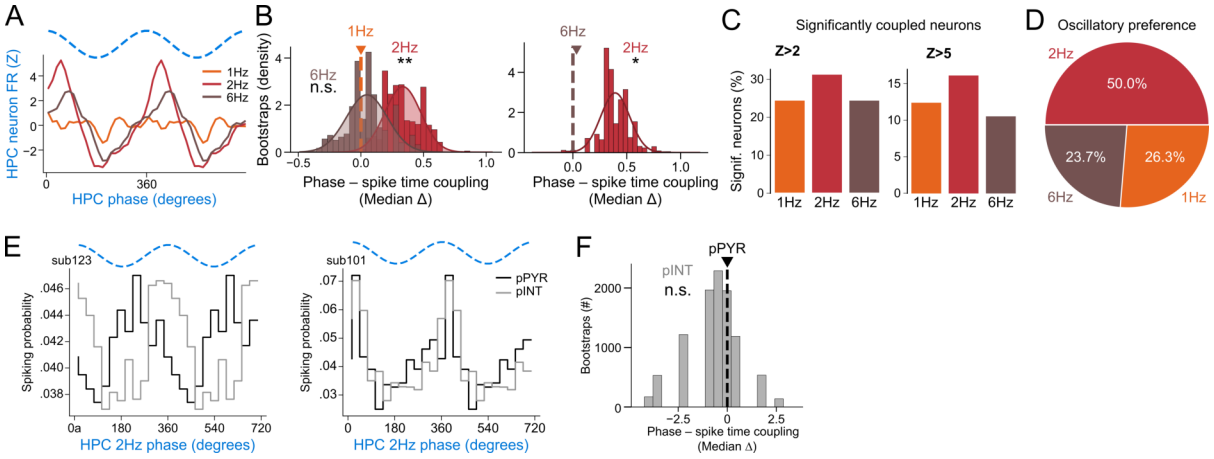


Figure 5.3: **Hippocampal single-neurons preferentially lock to the phase of 2-Hz oscillations.** (**A**) Firing-phase histograms of an example neuron relative to 1-, 2-, and 6-Hz oscillations. (**B**) Spike-phase consistency (z-score) differences between 1-Hz and 2- or 6-Hz oscillations (left) and between 2- and 6-Hz oscillations (right) across hippocampal neurons. (**C**) Percentage of hippocampal neurons significantly coupled to 1-, 2-, or 6-Hz oscillations, defined by PPC z-scores above 2 (left) or 5 (right). (**D**) Proportion of hippocampal neurons preferring 1-, 2-, or 6-Hz oscillations. (**E, F**) Both putative hippocampal pyramidal neurons (pPYR) and interneurons (pINT) were coupled to hippocampal 2-Hz phase. (**E**) Firing-phase histograms from two example subjects showing pPYR and pINT cells with comparable 2-Hz modulation depth, and either similar (left) or different (right) preferred phases. (**F**) Median differences in spike-phase consistency at 2 Hz between pPYR and pINT cells. Data were analysed using two-sided paired permutation tests; ***P $<$ 0.001, **P $<$ 0.01, *P $<$ 0.05; n.s., not significant.

5.II.2 Hippocampal gamma oscillations are preferentially modulated at 2 Hz

5.II.2.a Hippocampal gamma activity is preferentially coupled to 2-Hz phase

In rodents, fast gamma oscillations reflect the activity of local networks, namely the interaction between pyramidal neurons and interneurons (Fernandez-Ruiz et al. 2023). First, we confirmed that neuronal spiking correlated with local gamma-band (60–160 Hz) activity in humans as well (see Chapter 2.I.3.b and (Manning et al. 2009; Miller 2010; Watson et al. 2018)). In addition, rodent gamma oscillations couple with theta, and this theta-gamma phase-amplitude coupling (PAC) is crucial for memory acquisition and recall (Lisman and Jensen 2013; Colgin 2016). Consequently, we then tested whether gamma-band activity was coupled to hippocampal 2-Hz phase. By measuring the average of gamma activity and population firing rate triggered by individual oscillatory cycles of 1-, 2- and 6-Hz oscillations, we showed clear entrainment of gamma activity at 2-Hz (Fig. 5.4).

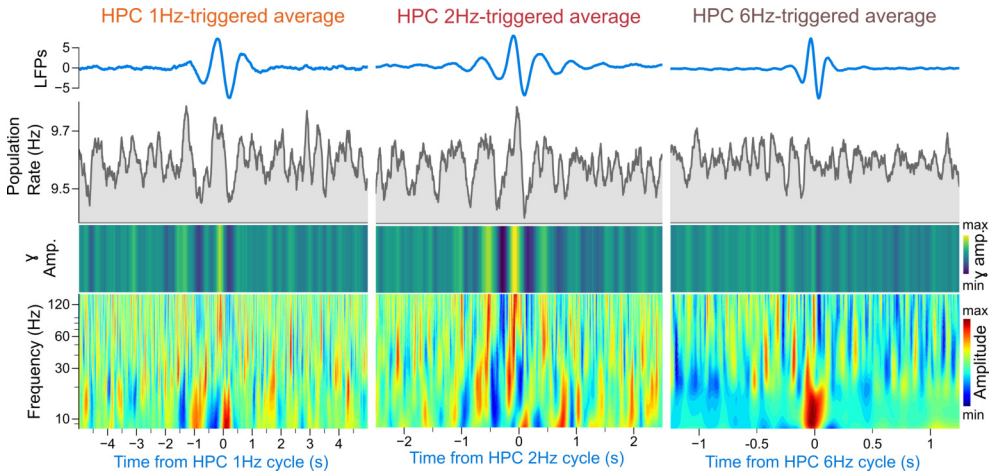


Figure 5.4: **Illustration of gamma and neuronal spiking co-modulation at 2-Hz.** Average hippocampal LFPs, instantaneous population firing rate, gamma amplitude, and corresponding spectrogram aligned to 1-Hz (left), 2-Hz (middle), and 6-Hz (right) oscillatory cycles in an example participant. This illustrates the modulation of local networks at 2-Hz.

Next, we quantified this relationship by measuring the coupling between local hippocampal gamma amplitude and the phase of 1-, 2- and 6-Hz oscillations, using EMD and the Kullback-Leibler divergence (see Chapter 2.II.5 for further details on the methodology). This measure of PAC was then compared to IMFs with randomly permuted phases, as we did in Chapter 5.II.1.b with neuronal spiking activity. Critically, because 2-Hz bursts are profoundly non-linear (see Fig. 4.4 and (Penner et al. 2022)), it is essential to use methods that are adapted to this type of signal, like the EMD. Indeed, using conventional linear filters would otherwise result in spurious PAC (Juan et al. 2021). In our data, gamma amplitude was significantly more strongly coupled to the 2-Hz phase than to the 1- or 6-Hz phases (Fig. 5.5), which shows that 2-Hz oscillations also entrain gamma activity locally in the hippocampus.

The antero-posterior axis of the human hippocampus is analogous to the dorso-ventral axis of the rodent hippocampus (Strange et al. 2014) along which substantial histological, anatomical, and functional diversity has been reported (Moser and Moser 1998; Fanselow and Dong 2010). Important differences between anterior and posterior subdivisions have also been described in humans (González-Arnay et al. 2024). Notably, the cellular layer is more compact in the posterior hippocampus, which could produce a more organized dipole and potentially stronger slow oscillations. We therefore measured gamma coupling separately in the anterior and posterior hippocampus and found that gamma activity was more strongly coupled to the 2-Hz than to 1- or 6-Hz oscillations in both regions (Fig. 5.6A), despite weaker statistical power in the posterior hippocampus (Fig 4.2C). LMEM analyses confirmed that gamma coupling to 2-Hz did not correlate with the antero-posterior position of the macrocontacts along the hippocampus (Fig. 5.6B).

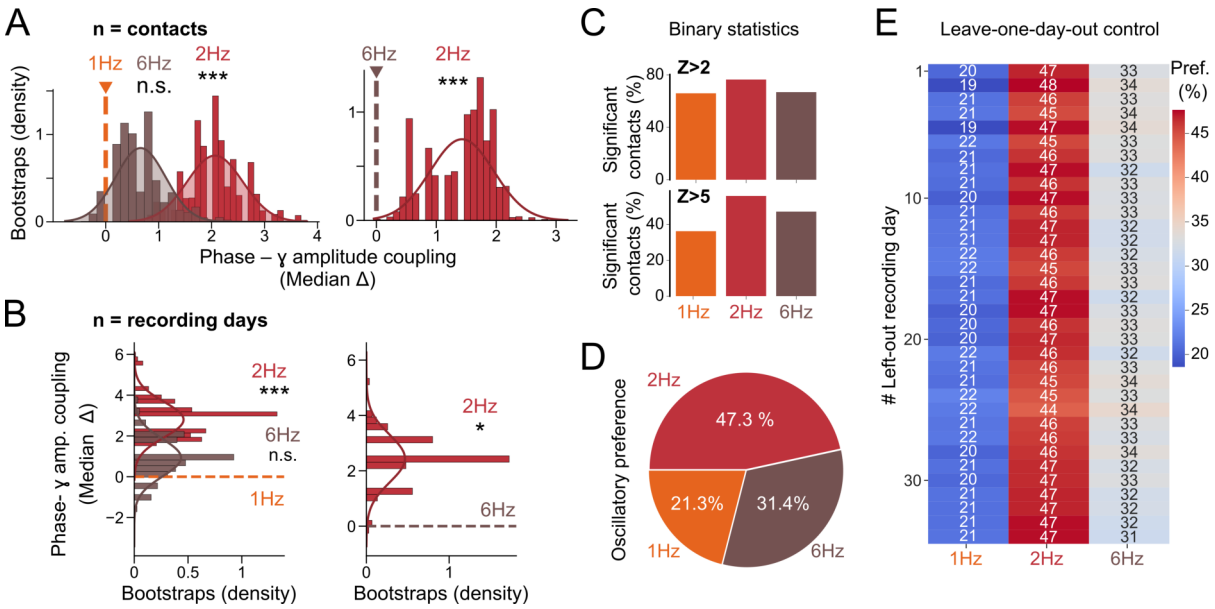


Figure 5.5: **Gamma activity coupling to hippocampal oscillations.** (**A**) Median differences in PAC (z-score) for hippocampal gamma envelopes between 1-Hz and 2- or 6-Hz oscillations (left) and between 2- and 6-Hz oscillations (right). (**B**) Estimation plots showing median PAC (z-score) differences between 1-Hz and 2- or 6-Hz oscillations (left), and between 2- and 6-Hz oscillations (right) when coupling values were averaged per recording day. (**C**) Percentage of hippocampal macrocontacts with gamma activity significantly coupled to 1-, 2-, or 6-Hz oscillations, defined by PAC z-scores above 2 (top) or 5 (bottom). (**D**) Proportion of hippocampal macrocontacts showing gamma-coupling preference for 1-, 2-, or 6-Hz oscillations. (**E**) Leave-one-day-out analysis of oscillatory preference demonstrating that the 2-Hz preference is not driven by any single recording day. Data were analysed using two-sided paired permutation tests; ***P $<$ 0.001, *P $<$ 0.05; n.s., not significant.

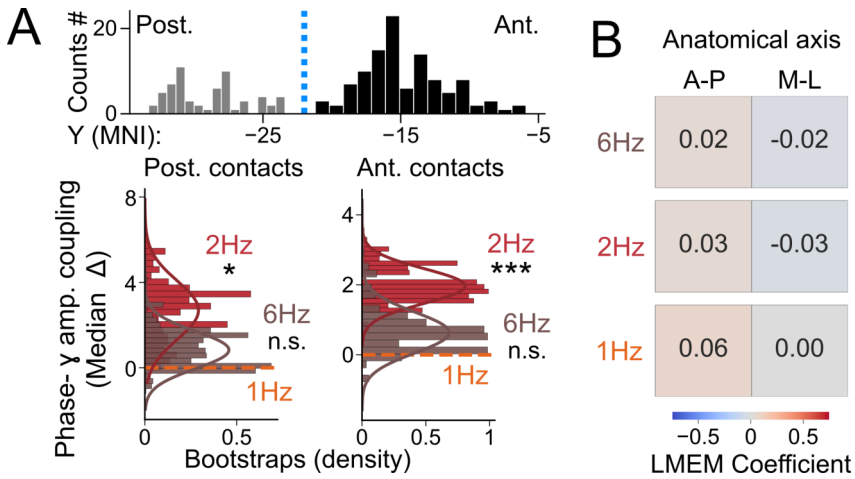


Figure 5.6: **Anatomical gradients of gamma coupling to hippocampal slow oscillations.** (**A**) Top: Distribution of hippocampal macrocontacts along the antero-posterior axis, separating anterior (black) and posterior (gray) sites. Bottom: Median PAC (z-score) differences between 1-Hz and 2- or 6-Hz oscillations across posterior (left) and anterior (right) contacts, showing a consistent 2-Hz preference in both regions. Data were analysed using two-sided paired permutation tests; ***P < 0.001, *P < 0.05; n.s., not significant. (**B**) Heatmap of β coefficients from linear regression predicting PAC (z-score) to 1-, 2-, or 6-Hz oscillations as a function of antero-posterior or medio-lateral macrocontact position. No coefficients reached significance.

5.II.2.b Holo-Hilbert amplitude modulation analysis confirms prevailing 2-Hz hippocampal modulation of gamma activity

Because measures of PAC can be influenced by signal-processing choices, in particular by band-pass filtering of fast-frequency activity (Juan et al. 2021), we next sought to confirm these results using an independent and fully unsupervised approach. For this, we applied Holo-Hilbert Spectral Analysis (HHSA), a method based on EMD and the Hilbert transform that identifies rhythmic fluctuations in the instantaneous amplitude of IMFs. Unlike conventional filtering-based approaches, HHSA does not require predefined frequency bands and is robust to spurious PAC introduced by linear filters (Huang et al. 1998; Juan et al. 2021). This makes HHSA a useful unsupervised method for characterizing cross-frequency interactions directly from the structure of the gamma amplitude itself. A mathematical intuition for HHSA is provided in Chapter 2.II.5.

Using this approach, we confirmed that gamma amplitude was predominantly modulated at 2 Hz (Fig. 5.7A,B), particularly at electrode contacts free from IEDs (Fig. 5.7C). Additional analyses from mouse dorsal CA1 revealed a clear modulation of gamma amplitude at ~7 Hz, further validating the sensitivity of this method for detecting genuine cross-frequency coupling (Fig. 5.7D,E). Thus, the preferential coupling between hippocampal gamma activity and 2-Hz phase in humans was recovered using two independent analytical frameworks: conventional phase-amplitude coupling analyses and the fully unsupervised HHSA.

Taken together, these results show that the hippocampal 2-Hz rhythm is fast enough to organize neuronal firing and gamma activity locally within the hippocampus. They also

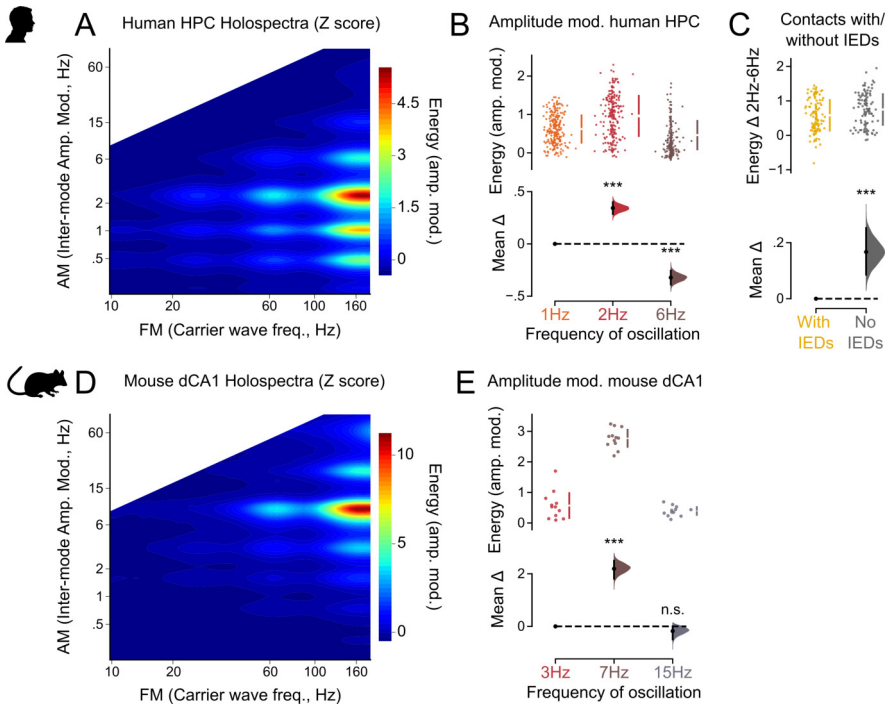


Figure 5.7: **Holo-Hilbert spectral analysis reveals gamma amplitude modulation by 2-Hz in the human hippocampus.** (**A**) Holospectrum averaged across time, IMFs, and hippocampal macrocontacts (z-scored), showing preferential modulation of fast-frequency signals by 2-Hz oscillations in humans. (**B**) Estimation plot showing mean differences in amplitude modulation between 1-Hz and 2- or 6-Hz oscillations across hippocampal macrocontacts. (**C**) Estimation plot showing stronger 2-Hz versus 6-Hz modulation in contacts free of IEDs compared with those containing IEDs. (Unpaired test.) (**D**) Holospectrum averaged over dorsal CA1 hippocampal contacts in mice, revealing preferential modulation of fast-frequency signals by ~7-Hz oscillations. (**E**) Quantification of panel D using the same method as in panel B, showing dominant amplitude modulation at ~7 Hz in mice (n = 12 sessions, 6 mice). Data were analysed using two-sided paired permutation tests, except in (C), where an unpaired test was applied; ***P < 0.001; n.s., not significant.

provide additional evidence that 2-Hz oscillations entrain local network activity and do not merely reflect volume conduction. However, hippocampal theta in animal models is not restricted to local circuits, but also synchronizes activity across distributed brain regions. Therefore, we next asked whether hippocampal 2-Hz similarly coordinates neuronal and oscillatory activity across the broader MTL network.

5.III Hippocampal 2-Hz synchronizes neuronal activity across MTL regions

In rodents, theta oscillations synchronize neuronal activity in various distributed brain regions including the entorhinal cortex (Mizuseki et al. 2009; Fernández-Ruiz et al. 2021), amygdala (Seidenbecher et al. 2003; Lesting et al. 2011; Bienvenu et al. 2012), prefrontal cortex (Adhikari et al. 2010; Lesting et al. 2011), medial septum (Hangya et al. 2009; Fuhrmann et al. 2015; Király et al. 2023), and brainstem nuclei (Vertes and Kocsis 1997; Lu et al. 2020). In humans, the MTL (hippocampus, entorhinal cortex, parahippocampal cortex and amygdala) shares dense anatomical connections with the hippocampus (Lavenex and Amaral 2000), making it a suitable candidate for functional connectivity at 2 Hz. To illustrate this, we used openly available structural data (Škoch et al. 2022) obtained from diffusion-weighted MRI (DW-MRI) in 88 human participants. Because the relational memory task we employed was based on the presentation of visual stimuli, in this analysis we focussed on the connectivity of the hippocampus with regions located along the ventral visual stream: MTL, temporal and occipital lobes. The hippocampus showed preferential connectivity with the entorhinal and parahippocampal cortices, followed by the amygdala, the temporal pole and the fusiform gyrus (Fig. 5.8), confirming the relevance of MTL structures for studying functional connectivity with the hippocampus at 2 Hz.

Because epilepsy networks involve distributed brain regions, participants recruited in this study had electrodes targeting other MTL regions (entorhinal cortex, amygdala, parahippocampal cortex) and areas outside the MTL (e.g., temporal cortices) (Fig. 5.9). Hence, these recordings allowed us to assess whether 2-Hz oscillations organized neuronal firing and gamma activity in other partner structures of the hippocampus located in the temporal lobe.

5.III.1 2-Hz oscillations are preferentially observed in the MTL

5.III.1.a 2-Hz power dominates in the MTL and particularly in the hippocampus

The first question we addressed is whether 2-Hz oscillations can be observed in the LFPs recorded from the MTL, and how they compared with hippocampal 6 Hz oscillations. By computing the average of MTL LFPs triggered by the 2-Hz cycles detected in the hippocampus in an example subject, we revealed clear 2-Hz oscillations synchronized across MTL structures (Fig. 5.10). This effect was not as clear in a control temporal cortical region (inferior temporal cortex). Interestingly, the peak of the 2-Hz burst was time-shifted across the MTL, beginning in the entorhinal cortex, followed by the hippocampus, the

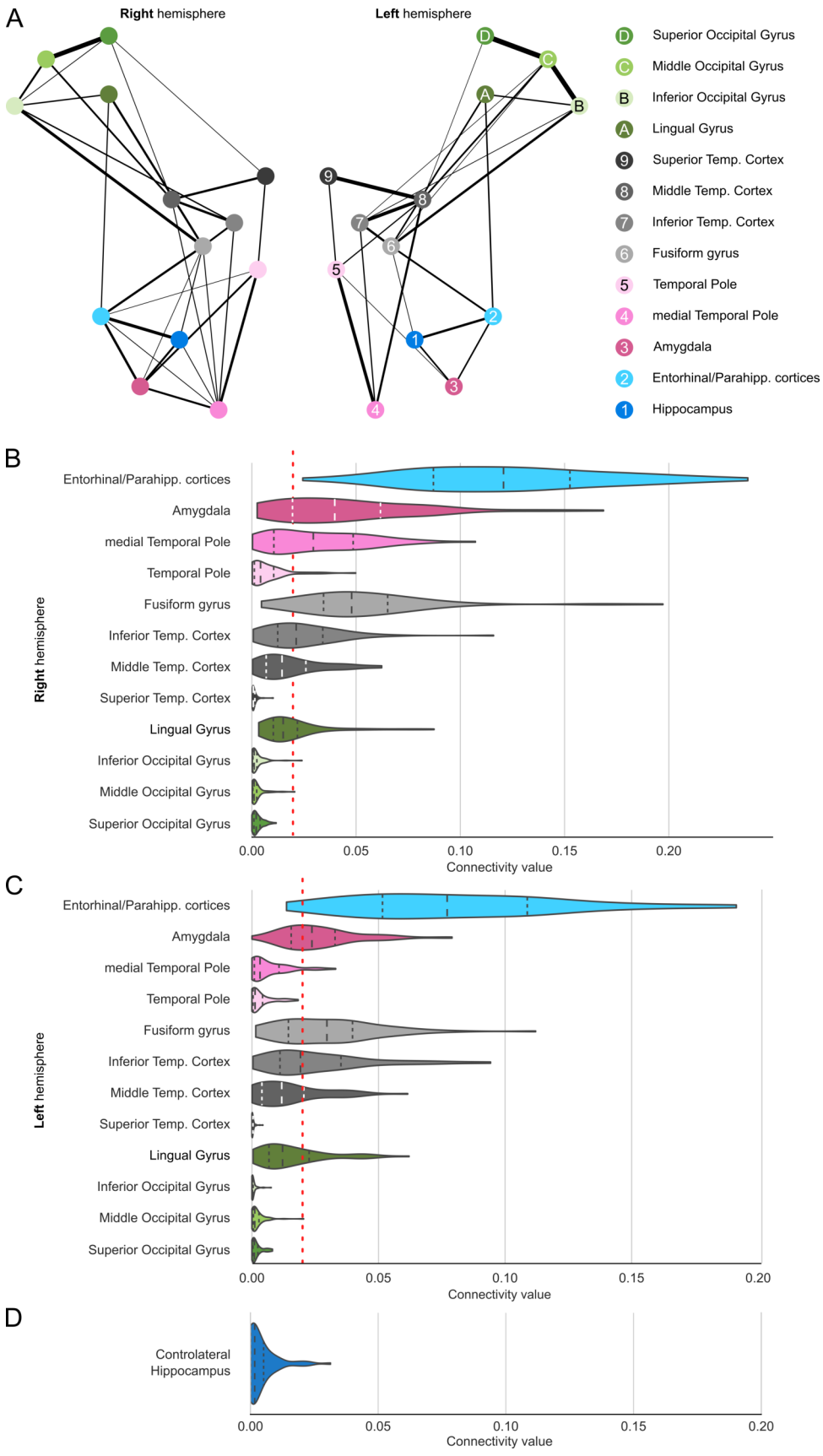

A
Right hemisphere
Left hemisphere
D Superior Occipital Gyrus
C Middle Occipital Gyrus
B Inferior Occipital Gyrus
A Lingual Gyrus
9 Superior Temp. Cortex
8 Middle Temp. Cortex
7 Inferior Temp. Cortex
6 Fusiform gyrus
5 Temporal Pole
4 medial Temporal Pole
3 Amygdala
2 Entorhinal/Parahipp. cortices
1 Hippocampus
B
Right hemisphere
Entorhinal/Parahipp. cortices
Amygdala
medial Temporal Pole
Temporal Pole
Fusiform gyrus
Inferior Temp. Cortex
Middle Temp. Cortex
Superior Temp. Cortex
Lingual Gyrus
Inferior Occipital Gyrus
Middle Occipital Gyrus
Superior Occipital Gyrus
0.00
0.05
0.10
0.15
0.20
Connectivity value
C
Left hemisphere
Entorhinal/Parahipp. cortices
Amygdala
medial Temporal Pole
Temporal Pole
Fusiform gyrus
Inferior Temp. Cortex
Middle Temp. Cortex
Superior Temp. Cortex
Lingual Gyrus
Inferior Occipital Gyrus
Middle Occipital Gyrus
Superior Occipital Gyrus
0.00
0.05
0.10
0.15
0.20
Connectivity value
D
Controlateral Hippocampus
0.00
0.05
0.10
0.15
0.20
Connectivity value

Figure 5.8: **Hippocampal structural connectivity with temporal and occipital regions.** (**A**) Average structural connectivity derived from DW-MRI data (Škoch et al. 2022) showing the mean connectivity value between MTL, temporal cortex and occipital cortex regions. Mean connectivity is represented by the width of the edges of the graph, and is thresholded at 0.02 for simplicity. (**B** and **C**) Violin plot showing the distribution of connectivity values between the right (B) and left (C) hippocampi and all other regions presented in A. For clarity, only ipsilateral connections are displayed. The red vertical line indicates the threshold used in (A). (**D**) Connectivity between contralateral hippocampi was modest.

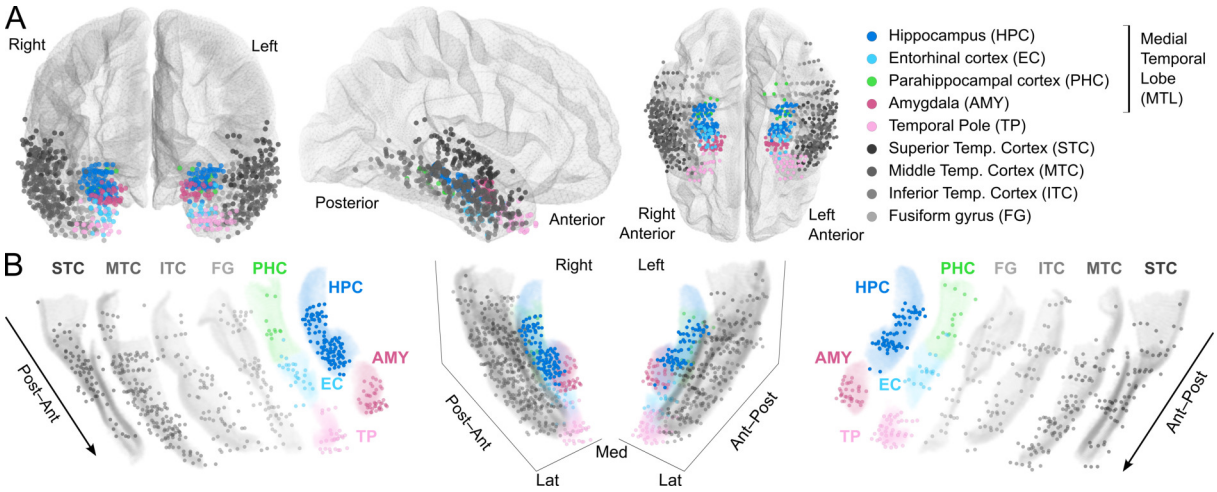


Figure 5.9: **Electrode contact localization across temporal lobe regions.** (**A**) MNI template brain showing electrode contact locations across temporal lobe regions in all participants. In this study, the MTL consisted of the hippocampus, the entorhinal cortex, the parahippocampal cortex and the amygdala. (**B**) 3D projection of electrode contacts on the MNI brain. Left and right hemispheres are expanded for clarity (axes: Post-Ant, posterior-anterior; Med-Lat, medio-lateral; Sup-Inf, superior-inferior).

parahippocampal cortex, the amygdala and the temporal pole. This observation suggests a propagation of the 2-Hz bursts across MTL regions as well as the temporal pole.

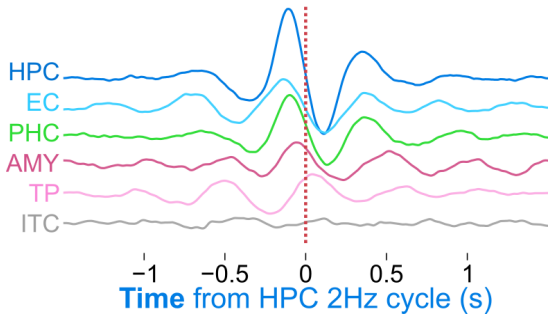


Figure 5.10: **Trigger average of MTL LFPs by hippocampal 2-Hz**, illustrating entrainment of MTL LFPs at 2 Hz and showing that 2-Hz oscillations propagate across MTL structures.

Next, to quantify this phenomenon, we measured the power spectral density (PSD) in macrocontacts located across MTL and non-MTL structures. Extra-hippocampal MTL regions had significantly higher power at 2 Hz than 6 Hz, whereas non-MTL temporal cortices were dominated by 6–8-Hz oscillations (Fig. 5.11).

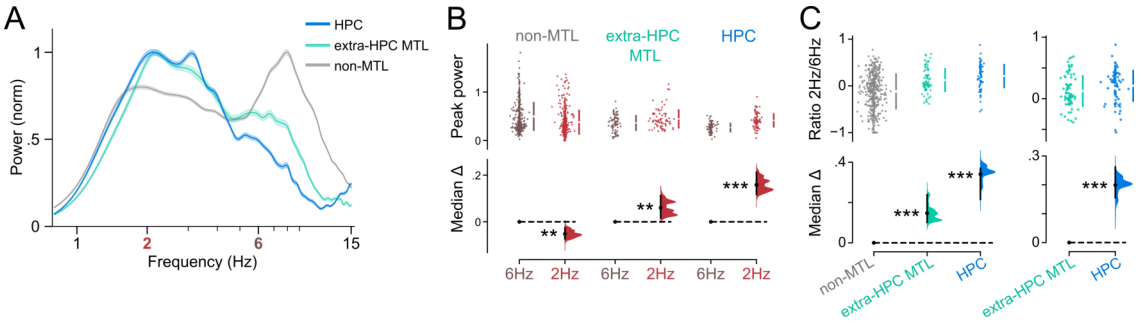


Figure 5.11: **Slow-frequency oscillations across the temporal lobe.** (**A**) PSDs corrected for the power law and averaged across hippocampal (HPC), extra-hippocampal MTL (extra-HPC MTL), and non-MTL temporal macrocontacts free of IEDs. Shaded areas indicate mean ± SEM. (**B**) Estimation plots showing mean differences between corrected 2-Hz and 6–8-Hz peak power in the regions shown in panel A. (**C**) Estimation plots showing higher 2-Hz/6–8-Hz power ratios in extra-HPC MTL and hippocampal contacts compared with non-MTL regions (left), and higher 2-Hz/6–8-Hz power ratios in hippocampal compared with extra-HPC MTL regions (right). Data were analysed using two-sided paired permutation tests; ***P $<$ 0.001, **P $<$ 0.01.

These results show that despite a stronger prevalence of 2-Hz oscillations in the hippocampus, this oscillation is also prominent in other MTL structures, but not in temporal neocortical regions (fusiform gyrus, inferior, middle and superior temporal cortices) which are primarily paced by a 6–8-Hz oscillation.

5.III.1.b Prominent 6–8-Hz oscillations in the non-MTL were detected using tmEMD

In other temporal cortices, 6–8-Hz oscillations dominated. We took advantage of this clear distinction between 2-Hz and 6–8-Hz oscillations to verify that the tmEMD algorithm was able to detect 6-Hz oscillations in these regions. Using recordings from the superior temporal cortex, we showed that 6–8-Hz oscillations could be reliably detected across macrocontacts, confirming the viability of the tmEMD method in detecting oscillations in this frequency band in our dataset (Fig. 5.12).

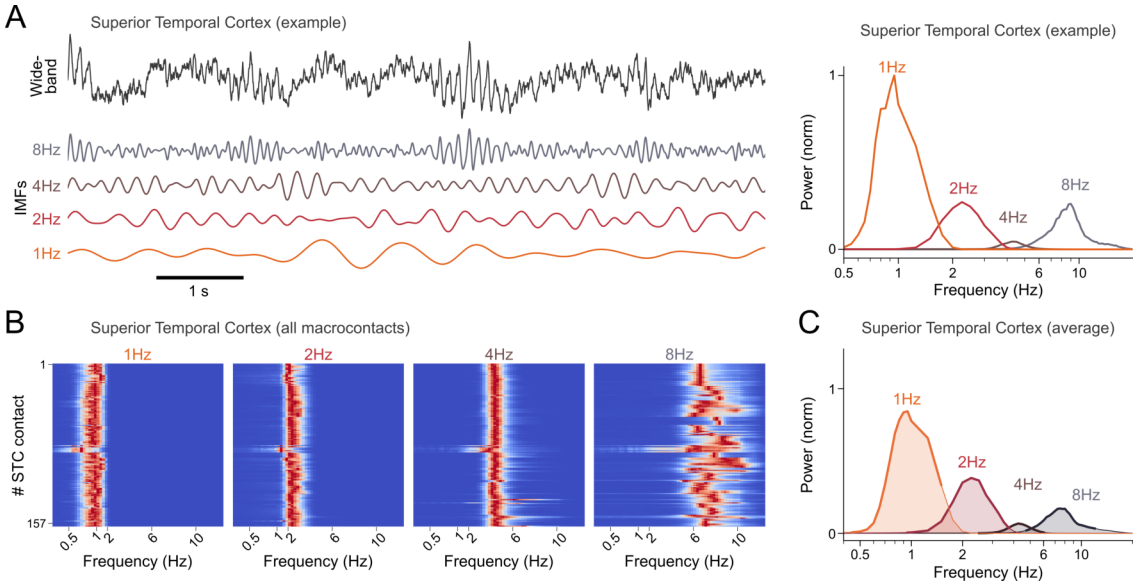


Figure 5.12: **Slow-frequency oscillatory components in the superior temporal cortex.** (**A**) LFPs signals recorded from Superior Temporal Cortex (STC) contacts revealed four oscillatory components detected by tmEMD, with peak frequencies near 1 Hz (peak [80% power band, PB]: 1.0 [0.45–1.50] Hz), 2 Hz (2.4 [0.95–3.75] Hz), 4 Hz (4.3 [2.50–6.00] Hz), and 8 Hz (8.4 [4.75–12.00] Hz). Importantly, note that these oscillations are not continuous, but also manifest as transient bursts. Left: Example STC wide-band LFPs trace with its constituent IMFs. Right: Corresponding PSDs. Note that the 8-Hz component showed a prominent peak whose amplitude was well above what could be expected from the power law. (**B**) Heatmaps showing power distributions of 1-, 2-, 4-, and 8-Hz IMFs across all STC contacts. (**C**) Average PSDs across STC contacts, normalized to the maximal 2-Hz power in the hippocampus for comparison with Fig. 4.3 (thick lines denote 80% power bands).

5.III.1.c 2-Hz oscillations are not directly evoked by mnemonic cues outside the hippocampus

Because 2-Hz oscillations dominated in extra-hippocampal MTL structures, we further tested whether they were related to the onset of visual photographs. ERPs were clearly visible in the amygdala, but in contrast to the hippocampus, recalling photographs elicited weaker ERP deflections than viewing photographs (Fig. 5.13A). In addition, there was no difference between the ERPs evoked by best and worst recalled pairs (Fig. 5.13B). These

findings together suggest that amygdala ERPs were not specifically linked to mnemonic processing, but were instead more strongly influenced by stimulus novelty.

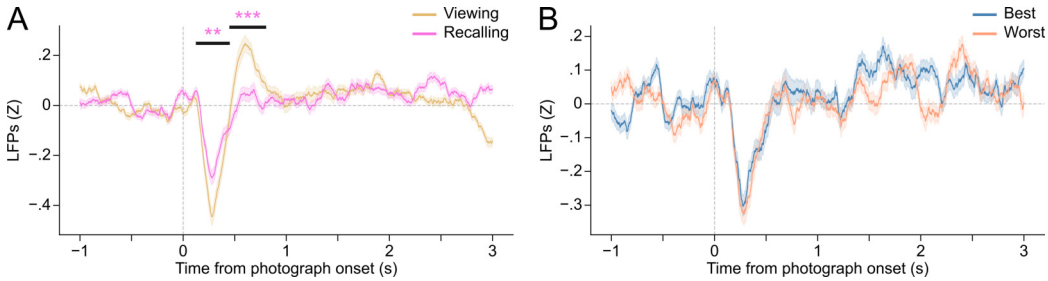


Figure 5.13: **ERPs in the amygdala.** (**A**) ERPs deflections were weaker after the onset of recall compared with viewing photographs. (**B**) ERPs deflections were not different between best and worst recalled associations in the recall session. Data were analysed using cluster-based permutation tests; ***P $<$ 0.001, **P $<$ 0.01.

In order to better characterize the link between cue onset and 2-Hz oscillations in the MTL, we computed the correlation between the magnitude of the ERP deflection and the amplitude of the evoked oscillations at 1-, 2- and 6-Hz in the recall session, like we did for hippocampal macrocontacts in Chapter 4.III.2. Importantly, ERPs deflection did not correlate with evoked 2-Hz bursts outside the hippocampus (Fig. 5.14). Overall, these results suggest that 2-Hz oscillations are primarily evoked by mnemonic cues in the hippocampus.

5.III.2 MTL local activity is paced by hippocampal 2-Hz

After having observed the presence of 2-Hz oscillations in MTL LFPs, we tested whether local activity in the MTL (single-neurons and gamma) was also entrained by hippocampal 2-Hz.

5.III.2.a MTL neurons are paced at 2-Hz

Some participants had hybrid micro-macro electrodes in MTL regions, allowing us to record from single-neuron activity in the MTL. This provided the opportunity to test whether the 2-Hz rhythm could also be observed in the autocorrelograms of these neurons. Even though these recordings were relatively sparse (n = 46 total extra-hippocampal MTL neurons), single-neuron spike trains across MTL regions exhibited prominent 2-Hz rhythmicity (Fig. 5.15), as described above in the hippocampus (Fig. 5.2).

In addition, in two participants we recorded single-neurons from temporal neocortical regions. This was permitted by the introduction of new hybrid electrodes with tetrodes protruding between the eight and ninth macrocontacts (see Chapter 2.I.1 on electrode models for further details). Notably, some neurons recorded outside the MTL (e.g., superior temporal cortex) displayed 6-Hz rhythmicity (Fig. 5.15, bottom row). This result confirmed that the 6–8-Hz oscillations observed in raw LFPs recorded from temporal neocortical regions could also pace local neuronal activity (Fig. 5.12).

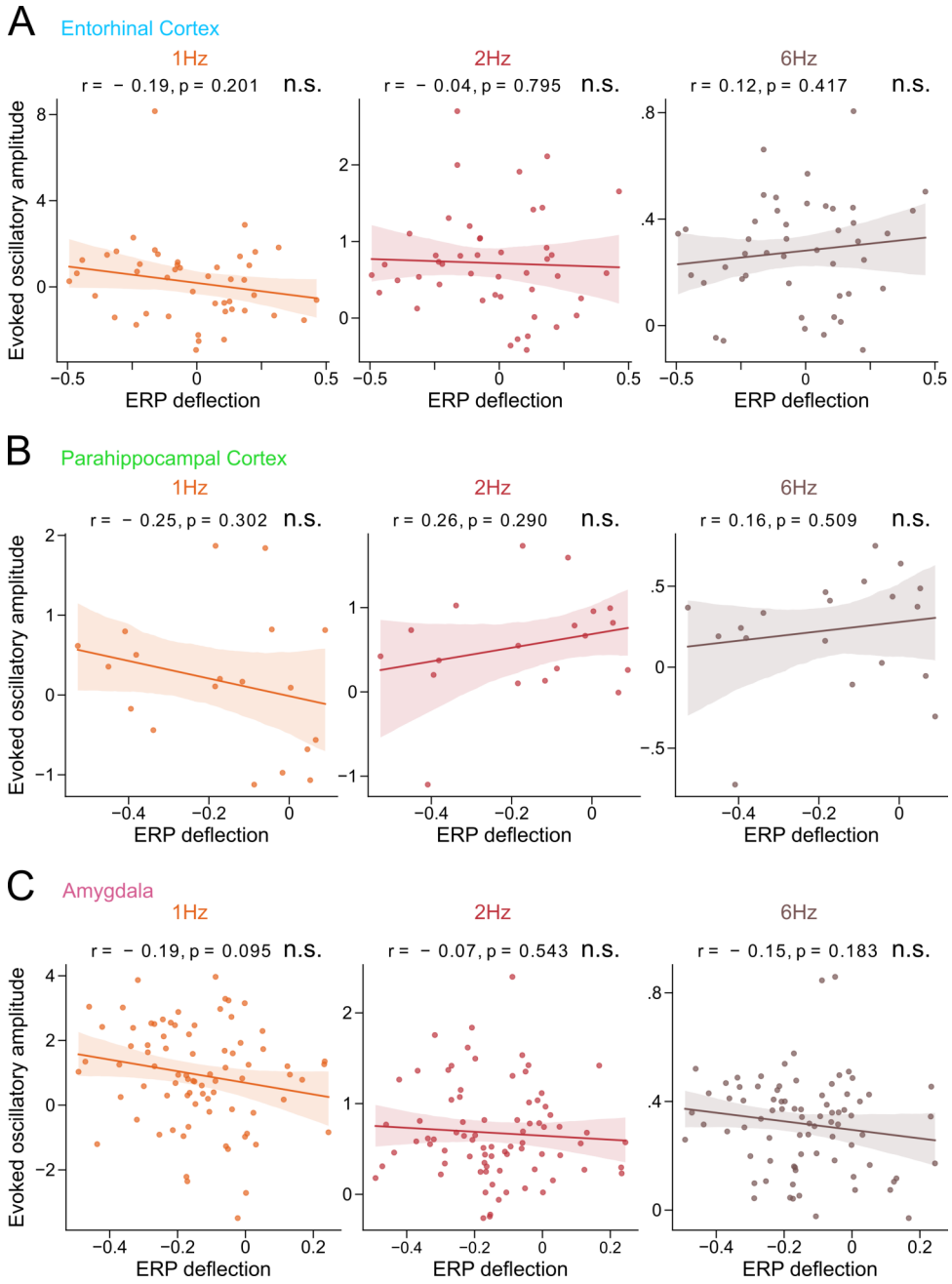


Figure 5.14: **ERP deflection does not correlate with evoked 2-Hz bursts outside the hippocampus.** (**A**–**C**) Correlations between ERPs deflection and evoked 1-, 2-, and 6-Hz amplitudes during recall in the entorhinal cortex (A), parahippocampal cortex (B), and amygdala (C). No correlation reached significance (n.s.). Note that the mean ERP deflection was measured over post-stimulus time windows corresponding to the main negative deflection observed in the grand averages for each region: 0.3–0.9 s for entorhinal cortex, 0.15–0.6 s for parahippocampal cortex, and 0.15–0.5 s for amygdala macrocontacts (see Fig. 5.13A for an example using contacts in the amygdala). Alternative time windows were also tested, but none revealed significant correlations with evoked oscillatory amplitude.

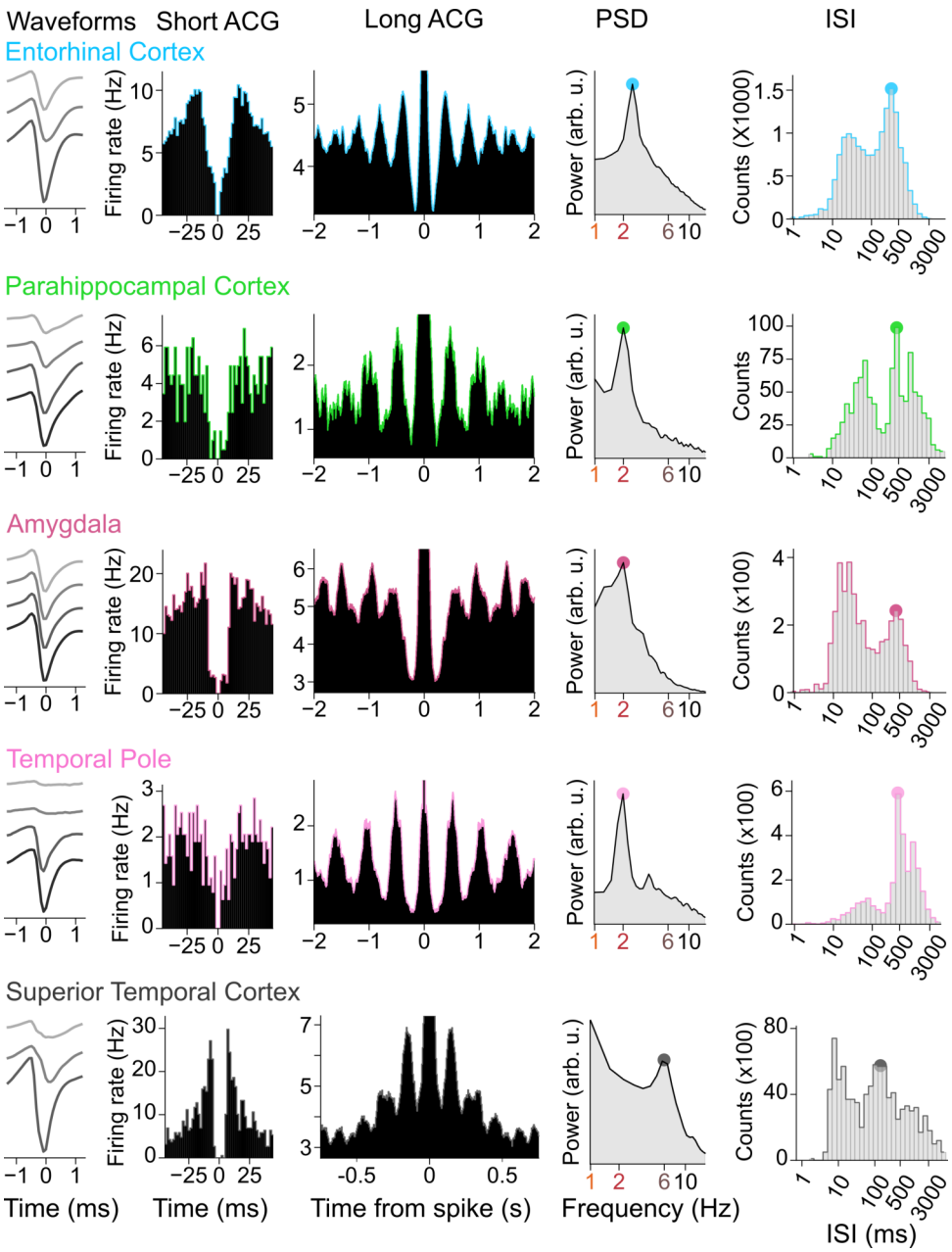


Figure 5.15: **2-Hz rhythmicity of MTL neurons.** Example neurons recorded from MTL tetrodes exhibiting 2-Hz rhythmicity, compared with a neuron recorded in the superior temporal cortex showing 6-Hz rhythmicity (bottom). From left to right: mean spike waveform across tetrode channels; short- (millisecond) and long- (second) timescale spike autocorrelograms (ACGs); PSDs; and ISI distributions. Long-timescale autocorrelograms (ACGs) are cropped at $t = 0$ for clarity.

To confirm that MTL neurons were entrained by 2-Hz oscillations detected in the hippocampus, we next measured PPC between extra-hippocampal MTL neurons and hippocampal phase. Consistently, MTL neurons better locked to hippocampal 2-Hz than to 1- or 6-Hz oscillatory phase (Fig. 5.16) and showed a strong preference for the phase of 2-Hz oscillations. Unfortunately, our single-neuron recordings in the temporal cortex were too sparse and provided too few neurons in these regions to run statistical measurements of phase-locking to the hippocampus. To overcome this technical limitation, in the next section we focus on gamma oscillations recorded from macrocontacts in the MTL and non-MTL regions, interpreted as a proxy for local neuronal activity (see Chapter 2.I.3.b and Fig. 2.3).

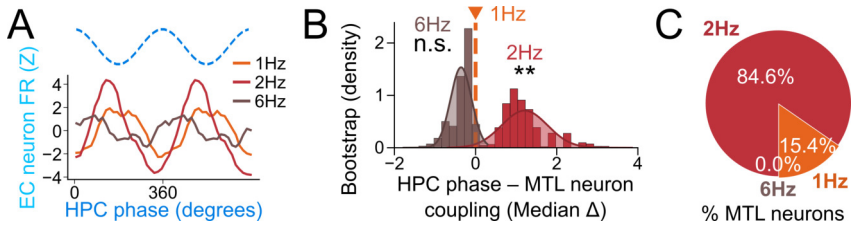


Figure 5.16: **MTL neurons preferentially couple to the phase of hippocampal 2-Hz oscillations.** (**A**) Firing-phase histograms of an example entorhinal cortex (EC) neuron relative to 1-, 2-, and 6-Hz hippocampal oscillations. (**B**) Median differences in pairwise spike-phase consistency (PPC, z-score) between hippocampal 1-Hz and 2- or 6-Hz rhythms for MTL neurons. (**C**) Percentage of MTL neurons preferentially coupled to 1-, 2-, or 6-Hz hippocampal oscillations.

5.III.2.b Hippocampal 2-Hz synchronizes MTL gamma oscillations

Next, we assessed whether the amplitude of extra-hippocampal MTL gamma activity was preferentially coupled to the phase of hippocampal slow oscillations. We computed PAC between all pairs of MTL-hippocampus macrocontacts, which also revealed preferential coupling at 2-Hz (Fig. 5.17A,B, D-F). We then trained a LMEM on gamma activity recorded in the MTL and the temporal cortex to compare the interaction between frequency (1-, 2- and 6-Hz) and region (MTL versus non-MTL). We included the anatomical (euclidean) distance between pairs of contacts as a fixed effect in the model, while recording days were treated as a random effect. This analysis revealed a synergistic effect between MTL region and 2-Hz (Fig. 5.17C, significant frequency x region interaction term), confirming that the hippocampal 2-Hz oscillations preferentially modulated gamma activity in the MTL.

Finally, we evaluated whether this preferential modulation of gamma MTL at 2-Hz translated into synchronization relevant for mnemonic processes. For each hippocampal contact, we computed the difference between all MTL or non-MTL preferred 2-Hz phase (Fig. 5.17A, see Chapter 2.II.5 for further details). By taking the inverse of this phase difference, we obtained a measure of phase synchronization between MTL and non-MTL contacts, reporting the tendency of gamma activity to be locked at the same hippocampal 2-Hz phase. Phase synchronization was higher for MTL contacts than non-MTL contacts only during the learning and the recalling sessions, a difference not observed at 1 or 6 Hz (Fig. 5.18).

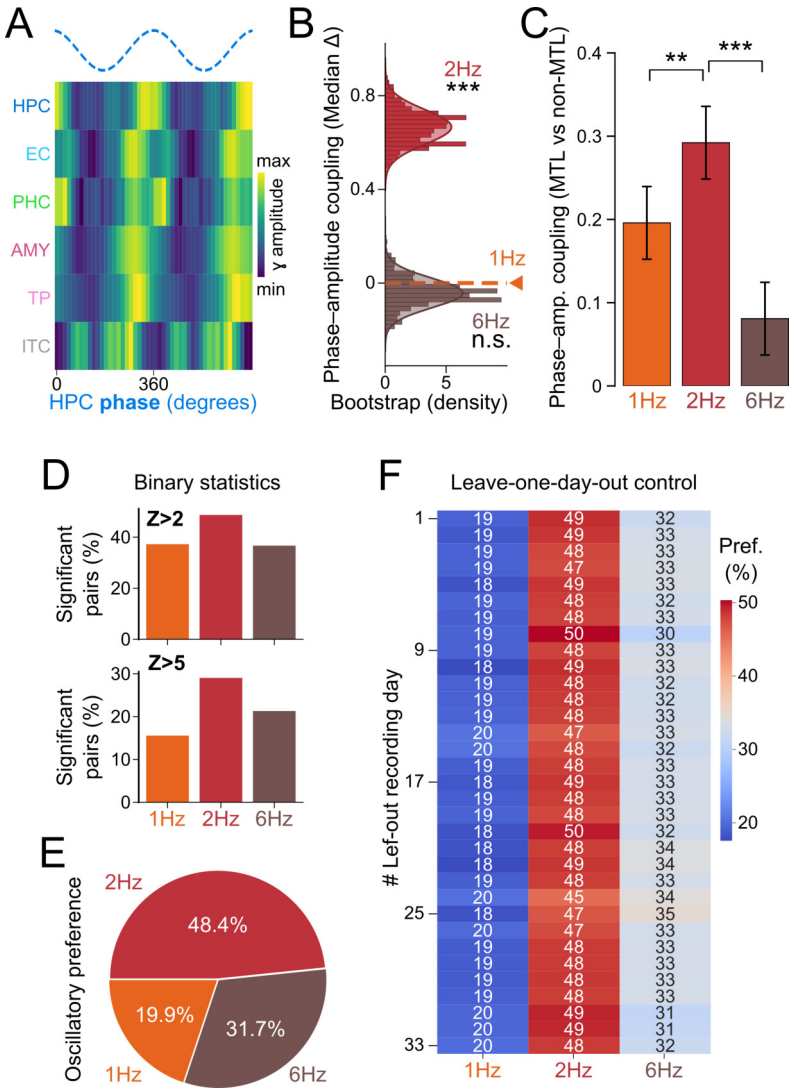


Figure 5.17: **Gamma coupling to hippocampal slow oscillations in the MTL.** (**A**) Gamma amplitude averaged across hippocampal 2-Hz phase bins, revealing phase synchronization within the MTL: the preferred 2-Hz phase of gamma patterns is consistent between MTL contacts, but not non-MTL ones (e.g., inferior temporal cortex, ITC). (**B**) Median differences in phase-amplitude coupling (z-score) between hippocampal 1-Hz and 2- or 6-Hz rhythms for MTL gamma envelopes. (**C**) Regression coefficients showing the MTL versus non-MTL contribution to phase-amplitude coupling across 1-, 2-, and 6-Hz rhythms. Statistics indicate the frequency x region interaction term. (**D**) Percentage of MTL contacts significantly coupled to 1-, 2-, or 6-Hz hippocampal oscillations, defined by pairwise spike-phase consistency z-scores above 2 (top) or 5 (bottom). (**E**) Proportion of MTL contacts preferring 1-, 2-, or 6-Hz hippocampal oscillations. (**F**) Leave-one-day-out analysis of oscillatory preference, showing that no individual recording day accounted for the observed preference of MTL gamma amplitude to the hippocampal 2-Hz phase. Data were analysed by two-sided paired permutation tests, except in (C), where Wald t-tests on LMEM coefficients were used; ***P $<$ 0.001, **P $<$ 0.01; n.s., not significant.

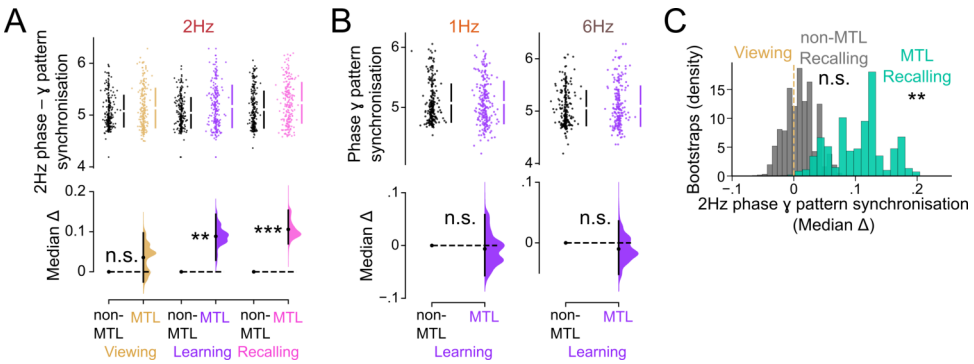


Figure 5.18: **Synchronization of MTL gamma patterns by 2-Hz phase.** (**A**) Estimation plot showing the difference in 2-Hz phase synchronization between MTL and non-MTL gamma patterns across viewing, learning, and recalling sessions. (**B**) Estimation plot showing median differences in 1-Hz (left) and 6-Hz (right) phase synchronization between MTL and non-MTL gamma patterns during learning, revealing no effect at 1 and 6 Hz. (**C**) Estimation plot showing median differences in 2-Hz phase synchronization between MTL and non-MTL gamma patterns during recall relative to viewing, revealing no effect for non-MTL contacts. Data were analysed by two-sided paired permutation tests; ***P $<$ 0.001, **P $<$ 0.01; n.s., not significant.

We then tested whether this coordination was preferentially expressed in slow-oscillatory burst events by comparing neuronal and network activity inside versus outside hippocampal 2-Hz bursts during learning and recall. Phase-amplitude coupling between hippocampal 2-Hz and MTL gamma-band activity was stronger inside than outside them (Fig. 5.19A). Gamma activity across MTL regions also showed stronger phase synchronization to hippocampal 2-Hz oscillations inside bursts (Fig. 5.19B). At the population level, MTL neuron spiking coactivity was elevated during in-burst compared to out-of-burst periods (Fig. 5.19C, Chapter 2.III.2 and Chapter 6.III for details on the measure of coactivity). Together, these results indicate that the hippocampal slow-oscillatory architecture coordinates neural activity across the MTL, with coordination concentrated within transient burst events that synchronize distributed population dynamics during human memory processing.

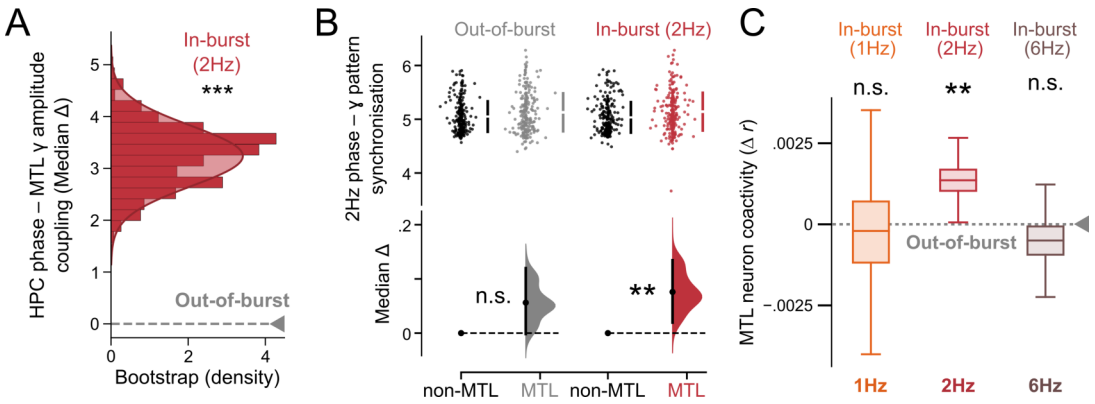


Figure 5.19: **Synchronization of MTL gamma patterns in oscillatory bursts.** (**A**) Phase-amplitude coupling difference for MTL gamma envelopes relative to hippocampal 2-Hz rhythm during (in-burst) versus outside (out-of-burst) 2-Hz burst events. (**B**) Estimation plot showing higher oscillatory phase synchronization in MTL versus non-MTL gamma activity patterns inside but not outside 2-Hz bursts. (**C**) Median differences in MTL neuron coactivity for in-burst versus out-of-burst periods at 1-, 2- and 6-Hz. Increased coactivity during hippocampal 2-Hz but not 1- and 6-Hz bursts indicates that 2-Hz bursts were specifically associated with a stronger organization of neuronal coactivity motifs across the MTL. Statistics were assessed using two-sided paired permutation tests. ***P $<$ 0.001, **P $<$ 0.01; n.s., not significant.

5.IV Discussion

In this chapter, I showed that the hippocampal 2-Hz rhythm organizes neuronal activity locally within the human hippocampus and across distributed MTL regions. At the local level, hippocampal neurons preferentially locked to the phase of 2-Hz oscillations, and gamma activity was more strongly modulated at 2 Hz than at neighbouring slow frequencies (1 and 6 Hz). These findings indicate that the 2-Hz rhythm structures both neuronal firing and local network dynamics, consistent with the properties expected from a theta-like oscillation. Although I had too few tetrodes with both putative pyramidal neurons and interneurons to draw strong cell-type conclusions, both cell classes were nonetheless phase-locked to 2-Hz, supporting the view that this rhythm acts at the level of the neuronal population.

Importantly, this organization extended beyond the hippocampus itself. Extra-hippocampal MTL regions also showed prominent 2-Hz oscillations, and neuronal as well as gamma-band activity in these regions synchronized preferentially to hippocampal 2-Hz phase. Notably, this pattern was observed in the entorhinal cortex and amygdala, two structures known in rodents to synchronize with hippocampal theta during memory-related states. This coordination was especially visible during learning and recall, and was stronger during 2-Hz burst periods than outside them. In addition, MTL neuronal coactivity was increased during hippocampal 2-Hz bursts, suggesting that these events were associated with a stronger organization of population activity across the MTL. Overall, these observations indicate that transient 2-Hz bursts contribute to the online coordination of distributed neuronal assemblies during memory-guided behaviour.

This effect was most prominent in the hippocampus, but 2-Hz oscillations were also present in extra-hippocampal MTL structures. In contrast, temporal neocortical regions were dominated by 6–8-Hz oscillations. However, the single-neuron recordings in the temporal cortex were sparse, which limited my ability to assess the functional relevance of these oscillations in detail. Further studies could therefore explore whether these 6–8-Hz rhythms support different forms of temporal-lobe processing, and how they relate to the slower hippocampal rhythm described here.

Because measures of phase-amplitude coupling (PAC) can be affected by signal-processing choices, particularly when the underlying oscillation is strongly non-linear, I used methods based on empirical mode decomposition and Holo-Hilbert Spectral Analysis (HHSA) to confirm the gamma findings. These approaches are designed to avoid the biases introduced by conventional filtering. In this dataset, they confirmed that gamma activity was preferentially modulated at 2 Hz, supporting the view that this effect reflects genuine cross-frequency organization rather than an analysis artefact.

The previous chapter showed that hippocampal 2-Hz is selectively evoked during mnemonic engagement, while the present one shows that this rhythm organizes neuronal coactivity across the MTL. Together, these findings raise the question of whether the coordinated activity patterns formed during wakefulness are later reactivated during offline states. According to the two-stage model of memory (Chapter 1.III.3), neuronal assemblies engaged during active wake states should subsequently be reactivated during hippocampal ripple events, supporting memory consolidation. In addition, because theta oscillations in other mammals are also prominently expressed during REM sleep (Chapter 1.III.2), an important remaining question is whether the hippocampal 2-Hz rhythm also re-expresses during human REM sleep. However, direct evidence for these two phenomena are currently lacking in humans (see Chapter 1.IV.1 and Chapter 1.IV.2). Therefore, in the next chapter, I investigate hippocampal activity during rest and sleep, focusing on the relationship between 2-Hz oscillations, ripple events, and the reactivation of neuronal coactivity patterns formed during task wake states.

6 Results: Neural activity in the offline human hippocampus

"Ce que voit un sujet dépend à la fois de ce qu'il regarde et de ce que son expérience antérieure, visuelle et conceptuelle, lui a appris à voir."

"What one sees depends both on what one is looking at and also upon what his previous visual-conceptual experience has taught him to see."

— Thomas S. Kuhn, The Structure of Scientific Revolutions (1962)

Contents

6.I Introduction 140

6.II Hippocampal physiology across sleep stages 141

6.II.1 Hippocampal 2-Hz features REM sleep but not SWS 142

6.II.2 Validation of hippocampal ripples 144

6.III Neuronal coactivity motifs in 2-Hz bursts reactivate in post-learning hippocampal ripples 154

6.III.1 Coactivity motifs formed during 2-Hz bursts reactivate in post-learning hippocampal ripples 154

6.III.2 Reactivation is relevant for behavioural performance 155

6.IV Discussion 157

6.I Introduction

The previous chapters identified a prominent 2-Hz rhythm in the human hippocampus which exhibited properties expected from a theta-like oscillation. Hippocampal 2-Hz bursts were more prevalent during mnemonic engagement, were evoked by memory-relevant cues, and organized neuronal firing and gamma activity locally within the hippocampus and across distributed MTL regions. In particular, transient 2-Hz bursts were associated with increased neuronal coactivity, suggesting that this rhythm contributes to the online coordination of neuronal assemblies during memory processing.

According to the two-stage model of memory, however, memory formation does not end with the online coordination of neuronal activity during active wake states. Instead, activity motifs formed during learning are reactivated during offline states such as rest

and sleep, thereby supporting memory consolidation (Buzsáki 1989; McClelland et al. 1995; Wilson and McNaughton 1994). In rodents, this offline stage is associated with hippocampal sharp-wave ripples occurring predominantly during low-cholinergic states such as slow-wave sleep and rest (Buzsáki 1986; Wilson and McNaughton 1994; Girardeau et al. 2009; Ego-Stengel and Wilson 2009; Roux et al. 2017). In parallel, theta oscillations re-express during REM sleep, suggesting that complementary oscillatory states organize online and offline memory processes across behavioural states (Jouvet et al. 1959; Jouvet 1969; Winson 1972).

The results obtained so far therefore raise two related questions. First, if hippocampal 2-Hz is a genuine theta-like rhythm, does it also characterize human REM sleep, as theta does in other mammals? Second, do the neuronal coactivity motifs coordinated during waking 2-Hz bursts subsequently reactivate during hippocampal ripple events in offline states? Addressing these questions is essential to determine whether the physiological organization described in the previous chapters extends to the offline stage of the two-stage memory model.

In this chapter, I therefore investigate hippocampal activity during rest and overnight sleep. I first characterize the expression of 2-Hz oscillations and ripple events across behavioural states, and compare their physiological properties with those previously described in animal models. I then test whether neuronal coactivity motifs formed during waking 2-Hz bursts are preferentially reactivated during post-learning hippocampal ripples. Finally, I evaluate whether this reactivation relates to behavioural performance, thereby linking online network coordination with offline memory consolidation in humans.

6.II Hippocampal physiology across sleep stages

We conducted overnight polysomnography in seven participants who enrolled in the memory task. These participants were recorded continuously for the entire duration of their stay at the hospital (24-hour recordings), and underwent three nights of polysomnography according to the American Academy of Sleep Medicine guidelines (Troester et al. 2023). Sleep stages were detected by a trained clinician using scalp EEG, electrooculography (EOG) and electromyography (EMG), and were grouped into the following: wake, light-sleep (N1), slow-wave sleep (SWS; N2 and N3), REM (Fig. 6.1). Note that for all analyses presented in this chapter, "wake" does not include micro-arousals detected during the night, but refers to epochs of clear wake occurring during the day.

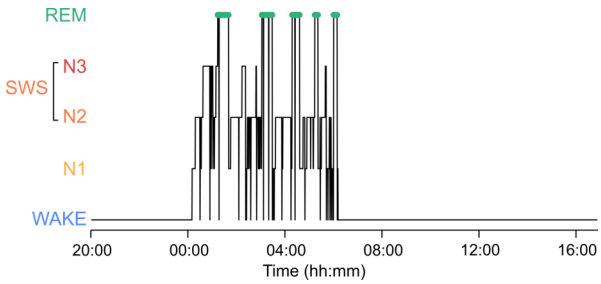


Figure 6.1: **Example of sleep staging in one participant.**

6.II.1 Hippocampal 2-Hz features REM sleep but not SWS

We first inspected hippocampal LFP raw traces to evaluate whether 2-Hz oscillations were visible in hippocampal LFPs during REM sleep in humans. Importantly, 2-Hz bursts were directly identifiable in the raw traces during REM sleep but not SWS (Fig. 6.2). Instead, SWS showed non-oscillatory, "de-structured" LFPs, consistent with what can be seen from the rodent hippocampus. This signature typically reflects the sum of transient delta waves occurring on a broadband, aperiodic background. Note that the REM oscillatory cycles were more symmetrical than those occurring during the memory task (Fig. 4.4), a characteristic previously reported in rodents (Buzsáki et al. 1983) referred to as "most regular rhythmic slow activity in REM sleep" (Belluscio et al. 2012). We further verified that 2-Hz bursts were observed alongside rapid eye movements recorded from the electrooculograms (Fig. 6.3).

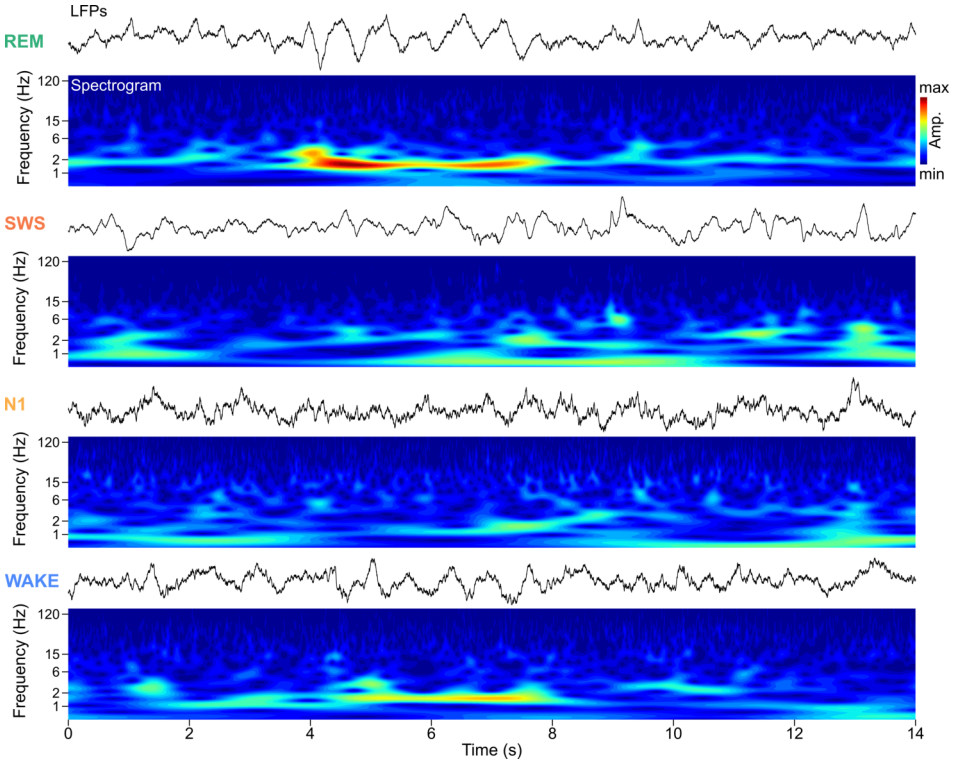


Figure 6.2: **Raw hippocampal LFPs display 2-Hz bursts in human REM sleep but not during SWS.** Example 14-s recording epochs from different recording epochs of an example night with wake, N1, SWS, and REM stages showing hippocampal LFPs and corresponding spectrograms, revealing a clear 2-Hz burst during REM sleep. Note the symmetrical oscillatory cycles during REM sleep compared with the asymmetrical cycles reported during task engagement (Fig. 4.4), and the aperiodic signal occurring during SWS.

Next, to quantify the presence of 2-Hz oscillations in REM sleep, we computed PSDs on 30-second epochs after matching the number of epochs detected between sleep stages. PSDs obtained from the example contact shown in Fig. 6.2 are presented in Fig. 6.4A. Across all recording nights, 2-Hz but neither 1-Hz nor 6-Hz power was higher in REM compared with SWS (Fig. 6.4B), confirming the presence of 2-Hz oscillations in REM but

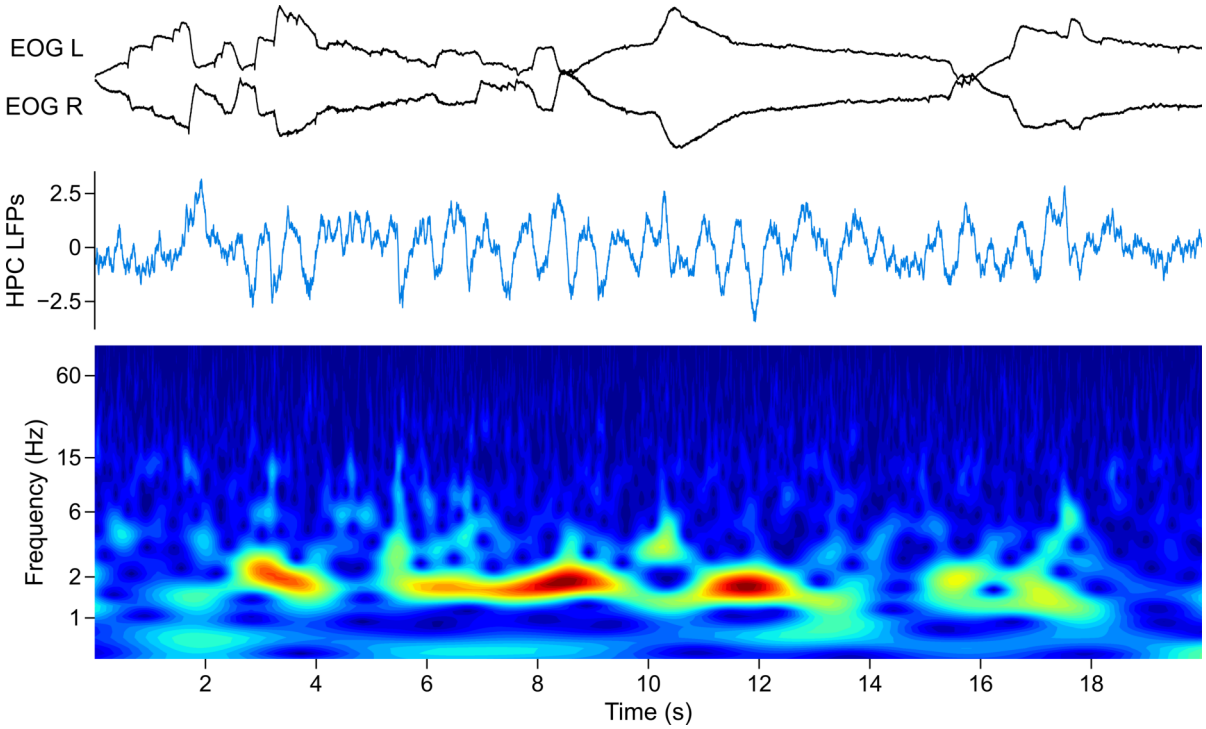


Figure 6.3: **2-Hz bursts can be observed alongside rapid eye movements.** Example 20-s recording epochs during REM stage showing right (EOG R) and left (EOG L) electrooculograms, hippocampal LFPs and corresponding spectrogram, with example 2-Hz bursts during REM. Rapid eye movements were clearly visible in the electrooculograms, confirming the correct staging of REM sleep.

not SWS in the human hippocampus. This result is in line with earlier work in rodents and cats, which describe theta oscillations emerging during REM sleep (Buzsáki et al. 1983). Moreover, by replicating analogous observations obtained from several other studies in humans (Freemon and Walter 1970; Giaquinto 1973; Bódizs et al. 2001; Clemens et al. 2009), these data further suggest that the 2-Hz rhythm is a putative homologue of rodent theta.

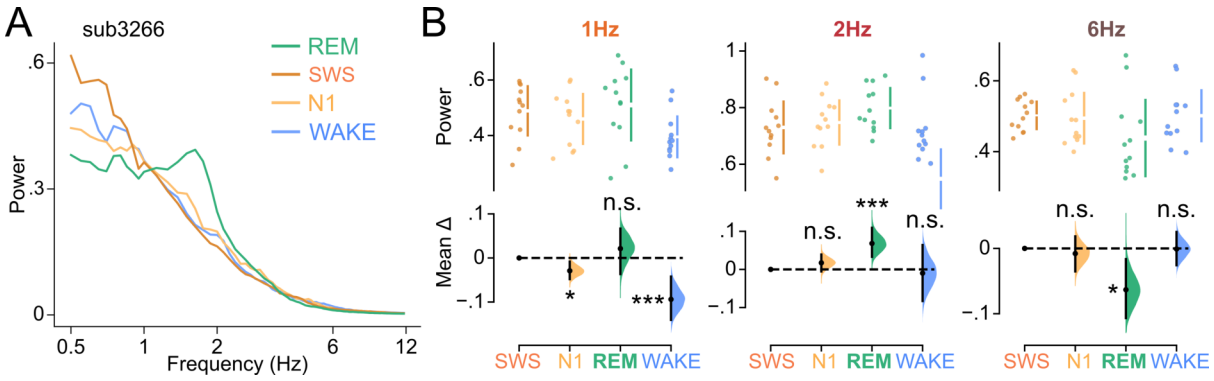


Figure 6.4: **2-Hz oscillations feature human hippocampal LFPs during REM sleep.** (**A**) Power spectral densities from the same contact used in Fig. 6.2, averaged over at least 100 randomly selected epochs per stage, showing prominent 2-Hz power featuring REM sleep. Note the elevated <1-Hz power during SWS, without a clearly identifiable peak in the PSD. This is consistent with the broadband, aperiodic nature of the raw LFPs traces. (**B**) Estimation plots showing mean differences in 1-, 2-, and 6-Hz power across sleep stages, revealing consistently higher 2-Hz, but not 1- or 6-Hz, power in REM compared with SWS. Data were analysed using two-sided paired permutation tests; ***P < 0.001, *P < 0.05; n.s., not significant.

6.II.2 Validation of hippocampal ripples

6.II.2.a Hippocampal ripples feature SWS and rest sessions

In animal models, fast-frequency ripple events (100–250 Hz) occur during rest and sleep and support offline memory consolidation (Wilson and McNaughton 1994). Hippocampal ripples also occur in humans (Bragin et al. 1999a; Clemens et al. 2007; Staresina et al. 2015; Chen et al. 2021; Staresina et al. 2023), where they could similarly support post-learning consolidation. To validate the ripple detection algorithm employed in our dataset, we first examined hippocampal ripple activity during sleep, as well as during pre- and post-learning rest sessions of the relational memory task. Ripples showed fast-frequency oscillatory cycles clearly visible in the raw LFPs traces (Fig. 6.5) and were associated with the characteristic slow-frequency, high-amplitude delta-waves described earlier (Fig. 6.2). Notably, the amplitude and the phase of the delta-waves but not the ripples were dramatically impaired by bipolar referencing (Fig. 6.6).

We further characterized the ripples detected in our dataset by measuring their central frequency using phase unwrapping (see Chapter 2.III.1.b for additional details), which does not rely on amplitude normalization. Even though ripples had a central frequency

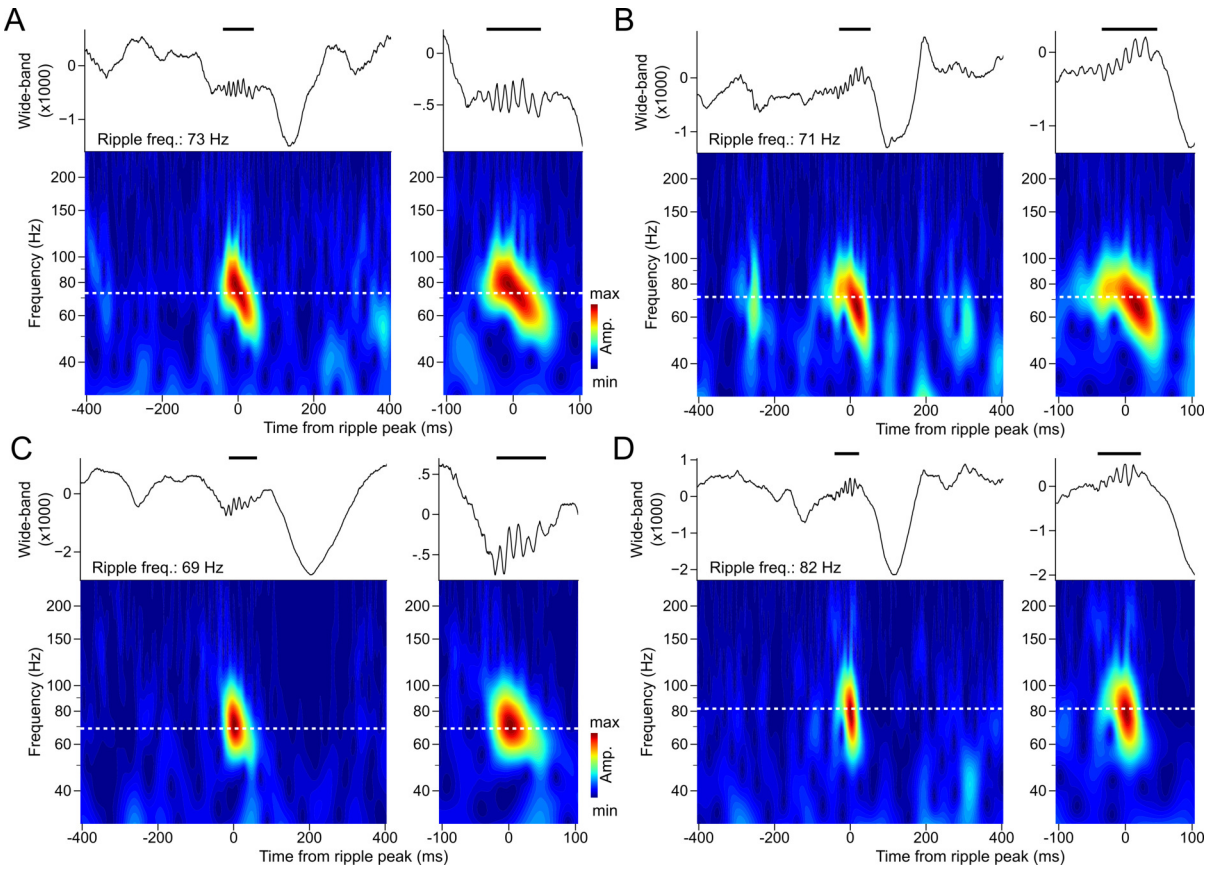


Figure 6.5: **Example of detected ripples.** (**A-D**) Representative ripples detected during SWS on a single macrocontact with corresponding wide-band LFPs and spectrograms. In this macrocontact, median and mean ripple frequencies were 73.9 Hz and 74.3 Hz, respectively. Right insets provide magnified views of individual ripples. Black horizontal bars indicate ripple duration (onset to offset), and white, dotted horizontal lines mark the ripple central frequency measured using phase unwrapping (see Chapter 2.III.1.b for further methodological details).

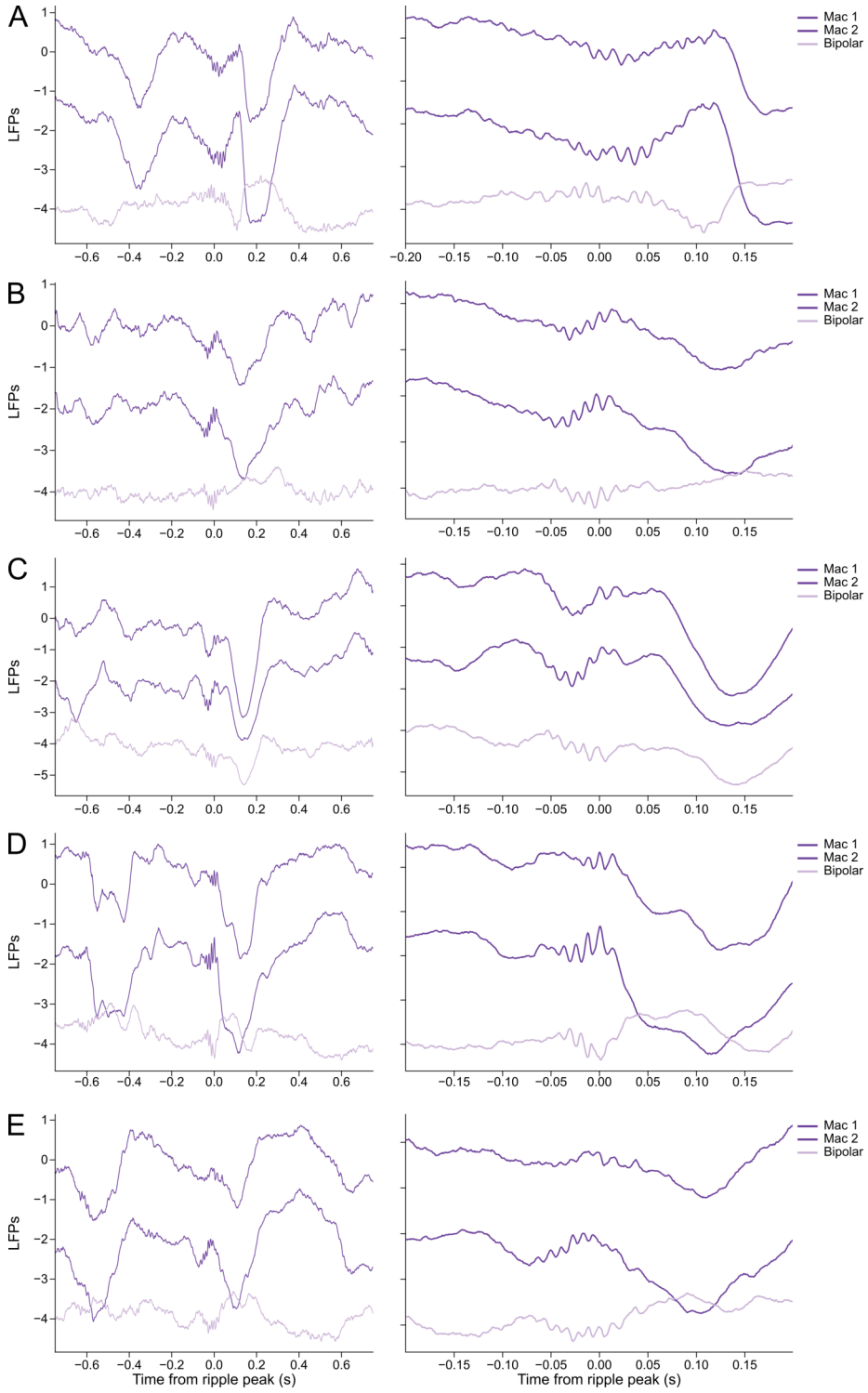


Figure 6.6: **Bipolar referencing impairs the delta-waves.** (**A**–**E**) LFPs traces centred on five example ripples before (Mac 1, Mac 2) and after bipolar referencing. Note that the bipolar referencing behaves unexpectedly: the slow component of the delta-wave is sometimes lost (**B**), preserved and reduced (**C**), or, most often, flipped in polarity (**A**, **D** and **E**).

distributed around 70 Hz [mean (95% CI): 70.60 (69.92–71.28) Hz] (Fig. 6.7A–C), despite the use of a broad ripple frequency band during initial detection of the ripples (60–180 Hz, see Chapter 2.III.1). In addition, ripple central frequency was comparable between SWS, N1 and task rest sessions (Fig. 6.7D–F), confirming that we detected similar events during task rest sessions and overnight sleep.

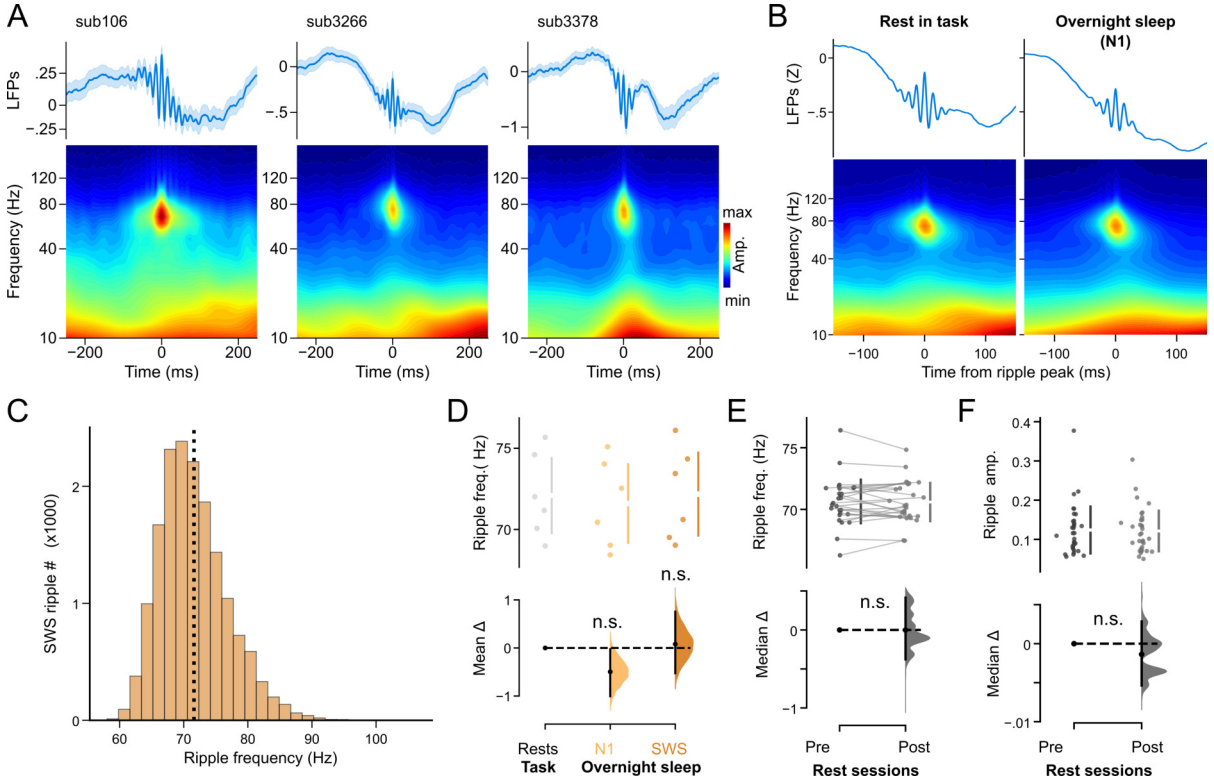


Figure 6.7: **Characterization of ripple frequency.** (**A**) Ripple-triggered average LFPs and spectrograms from hippocampal macrocontacts across participants. Shaded areas indicate mean ± SEM. (**B**) Average LFPs and spectrograms triggered by hippocampal ripples during rest or overnight sleep N1, recorded from the same macrocontact in the same participant, showing that ripples had the same morphology across these states. (**C**) Distribution of ripple central frequencies across all detected SWS ripples, pooled across participants used in F. Note that our algorithm detected ripples up to 90 Hz. Black vertical dotted line indicates the median frequency (70.9 Hz, mean = 71.6 Hz). (**D**) Estimation plot showing mean paired differences in ripple central frequency between rest and overnight N1 or SWS sessions (using the same contacts from the same subjects; n = 6 participants recorded across all sessions). (**E** and **F**) Estimation plots showing comparable ripple central frequency (E) and amplitude (F) between pre- and post-learning rest. Data were analysed using two-sided paired permutation tests; ***P < 0.001, **P < 0.01; n.s., not significant.

Ripples detected in our human dataset had a central frequency slower than that of events reported from the mouse hippocampus (Buzsáki 1986), which is consistent with canonical description in humans (Bragin et al. 1999a; Liu et al. 2022; Maslarova et al. 2025). However, mouse ripples were recorded from microelectrodes (tetrodes, silicon probes), which have different electrical properties than the macrocontacts used in our study and could thus affect the frequency of the ripples. Hence, we tested whether the

difference in ripple frequency could be explained by different electrode types by visualizing LFPs recorded simultaneously from a hippocampal macrocontact and a local tetrode (from the same hybrid micro-macro electrode), in a 10-min rest session (Fig. 6.8A).

PSDs computed over the entire recording session displayed a peak at 70 Hz in both hippocampal macrocontact and the local tetrode, indicating a similar frequency content overall (Fig. 6.8B). As a control, we used another, distal tetrode located in a non-MTL region which exhibited a prominent peak in the ripple band (90 Hz). Then, we computed the average LFPs on the local and the distal tetrodes, triggered by ripples detected from macrocontacts (Fig. 6.8C). In the hippocampal tetrode, but not in the non-MTL tetrode, ripples were clearly visible on this average trace. Moreover, the central frequency of the ripples was comparable in the hippocampal tetrode and the macrocontact, showing that electrode type is not likely to explain the difference observed between human and mouse ripples. Interestingly, the phase of the delta-wave was reversed between macrocontact and tetrode events (Fig. 6.8A,C), mirroring the phase reversal reported with laminar electrodes penetrating the dorsal CA1 pyramidal layer dipole in mice (Castelli et al. 2025; Lopes-Dos-Santos et al. 2025).

On a side note, during one recording day we recorded fast-ripples using tetrodes located in the seizure onset zone (Fig. 6.9). These events were clearly visible in the raw LFP traces of the tetrodes and in their corresponding spectrograms. Consistent with previous reports describing these pathological events (Bragin et al. 1999a; Bragin et al. 1999b; Foffani et al. 2007; Valero et al. 2017; Liu et al. 2022), fast-ripples had a central frequency of ~300 Hz. The layout of our hybrid electrodes provided useful information about fast-ripples: as they protrude between the two deepest macrocontacts at ~45 degrees angle, tetrodes were usually spaced by a few millimeters. In this example, one tetrode recorded extracellular action potentials (Tetrode 1), while the other did not (Tetrode 2). Fast-ripples were visible on both tetrodes, with the amplitude of the events being most prominent on the tetrode containing spiking activity. This observation confirms that oscillatory events with a central frequency above 100 Hz could be recorded with high signal-to-noise ratio in our setup, which provides greater confidence about the validity of the "physiological" ripples (with central frequency of ~70 Hz) used throughout this manuscript. Note that this recording day was not included in the main analyses of this manuscript.

In rodents, ripples occur at a higher rate in low-cholinergic behavioural states like slow-wave sleep and rest compared with active exploration, movement and REM sleep. However, previous studies in humans reported ripples in both high and low cholinergic states (Axmacher et al. 2008; Chen et al. 2021; Dickey et al. 2022b; Dickey et al. 2022a), raising questions about the behavioural state dependence of ripples in humans. In our dataset, ripples were more frequent in slow-wave and N1 sleep than wake and REM (Fig. 6.10A,B), and during rest sessions compared with active sessions of the memory task (Fig. 6.10C). Note that the ripple rate was comparable between N1 sleep and rest sessions of the memory task (Fig. 6.10A). This observation is consistent with the state of drowsiness characteristic of these short (10-min) rest sessions, which is the behavioural definition of N1 sleep. These results are consistent with the mouse literature, suggesting that the biological pathways giving rise to ripples in humans are down-regulated during high-cholinergic states (Maslarova et al. 2025).

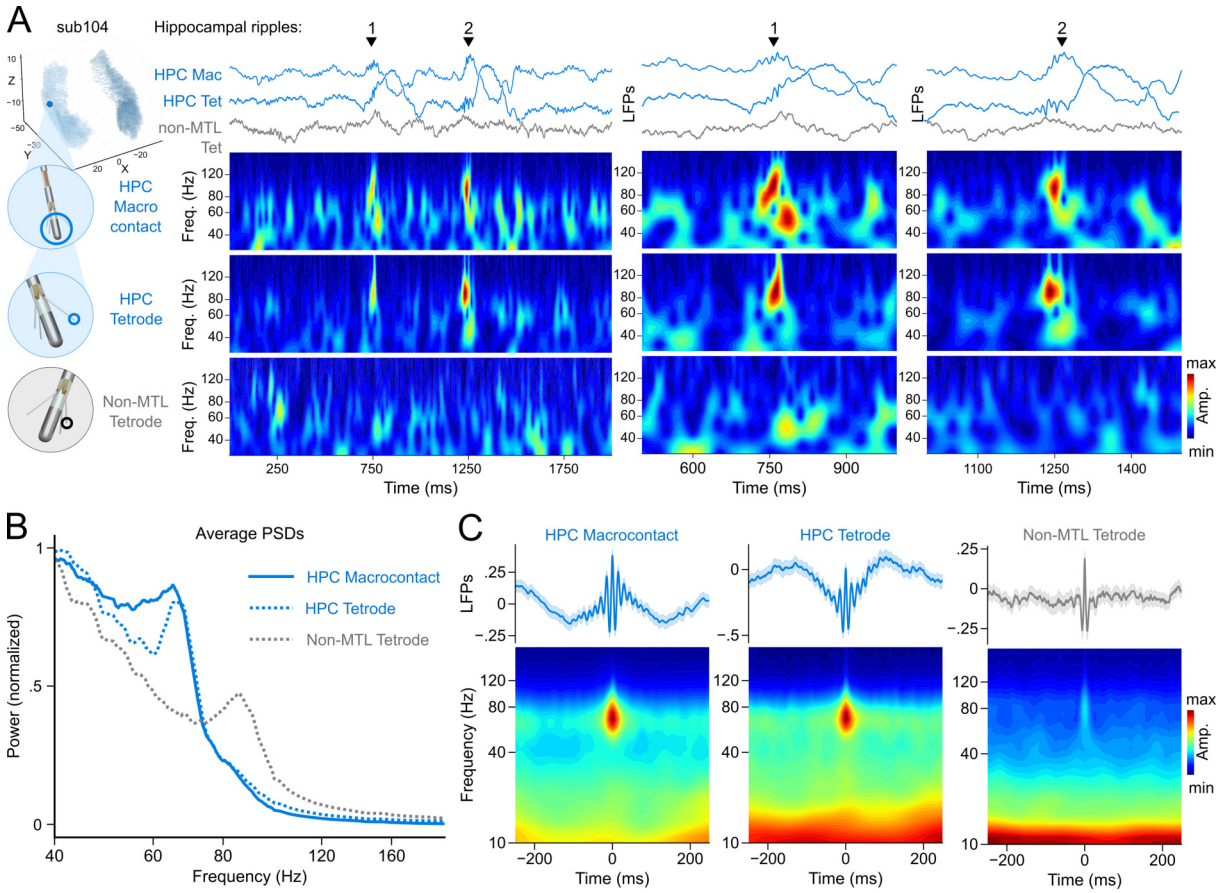


Figure 6.8: **Hippocampal ripples share the same properties between macrocontacts and tetrodes.** (**A**) Example 2-s rest recording showing LFP traces and corresponding spectrograms from a hybrid hippocampal electrode (macrocontact and local tetrode) and from a distal, non-MTL tetrode serving as a control. Insets: 500-ms magnified views around detected ripples. Black arrowheads indicate two example hippocampal ripples detected on the macrocontact. (**B**) Average power spectral densities across pre- and post-learning rest sessions showing a peak at 70 Hz on the macrocontact and hippocampal tetrode. The distal tetrode shows a peak at 90 Hz. (**C**) Ripple-triggered average LFPs and spectrograms aligned to the local peak of the macrocontact or tetrode signals, showing that ripples were visible and had the same frequency on both the hippocampal macrocontact and local tetrode but not on the distal, non-MTL tetrode.

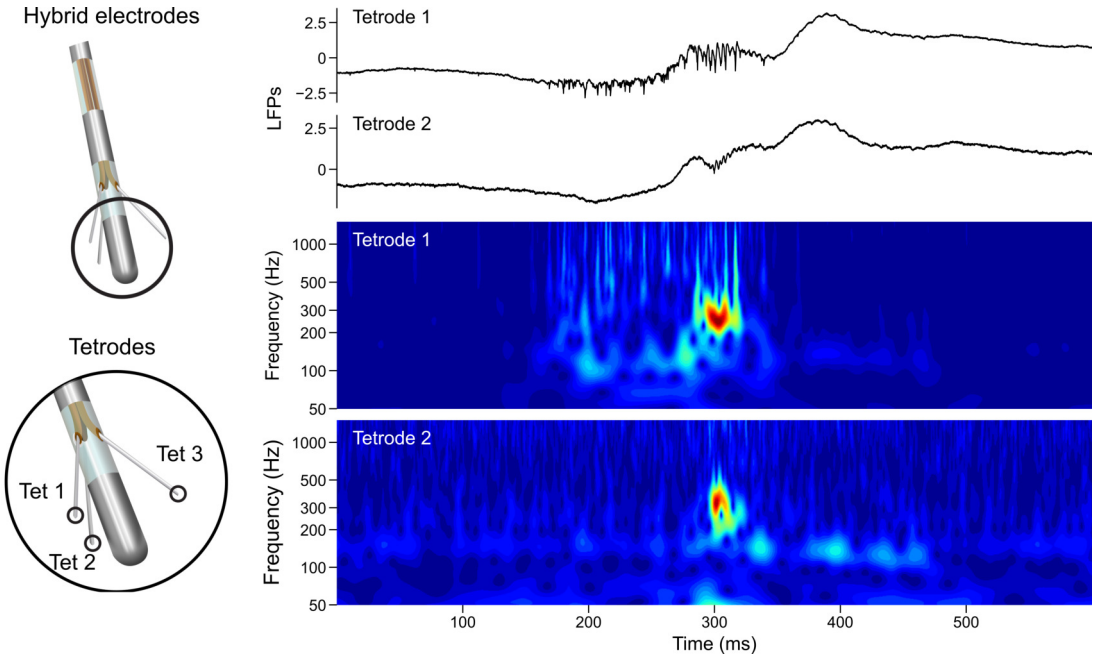


Figure 6.9: **Example hippocampal fast-ripple detected in one participant.** Left: Schematic of the hybrid electrodes used. Right: Example hippocampal fast-ripple detected using two tetrodes located on the same hybrid electrode. Tetrode 1 recorded spiking activity while tetrode 2 did not. Fast-ripples were clearly identifiable on both tetrodes. Note that in this example, the signal was downsampled to 20,000 Hz instead of 1,250 Hz to improve visibility of the oscillatory components >500 Hz.

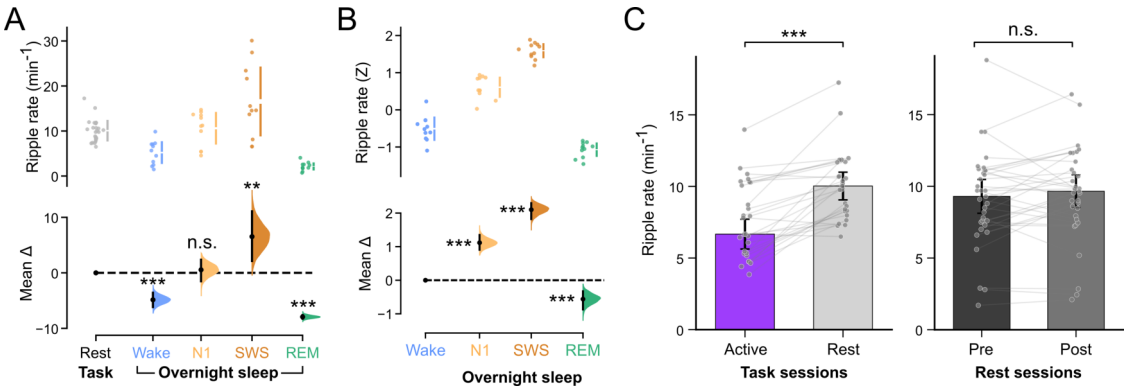


Figure 6.10: **Hippocampal ripples are predominant in task rests, N1 and slow-wave sleep.** (**A**) Estimation plot showing mean differences in ripple rate between rest sessions of the memory task and overnight sleep stages. (**B**) Estimation plot showing mean differences in ripple rate (z-score) across overnight sleep stages. (**C**) Bar plots showing higher ripple rates during rest (pre- and post-learning) than during active memory-task sessions (viewing, learning, recall), with no difference between pre- and post-learning rest. Data were analysed using two-sided paired permutation tests except in **A** where unpaired tests were employed; ***P $<$ 0.001, **P $<$ 0.01; n.s., not significant.

6.II.2.b Ripple modulation of neuronal activity and propagation to the MTL

To further validate that the events detected were genuine ripples, we tested whether single-neuron activity was modulated by hippocampal ripples. We leveraged rest recordings to compute single-neuron averages triggered by ripples (Fig. 6.11A). This analysis revealed up- and downregulated neurons by hippocampal ripples, consistent with earlier findings (Maslarova et al. 2025) and suggesting that single-neuron activity is modulated by ripples in our recordings. However, these averages showed substantial variability due to the relatively low number of ripples detected during rest sessions. In addition, some ripples were detected from hippocampal macrocontacts located at a distance from the tetrodes used to record neuronal spiking (for example anterior versus posterior hippocampus), which likely contributed to temporal shifts between ripple events and local neuronal modulation. To obtain a more reliable estimate of ripple-related neuronal dynamics, we therefore computed ripple-triggered averages using overnight sleep recordings, which contained a larger number of ripples (Fig. 6.11B). This analysis revealed a clear positive modulation of the neurons recorded from the hippocampus, and a refractory period following each ripple for up to +250 ms. This result confirms that ripples modulate neuronal activity in the hippocampus.

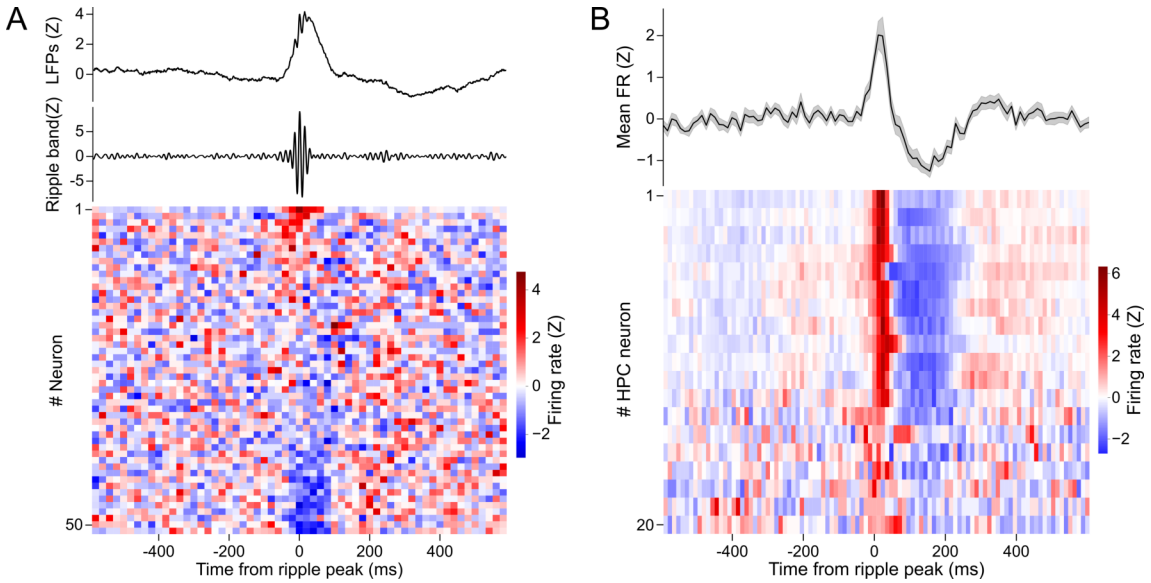


Figure 6.11: **Hippocampal single-neuron activity is modulated by ripples.** (**A**) Wide-band (z-score) and ripple-band (z-score) LFP traces averaged around ripples detected from an example subject (top), together with a heatmap representing single-neuron activity (z-score) averaged around ripples. (**B**) Average firing rate of hippocampal neurons (z-score) around ripples (top), together with a heatmap representing single-neuron activity (z-score, bottom) detected during SWS. Note the refractory period of up to +250 ms.

Next, we tested whether ripples propagated to other structures of the MTL, beyond the hippocampus. We used LFP traces recorded during overnight sleep, and extracted ripple-band amplitude from MTL and non-MTL regions around ripples (Fig. 6.12). Average ripple-band activity in the MTL was significantly elevated, thereby confirming that hippocampal ripples propagated preferentially to other MTL regions.

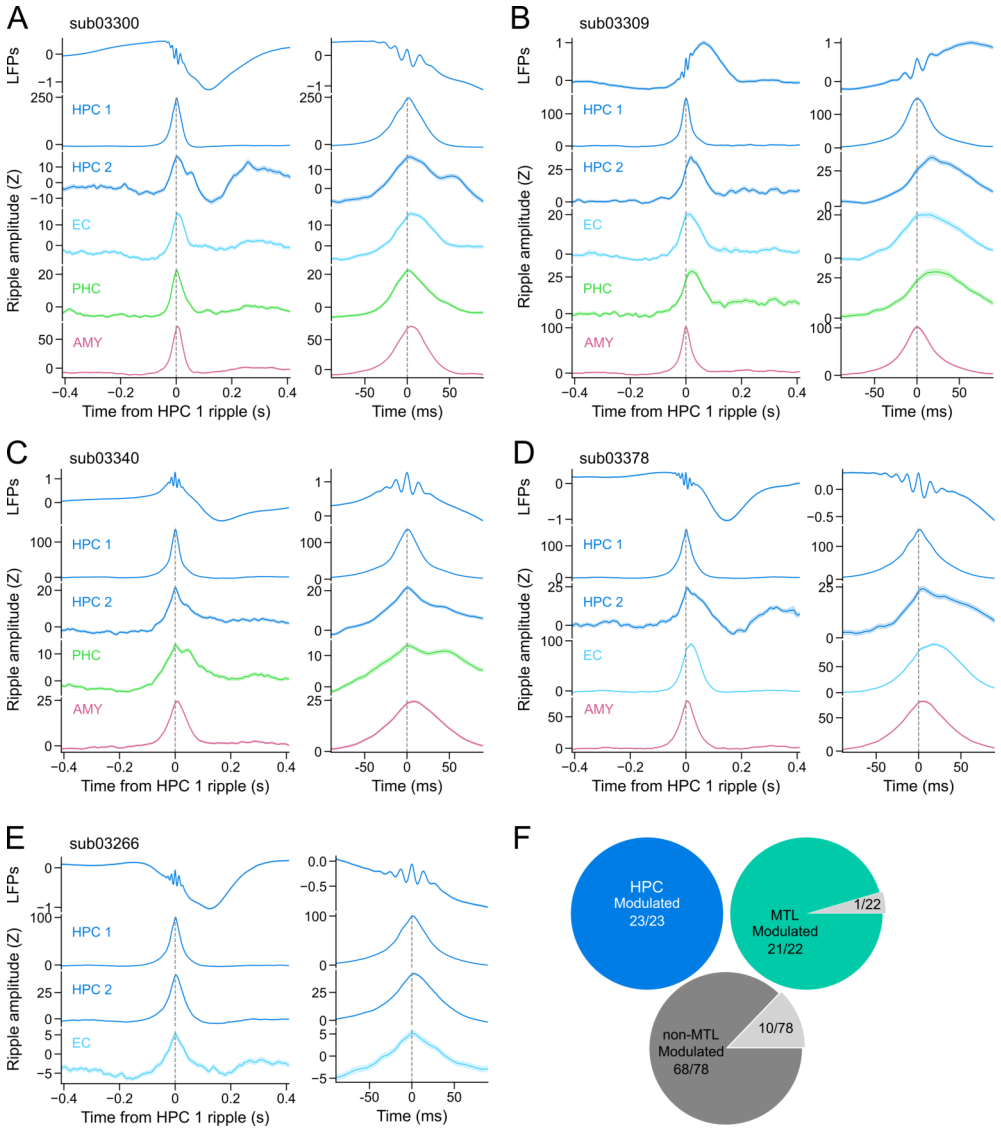


Figure 6.12: **Hippocampal ripples propagate preferentially to MTL regions.** (**A**–**E**) Average wide-band hippocampal LFPs traces (top) with ripple-band MTL instantaneous amplitude (bottom) around ripples detected in the hippocampus during SWS. "HPC 1" refers to the channel used for hippocampal detection, whereas "HPC 2" refers to a channel located in another hippocampal site (e.g., anterior site if ripples are detected posteriorly). A magnified view is displayed on the right to improve visibility at short time-lags. Five example subjects are shown. (**F**) Proportion of hippocampal, extra-hippocampal MTL, and non-MTL contacts in which the ripple-band amplitude signal was significantly modulated around the detected ripples.

6.II.2.c Temporal constraints in the occurrence of hippocampal ripples

Ripples are transient events that are followed by a refractory period during which the probability of observing another ripple is reduced. This phenomenon is thought to reflect the time required for the hippocampal network to recover after a ripple event, and has been observed in rodents (Buzsáki 1986). We thus tested whether ripples detected in our dataset were followed by a refractory period, and whether this refractory period was consistent with that observed in rodents. To do this, we computed the distribution of inter-ripple intervals during overnight slow-wave sleep in humans (Fig. 6.13A,B), and in mice (Fig. 6.13C,D). In humans, we observed a peak in the distribution of inter-ripple intervals at 620 milliseconds (Fig. 6.13B), confirming that ripples are followed by a refractory period. Interestingly, the distribution of inter-ripple intervals in mice also showed a peak, but at a much shorter interval of 120 milliseconds (Fig. 6.13D). Also, ripple-triggered averages of single-neuron activity in humans showed a refractory period of up to +250 ms (Fig. 6.11B), which may also reveal internal temporal constraints on the hippocampal network to produce consecutive ripples.

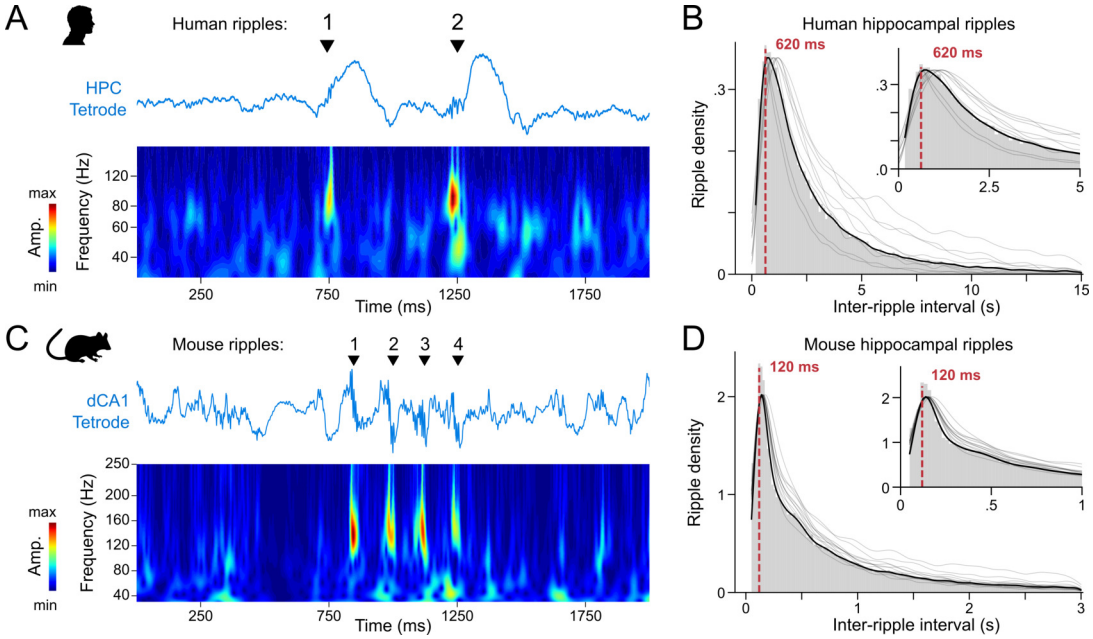


Figure 6.13: **Inter-ripple intervals of hippocampal ripples in mice and humans.** (**A**) Example 2-second tetrode recording from the human hippocampus showing the LFPs and corresponding spectrogram of consecutive ripples. (**B**) Histogram and kernel density estimations (black curve) showing the distribution of intervals between consecutive ripples detected in the human hippocampus during overnight slow-wave sleep (SWS); grey curves indicate inter-ripple interval statistics from individual recording nights; red dashed line indicates the peak of the distribution (620 milliseconds). (**C**) Example 2-second tetrode recording from the mouse hippocampus (dorsal CA1) showing the LFPs and corresponding spectrogram of consecutive ripples. Note that ripple central frequency is faster in mice. (**D**) Same as in **A** for 12 mice recorded during >90 minutes, showing that inter-ripple intervals peak at 120 milliseconds in mice.

6.III Neuronal coactivity motifs in 2-Hz bursts reactivate in post-learning hippocampal ripples

In Chapter 6.II.2 we showed that human hippocampal ripples occurred predominantly during slow-wave sleep and rest, modulated local neuronal activity and propagated to the MTL. The core aim of this chapter is to test whether ripples play a functional role in memory. In this section, we thus address the following hypothesis: are coactivity motifs formed in 2-Hz bursts during learning reactivated in hippocampal ripples during post-learning rest? To do this, we first define coactivity motifs, then test whether coactivity motifs formed in 2-Hz bursts are preferentially reactivated in ripples, and finally explore the link between reactivation and memory performance.

6.III.1 Coactivity motifs formed during 2-Hz bursts reactivate in post-learning hippocampal ripples

The notion of coactivity (or cofiring) derives from the theory of neuronal assemblies (Hebb's theory, (Hebb 1949)) according to which pairs of neurons which send action potentials in synchrony are part of the same functional units and jointly encode information about the world (Buzsáki 2010). In this view, coactivity reports the tendency of two neurons to be active together, and can be measured using correlations. Because all neurons of a given population are exposed to the same electrical environment, their activity co-fluctuates. This results in a high correlation between neurons in the same population, which blurs the information contained in the joint activity of neuronal pairs. Hence, it is necessary to control for the activity of the population when computing the correlation between the spike trains of two single neurons in order to identify the specific statistical relationship (i.e., coactivity) between these two neurons.

To assess reactivation, we continuously monitored MTL neurons across task sessions and we extracted spiking coactivity motifs computed within hippocampal 2-Hz bursts detected during viewing and learning, and compared these in-burst coactivity motifs with those during hippocampal ripples in pre- and post-learning rest (Fig. 6.14A). We also extracted waking spiking motifs outside 2-Hz bursts during viewing and learning, and compared these out-of-burst motifs with ripple activity in pre- and post-learning rest. Pre-learning ripples constitute a necessary control to isolate experience-dependent reactivation from intrinsic ripple-related synchrony (Wilson and McNaughton 1994; O'Neill et al. 2008; Dupret et al. 2010; van de Ven et al. 2016; Lopes-dos-Santos et al. 2018; Tingley and Peyrache 2020; Castelli et al. 2025). Without this control, an increase in neuronal coactivity could be attributed to offline reactivation of the wake experience (e.g., learning) while in fact it may instead reflect the intrinsically high synchrony of hippocampal ripples (Buzsáki 2015), which can occur in the absence of experience-specific reactivation (Giri et al. 2024).

For each task session, we computed MTL coactivity motifs using pairwise neuron-neuron (i,j) correlations while regressing out the activity of the remaining population (Fig. 6.14B; n = 603 coactivity motifs from 6 participants with at least 5 simultaneously recorded MTL neurons). This procedure returned correlation matrices representing

the population coactivity structure in each session. Offline reactivation was quantified using GLMs predicting ripple coactivity from waking motifs, with the interaction term capturing changes in waking-ripple correlation between post- and pre-learning rest. Further methodological details on the reactivation analyses can be found in Chapter 2.III.3.

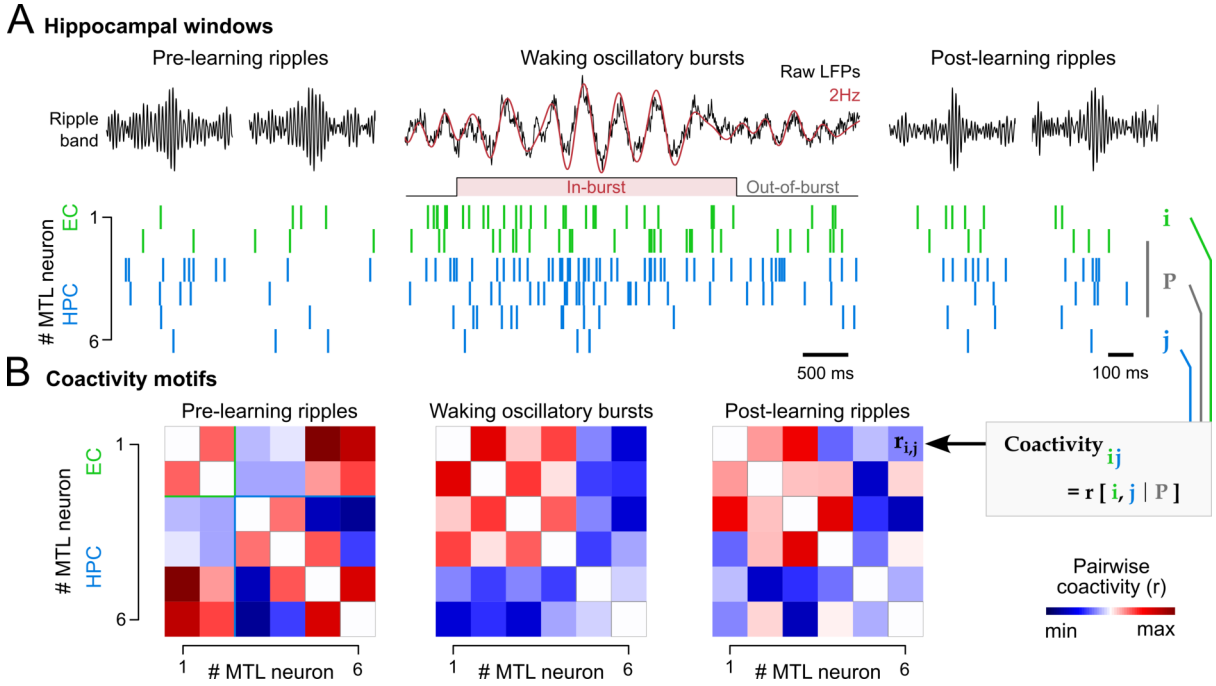


Figure 6.14: **Coactivity motifs detected from neuronal activity in the MTL.** (**A and B**) Reactivation of waking (viewing and learning sessions) MTL coactivity motifs during hippocampal ripples. MTL ensemble spike trains in hippocampal ripples from both pre- and post-learning rest, and those in waking 2-Hz bursts (in-burst) versus those outside (out-of-burst) were extracted (**A**). Coactivity motifs were derived from neuron-neuron (i,j) correlations after regressing out population activity P (**B**).

Following learning, ripples exhibited significantly stronger reactivation for coactivity motifs nested within 2-Hz bursts than for those outside 2-Hz bursts (Fig. 6.15A; in-burst, $P < 0.001$; out-of-burst, $P = 0.202$; in-burst versus out-of-burst, $P = 0.025$; Wald tests). This was not the case for coactivity motifs detected within 1-Hz or 6-Hz bursts which were not reactivated in post-learning ripples (Fig. 6.15B). These results show that spiking motifs structured by 2-Hz oscillatory bursts are preferentially reactivated during post-learning rest ripples.

6.III.2 Reactivation is relevant for behavioural performance

We next evaluated whether MTL neuronal coactivity motifs formed during different stages of the memory task were differently reactivated. To do this, we constructed coactivity motifs after the onset of photographic stimuli during the learning or the viewing sessions. Population coactivity evoked by photographic stimuli during learning reactivated more strongly in post-learning ripples than that evoked during viewing (Fig. 6.16A, $P < 0.001$; viewing, $P = 0.622$; learning versus viewing, $P < 0.001$; Wald tests). Moreover,

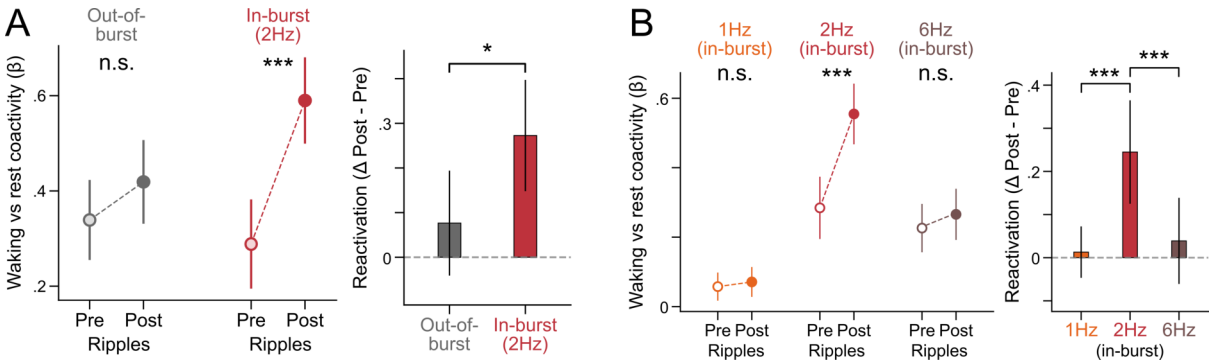


Figure 6.15: **Preferential reactivation of 2-Hz structured spiking motifs in hippocampal ripples.** (**A**) β coefficients from GLMs quantifying the similarity between waking (in-burst or out-of-burst) and ripple coactivity motifs in pre- and post-learning rest (left), and corresponding reactivation (right, post-learning minus pre-learning β). (**B**) β coefficients from GLMs quantifying the relationship between in-burst waking (1-, 2- and 6-Hz) and ripple coactivity motifs in pre- and post-learning rest, and corresponding reactivation (post minus pre). Reactivation was significant only for 2-Hz bursts. Error bars show ±95% confidence intervals. Data were analysed by two-sided Wald t-tests on GLM coefficients; ***P $<$ 0.001, *P $<$ 0.05; n.s., not significant.

coactivity in 2-Hz bursts elicited by photographs that were later best remembered showed the strongest post-learning ripple reactivation (Fig. 6.16B; best and worst recalled, both Ps $<$ 0.001; best versus worst recalled, P = 0.043; Wald tests).

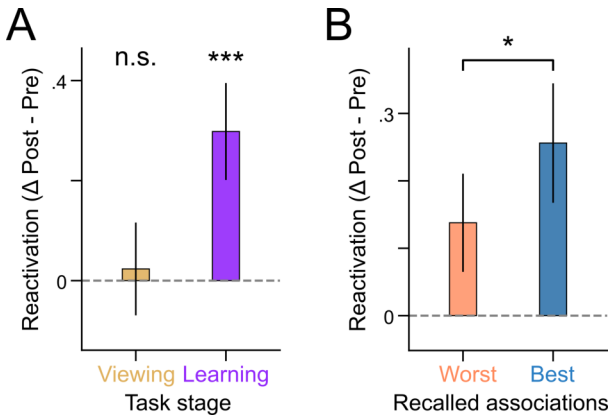


Figure 6.16: **Reactivation and memory consolidation.** (**A**) Reactivation of learning- but not viewing-related coactivity motifs. (**B**) Reactivation of coactivity motifs detected during learning trials leading to best versus worst subsequent memory performance. Error bars show ±95% confidence intervals. Data were analysed by two-sided Wald t-tests on GLM coefficients; ***P $<$ 0.001, *P $<$ 0.05; n.s., not significant.

We finally ran several controls to confirm that these results were robust and reliable. First, we computed reactivation from coactivity motifs detected in individual subjects, to show that reactivation was consistently present across participants (Fig. 6.17A). We further verified that the difference between learning and viewing was not explained by differences in firing rate in these two states (Fig. 6.17B). Next, to test the specific contribution of ripples to reactivation, we measured it using coactivity motifs constructed from epochs

as distant as possible from ripples. Indeed, reactivation was specific to ripple events as it did not occur outside ripples (Fig. 6.17C). Finally, to verify that this effect could be attributed to genuine pairwise coactivity formed during wake, we shuffled the neuronal identity before building the coactivity motifs. This control preserves the total number of spikes and their precise timing but destroys the specific pairwise relations between individual neurons. Under these conditions, reactivation was strongly reduced, whereas reactivation computed from the original coactivity structure remained significantly above chance levels (Fig. 6.17D). Further methodological details can be found in Chapter 2.III.2. Together, these control analyses confirm that the observed reactivation reflected the selective re-expression of neuronal coactivity motifs formed during active wakefulness, specifically during hippocampal ripple events, rather than nonspecific changes in firing rate or random spike coincidences.

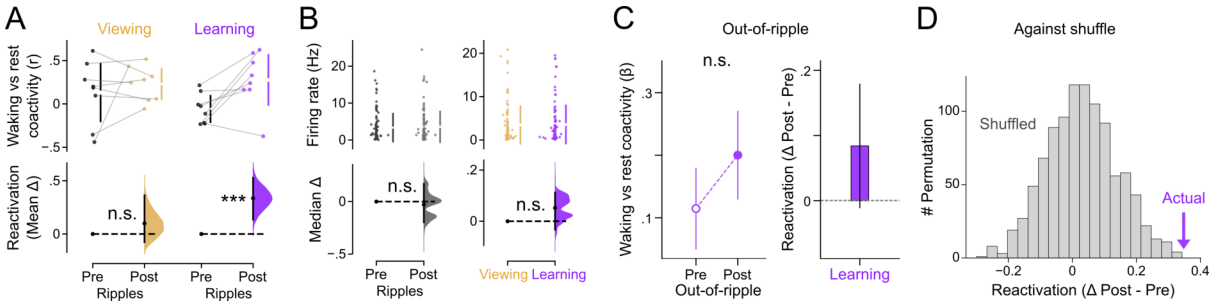


Figure 6.17: **Reactivation controls.** (**A**) Estimation plots showing matrix-wise correlations between viewing- or learning-related coactivity motifs and pre- or post-learning ripples (n = 8 recording days, 6 subjects). Out of the 8 recording days, 6 showed significant reactivation of learning-related coactivity motifs. (**B**) Estimation plots showing similar single-neuron firing rates between pre- and post-learning ripples (left) and between viewing and learning sessions (right), ruling out firing-rate differences as a confound. (**C**) β coefficients from GLMs quantifying the relationship between waking (in-burst or out-of-burst) and out-of-ripple coactivity motifs in pre- and post-learning rest, and corresponding reactivation (post minus pre). Out-of-ripple epochs were defined as periods most distant from ripple events. (**D**) Reactivation measured from coactivity motifs computed on shuffled versus intact (actual) spike trains. For each time bin, neuron identities were permuted to disrupt pairwise correlations. The actual reactivation exceeded the shuffled distribution by 2.80 standard deviations. Error bars show ±95% confidence intervals. Data were analysed using two-sided paired permutation tests (A and B), and Wald t-tests on GLM coefficients (C); ***P $<$ 0.001, n.s., not significant.

Together, these findings show that 2-Hz-structured waking neuronal coactivity motifs are preferentially reactivated within hippocampal ripples, supporting offline consolidation in humans.

6.IV Discussion

In this chapter, I investigated hippocampal activity during offline states and tested whether the physiological organization observed during wakefulness extends to rest and sleep in humans. I first showed that the hippocampal 2-Hz rhythm, previously associated

with mnemonic engagement during wake, was also prominently expressed during REM sleep but not during SWS. This behavioural-state dependence resembles the expression of theta oscillations in other mammals and further supports the view that hippocampal 2-Hz constitutes a human theta-like rhythm. Importantly, this result suggests that the 2-Hz rhythm is not restricted to active wakefulness, but may instead reflect a more general hippocampal state associated with information processing across behavioural states, whether driven by external sensory input or generated internally.

In parallel, I characterized hippocampal ripples during rest and overnight sleep. These events exhibited the physiological features expected from ripples described in animal models: they occurred predominantly during low-cholinergic states such as SWS and rest, displayed characteristic ripple-frequency oscillations coupled to slower deflections, and modulated neuronal activity within the hippocampus. Ripple-band activity also propagated preferentially to other MTL structures, consistent with the distributed anatomical organization of the hippocampal network. In addition, although human ripples occurred at a slower central frequency and with longer inter-ripple intervals than in mice, they nevertheless displayed similar physiological constraints and behavioural-state dependence. Together, these observations indicate that the human hippocampus alternates between distinct oscillatory regimes across behavioural states, with 2-Hz activity predominating during active wakefulness and REM sleep, and ripple events predominating during offline rest and SWS.

Most importantly, I showed that neuronal coactivity motifs formed during waking 2-Hz bursts were preferentially reactivated during hippocampal ripples in post-learning rest. This reactivation was specific to motifs formed within 2-Hz bursts, was not observed for neighbouring slow rhythms, and was strongest for learning-related and subsequently remembered associations. These findings therefore link online coordination during waking 2-Hz bursts with offline ripple-associated reactivation, supporting the idea that transient 2-Hz states contribute to the formation of neuronal assemblies that are later re-expressed during memory consolidation. Importantly, these effects were observed consistently across participants and remained robust after controlling for firing-rate differences, ripple occurrence, and random pairwise spike relationships.

Although overnight polysomnography was available in a subset of participants, the recordings nevertheless provided sufficient coverage to compare hippocampal activity across wakefulness, REM, and SWS within the same individuals. Further studies combining long-term recordings with larger neuronal samples will, however, be useful to better characterize how 2-Hz oscillations and ripple dynamics interact across sleep stages in humans.

Taken together, these results provide converging evidence that the human hippocampus exhibits a two-stage organization of memory-related activity analogous to that described in animal models. During active wake states, 2-Hz oscillations organize neuronal and network activity during mnemonic processing, whereas during offline states, hippocampal ripples support the re-expression of these coordinated activity patterns.

7 General discussion

"Le comportement acquis repose sur le raffinement et le développement ultérieur de circuits cérébraux
ayant évolué pour produire des comportements adaptés à l'environnement naturel."

"Learned behavior is dependent on a refinement and further development of brain circuitry that has evolved to generate adaptive behavior in the natural environment."

— C.H. Vanderwolf and D.P. Cain,
The behavioral neurobiology of learning and memory: a conceptual reorientation (1994)

Contents

7.I Summary of the main findings 159
7.II Is human hippocampal 2-Hz a putative homologue of type 2 theta? 161
7.III Why would human hippocampal rhythms be slower? 163
7.IV Why has hippocampal 2-Hz remained elusive? 164
7.V Limitations 166
7.VI Future directions 167

7.I Summary of the main findings

The aim of this thesis was to test whether key principles of the two-stage model of memory extend to the human hippocampal system (Buzsáki 1989). In animal models, memory-related activity is organized across two complementary states. During active wakefulness, theta oscillations coordinate neuronal assemblies involved in encoding and retrieval (Chapter 1.III.2). During offline states, hippocampal ripples promote the reactivation of these assemblies and support memory consolidation (Girardeau and Lopes-dos-Santos 2021) (Chapter 1.III.2.b). The main question addressed here was whether a comparable organization could be identified in humans using direct recordings of hippocampal and MTL activity.

The first step was to establish a behavioural task adapted for evaluating the two-stage memory model in humans (Chapter 3). I used a relational memory task in which participants learned associations between members of a social community. This task was designed to engage hippocampus-dependent memory while providing well-defined visual

and motor events for electrophysiological analyses. Participants with epilepsy were able to learn and later recall the associations above chance, although they performed worse and responded more slowly than paired controls. Notably, performance varied across participants and across paired associates. This variability was essential for the rest of the thesis, because it allowed neural activity to be related not only to task events, but also to memory performance.

The second step was to characterize hippocampal activity during active wakefulness (Chapter 4). I identified a prominent slow oscillation centred around 2 Hz in the human hippocampus. This oscillation was visible in the raw LFPs, was detected using unsupervised spectral decomposition, and occurred as transient bursts rather than as a continuous rhythm. Importantly, hippocampal 2-Hz was strongest in contacts without IEDs, sometimes showed a clear laminar phase reversal, and was impaired by local referencing. Moreover, 2-Hz oscillations were observed directly from single-neuron autocorrelograms. These features indicate that the 2-Hz rhythm is a physiological oscillation that can be detected in the human hippocampus when spatially distributed activity is preserved.

The behavioural correlates of this rhythm were central to the interpretation of the thesis. Hippocampal 2-Hz bursts were selectively recruited during mnemonic engagement: they were stronger during learning and recall than during passive viewing, were evoked by memory-relevant visual cues, decreased as learning progressed, and were associated with better subsequent recall. In contrast, comparable effects were not observed for neighbouring 1- or 6-Hz rhythms. Repetitive stepping movements did not robustly elicit hippocampal 2-Hz, although this control should be interpreted cautiously because it was limited to a small number of participants and did not reproduce natural locomotion. Together, these results support the view that hippocampal 2-Hz oscillations are linked to memory-guided behaviour but not visual stimulation or movement alone.

The third step was to determine whether this rhythm has the physiological properties expected from a theta-like coordination mechanism (Chapter 5). I showed that hippocampal neurons phase-locked preferentially to 2-Hz cycles, and that hippocampal gamma activity was more strongly modulated at 2 Hz than at neighbouring slow frequencies. This organization was not restricted to the hippocampus. Extra-hippocampal MTL regions, that is the entorhinal cortex, parahippocampal cortex and amygdala, also synchronized their neuronal and gamma-band activity to hippocampal 2-Hz phase. In addition, neuronal coactivity across the MTL increased during hippocampal 2-Hz bursts specifically. These findings indicate that transient 2-Hz events define temporal windows during which distributed neuronal ensembles are coordinated across the human MTL. The observation of subsequent memory effects at 2 Hz further suggests that these bursts are linked to behaviourally relevant memory processing.

The final step was to test whether the online coactivity motifs formed during 2-Hz bursts reappeared during offline states (Chapter 6). First, I showed that hippocampal 2-Hz activity was expressed during REM sleep but not during SWS, whereas hippocampal ripples were most frequent during rest and SWS. This state dependence resembles the alternation between theta-associated and ripple-associated regimes described in other mammals. Second, I showed that neuronal coactivity motifs formed during waking 2-Hz bursts were preferentially reactivated during hippocampal ripples in post-learning rest, controlling for pre-learning rest effects. This reactivation was stronger for learning-related motifs and for associations that were later remembered. Together, these findings raise the possibility that

transient 2-Hz bursts may "tag" behaviourally relevant neuronal assemblies for subsequent consolidation. In this interpretation, 2-Hz bursts would not simply coordinate ongoing mnemonic processing, but could also transiently mark distributed assemblies for later reactivation during hippocampal ripples. To my knowledge, this provides the first direct evidence in humans that single-neuron coactivity motifs formed during memory-guided behaviour are reactivated during offline, post-learning hippocampal ripples.

Overall, these findings support the main hypothesis of the thesis. The human hippocampal system exhibits an organization consistent with the two-stage memory model (Fig. 0.1). During active wakefulness, transient 2-Hz bursts coordinate neuronal activity across the MTL. During offline states, hippocampal ripples reactivate coactivity motifs formed during these bursts. The frequency of the organizing rhythm differs from the canonical rodent theta range, but the functional logic is comparable: slow oscillatory events organize population activity during online memory processing and link it to ripple-mediated offline reactivation.

7.II Is human hippocampal 2-Hz a putative homologue of type 2 theta?

A central issue raised by these results is whether hippocampal 2-Hz activity should be considered a putative human homologue of theta oscillations. This question cannot be answered by analysing the frequency band alone. In animal models, theta is not simply a band-limited oscillation. It is a state-dependent hippocampal rhythm generated by specific pathways, shaped by neuromodulatory tone (in particular acetylcholine), and defined by its ability to coordinate neuronal firing and network activity (Chapter 1.III.2). Therefore, the relevant comparison is not whether human hippocampal activity falls within the same frequency range as rodent theta, but whether it shares the same functional and physiological organization.

In this view, the 2-Hz rhythm described in this thesis resembles a putative homologue of type 2 theta (Chapter 1.III.2). In rodents and rabbits, type 1 theta is classically associated with locomotion and movement-related exploration, whereas type 2 theta is slower, disrupted by anticholinergic drugs, and expressed during immobility, arousal, and sensory processing (Vanderwolf 1969; Kramis et al. 1975; Vanderwolf 1975). The human 2-Hz rhythm described here was not primarily linked to movement. It was evoked by mnemonic visual cues and increased during learning and recall. These properties are closer to a type 2-like state than to a movement-related type 1 theta state. Critically, the re-expression of hippocampal 2-Hz bursts during REM sleep is another strong argument in favour of the homology hypothesis.

This interpretation is consistent with the broader comparative literature. In species outside the canonical rat and mouse model, including rabbits, cats, bats and non-human primates, hippocampal rhythmic activity is often less continuous and more closely linked to active sensing and mnemonic demands than to locomotion alone (Green and Arduini 1954; Ulanovsky and Moss 2007; Jutras et al. 2013). In this respect, the intermittency of human hippocampal 2-Hz should not be viewed as a weakness of the analogy. It may instead be one of the relevant comparative features. Although rodent theta often appears continuous

during active exploration, it is itself strongly state-dependent, tracking locomotion (type 1) and states of high arousal (type 2). During natural exploration, continuous locomotion, head movements, sniffing and other forms of olfactory sampling may therefore create the appearance of a sustained rhythm in rodents. More generally, neural oscillations are expressed in many brain regions as transient bursts rather than continuous rhythms, including theta in the temporal (Fig. 5.12A) and frontal cortices, alpha in the occipital cortex during cognitive tasks, and beta in the motor cortex (Raghavachari et al. 2001; Feingold et al. 2015; Zhang et al. 2018a; Halgren et al. 2019; Tal et al. 2020; West et al. 2023; Boroujeni and Womelsdorf 2023; Schmidt et al. 2023). The human hippocampus may therefore transiently enter slow oscillatory states when memory-guided behaviour requires coordinated network activity.

Recent pharmacological evidence also supports this interpretation. Scopolamine, a muscarinic antagonist, disrupted human hippocampal "slow-theta" in the 2–4 Hz range during memory encoding, and this effect was specific to visually-evoked oscillations (Gedankien et al. 2023; Gedankien et al. 2026). These findings are important because cholinergic sensitivity is one of the classical criteria distinguishing type 2 theta in animal models (Vanderwolf 1975; Kramis et al. 1975; Sainsbury and Montoya 1984). Although these pharmacological studies in humans employed a different cognitive task from the one used in this thesis, they support the idea that 2-Hz rhythm I identified here could also be dependent on cholinergic inputs.

The present findings also agree with the view proposed by Jacobs and colleagues that human hippocampal theta should be understood as a slower rhythm than rodent theta, rather than as a direct 8-Hz replica (Jacobs 2014). The data presented here extend this view by showing that a 2-Hz hippocampal rhythm is not merely present during memory tasks: it organizes neuronal firing, gamma activity, MTL-wide coactivity, and subsequent ripple-associated reactivation. Thus, the putative homology lies less in the absolute frequency than in the function of the rhythm as a state-dependent coordination mechanism.

At the same time, the present work does not exclude the existence of other theta-like states in humans. In particular, type 1 theta remains largely unresolved. The stepping control used here was useful because it isolated rhythmic movement from explicit memory demands, but it did not reproduce real-world locomotion, vestibular input, active navigation or sensorimotor exploration. Human studies using ambulatory recordings have reported theta-range effects during spatial navigation and movement-related behaviour (Aghajan et al. 2017; Stangl et al. 2021; Maoz et al. 2023; Seeber et al. 2025). Future work will therefore need to determine whether humans express multiple theta-like regimes, including a movement-related rhythm, and how these regimes relate to the 2-Hz mnemonic rhythm described in this thesis.

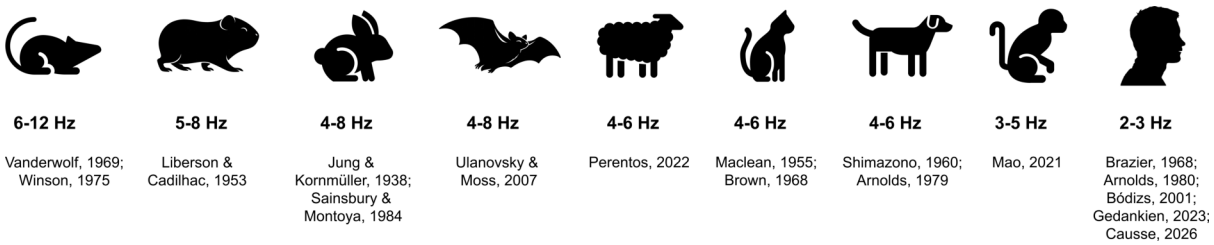


Figure 7.1: **Human 2-Hz in a putative evolutionary continuum.** In this thesis, I propose that transient hippocampal 2-Hz oscillations extend an evolutionary continuum of theta-like rhythms in mammals (Vanderwolf 1969; Winson 1974; Liberson and Cadilhac 1953; Jung and Kornmüller 1938; Sainsbury and Montoya 1984; Ulanovsky and Moss 2007; Perentos et al. 2022; Maclean et al. 1955; Brown 1968; Shimazono et al. 1960; Arnolds et al. 1979a; Mao et al. 2021; Brazier 1968; Arnolds et al. 1980), because they are recruited during mnemonic engagement (Chapter 4), are evoked by behaviourally relevant cues (Chapter 4), coordinate single-neuron and gamma activity across the hippocampus and other MTL regions (Chapter 5), are re-expressed during REM sleep (Chapter 6, (Freemon and Walter 1970; Giaquinto 1973; Bódizs et al. 2001; Clemens et al. 2009)), and are disrupted by anticholinergic drugs (Gedankien et al. 2023; Gedankien et al. 2026).

7.III Why would human hippocampal rhythms be slower?

The identification of a 2-Hz hippocampal oscillation raises a larger question: why is the dominant organizing rhythm of the human hippocampus slower than the theta oscillation typically reported in rodents? One possibility is that this frequency difference reflects scaling constraints (Perentos et al. 2022; Mao et al. 2021). As brains increase in size, axonal conduction paths become longer and communication between distant regions becomes more difficult to coordinate precisely. Slow rhythms provide broader temporal windows for synchronization, which may facilitate bidirectional interactions across distributed circuits despite longer conduction delays (Buzsáki et al. 2013). From this perspective, slower hippocampal rhythms in humans may preserve the logic of theta coordination while adapting it to the temporal constraints of a larger brain.

This explanation is probably incomplete on its own. Brain size affects conduction delays, but the frequency of hippocampal rhythms is also shaped by cellular morphology, synaptic integration and circuit architecture. Recent work on human hippocampal tissue suggests that human pyramidal neurons differ substantially from their rodent counterparts. Human CA1 pyramidal neurons have larger dendritic trees, more oblique dendrites and membrane properties tuned to slow theta frequencies (3-Hz resonance, (Mertens et al. 2024)). Human CA3 circuits also appear to use sparse and broad recurrent connectivity, with synaptic properties favouring reliable integration over longer temporal windows (Watson et al. 2024). More generally, comparative histological studies indicate that human cortical and hippocampal tissue is characterized by lower neuronal density and greater inter-neuronal distances than in rodents, together with increased dendritic complexity and higher perisomatic branching density (Kanari et al. 2025). These observations suggest that slow hippocampal rhythms may emerge from a sparse but spatially extended circuit

architecture, in which distributed neurons require broader temporal windows for effective coordination.

The sparse nature of human hippocampal coding may further favour slow coordination (Waydo et al. 2006; Wixted et al. 2014; Urgolites et al. 2022; Tallman et al. 2025). Importantly, this form of sparsity differs from the anatomical sparsity discussed above. Here, sparsity refers to the selectivity and distribution of neuronal representations. Human single-neuron studies have repeatedly shown highly selective responses to concepts, persons, places or episodes (Quiroga et al. 2005). If the neurons contributing to a given neuronal assembly are sparsely distributed across the hippocampus and connected MTL regions, then coordinating them may require wider temporal integration windows than those used by compact local assemblies located in the denser dorsal CA1 pyramidal layer of the rodent (Kanari et al. 2025). A 2-Hz rhythm provides such a window. It can organize local neuronal firing and gamma-band activity while allowing enough time for distributed regions of the MTL to align their excitable windows (Fries 2005).

The same scaling logic may also apply to hippocampal ripples. In rodents, ripple frequencies often lie above 120 Hz, whereas human hippocampal ripples are commonly observed at slower frequencies, around 70–90 Hz (Bragin et al. 1999a; Liu et al. 2022). In this thesis, ripples showed the expected physiological properties and state dependence, but their frequency and their temporal organization was slower than in mice. This suggests that both theta-like and ripple-like regimes may be shifted toward slower timescales in humans. The important point is that the relationship between rhythms is preserved: a slow oscillatory regime coordinates neuronal activity during wake and REM sleep, whereas a faster ripple regime is expressed during offline rest and SWS.

This interpretation argues against a strict frequency-band definition of hippocampal physiology. If the same organizing principle is implemented at different timescales across species, then frequency bands defined in rodents cannot simply be transferred to humans. An oscillation should instead be defined by its state dependence, anatomical pathways, cellular correlates, cross-frequency interactions and behavioural relevance (Fernandez-Ruiz et al. 2023). In this sense, the hippocampal 2-Hz rhythm described here is not important because it occupies a particular frequency range. It is important because it coordinates the relevant biological levels: neuronal spikes, local gamma activity and distributed MTL networks.

7.IV Why has hippocampal 2-Hz remained elusive?

One important aspect of the present findings is that the 2-Hz hippocampal oscillation was prominent in our dataset, yet it has not become central in the human sEEG literature. Several methodological and conceptual factors may explain this discrepancy.

First, human sEEG studies have often inherited frequency definitions from rodent electrophysiology and scalp EEG. As a result, analyses frequently focus on theta ranges beginning at 3 or 4 Hz, whereas activity below this limit is treated as delta, baseline drift, sleep-related activity or pathology. This convention can make a 2-Hz rhythm invisible by definition. If the high-pass filter is set above 1 Hz and the theta band begins at 3 Hz, a rhythm centred around 2 Hz may be attenuated, excluded or interpreted as non-specific

slow activity. This is especially problematic in the hippocampus, where the relevant human rhythm may fall precisely at the boundary between conventional delta and theta bands.

Second, referencing strongly affects the visibility of slow, spatially distributed oscillations. In Appendix A, I showed that local referencing (local microwires or bipolar reference) can cancel slow oscillations when adjacent contacts contain similar signals, or distort them when the phase relationship differs across contacts. This effect is expected to be more dramatic for slow rhythms than for spatially localized faster activity. Previous studies using bipolar or local referencing may therefore have underestimated hippocampal 2-Hz oscillations, especially if the rhythm was coherent across nearby contacts. This point is consistent with early reports of human hippocampal rhythmic slow oscillations during REM sleep which were abolished using bipolar referencing (Bódizs et al. 2001).

Third, because sEEG recordings are usually obtained in patients with epilepsy, slow activity is often interpreted as abnormal. This caution is justified, particularly near the seizure onset zone or in contacts with IEDs. However, it can also lead to excessive dismissal of physiological slow rhythms. The solution is not to ignore pathology, but to separate physiological from pathological activity using anatomical location, interictal markers, behavioural state, phase organization, neuronal coupling and by reproducing observations across participants and studies. Large-scale normative sEEG datasets based on recordings from non-epileptic regions, such as the atlas described by Frauscher and colleagues, are useful in this respect (Frauscher et al. 2018). Importantly, this study explored data from 106 patients and also reported prominent delta-band (0.75–2.25 Hz), but not theta-band power in the "normal" human hippocampus. This provides additional confidence in the physiological relevance of the 2-Hz oscillations described in this thesis.

Finally, many memory tasks use short inter-stimulus intervals. This is partly because experiments in clinical settings are constrained by time, but also because longer delays between stimuli can make cognitive tasks feel less natural and less engaging for participants. These tasks therefore focus on time windows of a few hundred milliseconds after stimulus onset. However, as I showed in Figs. 4.16, 4.14 and 4.15, the hippocampus is characterized by large ERP deflections caused by visual stimuli, in particular when the images are presented several times and have mnemonic value. These ERPs are characterized by prominent, transient deflections in the LFPs which can spread across frequencies, in particular in the theta-band range (Fig. 4.16). Moreover, because 2-Hz oscillations have a period of approximately 500 ms, detecting them requires long analysis windows in order to capture several cycles of the oscillation. This is necessary to disentangle transient deflections from genuine oscillatory events. Consequently, prominent ERPs may confound the detection of genuine slow oscillatory activity in the hippocampus.

Together, these factors suggest that hippocampal 2-Hz has remained elusive not because it is weak or irrelevant, but probably because it falls between conventional analytical categories. Indeed, it is slower than the theta band usually inherited from rodent studies, more spatially extended than rhythms preserved by bipolar referencing, and can be difficult to distinguish from large stimulus-evoked ERPs.

7.V Limitations

Several limitations should be considered when interpreting these findings. The first concerns the study population. All electrophysiological recordings were obtained from patients with drug-resistant epilepsy. This population provides rare access to human hippocampal and single-neuron activity, but it also introduces potential confounds related to interictal activity, anti-seizure medication, brain lesions and sleep disruption. I reduced these confounds by focusing on contacts outside irritative regions when possible, excluding epochs with IEDs, and showing that 2-Hz oscillations were strongest in physiologically "cleaner" contacts. Despite this caution, controls cannot make the dataset equivalent to recordings from healthy participants. However, it is important to note that early sEEG recordings in patients with schizophrenia also reported hippocampal LFPs activity "almost entirely dominated by delta activity" during wakefulness and REM sleep (Brazier 1968; Brazier 1970; Freemon and Walter 1970). Obtained in a different clinical population, these observations suggest that prominent slow hippocampal oscillations are not specific to epilepsy and may instead reflect a general feature of human hippocampal physiology.

Patients with epilepsy often exhibit significant cognitive impairments, which can affect performance across a wide range of memory tasks (Black et al. 2010; Dinkelacker et al. 2016; Wang et al. 2020; Phuong et al. 2021). Using paired controls and standardized neuropsychological assessments, I was able to replicate this observation in the population studied here. This point is important for interpreting the results. When separating participants into "best and worst" performers, it is possible that these groups partly reflected differences in the severity of the underlying pathology, with the best performers corresponding to patients whose brain function was relatively preserved. Interestingly, the most prominent hippocampal 2-Hz bursts were observed in these better-performing participants, which further supports the idea that 2-Hz represents a physiological mode of hippocampal activity rather than a pathological phenomenon.

Importantly, epilepsy is also associated with impairments in social cognition (Monti and Meletti 2015; Bora and Meletti 2016; Ziaei et al. 2023). Although the present task did not involve natural social interactions, it relied on learning friendships and navigating a social community structure, which may have introduced additional cognitive demands for this patient population. Future studies combining sEEG with more ecologically valid social paradigms could therefore help clarify how hippocampal and MTL dynamics contribute to social cognition in epilepsy, and whether disruptions of transient oscillatory coordination participate in the social and relational difficulties frequently observed in these patients.

A related limitation is sparse implantation schemes, resulting in sparse sampling of brain regions. Electrode placement was determined solely by clinical need. Consequently, coverage was uneven across hippocampal subfields, MTL regions and temporal cortical areas. This is especially important for the single-neuron analyses. Although the results show phase-locking and coactivity effects across neurons, the number of simultaneously recorded units in any given region was limited. Therefore, I think that the coactivity motifs studied here should be viewed as partial samples of larger assemblies. Denser recordings will be required to determine how these motifs are organized across hippocampal subfields and how they interact with entorhinal, amygdala and neocortical populations (Paulk et al. 2022; Lee et al. 2024).

Another limitation in the experimental setup employed in this thesis is the absence of an eye-tracking system. The visual cues used in the task were photographs of people, and it has been previously reported that eye movements can influence hippocampal and MTL activity (Jutras et al. 2009; Hoffman et al. 2013; Katz et al. 2020; Katz et al. 2022). Although the design minimized motor confounds by using a fixed cross in the center of the screen between visual stimuli and by comparing memory cues with passive viewing, it did not directly measure gaze and fixation. Even though it is technically challenging to implement in the clinical setting, future studies should combine sEEG with eye tracking to determine how hippocampal 2-Hz bursts relate to visual sampling and saccades.

In addition, the offline reactivation analyses were performed during rest rather than during full overnight sleep. This was a practical and conceptual choice. Rest sessions were acquired immediately before and after learning, allowing comparison of pre- and post-learning ripples while maintaining stable single-neuron recordings. However, long sleep recordings would provide a more complete test of memory consolidation. Such experiments are technically demanding because they require stable tracking of single neurons across pre-learning sleep, task wakefulness and post-learning sleep, often over more than 36 hours. This remains particularly difficult with current clinical microwire recordings. Nevertheless, it is an important future goal, because it would allow direct testing of whether 2-Hz-coordinated motifs reactivate during SWS ripples and whether this predicts memory retention after a full night of sleep (van Beest et al. 2025).

The interpretation of homology should also remain cautious. The data support a putative theta-like role for human hippocampal 2-Hz, but they do not establish a one-to-one identity with rodent theta. Homology requires converging evidence across anatomy, development, microcircuit mechanisms, pharmacology and behaviour. The present thesis contributes behavioural-state, electrophysiological and neuronal evidence, but it does not directly test septal inputs, cholinergic dependence, or the precise cellular generators of the rhythm. At the same time, the interpretation proposed here is closer to homology than analogy because it is based on comparative observations across mammals, sharing a common ancestry. In this interpretation, the human 2-Hz oscillation would not represent an independently evolved solution to cross-regional neuronal coordination, but rather a species-adapted expression of an ancestral hippocampal organizing mechanism operating at a slower timescale. Nevertheless, this interpretation remains speculative, and for this reason I have used the term "theta-like" or "putative" homologue throughout this thesis.

Finally, the results are mainly correlational. The association between 2-Hz bursts, neuronal coordination, ripple reactivation and memory performance is consistent with a causal role, but it does not prove one. Establishing causality will require perturbation. This could involve electrical stimulation (Suthana et al. 2012; Jacobs et al. 2016; Titiz et al. 2017) or pharmacological manipulation (Gedankien et al. 2023; Gedankien et al. 2026). However, such experiments are challenging to implement in humans, in particular in this clinical context.

7.VI Future directions

The results of this thesis open several directions for future work. A first question is whether hippocampal 2-Hz bursts are specific to visual associative memory or reflect a more

general state of mnemonic engagement, arousal, or both. The relational memory task used photographs and names, and the most prominent bursts were evoked by visual memory cues. Future studies could test auditory, tactile, olfactory or multimodal associations. If 2-Hz bursts are consistently evoked by memory-relevant cues across sensory modalities, this would support the idea that they reflect mnemonic engagement rather than visual processing. Such experiments could also help determine whether 2-Hz bursts actively contribute to the selection or "tagging" of neuronal assemblies for subsequent offline reactivation, or whether they simply accompany successful encoding states. Conversely, modality-specific differences could reveal how hippocampal processes adapt to distinct sensory modalities engaging different brain networks and behavioural demands.

A second and related perspective is to test more natural forms of episodic memory. The social-community task captured relational learning, but everyday memory often involves temporally extended events, spatial context, goals or emotions. In addition, everyday memory relies on fluctuating internal states, which can shape what will be remembered, and the strength or persistence of memories. Recent developments in chronic neurostimulation implants for epilepsy (Silva et al. 2021) now make it possible to track hippocampal dynamics continuously across days or weeks (van Rheede et al. 2022). Such approaches could help determine how hippocampal 2-Hz bursts evolve across behavioural states and whether they predict long-term memory formation and maintenance. Future paradigms could therefore combine chronic recordings with short narrative episodes, naturalistic videos or virtual environments experienced repeatedly over extended periods. These approaches would allow testing whether 2-Hz bursts organize the binding of items, places and temporal context, and whether they contribute to the later reconstruction of rich episodic experiences rather than simple recall of learned associations.

Navigation remains a particularly important case. Human navigation studies have reported hippocampal theta-range activity, but results vary across tasks, recording methods and referencing schemes (Ekstrom et al. 2005; Watrous et al. 2011; Clemens et al. 2013; Watrous et al. 2013; Aghajan et al. 2017; Stangl et al. 2021; Maoz et al. 2023; Seeber et al. 2025). The present findings suggest that future navigation studies should avoid assuming that the relevant hippocampal rhythm must lie in the rodent theta range. They should preserve slow oscillations, avoid local bipolar referencing when possible, and distinguish hippocampal 2-Hz from temporal neocortical 6–8-Hz oscillations. Real-world navigation, vestibular stimulation and active locomotion will be especially useful to determine whether humans express a movement-related theta-like rhythm distinct from the mnemonic 2-Hz rhythm described in this thesis (Topalovic et al. 2020; Topalovic et al. 2023).

A third direction concerns the 6–8-Hz rhythm observed in the temporal neocortex. In this thesis, temporal cortical regions outside the MTL were dominated by 6–8-Hz oscillations, whereas the hippocampus was dominated by 2-Hz bursts. The functional relationship between these rhythms remains unclear. One possibility is that they reflect distinct coordination regimes. Alternatively, they could form a cross-regional hierarchy, in which temporal cortical theta-band oscillations are nested within slower hippocampal windows. Future analyses examining cross-frequency nesting between hippocampal 2-Hz and temporal neocortical 6–8-Hz oscillations could help clarify this relationship.

A fourth direction is to study what happens outside 2-Hz bursts. The absence of a detected oscillatory burst does not mean that the hippocampus is "silent" or disconnected from other brain regions. Out-of-burst epochs may contain higher firing rates, stronger

aperiodic activity, different fractal dynamics, or non-oscillatory forms of communication. They may support local processing, sensory updating, or transitions between network states. Understanding these periods is important because the most distinctive feature of the human hippocampal rhythm may be its intermittency. Unlike rodent theta during locomotion, the human 2-Hz rhythm does not appear to pace hippocampal activity continuously. The alternation between burst and non-burst states may therefore be central to human hippocampal function.

Another interesting direction concerns the relationship between hippocampal 2-Hz bursts during REM sleep and the "sawtooth waves" previously described in scalp EEG. Sawtooth waves have traditionally been treated as a distinct REM sleep phenomenon, although sEEG studies reported prominent 2–4 Hz oscillations in mesiotemporal regions during these events (Frauscher et al. 2020). The spectral and behavioural similarities with the hippocampal 2-Hz bursts described in this thesis suggest that these phenomena may be related. At the same time, an important difference concerns ripple dynamics, since the present results showed lower hippocampal ripple rates during REM sleep, consistent with results from other studies in mammals. Future work should therefore directly compare hippocampal 2-Hz bursts and scalp-detected sawtooth waves, determine whether they recruit similar hippocampo-cortical networks, and clarify whether they reflect the same or partially distinct REM sleep processes.

Finally, future studies should aim for denser and longer recordings of human single-neuron activity. The present results show that coactivity motifs formed during waking 2-Hz bursts can reactivate during post-learning ripples, but they capture only a small fraction of the underlying neuronal population. High-density microelectrode arrays (Paulk et al. 2022; Lee et al. 2024) could allow neuronal assemblies to be formally detected and tracked across the day and overnight sleep (Lopes-dos-Santos et al. 2013). This would provide a direct test of the full two-stage model in humans (Buzsáki 1989), from online assembly formation to sleep reactivation and long-term memory retention.

Beyond their theoretical implications, these findings may also have translational relevance. If memory formation depends on transient 2-Hz coordination across hippocampal and limbic networks, then restoring or reinforcing this coordination could represent a potential target for neuromodulation. Recent work showed that stimulation of the Papez circuit at 2 Hz (anterior thalamus) reduced seizures and was associated with improved memory outcomes in patients with temporal lobe epilepsy (Kremen et al. 2025). Although these effects should not be interpreted as a direct replication of the physiological rhythm described in this thesis, they support the broader idea that slow-frequency modulation of hippocampo-limbic circuits can influence both memory and network excitability. Future studies should therefore test whether memory-related stimulation effects depend not only on stimulation frequency, but also on behavioural state and ongoing physiological oscillatory dynamics.

A Appendix: Local referencing

In Chapter 4.II.4.c, we observed that local referencing methods such as bipolar or local referencing impairs the detection of slow oscillations in the LFPs. This observation arises from the fact that slow oscillations are often spatially widespread and can be detected across multiple contacts located in the same region of interest. When using bipolar or local referencing, the subtraction of adjacent contacts can lead to the cancellation of these slow oscillatory components, making them less visible or even undetectable in the re-referenced signal (Fig. 4.11A). However, this is true only if the oscillatory cycles detected from two adjacent contacts have the same phase. To illustrate this phenomenon, we time-shifted one of the macrocontact signals presented in Fig. 4.11A (100, 280, 460 ms), and repeated the bipolar subtraction on these rolled signals (Fig. A.1). Interestingly, when the two signals were in phase, bipolar referencing led to the cancellation of the 2-Hz oscillatory burst (Fig. A.1A, D, 0 ms and 460 ms). However, when the two signals were out of phase, bipolar referencing resulted in an apparent increase in 2-Hz power, associated with a phase distortion of the resulting signal (Fig. A.1B, C, 100 ms and 260 ms).

Although visually striking, these examples were obtained by artificially shifting one signal's phase by a substantial time interval. This may not occur in real recordings, as the phase delay of an oscillation detected on adjacent macrocontacts is constrained by their distance, the propagation speed of the oscillation, and the underlying dipole orientations. We therefore examined whether such amplification of the 2-Hz bursts could occur in our data. In some instances, bipolar referencing produced an apparent increase in 2-Hz power, accompanied by phase distortion of the resulting signal (Fig. A.2). Although rare, these cases show that bipolar referencing can yield either a decrease or an increase in 2-Hz power, depending on the phase relationship between the original signals.

Next, we investigated whether the phase difference between two adjacent macrocontacts could predict the change in 2-Hz amplitude induced by bipolar referencing across detected 2-Hz bursts. LFPs signals recorded in viewing, learning and recall sessions from two adjacent macrocontacts (Mac 1, Mac 2; common median reference) were aggregated and z-scored. A bipolar signal was constructed by subtracting the signals recorded from the two adjacent macrocontacts and subsequently z-scored. IMFs were extracted using tmEMD, and the instantaneous phase and amplitude of the 2-Hz IMF were obtained for each of the three signals ("Mac 1", "Mac 2" and "Bipolar"). For each 2-Hz burst initially detected on the deepest macrocontact, we computed the mean phase difference between the 2-Hz IMF of the two adjacent macrocontacts before bipolar referencing ("Mac 1" and "Mac 2"). Phase differences were computed using circular subtraction and summarized using the circular mean, and expressed in absolute phase values. Consequently, a phase difference of 0° indicates that the two signals are in phase, while a phase difference of 180°

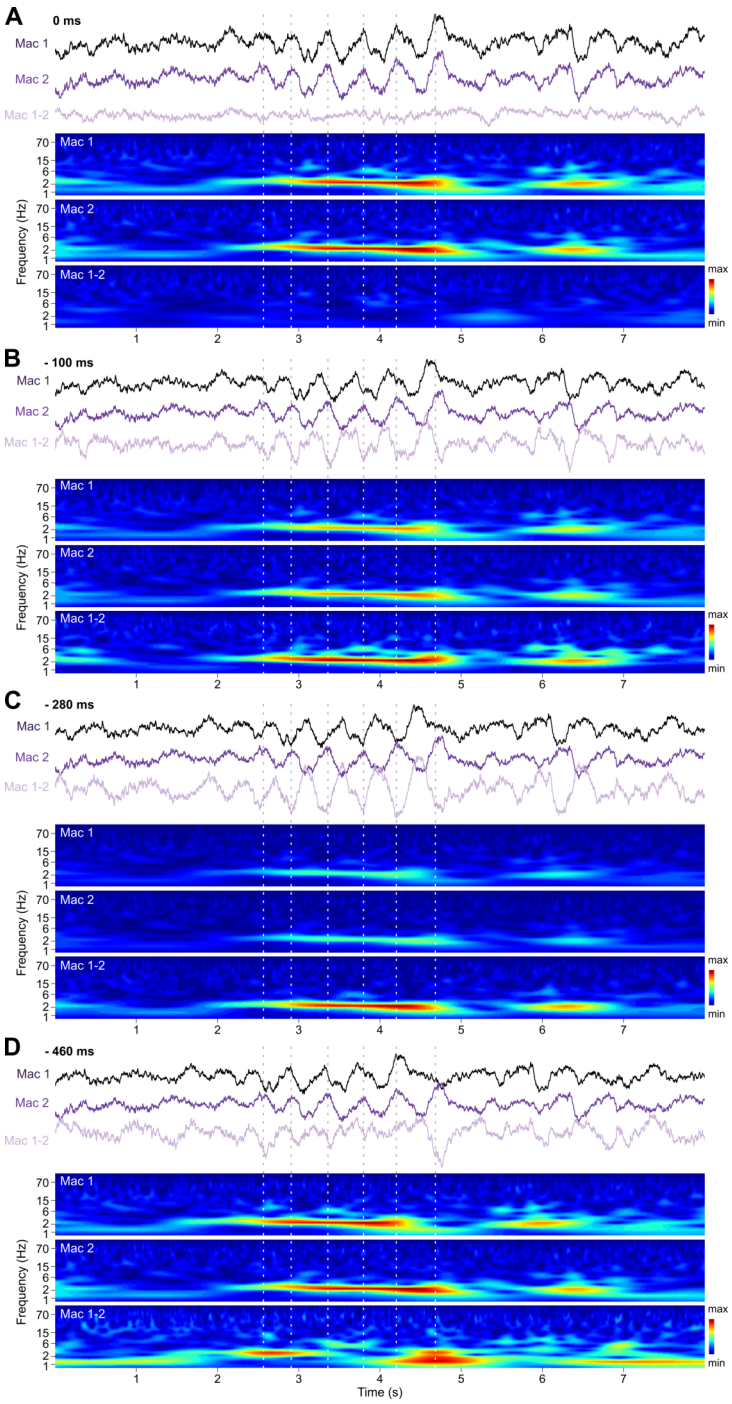


Figure A.1: **Bipolar reference with different phase relationships.** (**A**) Example LFP signals from two adjacent macrocontacts (top) and their bipolar reference (bottom), as in Fig. 4.11A. The 2-Hz oscillatory burst is visible in both common median referenced signals, but it is cancelled in the bipolar reference due to the in-phase relationship between the two macrocontacts. (**B, C**) Same as **A**, but with one signal shifted by 100 ms (**B**) and 260 ms (**C**). The 2-Hz burst is now out of phase, leading to an apparent increase in 2-Hz power in the bipolar-referenced signal. (**D**) Same as **A**, but with one signal shifted by 460 ms (one period of a 2-Hz oscillation). By restoring the in-phase relationship, 2 Hz oscillatory bursts are attenuated in the bipolar-referenced signal.

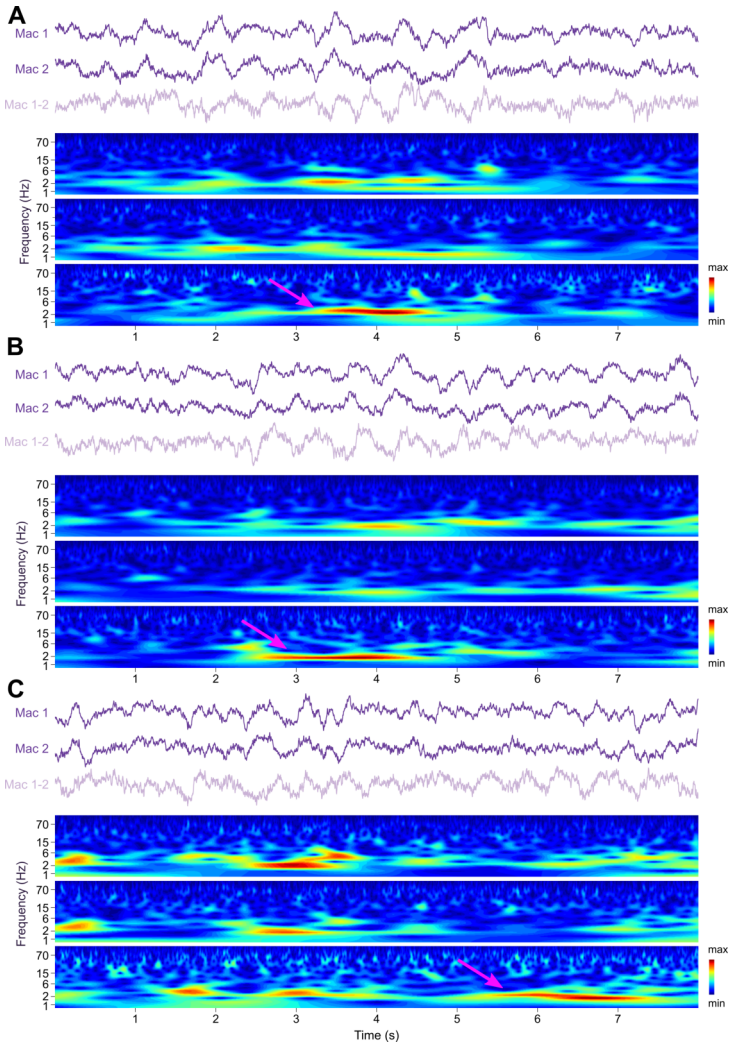


Figure A.2: **Example of phase distortions induced by bipolar reference.** (**A**–**C**) Example LFP signals from two adjacent macrocontacts (top) and their bipolar reference (bottom). The 2-Hz oscillatory burst is faintly visible in both common median referenced signals, and it is enhanced in the bipolar reference due to the out-of-phase relationship between the two macrocontacts. Purple arrows indicate the bursts detected in the bipolar reference, which were not obvious in the common median referenced LFP signals.

indicates that the two signals are in anti-phase. We observed that the phase difference between adjacent macrocontacts varied across bursts and participants, with most of the bursts showing modest phase differences (below 50°, Fig. A.3) and a few showing larger differences. Note that at 2 Hz, a phase difference of 50° corresponds to a time delay of approximately 70 ms.

We then measured the mean instantaneous amplitude of the 2-Hz IMF within each burst for the bipolar signal and for each median-referenced macrocontact. The median-referenced amplitude was defined as the average across the two macrocontacts. The change in 2-Hz amplitude induced by bipolar referencing was quantified, for each burst, as the relative difference between the bipolar and median-referenced amplitudes (in %). Finally, we computed the correlation between the phase difference and the change in 2-Hz amplitude across all detected bursts. We observed significant positive correlations, indicating that larger phase differences were associated with greater increases in 2-Hz amplitude when using the bipolar reference (Fig. A.3).

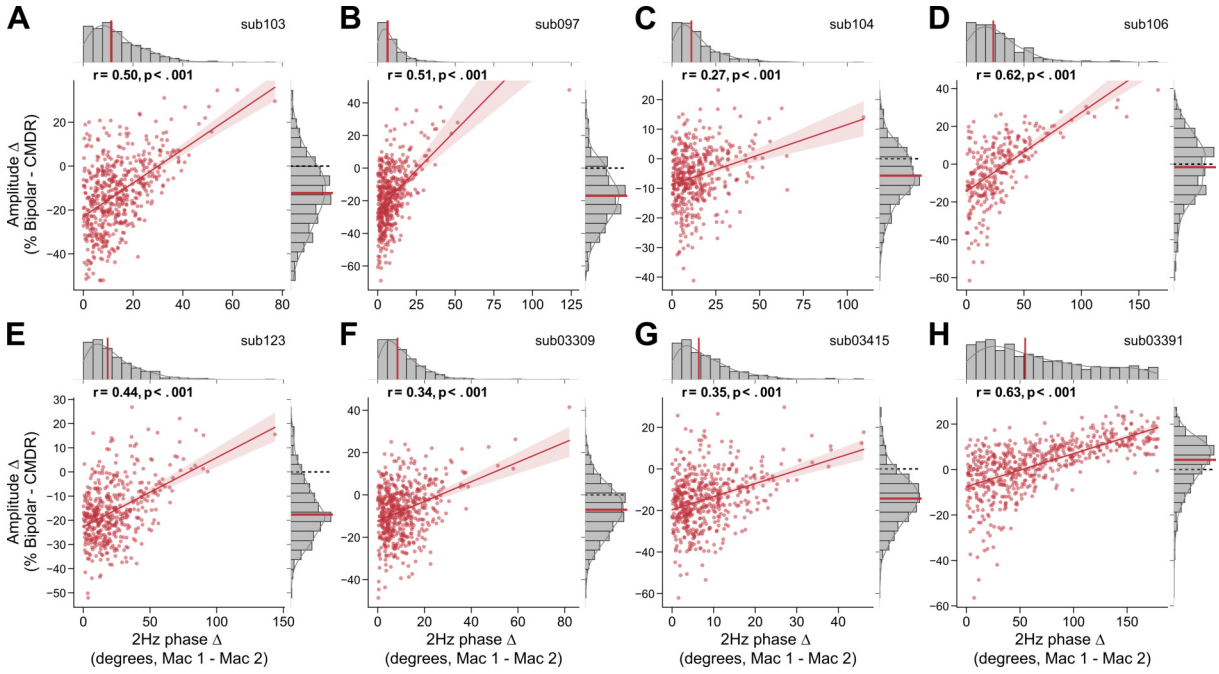


Figure A.3: **Correlation between phase difference and 2-Hz amplitude change induced by bipolar referencing.** (**A**–**H**) Scatter plots showing the relationship between the phase difference of the 2-Hz oscillation detected on two adjacent macrocontacts and the change in 2-Hz amplitude induced by bipolar referencing for eight participants. Each point represents a 2-Hz burst, with the x-axis representing the phase difference (in degrees, absolute phase values) and the y-axis representing the change in 2-Hz amplitude (in %) induced by bipolar referencing. Significant positive correlations were observed, indicating that larger phase differences are associated with greater increases in 2-Hz amplitude in the bipolar reference. CMDR, common median reference; Bipolar, bipolar reference. Correlations were computed using Pearson's correlation coefficient.

To further illustrate this relationship, we computed the correlation between the phase difference and the change in amplitude induced by bipolar referencing across participants. We observed significant positive correlations for the 1- and 2-Hz oscillations, but not for

the 6-Hz oscillation (Fig. A.4A-C). Similar correlations were obtained when considering all detected bursts pooled across participants (Fig. A.4D-F). This is consistent with the fact that 6-Hz oscillations are more spatially localized, making them less sensitive to bipolar referencing.

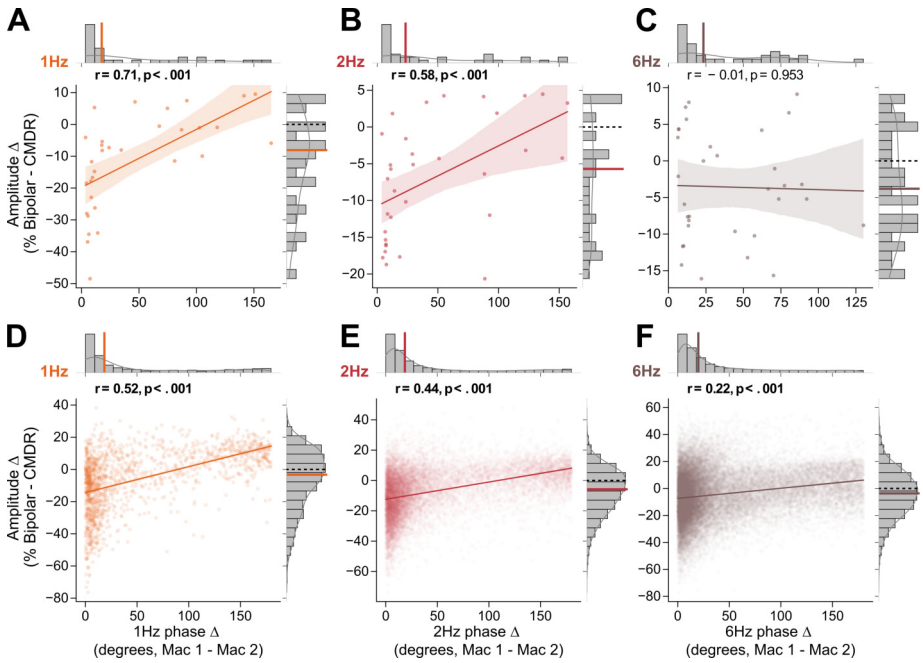


Figure A.4: **Correlation between phase difference and amplitude changes induced by bipolar referencing across participants.** (**A**–**C**) Scatter plots showing the relationship between the phase difference of the 1- (**A**), 2- (**B**) and 6-Hz (**C**) oscillations and the change in amplitude induced by bipolar referencing across participants. Note the absence of correlation at 6 Hz (**C**). (**D**–**F**) Scatter plots showing the relationship between the phase difference of the 1- (**D**), 2- (**E**) and 6-Hz (**F**) oscillations and the change in amplitude induced by bipolar referencing across all detected bursts. Correlations were computed using Spearman's rank correlation coefficient. Note that the magnitude of the average amplitude change induced by bipolar referencing is maximal for 2-Hz oscillations (-5.8%) compared to the 1- (-3.2%) and the 6-Hz (-3.7%) oscillations. This is visible on the joint histograms presented on the right of individual scatter plots.

Taken together, these results show that the phase relationship between adjacent contacts is an important factor to consider when interpreting the effects of bipolar referencing on slow oscillations. This further supports our decision to use the CAR for all analyses in this manuscript, as it better preserves slow oscillatory components without introducing phase distortions. It may also explain the variability in the detection of slow oscillations across studies using bipolar referencing, in particular for 2-Hz oscillations in the hippocampus. In our dataset, 6-Hz oscillations were less affected by bipolar referencing (Fig. 4.11C and Fig. A.4C), which could provide an explanation for the focus on this frequency band in previous hippocampal sEEG studies.

In addition, recent studies have shown that slow oscillations can be interpreted as travelling waves in the hippocampus, with phase shifts across adjacent macrocontacts (Zhang and Jacobs 2015; Zhang et al. 2018a; Kleen et al. 2021). Depending on the orientation of the electrode shaft across the dipole generating the slow oscillation, and the

direction of propagation of the travelling wave, the phase relationship between adjacent macrocontacts may vary across individual bursts. Indeed, our results point to the fact that not all bursts are affected identically by bipolar referencing, and not all participants show the same effect (Fig. A.4). This suggests that previous studies using bipolar referencing may have detected only a subset of the slow oscillatory bursts present in their recordings, and amplified those with strong phase shifts between adjacent macrocontacts.

In conclusion, our results highlight the importance of carefully considering the choice of referencing method when analysing slow oscillations in sEEG recordings, as it can have a significant impact on the detectability and interpretation of these oscillations.

B Appendix: Gamma oscillations

B.I Definition of gamma oscillations

Gamma oscillations are a fundamental property of brain networks, observed across many animal models and brain regions (Chapter 1.III.2). In rodents, although historically defined by the broad frequency band (30-150 Hz) used to extract them from LFPs, they are now believed to report (or even constitute) the activity of diverse neural circuits and pathways (Fernandez-Ruiz et al. 2023).

In humans, by contrast, gamma activity is frequently studied under the label of "broadband gamma" (typically 60–160 Hz). In this view, gamma is treated as a wide spectral component defined primarily by its frequency range, rather than by the specific biological circuit that generates it. Broadband gamma has been widely used in sEEG studies to investigate neural representations of external stimuli (e.g., visual or auditory features), movement, and internal states (Miller et al. 2009a; Ghuman et al. 2014; Miller et al. 2014; Miller et al. 2016; Gueguen et al. 2021; Broday-Dvir et al. 2023). Although useful for achieving tractable decoding accuracies, broadband gamma, as currently defined in the human sEEG literature, does not satisfy the criteria of a neural oscillation (Fernandez-Ruiz et al. 2023).

Here, I propose that the absence of a clear definition of gamma oscillations in humans can be attributed, at least in part, to technical constraints inherent to clinical sEEG recordings.

First, electrode contacts used for clinical epilepsy monitoring are substantially larger than the microelectrodes typically employed in animal models. Because these macroelectrodes record neural activity across multiple cortical layers simultaneously, the measured signals represent an average of extracellular potentials from different layers, resulting in a loss of laminar and/or columnar specificity.

Second, interindividual variability in brain anatomy among patients with epilepsy is high, leading to electrode contacts being positioned at different locations and oriented at varying angles relative to the underlying neuronal current dipoles across subjects. In addition, uncertainty in the reconstruction of electrode contact locations using MRI/CT scan co-registration is considerable. Given that gamma oscillations are local (micrometre-resolved), this important variability in the location of electrode contacts decreases the chance of recording twice from the same network across subjects. It is thus very challenging to generalize across participants when referring to gamma-band phenomena.

Finally, recording setups employed in clinical settings often introduce line noise (50

or 60 Hz) into electrophysiological recordings, which can adversely affect the detection of genuine physiological gamma oscillations, particularly when notch filters are applied. Beyond these methodological considerations, it remains possible that gamma-band activity in the human brain differs fundamentally from that observed in rodents.

In this appendix, we aim to characterize the gamma-band phenomena observed in our recordings. We first examine hippocampal activity during task engagement, specifically assessing whether well-defined gamma oscillations can be identified directly in raw LFP signals. We then focus on regions of the ventral visual stream to determine whether stimulus onset elicits sustained oscillatory gamma activity in these areas.

B.II Analysis of gamma-band bursts in the human hippocampus

We first examined average PSDs computed from hippocampal LFPs over the entire learning session, focussing on the gamma band. We observed that some hippocampal macrocontacts displayed a clear spectral peak in the gamma range, whereas the vast majority of hippocampal macrocontacts showed a more typical power-law distribution (Fig. B.1A,B). The presence of IEDs was associated with a more pronounced power-law distribution (Fig. B.1C).

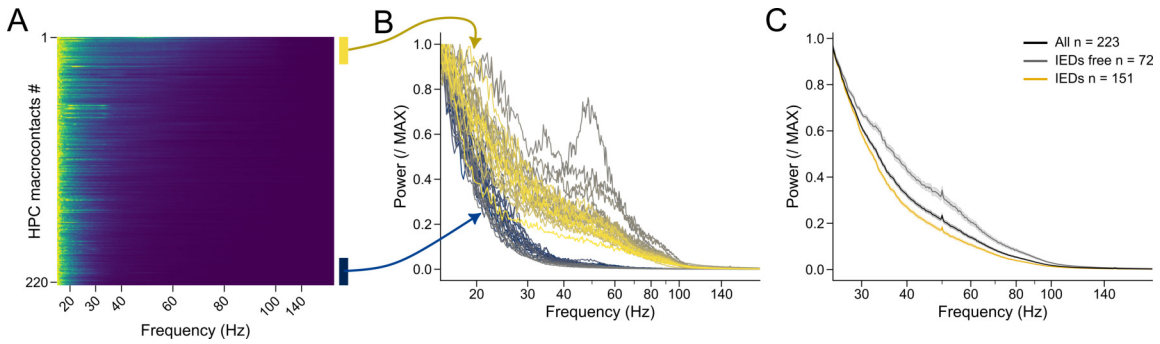


Figure B.1: **Hippocampal power spectral densities in the gamma band.** (**A**) Heatmap showing average PSDs across all hippocampal macrocontacts and subjects, normalized by the maximal power. Each row corresponds to a single macrocontact, sorted by the mean power in the 60–100 Hz range. (**B**) Average PSDs showing the top (yellow) and bottom (blue) hippocampal macrocontacts in terms of mean power in the 60–100 Hz range. Some of the top macrocontacts show a clear spectral peak in the gamma range (60–100 Hz), whereas the bottom macrocontacts show a more typical power-law distribution. (**C**) Average PSDs across either all macrocontacts (black), macrocontacts with (yellow) or without (grey) IEDs.

Next, we examined whether the presence of a gamma peak in the PSDs was associated with transient bursts of gamma activity in the time domain. We found that macrocontacts showing a clear gamma peak in the PSDs also displayed transient bursts of gamma activity, observed both in the LFP signals recorded from macrocontacts and local tetrodes (Fig. B.2A–C). However, gamma power was not higher in tetrode recordings, and the gamma bursts were not longer nor more pronounced than those observed in the

macrocontacts. Gamma bursts were also observed in other hippocampal macrocontacts showing a clear gamma peak in the PSDs, across different subjects (Fig. B.2D–I). However, this pattern was observed only in a small subset of all hippocampal macrocontacts, and the presence of gamma bursts was not consistent across subjects (data not shown). In addition, we were not able to find additional evidence for gamma bursts recorded on other hippocampal tetrodes in our dataset (data not shown). This is likely due to the sparse implantation of tetrodes and the important variability between participants.

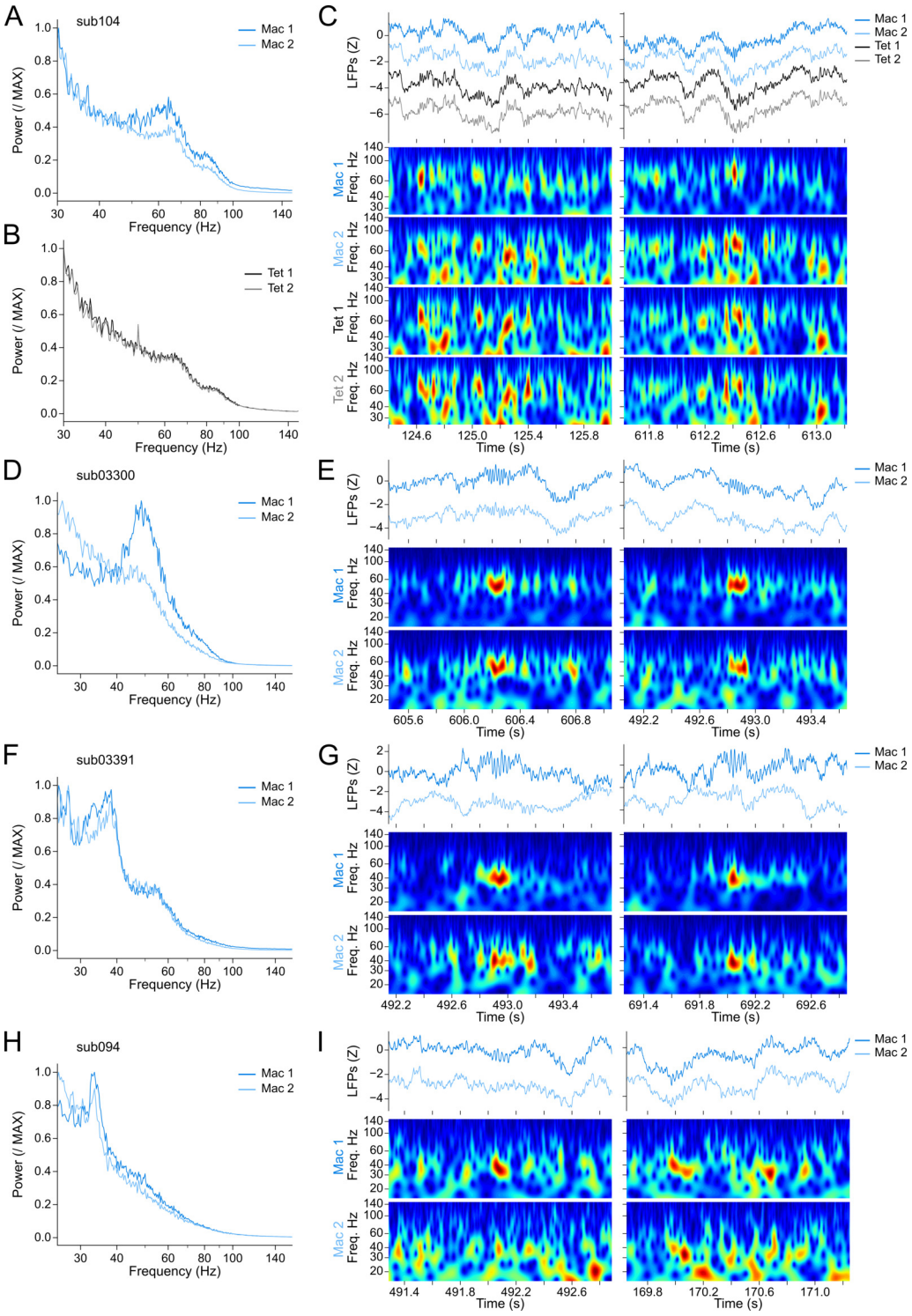


Figure B.2: **Gamma-band bursts in the human hippocampus.** (**A**–**C**) Some hippocampal recording sites displayed clear transient bursts of gamma activity. Average PSDs computed from two adjacent macrocontacts (**A**) and their local tetrodes (**B**) located in the human hippocampus. Clear peaks in the gamma range can be observed in the PSDs of both macrocontacts and local tetrodes. (**C**) Example LFPs traces from simultaneously-recorded macrocontacts and tetrodes shown in (**A**) and (**B**), with corresponding wavelet spectrogram, showing transient bursts of gamma activity in the time domain. (**D**–**I**) Same as (**A,C**) for other macrocontacts located in the hippocampus, showing clear gamma peaks in the PSDs (**D,F,H**) and transient bursts of gamma activity in the time domain (**E,G,I**).

B.III Gamma-band responses in the ventral visual stream

To better understand the nature of this broadband signal, we measured gamma responses in the entorhinal cortex, amygdala and fusiform gyrus to the presentation of photographs at various stages of the relational memory task (Fig. B.3, Fig. B.4, Fig. B.5). We selected these regions because they have previously been implicated in face processing and because the task we used presented photographs of people. Even though all three regions displayed comparable modulation strength (peak) after the onset of the visual cues in the recall questions (type 2 memory questions, see Fig. 3.1), the duration of this response was longer in the fusiform gyrus compared with the amygdala and the entorhinal cortex (Fig. B.3). Gamma responses in the amygdala and entorhinal cortex were transient (less than 100 ms) and consistent across electrode contacts and subjects.

In the amygdala, gamma responses were more prominent following the onset of learning photographs compared with viewing photographs (Fig. B.4A), a pattern not observed in the fusiform gyrus (Fig. B.5A). We therefore focused on the conditions eliciting the strongest gamma responses in each region: learning photographs for the amygdala and viewing photographs for the fusiform gyrus.

When broadband gamma activity was subdivided into three narrower frequency bands (20–60 Hz, 60–100 Hz, and 100–140 Hz), the gamma response in the amygdala was dominated by the 60–100 Hz component (Fig. B.4B). In contrast, gamma activity in the fusiform gyrus remained broadly distributed across frequencies (Fig. B.5B). In addition, the gamma response was markedly shorter in duration in the amygdala (less than ~100 ms) than in the fusiform gyrus (~500 ms).

To further characterize these differences at the level of individual recording sites, we selected the macrocontact exhibiting the strongest gamma response in each region (Fig. B.4C; Fig. B.5C). Measuring broadband gamma power across individual trials free of IEDs revealed that responses in the amygdala were highly consistent across trials, whereas those in the fusiform gyrus showed greater variability. In addition, average wavelet spectrograms demonstrated that gamma activity in the amygdala was well defined within the mid-gamma range (50–100 Hz), whereas in the fusiform gyrus it was distributed across a broader frequency spectrum.

We further confirmed these findings by computing the average LFPs time-locked to the peak amplitude of broadband gamma (60–160 Hz) in the amygdala (Fig. B.4D), and to narrower frequency bands (60–, 80–, 100–, and 120–160 Hz) in the fusiform gyrus (Fig. B.5D). This time-domain representation revealed that gamma responses in the amygdala consisted of transient, non-oscillatory events peaking at approximately 50–60 Hz (Fig. B.4E).

Finally, analysis at the single-trial level confirmed the transient nature of gamma responses in the amygdala (Fig. B.4F–H) and the sustained, broadband responses observed in the fusiform gyrus (Fig. B.5E–G). The latter pattern is consistent with the spectral tilt previously reported in the literature (Miller et al. 2009b).

Finally, we examined whether gamma responses were also present in occipital regions,

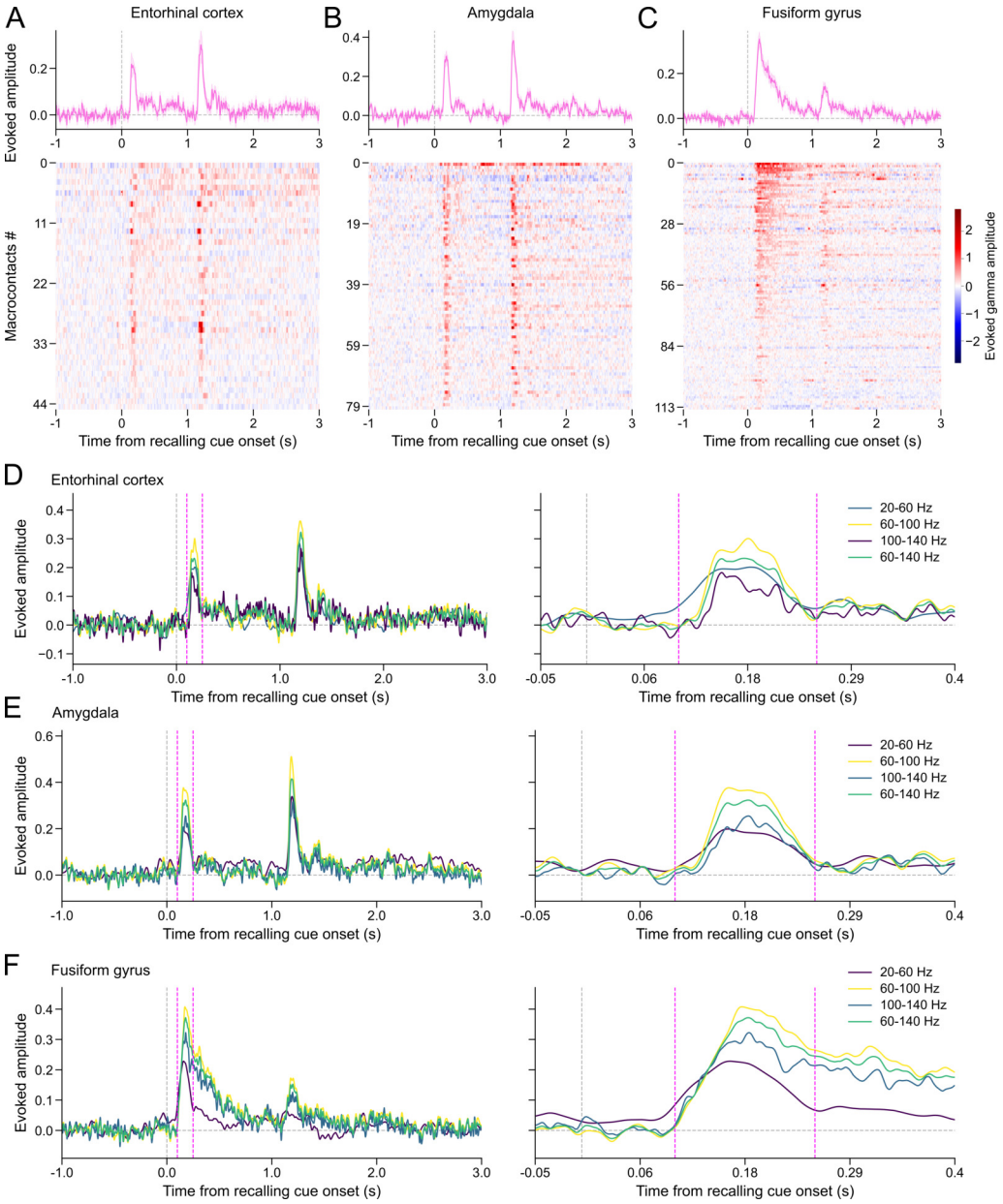
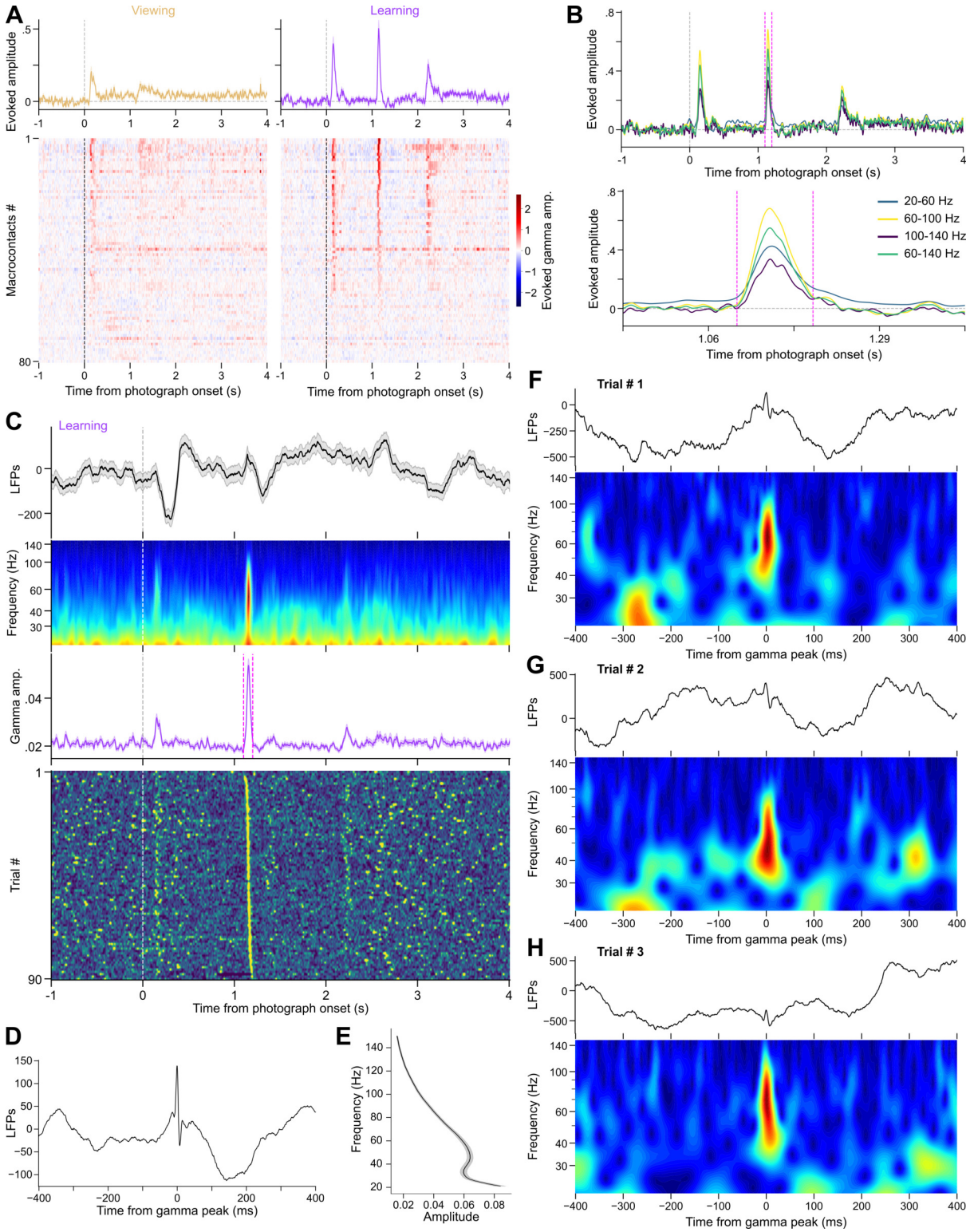


Figure B.3: **Gamma-band responses to photographs in the recall session.** (**A**–**C**) Broadband gamma (60–160 Hz) amplitude evoked by the onset of recalling photographs in the entorhinal cortex (**A**), amygdala (**B**) and fusiform gyrus (**C**). Top, average response across all macrocontacts. Bottom, heatmap showing traces obtained from individual macrocontacts, sorted by the amplitude of the first peak. Evoked gamma amplitude was obtained by z-scoring individual traces using the statistics from the baseline (-1 to -0.5 s). (**D**–**E**) Left, gamma amplitude evoked by the onset of recalling photographs for different frequency bands, averaged across all macrocontacts (20–60 Hz, 60–100 Hz, 100–140 Hz, 60–140 Hz). Right, zoom on the first gamma peak (-0.05 to +0.4 s). The colour of individual traces is sorted from darker to brighter tones based on the average amplitude in the selected epoch (+0.1 to +0.2 s) to reflect their modulation strength.


A
Viewing
Learning
Evoked amplitude
Macrocontacts #
Evoked gamma amp.
Time from photograph onset (s)
B
Evoked amplitude
Time from photograph onset (s)
20-60 Hz
60-100 Hz
100-140 Hz
60-140 Hz
C
Learning
LFPs
Frequency (Hz)
Gamma amp.
Trial #
Time from photograph onset (s)
D
LFPs
Time from gamma peak (ms)
E
Frequency (Hz)
Amplitude
F
Trial # 1
G
Trial # 2
H
Trial # 3

which are known to exhibit clear gamma-band oscillations in response to visual stimuli. To do this, we focussed on macrocontacts located in the lingual gyrus and lateral occipital cortex, which are part of the ventral visual stream. We found that some macrocontacts displayed a clear gamma modulation following the onset of visual stimuli (Fig. B.6A–D). Although the gamma bursts evoked by visual stimuli in these regions were quite prolonged, they showed substantial variability in frequency across trials (ranging from 60 to 140 Hz). Unfortunately, occipital regions were only sparsely covered in our recordings, and none of them had tetrodes in their vicinity, preventing us from further characterizing the nature of these gamma responses.

Taken together, these analyses revealed that some hippocampal macrocontacts displayed a clear gamma peak in the PSDs, which was associated with transient bursts of gamma activity directly visible in the raw LFP traces. These hippocampal gamma bursts could be observed both on macrocontacts and tetrodes, and they were equally prominent in the tetrode recordings. This suggests that the size of the recording contact does not necessarily impair the detection of gamma oscillations. However, this pattern was observed only in a subset of all hippocampal macrocontacts, and the presence of gamma bursts was not consistent across subjects. This observation is likely due to the important variability between participants and to the convoluted histology of the human hippocampus, which makes it particularly challenging to record twice from the same microcircuit.

In addition, we found that visual stimuli elicited sustained gamma responses in the fusiform gyrus, but transient gamma responses in the amygdala, which did not correspond to well-defined oscillations in the time domain. Moreover, even in regions known to exhibit clear gamma-band oscillations (the occipital cortex), we observed a mixture of convincing, oscillatory gamma bursts and broadband responses.

These results suggest that the gamma-band activity observed in our recordings may reflect a mixture of different network phenomena, including transient bursts of gamma oscillations and non-oscillatory broadband responses. The latter pattern is consistent with the spectral tilt previously reported in the literature (Miller et al. 2009b). Future studies combining high-density laminar recordings, microelectrodes, and improved anatomical reconstruction methods will be necessary to better characterize gamma-band phenomena in the human brain and to determine which components correspond to genuine oscillatory network activity versus broadband, non-oscillatory responses.

Figure B.4: **Gamma-band responses in the amygdala.** (**A**) Broadband gamma (60–160 Hz) amplitude evoked by the onset of viewing (left) or learning (right) photographs in the relational memory task. Top, average response across all amygdala macrocontacts. Bottom, heatmap showing traces obtained from individual amygdala macrocontacts, sorted by the amplitude of the second peak in the learning condition (+1.1 to +1.2 s). Evoked gamma amplitude was obtained by z-scoring individual traces using the statistics from the baseline (-1 to -0.5 s). (**B**) Top, average gamma amplitude evoked by the onset of learning photographs for different frequency bands (20–60 Hz, 60–100 Hz, 100–140 Hz, 60–140 Hz). Bottom, magnified view of the second gamma peak (+0.95 to +1.4 s). The colour of individual traces is sorted from darker to brighter tones based on the average amplitude in the +1.1 to +1.2 s epoch to reflect their modulation strength. (**C**) Example response from the amygdala macrocontact which showed the most prominent gamma modulation. From top to bottom: ERPs, with corresponding wavelet spectrogram, average broadband gamma (60–160 Hz) amplitude, and heatmap showing broadband gamma across individual trials (sorted). (**D**) Average LFPs triggered by gamma peaks detected in the (+1.1 to +1.2 s) time range, showing a transient gamma response nested on the first positive component of the typical amygdala visual ERPs. (**E**) PSDs computed from the wavelet spectrogram in the (+1.1 to +1.2 s) time range. (**F**–**H**) LFPs traces and spectrograms from three example trials centred on the peak of the gamma response detected as in **D**.

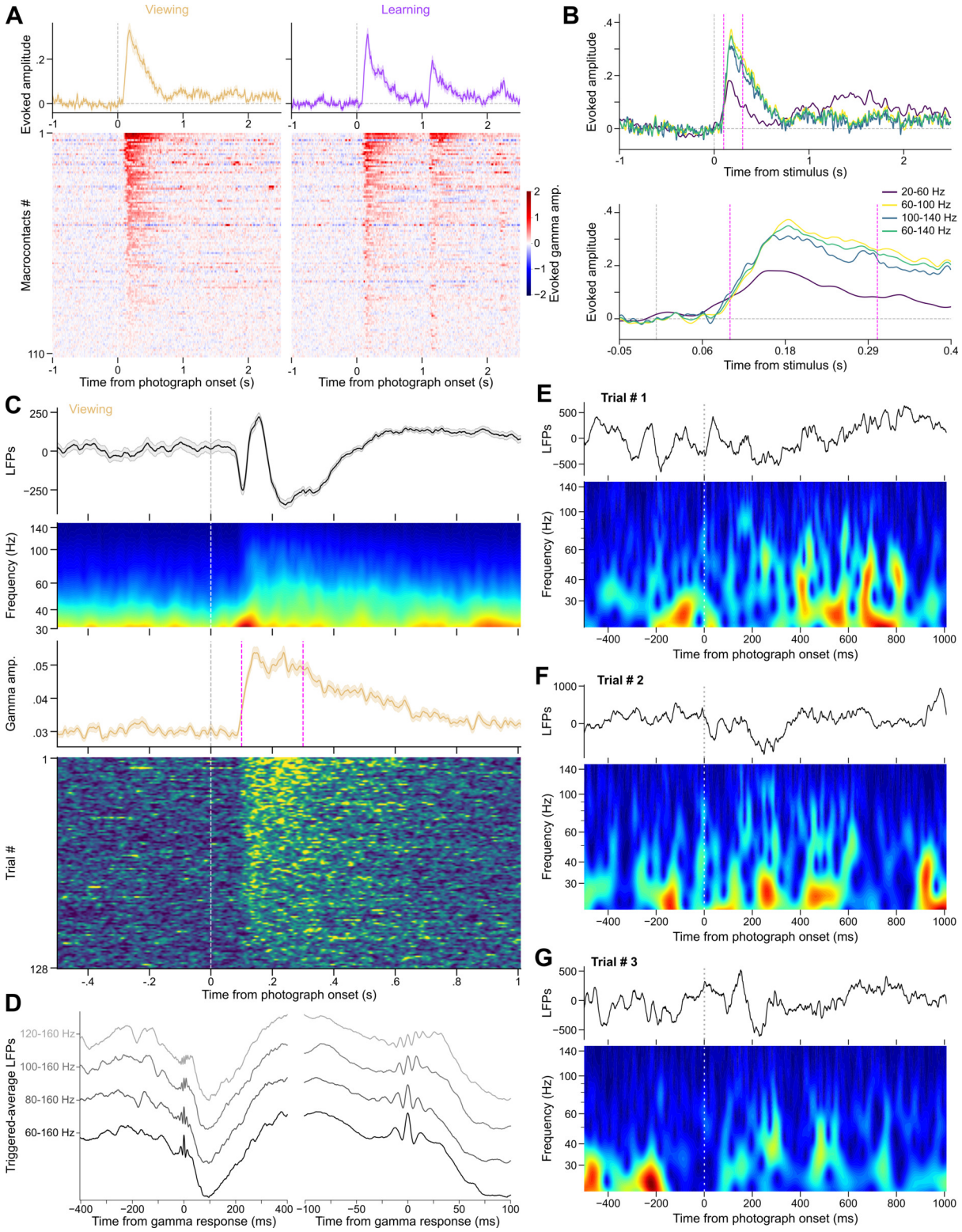

A
Viewing
Learning
Evoked amplitude
Macrocontacts #
Evoked gamma amp.
Time from photograph onset (s)
B
Evoked amplitude
Time from stimulus (s)
20-60 Hz
60-100 Hz
100-140 Hz
60-140 Hz
C
Viewing
LFPs
Frequency (Hz)
Gamma amp.
Trial #
Time from photograph onset (s)
D
Triggered-average LFPs
120-160 Hz
100-160 Hz
80-160 Hz
60-160 Hz
Time from gamma response (ms)
E
Trial # 1
F
Trial # 2
G
Trial # 3
Time from photograph onset (ms)

Figure B.5: **Gamma-band responses in the fusiform gyrus.** (**A**) Broadband gamma (60–160 Hz) amplitude evoked by the onset of viewing (left) or learning (right) photographs in the relational memory task. Top, average response across all fusiform gyrus macrocontacts. Bottom, heatmap showing traces obtained from individual fusiform gyrus macrocontacts, sorted by the amplitude of the first peak in the viewing condition (+0.1 to +0.3 s). Evoked gamma amplitude was obtained by z-scoring individual traces using the statistics from the baseline (-1 to -0.5 s). (**B**) Top, average gamma amplitude evoked by the onset of viewing photographs for different frequency bands (20–60 Hz, 60–100 Hz, 100–140 Hz, 60–140 Hz). Bottom, zoom on the first gamma peak (-0.05 to +0.4 s). The colour of individual traces is sorted from darker to brighter tones based on the average amplitude in the +0.1 to +0.3 s epoch to reflect their modulation strength. (**C**) Example response from the fusiform gyrus macrocontact which showed the most prominent gamma modulation. From top to bottom: ERPs, with corresponding wavelet spectrogram, average broadband gamma (60–160 Hz) amplitude, and heatmap showing broadband gamma across individual trials (sorted). (**D**) Average LFPs triggered by gamma peaks (60–, 80–, 100–, or 120–160 Hz) detected in the (+0.1 to +0.3 s) time range, showing a more sustained gamma response than that of the amygdala (Fig. B.4C). (**E**–**G**) LFPs traces and spectrograms from three example trials centred on the onset of the photograph as in **C**.

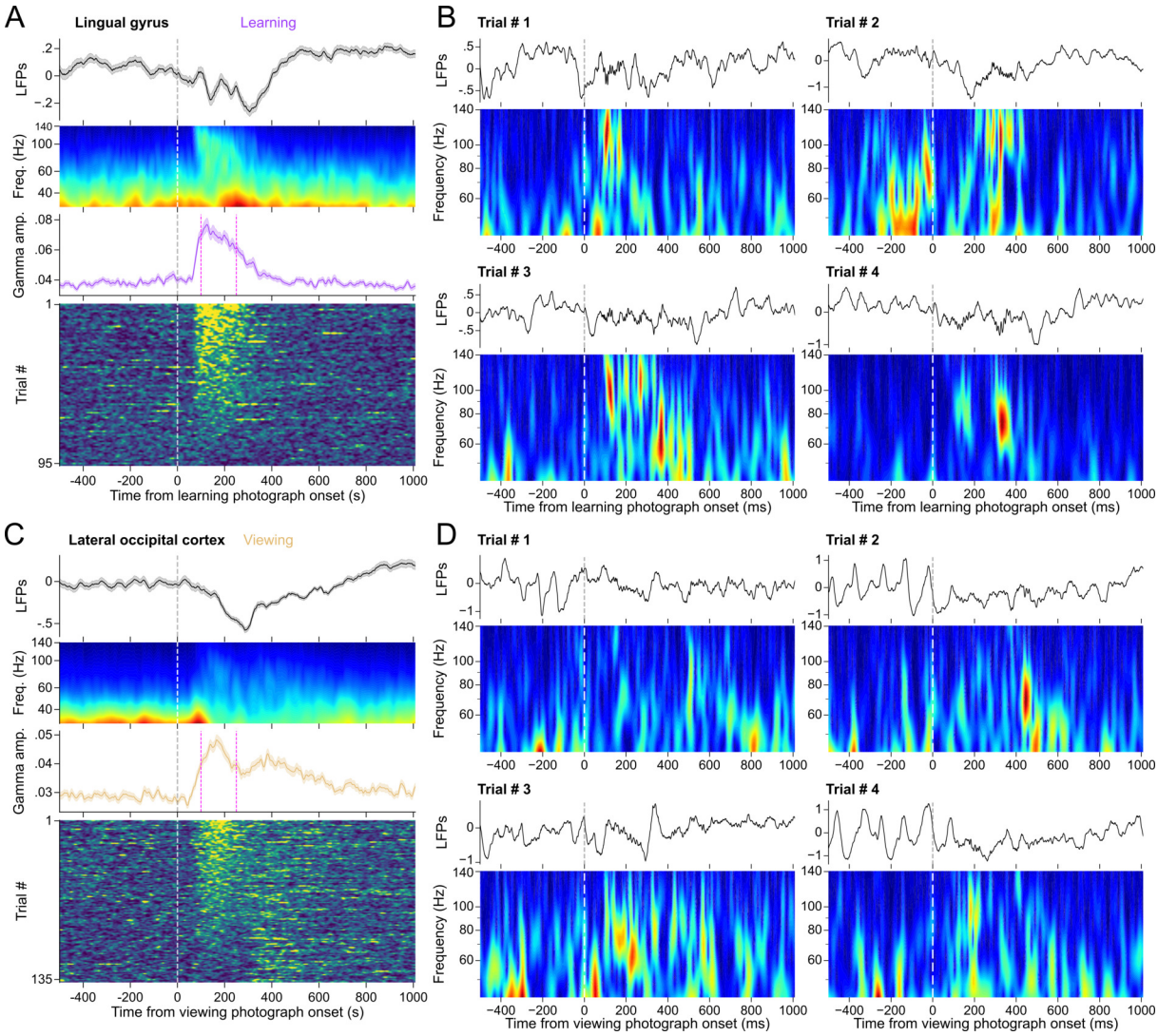


Figure B.6: **Gamma-band responses in regions of the occipital lobe.** (**A**) Example response from a macrocontact located in the lingual gyrus which showed the most prominent gamma modulation. From top to bottom: ERPs, with corresponding wavelet spectrogram, average broadband gamma (60–160 Hz) amplitude, and heatmap showing broadband gamma across individual trials (sorted). (**B**) LFPs traces and spectrograms from four example trials centred on the onset of the photograph. (**C** and **D**) Same as **A** and **B** for a contact in the lateral occipital cortex which displayed a prominent gamma modulation.

C Appendix: Analysis of the References used in this thesis

The references cited throughout a thesis reflect a series of intellectual choices and influences. Although the references employed in my thesis were used to support specific scientific arguments rather than to provide a systematic review of the literature, the collection of cited works nevertheless offers a glimpse into the research traditions that shaped the present thesis. Hence, the purpose of this appendix is twofold. First, it attempts to provide a transparent overview of potential biases in the selection of references. Second, it highlights the authors, journals, and periods of publication that most strongly influenced the theoretical background, methodological choices, and interpretation of the results presented throughout the thesis.

General approach: To describe the composition of the bibliography, I first parsed the compiled bibliographic file (.bib file generated by the LaTeX compiler) into a structured table with one row per cited work. For each entry, I extracted the citation key, document type, title, year, authors, and source (journal). I then cleaned the text to remove formatting artefacts, grouped author names at the surname level, and harmonised source names so that small spelling or formatting differences did not create separate categories. This produced a single dataset that could be used to summarise the bibliography by year, journal, and author. The bibliography contained ~636 citations, of which 589 were journal articles, including original research papers, reviews and opinion articles (Fig. C.1A).

Journals and years: I then examined the temporal distribution of the references by assigning each citation to a decade based on its publication year. This provides a broad overview of when the cited literature was published, without placing too much weight on year-to-year fluctuations (Fig. C.1B). In parallel, I summarised the journals and other sources represented in the bibliography after harmonising journal names and excluding book-like sources from the journal count. Out of the 589 journal articles, 548 were published in journals which could be automatically identified, disregarding single occurrences. For Fig. C.1C, I focused on the most frequently cited journals (top 20), as these give the clearest view of the publication landscape supporting the thesis (representing 72.3% of the article citations). The top-cited journals were: Neuron (14.4%), Science AAAS (10.6%), Nature Neuroscience (9.8%), Journal of Neuroscience (9.3%), Nature (7.6%), representing more than half of the citations in the selected journals (51.7%).

Authors: To summarise the authors of the bibliography, I counted citations at the surname level rather than at the full-name level, so that repeated references to the same author were grouped together. I took this decision because the first names varied considerably between citation formats and proved too challenging to track accurately.

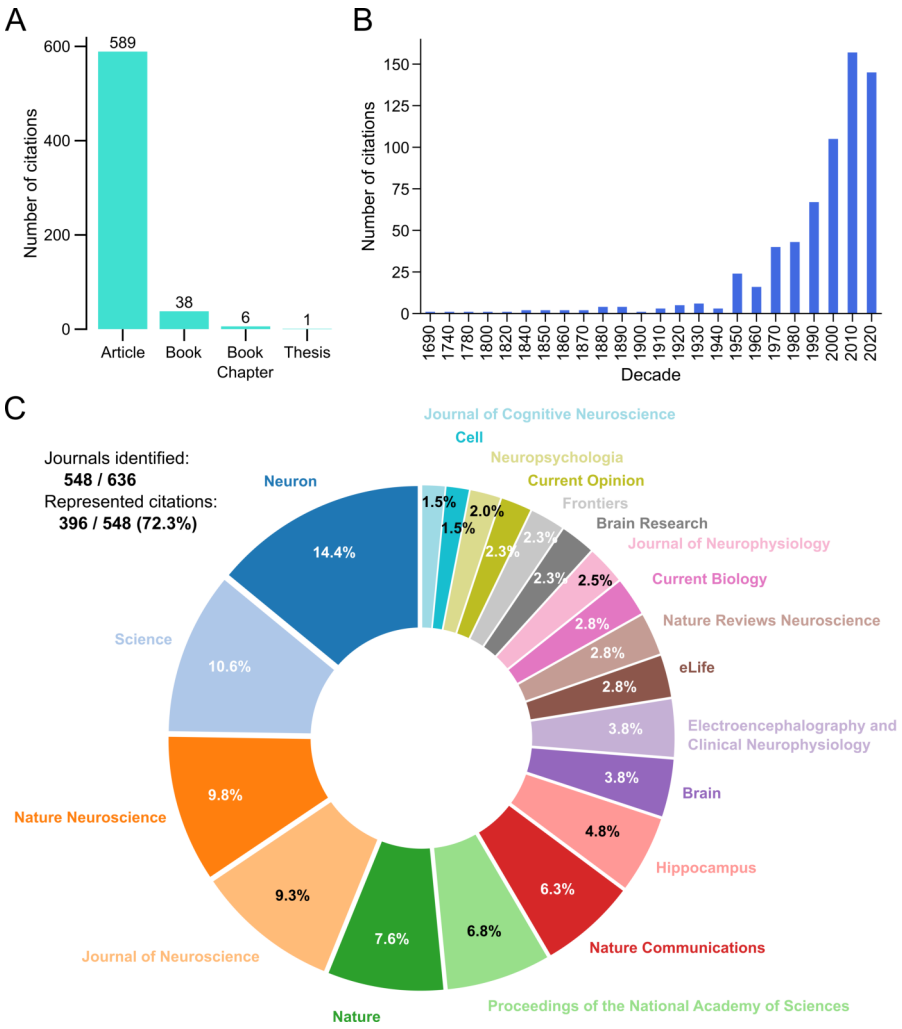


Figure C.1: **References: timeline and journals.** (**A**) Bar chart showing the main types of documents cited. (**B**) Bar chart showing the number of citations per decade. (**C**) Pie chart showing the distribution of the most frequently cited journals in the bibliography. Percentages indicate the proportion of references attributed to each journal, and the total number of included references is reported in the top left corner of the panel.

Where necessary, surnames were normalised to merge spelling variants while preserving the original form for display. I then identified the most frequently cited authors (Fig. C.2A).

To complement the citation counts, I examined the relationships between the most frequently cited authors using a co-occurrence network (*graph not shown*). In this network, two authors were connected when they appeared together on the same cited publication, irrespective of their position in the authors' list. I focused on two complementary measures. The first, weighted degree, quantifies the total strength of an author's connections by summing all co-authorship links (Fig. C.2B). For example, an author who repeatedly publishes with many other highly cited authors (in my thesis) would have a high weighted degree. The second, degree centrality, quantifies the proportion of authors in the network to whom a given author is connected, irrespective of how often those connections occur (Fig. C.2C). For example, an author who has collaborated at least once with many different authors would have a high degree centrality, even if each collaboration occurred only a single time. Together, these measures distinguish authors who are strongly embedded within collaboration networks from those whose work spans a broader range of connections across the citation network.

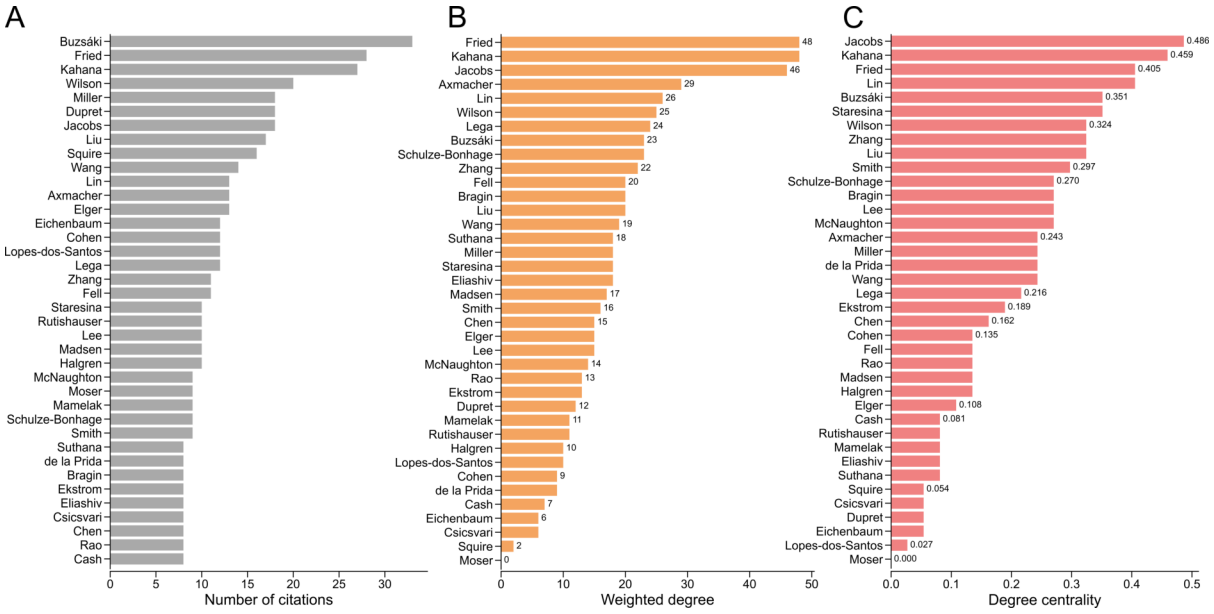


Figure C.2: **References: authors.** (**A**) Bar chart showing the most frequently cited authors in the bibliography, quantified at the surname level. (**B**) Bar chart showing the weighted degree of the most frequently cited authors in the co-occurrence network, reflecting the total strength of their connections to other highly-cited authors. (**C**) Bar chart showing the degree centrality of the same network, reflecting the proportion of authors to whom each author is connected.

References

Abbaspoor, S., A. Aljishi, and K. L. Hoffman (Aug. 12, 2025). Experience Reorganizes Content-Specific Memory Traces in Macaques. *bioRxiv*, p. 2025.04.08.647787. https://doi.org/10.1101/2025.04.08.647787(cit. on p. 34)

Adam, Y., J. J. Kim, S. Lou, Y. Zhao, M. E. Xie, D. Brinks, H. Wu, M. A. Mostajo-Radji, S. Kheifets, V. Parot, S. Chettih, K. J. Williams, B. Gmeiner, S. L. Farhi, L. Madisen, E. K. Buchanan, I. Kinsella, D. Zhou, L. Paninski, C. D. Harvey, H. Zeng, P. Arlotta, R. E. Campbell, and A. E. Cohen (May 2019). Voltage Imaging and Optogenetics Reveal Behaviour-Dependent Changes in Hippocampal Dynamics. *Nature* 569, 7756, pp. 413–417. https://doi.org/10.1038/s41586-019-1166-7(cit. on p. 35)

Adey, W. R., C. W. Dunlop, and C. E. Hendrix (July 1, 1960). Hippocampal Slow Waves: Distribution and Phase Relationships in the Course of Approach Learning. *Archives of Neurology* 3, 1, pp. 74–90. https://doi.org/10.1001/archneur.1960.00450010074007(cit. on p. 36)

Adhikari, A., M. A. Topiwala, and J. A. Gordon (Jan. 28, 2010). Synchronized Activity between the Ventral Hippocampus and the Medial Prefrontal Cortex during Anxiety. *Neuron* 65, 2, pp. 257–269. https://doi.org/10.1016/j.neuron.2009.12.002(cit. on p. 127)

Aggleton, J. P. and M. W. Brown (June 1999). Episodic Memory, Amnesia, and the Hippocampal-Anterior Thalamic Axis. *The Behavioral and Brain Sciences* 22, 3, 425–444, discussion 444–489. (Cit. on p. 32)

Aggleton, J. P. and M. Mishkin (1983). Visual Recognition Impairment Following Medial Thalamic Lesions in Monkeys. *Neuropsychologia* 21, 3, pp. 189–197. https://doi.org/10.1016/0028-3932(83)90037-4(cit. on p. 32)

Aghajan, Z. M., P. Schuette, T. A. Fields, M. E. Tran, S. M. Siddiqui, N. R. Hasulak, T. K. Tcheng, D. Eliashiv, E. A. Mankin, J. Stern, I. Fried, and N. Suthana (Dec. 18, 2017). Theta Oscillations in the Human Medial Temporal Lobe during Real-World Ambulatory Movement. *Current Biology* 27, 24, 3743–3751.e3. https://doi.org/10.1016/j.cub.2017.10.062(cit. on pp. 43, 116, 162, 168)

Ahissar, E., E. Vaadia, M. Ahissar, H. Bergman, A. Arieli, and M. Abeles (Sept. 4, 1992). Dependence of Cortical Plasticity on Correlated Activity of Single Neurons and on Behavioral Context. *Science* 257, 5075, pp. 1412–1415. https://doi.org/10.1126/science.1529342(cit. on p. 33)

Akam, T. and D. M. Kullmann (July 29, 2010). Oscillations and Filtering Networks Support Flexible Routing of Information. *Neuron* 67, 2, pp. 308–320. https://doi.org/10.1016/j.neuron.2010.06.019(cit. on p. 39)

Alba, J. W. and L. Hasher (1983). Is Memory Schematic? *Psychological Bulletin* 93, 2, pp. 203–231. https://doi.org/10.1037/0033-2909.93.2.203(cit. on p. 25)

Aleman-Zapata, A., M. M. Capitan, A. Samanta, P. Özsezer, K. Agarwal, T. Adam, A. Rayan, and L. Genzel (Feb. 21, 2025). Differential Contributions of CA3 and Entorhinal Cortex Inputs to Ripple Patterns in the Hippocampus. *iScience* 28, 2. https://doi.org/10.1016/j.isci.2025.111782(cit. on p. 38)

Anderson, R. C. and P. D. Pearson (Feb. 26, 1988). "A Schema-Theoretic View of Basic Processes in Reading Comprehension". In: *Interactive Approaches to Second Language Reading*. Ed. by P. L. Carrell, J. Devine, and D. E. Eskey. 1st ed. Cambridge University Press, pp. 37–55. https://doi.org/10.1017/CBO9781139524513.007 (cit. on p. 25).

Anderson, R. C., J. W. Pichert, and L. L. Shirey (1983). Effects of the Reader's Schema at Different Points in Time. *Journal of Educational Psychology* 75, 2, pp. 271–279. https://doi.org/10.1037/0022-0663.75.2.271(cit. on p. 25)

Andrillon, T. and S. Kouider (June 1, 2020). The Vigilant Sleeper: Neural Mechanisms of Sensory (de)Coupling during Sleep. *Current Opinion in Physiology* 15, pp. 47–59. https://doi.org/10.1016/j.cophys.2019.12.002(cit. on p. 37)

Arnolds, D. E., F. H. Lopes da Silva, J. W. Aitink, and A. Kamp (May 1979). Hippocampal EEG and Behaviour in Dog. I. Hippocampal EEG Correlates of Gross Motor Behaviour. *Electroencephalography and Clinical Neurophysiology* 46, 5, pp. 552–570. https://doi.org/10.1016/0013-4694(79)90009-9(cit. on pp. 36, 163)

Arnolds, D. E., F. H. Lopes da Silva, J. W. Aitink, and A. Kamp (May 1979). Hippocampal EEG and Behaviour in Dog. II. Hippocampal EEG Correlates with Elementary Motor Acts. *Electroencephalography and Clinical Neurophysiology* 46, 5, pp. 571–580. https://doi.org/10.1016/0013-4694(79)90010-5(cit. on p. 36)

Arnolds, D. E. A. T., F. H. Lopes Da Silva, J. W. Aitink, A. Kamp, and P. Boeijinga (Nov. 1, 1980). The Spectral Properties of Hippocampal EEG Related to Behaviour in Man. *Electroencephalography and Clinical Neurophysiology* 50, 3, pp. 324–328. https://doi.org/10.1016/0013-4694(80)90160-1(cit. on pp. 42, 163)

Assaf, S. and J. Miller (June 1978). The Role of a Raphe Serotonin System in the Control of Septal Unit Activity and Hippocampal Desynchronization. *Neuroscience* 3, 6, pp. 539–550. https://doi.org/10.1016/0306-4522(78)90018-0(cit. on p. 37)

Axmacher, N., C. E. Elger, and J. Fell (July 2008). Ripples in the Medial Temporal Lobe Are Relevant for Human Memory Consolidation. *Brain: A Journal of Neurology* 131, pp. 1806–1817. https://doi.org/10.1093/brain/awn103(cit. on pp. 45, 148)

Axmacher, N., M. M. Henseler, O. Jensen, I. Weinreich, C. E. Elger, and J. Fell (Feb. 16, 2010). Cross-Frequency Coupling Supports Multi-Item Working Memory in the Human Hippocampus. *Proceedings of the National Academy of Sciences* 107, 7, pp. 3228–3233. https://doi.org/10.1073/pnas.0911531107(cit. on pp. 44, 108)

Axmacher, N., F. Mormann, G. Fernández, M. X. Cohen, C. E. Elger, and J. Fell (July 18, 2007). Sustained Neural Activity Patterns during Working Memory in the Human Medial Temporal Lobe. *The Journal of Neuroscience: The Official Journal of the Society for Neuroscience* 27, 29, pp. 7807–7816. https://doi.org/10.1523/JNEUROSCI.0962-07.2007(cit. on pp. 42, 45)

Babb, T. L., E. Carr, and P. H. Crandall (Mar. 1973). Analysis of Extracellular Firing Patterns of Deep Temporal Lobe Structures in Man. *Electroencephalography and Clinical Neurophysiology* 34, 3, pp. 247–257. https://doi.org/10.1016/0013-4694(73)90252-6(cit. on p. 34)

Babiloni, C., F. Vecchio, G. Mirabella, M. Buttiglione, F. Sebastiano, A. Picardi, G. Di Gennaro, P. P. Quarato, L. G. Grammaldo, P. Buffo, V. Esposito, M. Manfredi, G. Cantore, and F. Eusebi (July 2009). Hippocampal, Amygdala, and Neocortical

Synchronization of Theta Rhythms Is Related to an Immediate Recall during Rey Auditory Verbal Learning Test. *Human Brain Mapping* 30, 7, pp. 2077–2089. https://doi.org/10.1002/hbm.20648(cit. on pp. 42, 44)

Bachevalier, J., J. K. Parkinson, and M. Mishkin (1985). Visual Recognition in Monkeys: Effects of Separate vs. Combined Transection of Fornix and Amygdalofugal Pathways. *Experimental Brain Research* 57, 3, pp. 554–561. https://doi.org/10.1007/BF00237842(cit. on p. 32)

Bain, A. (1855). *The Senses and the Intellect*. The Senses and the Intellect. London, England: John W Parker & Son, West Strand, pp. xxxi, 614. xxxi, 614. https://doi.org/10.1037/12115-000 (cit. on pp. 23, 27, 28).

Baldassano, C., U. Hasson, and K. A. Norman (Nov. 7, 2018). Representation of Real-World Event Schemas during Narrative Perception. *Journal of Neuroscience* 38, 45, pp. 9689–9699. https://doi.org/10.1523/JNEUROSCI.0251-18.2018(cit. on p. 25)

Baram, A. B., T. H. Muller, H. Nili, M. M. Garvert, and T. E. J. Behrens (Feb. 17, 2021). Entorhinal and Ventromedial Prefrontal Cortices Abstract and Generalize the Structure of Reinforcement Learning Problems. *Neuron* 109, 4, 713–723.e7. https://doi.org/10.1016/j.neuron.2020.11.024(cit. on p. 25)

Barba, C., M. Cossu, R. Guerrini, G. Di Gennaro, F. Villani, L. De Palma, L. Grisotto, A. Consales, D. Battaglia, N. Zamponi, P. d'Orio, M. Revay, M. Rizzi, S. Casciato, V. Esposito, P. P. Quarato, R. Di Giacomo, G. Didato, C. Pastori, G. C. Pavia, S. Pellacani, G. Matta, M. Pacetti, G. Tamburrini, E. Cesaroni, G. Colicchio, G. Vatti, S. Asioli, M. Caulo, T. S. Group, C. E. Marras, and L. Tassi (2021). Temporal Lobe Epilepsy Surgery in Children and Adults: A Multicenter Study. *Epilepsia* 62, 1, pp. 128–142. https://doi.org/10.1111/epi.16772(cit. on pp. 34, 97)

Barbeau, E. J., P. Chauvel, C. J. Moulin, J. Regis, and C. Liégeois-Chauvel (Apr. 2017). Hippocampus Duality: Memory and Novelty Detection Are Subserved by Distinct Mechanisms. *Hippocampus* 27, 4, pp. 405–416. https://doi.org/10.1002/hipo.22699(cit. on p. 108)

Barbeau, E. J., J. Pariente, O. Felician, and M. Puel (Sept. 2011). Visual Recognition Memory: A Double Anatomo-Functional Dissociation. *Hippocampus* 21, 9, pp. 929–934. https://doi.org/10.1002/hipo.20848(cit. on p. 30)

Barlow, H. B. (1972). Single Units and Sensation: A Neuron Doctrine for Perceptual Psychology? *Perception* 1, 4, pp. 371–394. https://doi.org/10.1068/p010371(cit. on p. 32)

Barron, H. C., R. Auksztulewicz, and K. Friston (Sept. 1, 2020). Prediction and Memory: A Predictive Coding Account. *Progress in neurobiology* 192, p. 101821. https://doi.org/10.1016/j.pneurobio.2020.101821(cit. on p. 27)

Barron, H. C., R. B. Mars, D. Dupret, J. P. Lerch, and C. Sampaio-Baptista (Jan. 4, 2021). Cross-Species Neuroscience: Closing the Explanatory Gap. *Philosophical Transactions of the Royal Society B: Biological Sciences* 376, 1815, p. 20190633. https://doi.org/10.1098/rstb.2019.0633(cit. on p. 28)

Barron, H. C., H. M. Reeve, R. S. Koolschijn, P. V. Perestenko, A. Shpektor, H. Nili, R. Rothaermel, N. Campo-Urriza, J. X. O'Reilly, D. M. Bannerman, T. E. Behrens, and D. Dupret (Oct. 2020). Neuronal Computation Underlying Inferential Reasoning in Humans and Mice. *Cell* 183, 1, 228–243.e21. https://doi.org/10.1016/j.cell.2020.08.035(cit. on pp. 28, 41)

Bartlett, F. C. (1932). *Remembering: A Study in Experimental and Social Psychology*. Remembering: A Study in Experimental and Social Psychology. New York, NY, US: Cambridge University Press, pp. xix, 317. xix, 317 (cit. on pp. 24, 25).

Bartsch, T., K. Alfke, R. Stingele, A. Rohr, S. Freitag-Wolf, O. Jansen, and G. Deuschl (Nov. 1, 2006). Selective Affection of Hippocampal CA-1 Neurons in Patients with Transient Global Amnesia without Long-Term Sequelae. *Brain* 129, 11, pp. 2874–2884. https://doi.org/10.1093/brain/awl248(cit. on p. 29)

Bastos, A. M., J. Vezoli, and P. Fries (Apr. 2015). Communication through Coherence with Inter-Areal Delays. *Current Opinion in Neurobiology* 31, pp. 173–180. https://doi.org/10.1016/j.conb.2014.11.001(cit. on p. 39)

Beach, F. A. (Apr. 1950). The Snark Was a Boojum. *American Psychologist* 5, 4, pp. 115–124. https://doi.org/10.1037/h0056510(cit. on p. 28)

Bédard, C. and A. Destexhe (Oct. 2011). Generalized Theory for Current-Source-Density Analysis in Brain Tissue. *Physical Review. E, Statistical, Nonlinear, and Soft Matter Physics* 84, p. 041909. https://doi.org/10.1103/PhysRevE.84.041909(cit. on p. 35)

Bédard, C., H. Kröger, and A. Destexhe (Mar. 2004). Modeling Extracellular Field Potentials and the Frequency-Filtering Properties of Extracellular Space. *Biophysical Journal* 86, 3, pp. 1829–1842. https://doi.org/10.1016/S0006-3495(04)74250-2(cit. on p. 35)

Behrens, T. E. J., T. H. Muller, J. C. R. Whittington, S. Mark, A. B. Baram, K. L. Stachenfeld, and Z. Kurth-Nelson (Oct. 24, 2018). What Is a Cognitive Map? Organizing Knowledge for Flexible Behavior. *Neuron* 100, 2, pp. 490–509. https://doi.org/10.1016/j.neuron.2018.10.002(cit. on p. 33)

Belluscio, M. A., K. Mizuseki, R. Schmidt, R. Kempter, and G. Buzsáki (Jan. 11, 2012). Cross-Frequency Phase–Phase Coupling between Theta and Gamma Oscillations in the Hippocampus. *Journal of Neuroscience* 32, 2, pp. 423–435. https://doi.org/10.1523/JNEUROSCI.4122-11.2012(cit. on p. 142)

Bergel, A., J. M. Schmidt, B. Barrillot, S. Arthaud, L. Averty, M. S. Blumberg, C. Carachet, A. Clair, I. Filchenko, C. Froidevaux, A. Herrel, B. Massot, N. C. Rattenborg, M. H. Schmidt, M. Tanter, G. Ungurean, and P.-A. Libourel (Dec. 29, 2025). Sleep-Dependent Infraslow Rhythms Are Evolutionarily Conserved across Reptiles and Mammals. *Nature Neuroscience*, pp. 1–8. https://doi.org/10.1038/s41593-025-02159-y(cit. on p. 28)

Berger, H. (Dec. 1, 1929). Über das Elektrenkephalogramm des Menschen. *Archiv für Psychiatrie und Nervenkrankheiten* 87, 1, pp. 527–570. https://doi.org/10.1007/BF01797193(cit. on p. 35)

Bernard, C. (.-1. A. du texte (1865). *Introduction à l'étude de la médecine expérimentale ([Reprod. en fac-sim.]) / par Claude Bernard...* (Cit. on p. 28).

Bienvenu, T. C., D. Busti, P. J. Magill, F. Ferraguti, and M. Capogna (June 21, 2012). Cell-Type-Specific Recruitment of Amygdala Interneurons to Hippocampal Theta Rhythm and Noxious Stimuli In Vivo. *Neuron* 74–20, 6, pp. 1059–1074. https://doi.org/10.1016/j.neuron.2012.04.022(cit. on p. 127)

Black, L. C., B. K. Schefft, S. R. Howe, J. P. Szaflarski, H.-s. Yeh, and M. D. Privitera (Mar. 2010). The Effect of Seizures on Working Memory and Executive Functioning Performance. *Epilepsy & Behavior: E&B* 17, 3, pp. 412–419. https://doi.org/10.1016/j.yebeh.2010.01.006(cit. on pp. 81, 84, 93, 94, 166)

Bódizs, R., S. Kántor, G. Szabó, A. Szûcs, L. Erõss, and P. Halász (Jan. 2001). Rhythmic Hippocampal Slow Oscillation Characterizes REM Sleep in Humans. *Hippocampus* 11, 6, pp. 747–753. https://doi.org/10.1002/hipo.1090(cit. on pp. 43, 104, 144, 163, 165)

Bohbot, V. D., M. S. Copara, J. Gotman, and A. D. Ekstrom (Feb. 14, 2017). Low-Frequency Theta Oscillations in the Human Hippocampus during Real-World and Virtual Navigation. *Nature Communications* 8, 1, p. 14415. https://doi.org/10.1038/ncomms14415(cit. on pp. 43, 116)

Bonnet, M. H., L. C. Johnson, and W. B. Webb (1978). The Reliability of Arousal Threshold During Sleep. *Psychophysiology* 15, 5, pp. 412–416. https://doi.org/10.1111/j.1469-8986.1978.tb01407.x(cit. on p. 37)

Bora, E. and S. Meletti (July 1, 2016). Social Cognition in Temporal Lobe Epilepsy: A Systematic Review and Meta-Analysis. *Epilepsy & Behavior* 60, pp. 50–57. https://doi.org/10.1016/j.yebeh.2016.04.024(cit. on p. 166)

Boroujeni, K. B. and T. Womelsdorf (Sept. 20, 2023). Routing States Transition during Oscillatory Bursts and Attentional Selection. *Neuron* 111, 18, 2929–2944.e11. https://doi.org/10.1016/j.neuron.2023.06.012(cit. on p. 162)

Bragin, A., J. Engel, C. L. Wilson, I. Fried, and G. Buzsáki (1999). High-Frequency Oscillations in Human Brain. *Hippocampus* 9, 2, pp. 137–142. https://doi.org/10.1002/(SICI)1098-1063(1999)9:2<137::AID-HIPO5>3.0.CO;2-0(cit. on pp. 44, 144, 147, 148, 164)

Bragin, A., G. Jandó, Z. Nádasdy, J. Hetke, K. Wise, and G. Buzsáki (Jan. 1995). Gamma (40-100 Hz) Oscillation in the Hippocampus of the Behaving Rat. *The Journal of Neuroscience: The Official Journal of the Society for Neuroscience* 15, pp. 47–60. https://doi.org/10.1523/JNEUROSCI.15-01-00047.1995(cit. on pp. 35, 37, 39, 45, 116, 119)

Bragin, A., G. Jandó, Z. Nádasdy, M. van Landeghem, and G. Buzsáki (Apr. 1995). Dentate EEG Spikes and Associated Interneuronal Population Bursts in the Hippocampal Hilar Region of the Rat. *Journal of Neurophysiology* 73, 4, pp. 1691–1705. https://doi.org/10.1152/jn.1995.73.4.1691(cit. on p. 38)

Bragin, A., J. Engel Jr., C. L. Wilson, I. Fried, and G. W. Mathern (1999). Hippocampal and Entorhinal Cortex High-Frequency Oscillations (100–500 Hz) in Human Epileptic Brain and in Kainic Acid-Treated Rats with Chronic Seizures. *Epilepsia* 40, 2, pp. 127–137. https://doi.org/10.1111/j.1528-1157.1999.tb02065.x(cit. on pp. 44, 148)

Bragin, A., I. Mody, C. L. Wilson, and J. Engel (Mar. 1, 2002). Local Generation of Fast Ripples in Epileptic Brain. *Journal of Neuroscience* 22, 5, pp. 2012–2021. https://doi.org/10.1523/JNEUROSCI.22-05-02012.2002(cit. on p. 44)

Brankack, J., M. Stewart, and S. E. Fox (July 2, 1993). Current Source Density Analysis of the Hippocampal Theta Rhythm: Associated Sustained Potentials and Candidate Synaptic Generators. *Brain Research* 615, 2, pp. 310–327. https://doi.org/10.1016/0006-8993(93)90043-m(cit. on p. 37)

Brazier, M. A. (Oct. 1968). Studies of the EEG Activity of Limbic Structures in Man. *Electroencephalography and Clinical Neurophysiology* 25, 4, pp. 309–318. https://doi.org/10.1016/0013-4694(68)90171-5(cit. on pp. 42, 163, 166)

Brazier, M. A. (Feb. 1970). Regional Activities within the Human Hippocampus and Hippocampal Gyrus. *Experimental Neurology* 26, 2, pp. 354–368. https://doi.org/10.1016/0014-4886(70)90132-9(cit. on pp. 42, 166)

Brewer, J. B., Z. Zhao, J. E. Desmond, G. H. Glover, and J. D. Gabrieli (Aug. 21, 1998). Making Memories: Brain Activity That Predicts How Well Visual Experience Will Be Remembered. *Science* 281, 5380, pp. 1185–1187. https://doi.org/10.1126/science.281.5380.1185(cit. on p. 110)

Brewer, W. F. and J. C. Treyens (1981). Role of Schemata in Memory for Places. *Cognitive Psychology* 13, 2, pp. 207–230. https://doi.org/10.1016/0010-0285(81)90008-6(cit. on p. 25)

Broday-Dvir, R., Y. Norman, M. Harel, A. D. Mehta, and R. Malach (June 2023). Perceptual Stability Reflected in Neuronal Pattern Similarities in Human Visual Cortex. *Cell Reports* 42, 6, p. 112614. https://doi.org/10.1016/j.celrep.2023.112614(cit. on p. 176)

Brooks, D. N. and A. D. Baddeley (1976). What Can Amnesic Patients Learn? *Neuropsychologia* 14, 1, pp. 111–122. https://doi.org/10.1016/0028-3932(76)90012-9(cit. on p. 30)

Brown, B. B. (Jan. 1, 1968). Frequency and Phase of Hippocampal Theta Activity in the Spontaneously Behaving Cat. *Electroencephalography and Clinical Neurophysiology* 24, 1, pp. 53–62. https://doi.org/10.1016/0013-4694(68)90066-7(cit. on pp. 36–38, 163)

Brown, S. and E. A. Sharpey-Schafer (Dec. 31, 1888). XI. An Investigation into the Functions of the Occipital and Temporal Lobes of the Monkey's Brain. *Philosophical Transactions of the Royal Society of London. (B.)*, 179, pp. 303–327. https://doi.org/10.1098/rstb.1888.0011(cit. on p. 30)

Buccino, A. P., C. L. Hurwitz, S. Garcia, J. Magland, J. H. Siegle, R. Hurwitz, and M. H. Hennig (Nov. 10, 2020). SpikeInterface, a Unified Framework for Spike Sorting. *eLife* 9, e61834. https://doi.org/10.7554/eLife.61834(cit. on p. 53)

Buckmaster, C. A., H. Eichenbaum, D. G. Amaral, W. A. Suzuki, and P. R. Rapp (Nov. 3, 2004). Entorhinal Cortex Lesions Disrupt the Relational Organization of Memory in Monkeys. *The Journal of Neuroscience: The Official Journal of the Society for Neuroscience* 24, 44, pp. 9811–9825. https://doi.org/10.1523/JNEUROSCI.1532-04.2004(cit. on p. 30)

Bunsey, M. and H. Eichenbaum (Jan. 1996). Conservation of Hippocampal Memory Function in Rats and Humans. *Nature* 379, 6562, pp. 255–257. https://doi.org/10.1038/379255a0(cit. on pp. 26, 31, 79)

Burke, J. F., K. A. Zaghloul, J. Jacobs, R. B. Williams, M. R. Sperling, A. D. Sharan, and M. J. Kahana (Jan. 2, 2013). Synchronous and Asynchronous Theta and Gamma Activity during Episodic Memory Formation. *Journal of Neuroscience* 33, 1, pp. 292–304. https://doi.org/10.1523/JNEUROSCI.2057-12.2013(cit. on pp. 42, 45)

Bush, D., J. A. Bisby, C. M. Bird, S. Gollwitzer, R. Rodionov, B. Diehl, A. W. McEvoy, M. C. Walker, and N. Burgess (Nov. 14, 2017). Human Hippocampal Theta Power Indicates Movement Onset and Distance Travelled. *Proceedings of the National Academy of Sciences of the United States of America* 114, 46, pp. 12297–12302. https://doi.org/10.1073/pnas.1708716114(cit. on p. 43)

Busigny, T., X. de Boissezon, M. Puel, J.-L. Nespoulous, and E. J. Barbeau (Apr. 2015). Proper Name Anomia with Preserved Lexical and Semantic Knowledge after Left Anterior Temporal Lesion: A Two-Way Convergence Defect. *Cortex; a Journal Devoted to the Study of the Nervous System and Behavior* 65, pp. 1–18. https://doi.org/10.1016/j.cortex.2014.12.008(cit. on p. 30)

Buzsaki, G., Z. Horvath, R. Urioste, J. Hetke, and K. Wise (May 15, 1992). High-Frequency Network Oscillation in the Hippocampus. *Science* 256, 5059, pp. 1025–1027. https://doi.org/10.1126/science.1589772(cit. on pp. 33, 37)

Buzsaki, G. (June 25, 2004). Neuronal Oscillations in Cortical Networks. *Science* 304, 5679, pp. 1926–1929. https://doi.org/10.1126/science.1099745(cit. on p. 39)

Buzsáki, G. (Nov. 29, 1986). Hippocampal Sharp Waves: Their Origin and Significance. *Brain Research* 398, 2, pp. 242–252. https://doi.org/10.1016/0006-8993(86)91483-6(cit. on pp. 38, 44, 45, 141, 147, 153)

Buzsáki, G. (1989). Two-Stage Model of Memory Trace Formation: A Role for "Noisy" Brain States. *Neuroscience* 31, 3, pp. 551–570. https://doi.org/10.1016/0306-4522(89)90423-5(cit. on pp. 40, 79, 141, 159, 169)

Buzsáki, G. (Jan. 31, 2002). Theta Oscillations in the Hippocampus. *Neuron* 33, 3, pp. 325–340. https://doi.org/10.1016/S0896-6273(02)00586-X(cit. on pp. 37, 38, 96)

Buzsáki, G. (May 2004). Large-Scale Recording of Neuronal Ensembles. *Nature Neuroscience* 7, 5, pp. 446–451. https://doi.org/10.1038/nn1233(cit. on p. 33)

Buzsáki, G. (Nov. 2010). Neural Syntax: Cell Assemblies, Synapsembles, and Readers. *Neuron* 68, 3, pp. 362–385. https://doi.org/10.1016/j.neuron.2010.09.023(cit. on pp. 33, 39, 96, 119, 154)

Buzsáki, G. (Oct. 2015). Hippocampal Sharp Wave-ripple: A Cognitive Biomarker for Episodic Memory and Planning. *Hippocampus* 25, 10, pp. 1073–1188. https://doi.org/10.1002/hipo.22488(cit. on pp. 37, 154)

Buzsáki, G., C. A. Anastassiou, and C. Koch (June 2012). The Origin of Extracellular Fields and Currents — EEG, ECoG, LFP and Spikes. *Nature Reviews Neuroscience* 13, 6, pp. 407–420. https://doi.org/10.1038/nrn3241(cit. on pp. 35, 103)

Buzsáki, G., L. Lai-Wo S., and C. H. Vanderwolf (Oct. 1, 1983). Cellular Bases of Hippocampal EEG in the Behaving Rat. *Brain Research Reviews* 6, 2, pp. 139–171. https://doi.org/10.1016/0165-0173(83)90037-1(cit. on pp. 36–38, 142, 144)

Buzsáki, G., N. Logothetis, and W. Singer (Oct. 30, 2013). Scaling Brain Size, Keeping Timing: Evolutionary Preservation of Brain Rhythms. *Neuron* 80, 3, pp. 751–764. https://doi.org/10.1016/j.neuron.2013.10.002(cit. on pp. 39, 44, 45, 163)

Cadilhac, J. (July 16, 1954). "Hippocampe et Épilepsie : à Propos d'une Série d'expériences Sur Le Cobaye et Le Chat et de l'exploration Électrique de La Corne d'Ammon Chez l'homme." (cit. on p. 28).

Calkins, M. W. (1896). *Association: An Essay Analytic and Experimental*. MacMillan. 68 pp. (cit. on p. 79).

Cameron, K. A., S. Yashar, C. L. Wilson, and I. Fried (Apr. 2001). Human Hippocampal Neurons Predict How Well Word Pairs Will Be Remembered. *Neuron* 30, 1, pp. 289–298. https://doi.org/10.1016/s0896-6273(01)00280-x(cit. on p. 34)

Cantero, J. L., M. Atienza, R. Stickgold, M. J. Kahana, J. R. Madsen, and B. Kocsis (Nov. 26, 2003). Sleep-Dependent Theta Oscillations in the Human Hippocampus and Neocortex. *The Journal of Neuroscience: The Official Journal of the Society for Neuroscience* 23, 34, pp. 10897–10903. https://doi.org/10.1523/JNEUROSCI.23-34-10897.2003(cit. on p. 43)

Cao, R., P. Brunner, P. N. Chakravarthula, K. L. Wahlstrom, C. Inman, E. H. Smith, X. Li, A. N. Mamelak, N. J. Brandmeir, U. Rutishauser, J. T. Willie, and S. Wang (Feb. 10, 2025). A Neuronal Code for Object Representation and Memory in the Human Amygdala and Hippocampus. *Nature Communications* 16, 1, p. 1510. https://doi.org/10.1038/s41467-025-56793-y(cit. on p. 34)

Caplan, J. B., J. R. Madsen, S. Raghavachari, and M. J. Kahana (July 2001). Distinct Patterns of Brain Oscillations Underlie Two Basic Parameters of Human Maze Learning. *Journal of Neurophysiology* 86, 1, pp. 368–380. https://doi.org/10.1152/jn.2001.86.1.368(cit. on p. 42)

Caplan, J. B., J. R. Madsen, A. Schulze-Bonhage, R. Aschenbrenner-Scheibe, E. L. Newman, and M. J. Kahana (June 1, 2003). Human Theta Oscillations Related to Sensorimotor Integration and Spatial Learning. *The Journal of Neuroscience: The Official Journal of the Society for Neuroscience* 23, 11, pp. 4726–4736. https://doi.org/10.1523/JNEUROSCI.23-11-04726.2003(cit. on p. 42)

Carrillo-Reid, L., W. Yang, Y. Bando, D. S. Peterka, and R. Yuste (Aug. 12, 2016). Imprinting and Recalling Cortical Ensembles. *Science* 353, 6300, pp. 691–694. https://doi.org/10.1126/science.aaf7560(cit. on p. 33)

Cash, S. S. and L. R. Hochberg (Apr. 8, 2015). The Emergence of Single Neurons in Clinical Neurology. *Neuron* 86, 1, pp. 79–91. https://doi.org/10.1016/j.neuron.2015.03.058(cit. on p. 34)

Castelli, M., V. Lopes-dos-Santos, G. P. Gava, R. Lambiotte, and D. Dupret (Oct. 2025). Hippocampal Ripple Diversity Organizes Neuronal Reactivation Dynamics in the Offline Brain. *Neuron*, S0896627325007007. https://doi.org/10.1016/j.neuron.2025.09.012(cit. on pp. 37, 41, 148, 154)

Causse, A. A., J. Curot, V. Lopes-dos-Santos, R. Nunes-da-Silva, H. C. Barron, V. Dornier, M. Denuelle, A. D. Barros, J.-C. Sol, J.-A. Lotterie, K. Lehongre, S. Fernandez-Vidal, V. Frazzini, V. Navarro, L. Valton, E. J. Barbeau, T. Denison, L. Reddy, and D. Dupret (June 1, 2026). A Learning-Evoked Slow-Oscillatory Architecture Paces Population Activity for Offline Reactivation across the Human Medial Temporal Lobe. *Neuron* 0, 0. https://doi.org/10.1016/j.neuron.2026.05.004(cit. on pp. 8, 9)

Chen, D., L. Kunz, W. Wang, H. Zhang, W.-X. Wang, A. Schulze-Bonhage, P. C. Reinacher, W. Zhou, S. Liang, N. Axmacher, and L. Wang (Oct. 22, 2018). Hexadirectional Modulation of Theta Power in Human Entorhinal Cortex during Spatial Navigation. *Current Biology* 28, 20, 3310–3315.e4. https://doi.org/10.1016/j.cub.2018.08.029(cit. on p. 43)

Chen, Y. Y., L. Aponik-Gremillion, E. Bartoli, D. Yoshor, S. A. Sheth, and B. L. Foster (June 29, 2021). Stability of Ripple Events during Task Engagement in Human Hippocampus. *Cell Reports* 35, 13, p. 109304. https://doi.org/10.1016/j.celrep.2021.109304(cit. on pp. 45, 144, 148)

Chomsky, N. (1959). Review of Verbal Behavior. *Language* 35, 1, pp. 26–58. https://doi.org/10.2307/411334(cit. on p. 24)

Cisek, P. (Oct. 2019). Resynthesizing Behavior through Phylogenetic Refinement. *Attention, Perception & Psychophysics* 81, 7, pp. 2265–2287. https://doi.org/10.3758/s13414-019-01760-1(cit. on pp. 24, 27, 28, 37)

Cisek, P. and A. M. Green (June 1, 2024). Toward a Neuroscience of Natural Behavior. *Current Opinion in Neurobiology* 86, p. 102859. https://doi.org/10.1016/j.conb.2024.102859(cit. on p. 28)

Clarke-Williams, C. (May 24, 2022). *tmEMD* (cit. on pp. 60, 98).

Clarke-Williams, C. J., V. Lopes-dos-Santos, L. Lefèvre, D. Brizee, A. A. Causse, R. Rothaermel, K. Hartwich, P. V. Perestenko, R. Toth, C. G. McNamara, A. Sharott, and D. Dupret (Jan. 18, 2024). Coordinating Brain-Distributed Network Activities in Memory Resistant to Extinction. *Cell* 187, 2, 409–427.e19. https://doi.org/10.1016/j.cell.2023.12.018(cit. on pp. 41, 60, 98)

Clemens, Z., B. Weiss, A. Szucs, L. Eross, G. Rásonyi, and P. Halász (Sept. 29, 2009). Phase Coupling between Rhythmic Slow Activity and Gamma Characterizes Mesiotemporal Rapid-Eye-Movement Sleep in Humans. *Neuroscience* 163, 1, pp. 388–396. https://doi.org/10.1016/j.neuroscience.2009.06.044(cit. on pp. 43, 144, 163)

Clemens, Z., C. Borbély, B. Weiss, L. Erőss, A. Szűcs, A. Kelemen, D. Fabó, G. Rásonyi, J. Janszky, and P. Halász (2013). Increased Mesiotemporal Delta Activity Characterizes Virtual Navigation in Humans. *Neuroscience Research* 76, 1–2, pp. 67–75. https://doi.org/10.1016/j.neures.2013.03.004(cit. on pp. 42, 168)

Clemens, Z., M. Mölle, L. Eross, P. Barsi, P. Halász, and J. Born (Nov. 2007). Temporal Coupling of Parahippocampal Ripples, Sleep Spindles and Slow Oscillations in Humans. *Brain: A Journal of Neurology* 130, pp. 2868–2878. https://doi.org/10.1093/brain/awm146(cit. on p. 144)

Cohen, N. J. and L. R. Squire (Oct. 10, 1980). Preserved Learning and Retention of Pattern-Analyzing Skill in Amnesia: Dissociation of Knowing How and Knowing That. *Science* 210, 4466, pp. 207–210. https://doi.org/10.1126/science.7414331(cit. on p. 30)

Colgin, L. L. (Apr. 1, 2015). Theta–Gamma Coupling in the Entorhinal–Hippocampal System. *Current Opinion in Neurobiology* 31, pp. 45–50. https://doi.org/10.1016/j.conb.2014.08.001(cit. on p. 45)

Colgin, L. L. (Apr. 2016). Rhythms of the Hippocampal Network. *Nature Reviews. Neuroscience* 17, 4, pp. 239–249. https://doi.org/10.1038/nrn.2016.21(cit. on pp. 40, 96, 122)

Colgin, L. L., T. Denninger, M. Fyhn, T. Hafting, T. Bonnevie, O. Jensen, M.-B. Moser, and E. I. Moser (Nov. 2009). Frequency of Gamma Oscillations Routes Flow of Information in the Hippocampus. *Nature* 462, 7271, pp. 353–357. https://doi.org/10.1038/nature08573(cit. on p. 35)

Corkin, S., D. G. Amaral, R. G. González, K. A. Johnson, and B. T. Hyman (May 15, 1997). H. M.'s Medial Temporal Lobe Lesion: Findings from Magnetic Resonance Imaging. *The Journal of Neuroscience: The Official Journal of the Society for Neuroscience* 17, 10, pp. 3964–3979. https://doi.org/10.1523/JNEUROSCI.17-10-03964.1997(cit. on p. 31)

Corkin, S. (June 1984). Lasting Consequences of Bilateral Medial Temporal Lobectomy: Clinical Course and Experimental Findings in H.M. *Seminars in Neurology* 4, 2, pp. 249–259. https://doi.org/10.1055/s-2008-1041556(cit. on p. 29)

Corkin, S. (Feb. 2002). What's New with the Amnesic Patient H.M.? *Nature Reviews Neuroscience* 3, 2, pp. 153–160. https://doi.org/10.1038/nrn726(cit. on p. 29)

Costa, M., D. Lozano-Soldevilla, A. Gil-Nagel, R. Toledano, C. R. Oehrn, L. Kunz, M. Yebra, C. Mendez-Bertolo, L. Stieglitz, J. Sarnthein, N. Axmacher, S. Moratti, and B. A. Strange (Oct. 27, 2022). Aversive Memory Formation in Humans Involves an Amygdala-Hippocampus Phase Code. *Nature Communications* 13, 1, p. 6403. https://doi.org/10.1038/s41467-022-33828-2(cit. on pp. 43, 44)

Courellis, H. S., J. Minxha, A. R. Cardenas, D. L. Kimmel, C. M. Reed, T. A. Valiante, C. D. Salzman, A. N. Mamelak, S. Fusi, and U. Rutishauser (Aug. 14, 2024). Abstract Representations Emerge in Human Hippocampal Neurons during Inference. *Nature*, pp. 1–9. https://doi.org/10.1038/s41586-024-07799-x(cit. on p. 34)

Courellis, H. S., S. U. Nummela, M. Metke, G. W. Diehl, R. Bussell, G. Cauwenberghs, and C. T. Miller (Dec. 9, 2019). Spatial Encoding in Primate Hippocampus during Free

Navigation. *PLOS Biology* 17, 12, e3000546. https://doi.org/10.1371/journal.pbio.3000546(cit. on p. 36)
Craik, F. I. M. and E. Tulving (1975). Depth of Processing and the Retention of Words in Episodic Memory. *Journal of Experimental Psychology: General* 104, 3, pp. 268–294. https://doi.org/10.1037/0096-3445.104.3.268(cit. on pp. 25, 30)
Craik, K. J. W. (Oct. 1967). *The Nature of Explanation*. CUP Archive. 140 pp. (cit. on p. 26).
Crespo-García, M., M. Zeiller, C. Leupold, G. Kreiselmeyer, S. Rampp, H. M. Hamer, and S. S. Dalal (Nov. 15, 2016). Slow-Theta Power Decreases during Item-Place Encoding Predict Spatial Accuracy of Subsequent Context Recall. *NeuroImage* 142, pp. 533–543. https://doi.org/10.1016/j.neuroimage.2016.08.021(cit. on p. 43)
Csicsvari, J., H. Hirase, A. Czurko, and G. Buzsáki (July 1998). Reliability and State Dependence of Pyramidal Cell-Interneuron Synapses in the Hippocampus: An Ensemble Approach in the Behaving Rat. *Neuron* 21, 1, pp. 179–189. https://doi.org/10.1016/s0896-6273(00)80525-5(cit. on p. 120)
Csicsvari, J., H. Hirase, A. Czurkó, A. Mamiya, and G. Buzsáki (Jan. 1, 1999). Oscillatory Coupling of Hippocampal Pyramidal Cells and Interneurons in the Behaving Rat. *Journal of Neuroscience* 19, 1, pp. 274–287. https://doi.org/10.1523/JNEUROSCI.19-01-00274.1999(cit. on pp. 116, 119, 120)
Csicsvari, J., B. Jamieson, K. D. Wise, and G. Buzsáki (Jan. 2003). Mechanisms of Gamma Oscillations in the Hippocampus of the Behaving Rat. *Neuron* 37, 2, pp. 311–322. https://doi.org/10.1016/S0896-6273(02)01169-8(cit. on p. 35)
D. Marr (July 1971). Simple Memory: A Theory for Archicortex. *Philosophical Transactions of the Royal Society of London. B, Biological Sciences* 262, 841, pp. 23–81. https://doi.org/10.1098/rstb.1971.0078(cit. on pp. 26, 40)
Darwin, C. (1872). *The Expression of the Emotions in Man and Animals*. New York : D. Appleton. 414 pp. (cit. on p. 27).
Daume, J., J. Kamiński, Y. Salimpour, A. G. P. Schjetnan, W. S. Anderson, T. A. Valiante, A. N. Mamelak, and U. Rutishauser (Dec. 4, 2024). Persistent Activity during Working Memory Maintenance Predicts Long-Term Memory Formation in the Human Hippocampus. *Neuron* 112, 23, 3957–3968.e3. https://doi.org/10.1016/j.neuron.2024.09.013(cit. on p. 34)
Daume, J., J. Kamiński, A. G. P. Schjetnan, Y. Salimpour, U. Khan, M. Kyzar, C. M. Reed, W. S. Anderson, T. A. Valiante, A. N. Mamelak, and U. Rutishauser (Apr. 17, 2024). Control of Working Memory by Phase–Amplitude Coupling of Human Hippocampal Neurons. *Nature*, pp. 1–9. https://doi.org/10.1038/s41586-024-07309-z(cit. on pp. 34, 44, 45)
Dayan, P., G. E. Hinton, R. M. Neal, and R. S. Zemel (Sept. 1, 1995). The Helmholtz Machine. *Neural Computation* 7, 5, pp. 889–904. https://doi.org/10.1162/neco.1995.7.5.889(cit. on p. 26)
De Sousa, A. F., A. Chowdhury, and A. J. Silva (Sept. 1, 2021). Dimensions and Mechanisms of Memory Organization. *Neuron* 109, 17, pp. 2649–2662. https://doi.org/10.1016/j.neuron.2021.06.014(cit. on p. 26)
Deitch, D., A. Rubin, and Y. Ziv (Oct. 11, 2021). Representational Drift in the Mouse Visual Cortex. *Current Biology* 31, 19, 4327–4339.e6. https://doi.org/10.1016/j.cub.2021.07.062(cit. on p. 33)

Derdikman, D. and J. J. Knierim, eds. (2014). *Space, Time and Memory in the Hippocampal Formation*. Vienna: Springer Vienna. https://doi.org/10.1007/978-3-7091-1292-2 (cit. on pp. 36, 96).

Desikan, R. S., F. Ségonne, B. Fischl, B. T. Quinn, B. C. Dickerson, D. Blacker, R. L. Buckner, A. M. Dale, R. P. Maguire, B. T. Hyman, M. S. Albert, and R. J. Killiany (July 1, 2006). An Automated Labeling System for Subdividing the Human Cerebral Cortex on MRI Scans into Gyral Based Regions of Interest. *NeuroImage* 31, 3, pp. 968–980. https://doi.org/10.1016/j.neuroimage.2006.01.021(cit. on p. 52)

Despouy, E., J. Curot, L. Reddy, L. G. Nowak, M. Deudon, J.-C. Sol, J.-A. Lotterie, M. Denuelle, A. Maziz, C. Bergaud, S. J. Thorpe, L. Valton, and E. J. Barbeau (July 15, 2020). Recording Local Field Potential and Neuronal Activity with Tetrodes in Epileptic Patients. *Journal of Neuroscience Methods* 341, p. 108759. https://doi.org/10.1016/j.jneumeth.2020.108759(cit. on p. 52)

Dickey, C. W., I. A. Verzhbinsky, X. Jiang, B. Q. Rosen, S. Kajfez, E. N. Eskandar, J. Gonzalez-Martinez, S. S. Cash, and E. Halgren (Aug. 30, 2022). Cortical Ripples during NREM Sleep and Waking in Humans. *Journal of Neuroscience*. https://doi.org/10.1523/JNEUROSCI.0742-22.2022(cit. on pp. 45, 148)

Dickey, C. W., I. A. Verzhbinsky, X. Jiang, B. Q. Rosen, S. Kajfez, B. Stedelin, J. J. Shih, S. Ben-Haim, A. M. Raslan, E. N. Eskandar, J. Gonzalez-Martinez, S. S. Cash, and E. Halgren (July 12, 2022). Widespread Ripples Synchronize Human Cortical Activity during Sleep, Waking, and Memory Recall. *Proceedings of the National Academy of Sciences of the United States of America* 119, 28, e2107797119. https://doi.org/10.1073/pnas.2107797119(cit. on pp. 45, 148)

Dinkelacker, V., X. Xin, M. Baulac, S. Samson, and S. Dupont (Sept. 2016). Interictal Epileptic Discharge Correlates with Global and Frontal Cognitive Dysfunction in Temporal Lobe Epilepsy. *Epilepsy & Behavior: E&B* 62, pp. 197–203. https://doi.org/10.1016/j.yebeh.2016.07.009(cit. on pp. 81, 84, 93, 94, 104, 166)

Donoghue, T., M. Haller, E. J. Peterson, P. Varma, P. Sebastian, R. Gao, T. Noto, A. H. Lara, J. D. Wallis, R. T. Knight, A. Shestyuk, and B. Voytek (Dec. 2020). Parameterizing Neural Power Spectra into Periodic and Aperiodic Components. *Nature Neuroscience* 23, 12, pp. 1655–1665. https://doi.org/10.1038/s41593-020-00744-x(cit. on pp. 63, 100)

Doya, K. (2007). *Bayesian Brain: Probabilistic Approaches to Neural Coding*. MIT Press. 341 pp. (cit. on p. 26).

Dragoi, G. and S. Tonegawa (Jan. 20, 2011). Preplay of Future Place Cell Sequences by Hippocampal Cellular Assemblies. *Nature* 469, 7330, pp. 397–401. https://doi.org/10.1038/nature09633(cit. on p. 41)

Duan, W., Z. Xu, D. Chen, J. Wang, J. Liu, Z. Tan, X. Xiao, P. Lv, M. Wang, K. A. Paller, N. Axmacher, and L. Wang (Mar. 12, 2025). Electrophysiological Signatures Underlying Variability in Human Memory Consolidation. *Nature Communications* 16, 1, p. 2472. https://doi.org/10.1038/s41467-025-57766-x(cit. on p. 46)

Dudai, Y. (2004). The Neurobiology of Consolidations, or, How Stable Is the Engram? *Annual Review of Psychology* 55, pp. 51–86. https://doi.org/10.1146/annurev.psych.55.090902.142050(cit. on p. 40)

Dudai, Y., A. Karni, and J. Born (Oct. 2015). The Consolidation and Transformation of Memory. *Neuron* 88, 1, pp. 20–32. https://doi.org/10.1016/j.neuron.2015.09.004(cit. on p. 40)

Dupret, D., J. O'Neill, and J. Csicsvari (Oct. 4, 2013). Dynamic Reconfiguration of Hippocampal Interneuron Circuits during Spatial Learning. *Neuron* 78, 1. https://doi.org/10.1016/j.neuron.2013.01.033(cit. on p. 33)

Dupret, D., S. Fusi, and S. Panzeri (Feb. 4, 2026). Neural Population Activity for Memory: Properties, Computations, and Codes. *Neuron* 114, 3, pp. 390–407. https://doi.org/10.1016/j.neuron.2025.11.007(cit. on p. 33)

Dupret, D., J. O'Neill, B. Pleydell-Bouverie, and J. Csicsvari (Aug. 2010). The Reorganization and Reactivation of Hippocampal Maps Predict Spatial Memory Performance. *Nature Neuroscience* 13, 8, pp. 995–1002. https://doi.org/10.1038/nn.2599(cit. on pp. 40, 154)

Dusek, J. A. and H. Eichenbaum (June 24, 1997). The Hippocampus and Memory for Orderly Stimulus Relations. *Proceedings of the National Academy of Sciences of the United States of America* 94, 13, pp. 7109–7114. (Cit. on pp. 31, 79)

Ebbinghaus, H. (1885). *Über das Gedächtnis Untersuchungen zur experimentellen Psychologie*. Duncker & Humblot. 187 pp. (cit. on p. 40).

— (1913). *Memory; a Contribution to Experimental Psychology*. New York city, Teachers college, Columbia university. 146 pp. (cit. on p. 23).

Ego-Stengel, V. and M. A. Wilson (2009). Disruption of Ripple-Associated Hippocampal Activity during Rest Impairs Spatial Learning in the Rat. *Hippocampus*, NA–NA. https://doi.org/10.1002/hipo.20707(cit. on pp. 40, 141)

Eichenbaum, H. and N. J. Cohen (June 1988). Representation in the Hippocampus: What Do Hippocampal Neurons Code? *Trends in Neurosciences* 11, 6, pp. 244–248. https://doi.org/10.1016/0166-2236(88)90100-2(cit. on p. 32)

Eichenbaum, H., A. Fagan, P. Mathews, and N. J. Cohen (June 1988). Hippocampal System Dysfunction and Odor Discrimination Learning in Rats: Impairment or Facilitation Depending on Representational Demands. *Behavioral Neuroscience* 102, 3, pp. 331–339. https://doi.org/10.1037//0735-7044.102.3.331(cit. on p. 26)

Eichenbaum, H., P. Mathews, and N. J. Cohen (Dec. 1989). Further Studies of Hippocampal Representation during Odor Discrimination Learning. *Behavioral Neuroscience* 103, 6, pp. 1207–1216. https://doi.org/10.1037//0735-7044.103.6.1207(cit. on p. 26)

Eichenbaum, H. and N. J. Cohen (Oct. 4, 1993). *Memory, Amnesia, and the Hippocampal System*. Cambridge, MA, USA: MIT Press. 326 pp. (cit. on pp. 26, 78).

— (2001). *From Conditioning to Conscious Recollection: Memory Systems of the Brain*. Oxford Psychology Series. Oxford University Press. https://doi.org/10.1093/acprof:oso/9780195178043.001.0001 (cit. on p. 26).

Einevoll, G. T., C. Kayser, N. K. Logothetis, and S. Panzeri (Nov. 2013). Modelling and Analysis of Local Field Potentials for Studying the Function of Cortical Circuits. *Nature Reviews Neuroscience* 14, 11, pp. 770–785. https://doi.org/10.1038/nrn3599(cit. on p. 35)

Ekstrom, A. D., J. B. Caplan, E. Ho, K. Shattuck, I. Fried, and M. J. Kahana (2005). Human Hippocampal Theta Activity during Virtual Navigation. *Hippocampus* 15, 7, pp. 881–889. (Cit. on pp. 42, 168)

Fanselow, M. S. and H.-W. Dong (Jan. 14, 2010). Are the Dorsal and Ventral Hippocampus Functionally Distinct Structures? *Neuron* 65, 1, pp. 7–19. https://doi.org/10.1016/j.neuron.2009.11.031(cit. on p. 123)

Farrell, J. S., E. Hwaun, B. Dudok, and I. Soltesz (Apr. 2024). Neural and Behavioural State Switching during Hippocampal Dentate Spikes. *Nature* 628, 8008, pp. 590–595. https://doi.org/10.1038/s41586-024-07192-8(cit. on p. 41)

Feingold, J., D. J. Gibson, B. DePasquale, and A. M. Graybiel (Nov. 3, 2015). Bursts of Beta Oscillation Differentiate Postperformance Activity in the Striatum and Motor Cortex of Monkeys Performing Movement Tasks. *Proceedings of the National Academy of Sciences* 112, 44, pp. 13687–13692. https://doi.org/10.1073/pnas.1517629112(cit. on p. 162)

Fell, J. and N. Axmacher (Feb. 2011). The Role of Phase Synchronization in Memory Processes. *Nature Reviews. Neuroscience* 12, 2, pp. 105–118. https://doi.org/10.1038/nrn2979(cit. on p. 39)

Fell, J., P. Klaver, H. Elfadil, C. Schaller, C. E. Elger, and G. Fernández (2003). Rhinal–Hippocampal Theta Coherence during Declarative Memory Formation: Interaction with Gamma Synchronization? *European Journal of Neuroscience* 17, 5, pp. 1082–1088. https://doi.org/10.1046/j.1460-9568.2003.02522.x(cit. on pp. 42, 43)

Fell, J., P. Klaver, K. Lehnertz, T. Grunwald, C. Schaller, C. E. Elger, and G. Fernández (Dec. 2001). Human Memory Formation Is Accompanied by Rhinal–Hippocampal Coupling and Decoupling. *Nature Neuroscience* 4, 12, pp. 1259–1264. https://doi.org/10.1038/nn759(cit. on pp. 43, 45, 79)

Fernández, G., A. Effern, T. Grunwald, N. Pezer, K. Lehnertz, M. Dümpelmann, D. Van Roost, and C. E. Elger (Sept. 3, 1999). Real-Time Tracking of Memory Formation in the Human Rhinal Cortex and Hippocampus. *Science* 285, 5433, pp. 1582–1585. https://doi.org/10.1126/science.285.5433.1582(cit. on pp. 108, 116)

Fernández-Ruiz, A., A. Oliva, M. Soula, F. Rocha-Almeida, G. A. Nagy, G. Martin-Vazquez, and G. Buzsáki (Apr. 2, 2021). Gamma Rhythm Communication between Entorhinal Cortex and Dentate Gyrus Neuronal Assemblies. *Science* 372, 6537, eabf3119. https://doi.org/10.1126/science.abf3119(cit. on pp. 36, 127)

Fernandez-Ruiz, A., A. Sirota, V. Lopes-dos-Santos, and D. Dupret (Apr. 2023). Over and above Frequency: Gamma Oscillations as Units of Neural Circuit Operations. *Neuron* 111, 7, pp. 936–953. https://doi.org/10.1016/j.neuron.2023.02.026(cit. on pp. 36, 38, 41, 56, 122, 164, 176)

Foffani, G., Y. G. Uzcategui, B. Gal, and L. Menendez De La Prida (Sept. 2007). Reduced Spike-Timing Reliability Correlates with the Emergence of Fast Ripples in the Rat Epileptic Hippocampus. *Neuron* 55, 6, pp. 930–941. https://doi.org/10.1016/j.neuron.2007.07.040(cit. on pp. 44, 148)

Foster, B. L., A. Kaveh, M. Dastjerdi, K. J. Miller, and J. Parvizi (June 19, 2013). Human Retrosplenial Cortex Displays Transient Theta Phase Locking with Medial Temporal Cortex Prior to Activation during Autobiographical Memory Retrieval. *Journal of Neuroscience* 33, 25, pp. 10439–10446. https://doi.org/10.1523/JNEUROSCI.0513-13.2013(cit. on p. 44)

Foster, D. and M. Wilson (Apr. 1, 2006). Reverse Replay of Behavioural Sequences in Hippocampal Place Cells during the Awake State. *Nature* 440, pp. 680–3. https://doi.org/10.1038/nature04587(cit. on p. 45)

Frank, L. M., E. N. Brown, and M. Wilson (July 2000). Trajectory Encoding in the Hippocampus and Entorhinal Cortex. *Neuron* 27, 1, pp. 169–178. https://doi.org/10.1016/s0896-6273(00)00018-0(cit. on p. 33)

Frauscher, B., N. von Ellenrieder, I. Dolezalova, S. Bouhadoun, J. Gotman, and L. Peter-Derex (Nov. 11, 2020). Rapid Eye Movement Sleep Sawtooth Waves Are Associated with Widespread Cortical Activations. *The Journal of Neuroscience: The Official Journal of the Society for Neuroscience* 40, 46, pp. 8900–8912. https://doi.org/10.1523/JNEUROSCI.1586-20.2020(cit. on p. 169)

Frauscher, B., N. von Ellenrieder, R. Zelmann, I. Doležalová, L. Minotti, A. Olivier, J. Hall, D. Hoffmann, D. K. Nguyen, P. Kahane, F. Dubeau, and J. Gotman (Apr. 1, 2018). Atlas of the Normal Intracranial Electroencephalogram: Neurophysiological Awake Activity in Different Cortical Areas. *Brain* 141, 4, pp. 1130–1144. https://doi.org/10.1093/brain/awy035(cit. on p. 165)

Freemon, F. R. and R. D. Walter (Nov. 1970). Electrical Activity of Human Limbic System during Sleep. *Comprehensive Psychiatry* 11, 6, pp. 544–551. https://doi.org/10.1016/0010-440x(70)90017-9(cit. on pp. 43, 144, 163, 166)

Freund, T. F. and M. Antal (Nov. 1988). GABA-containing Neurons in the Septum Control Inhibitory Interneurons in the Hippocampus. *Nature* 336, 6195, pp. 170–173. https://doi.org/10.1038/336170a0(cit. on pp. 37, 38)

Fried, I., K. A. MacDonald, and C. L. Wilson (May 1997). Single Neuron Activity in Human Hippocampus and Amygdala during Recognition of Faces and Objects. *Neuron* 18, 5, pp. 753–765. https://doi.org/10.1016/s0896-6273(00)80315-3(cit. on p. 34)

Fries, P., P. R. Roelfsema, A. K. Engel, P. Konig, and W. Singer (Nov. 11, 1997). Synchronization of Oscillatory Responses in Visual Cortex Correlates with Perception in Interocular Rivalry. *Proceedings of the National Academy of Sciences* 94, 23, pp. 12699–12704. https://doi.org/10.1073/pnas.94.23.12699(cit. on p. 35)

Fries, P. (Oct. 2005). A Mechanism for Cognitive Dynamics: Neuronal Communication through Neuronal Coherence. *Trends in Cognitive Sciences* 9, 10, pp. 474–480. https://doi.org/10.1016/j.tics.2005.08.011(cit. on pp. 39, 119, 164)

Fries, P. (2009). Neuronal Gamma-Band Synchronization as a Fundamental Process in Cortical Computation. *Annual Review of Neuroscience* 32, pp. 209–224. https://doi.org/10.1146/annurev.neuro.051508.135603(cit. on p. 39)

Friston, K. (Apr. 29, 2005). A Theory of Cortical Responses. *Philosophical Transactions of the Royal Society of London. Series B, Biological Sciences* 360, 1456, pp. 815–836. https://doi.org/10.1098/rstb.2005.1622(cit. on p. 26)

Friston, K. (Feb. 2010). The Free-Energy Principle: A Unified Brain Theory? *Nature Reviews Neuroscience* 11, 2, pp. 127–138. https://doi.org/10.1038/nrn2787(cit. on p. 26)

Friston, K. and S. Kiebel (May 12, 2009). Predictive Coding under the Free-Energy Principle. *Philosophical Transactions of the Royal Society B: Biological Sciences* 364, 1521, pp. 1211–1221. https://doi.org/10.1098/rstb.2008.0300(cit. on p. 26)

Fuhrmann, F., D. Justus, L. Sosulina, H. Kaneko, T. Beutel, D. Friedrichs, S. Schoch, M. K. Schwarz, M. Fuhrmann, and S. Remy (June 3, 2015). Locomotion, Theta Oscillations, and the Speed-Correlated Firing of Hippocampal Neurons Are Controlled by a Medial Septal Glutamatergic Circuit. *Neuron* 86, 5, pp. 1253–1264. https://doi.org/10.1016/j.neuron.2015.05.001(cit. on pp. 38, 127)

Fyhn, M., S. Molden, M. P. Witter, E. I. Moser, and M.-B. Moser (Aug. 27, 2004). Spatial Representation in the Entorhinal Cortex. *Science* 305, 5688, pp. 1258–1264. https://doi.org/10.1126/science.1099901(cit. on p. 33)

El-Gaby, M., A. L. Harris, J. C. R. Whittington, W. Dorrell, A. Bhomick, M. E. Walton, T. Akam, and T. E. J. Behrens (Dec. 2024). A Cellular Basis for Mapping Behavioural Structure. *Nature* 636, 8043, pp. 671–680. https://doi.org/10.1038/s41586-024-08145-x(cit. on p. 25)

El-Gaby, M., H. M. Reeve, V. Lopes-dos-Santos, N. Campo-Urriza, P. V. Perestenko, A. Morley, L. A. M. Strickland, I. P. Lukács, O. Paulsen, and D. Dupret (May 2021).

An Emergent Neural Coactivity Code for Dynamic Memory. *Nature Neuroscience* 24, 5, pp. 694–704. https://doi.org/10.1038/s41593-021-00820-w(cit. on p. 33)
Gaffan, D. (1994). Scene-Specific Memory for Objects: A Model of Episodic Memory Impairment in Monkeys with Fornix Transection. *Journal of Cognitive Neuroscience* 6, 4, pp. 305–320. https://doi.org/10.1162/jocn.1994.6.4.305(cit. on p. 32)
Gaffan, D. (Dec. 14, 2001). What Is a Memory System? Horel's Critique Revisited. *Behavioural Brain Research* 127, 1–2, pp. 5–11. https://doi.org/10.1016/s0166-4328(01)00360-6(cit. on p. 31)
Gaffan, D. and E. A. Gaffan (Dec. 1991). Amnesia in Man Following Transection of the Fornix. A Review. *Brain: A Journal of Neurology* 114 (Pt 6), pp. 2611–2618. https://doi.org/10.1093/brain/114.6.2611(cit. on p. 32)
Gaffan, D. (Aug. 29, 2002). Against Memory Systems. *Philosophical Transactions of the Royal Society of London. Series B: Biological Sciences* 357, 1424, pp. 1111–1121. https://doi.org/10.1098/rstb.2002.1110(cit. on p. 31)
Gattas, S., M. S. Larson, L. Mnatsakanyan, I. Sen-Gupta, S. Vadera, A. L. Swindlehurst, P. E. Rapp, J. J. Lin, and M. A. Yassa (Dec. 21, 2023). Theta Mediated Dynamics of Human Hippocampal-Neocortical Learning Systems in Memory Formation and Retrieval. *Nature Communications* 14, 1, p. 8505. https://doi.org/10.1038/s41467-023-44011-6(cit. on pp. 43, 44)
Gava, G. P., L. Lefèvre, T. Broadbelt, S. B. McHugh, V. Lopes-dos-Santos, D. Brizee, K. Hartwich, H. Sjoberg, P. V. Perestenko, R. Toth, A. Sharott, and D. Dupret (Sept. 6, 2024). Organizing the Coactivity Structure of the Hippocampus from Robust to Flexible Memory. *Science* 385, 6713, pp. 1120–1127. https://doi.org/10.1126/science.adk9611(cit. on pp. 33, 53)
Gava, G. P., S. B. McHugh, L. Lefèvre, V. Lopes-dos-Santos, S. Trouche, M. El-Gaby, S. R. Schultz, and D. Dupret (Mar. 1, 2021). Integrating New Memories into the Hippocampal Network Activity Space. *Nature neuroscience* 24, 3, pp. 326–330. https://doi.org/10.1038/s41593-021-00804-w(cit. on p. 33)
Gedankien, T., J. Kriegel, E. Zabeh, D. McDonagh, B. Lega, and J. Jacobs (Feb. 26, 2026). Cholinergic Blockade Reveals a Role for Human Hippocampal Theta in Memory Encoding but Not Retrieval. *eLife* 14. https://doi.org/10.7554/eLife.108972.2(cit. on pp. 162, 163, 167)
Gedankien, T., R. J. Tan, S. E. Qasim, H. Moore, D. McDonagh, J. Jacobs, and B. Lega (Aug. 30, 2023). Acetylcholine Modulates the Temporal Dynamics of Human Theta Oscillations during Memory. *Nature Communications* 14, 1, p. 5283. https://doi.org/10.1038/s41467-023-41025-y(cit. on pp. 111, 162, 163, 167)
Gelbard-Sagiv, H., R. Mukamel, M. Harel, R. Malach, and I. Fried (Oct. 3, 2008). Internally Generated Reactivation of Single Neurons in Human Hippocampus During Free Recall. *Science* 322, 5898, pp. 96–101. https://doi.org/10.1126/science.1164685(cit. on p. 45)
Genzel, L., G. Dragoi, L. Frank, K. Ganguly, L. de la Prida, B. Pfeiffer, and E. Robertson (Apr. 6, 2020). A Consensus Statement: Defining Terms for Reactivation Analysis. *Philosophical Transactions of the Royal Society B: Biological Sciences* 375, 1799, p. 20200001. https://doi.org/10.1098/rstb.2020.0001(cit. on p. 46)
George John Romanes (1882). *Animal Intelligence*. London : K. Paul, Trench. 582 pp. (cit. on p. 27).

Gerstein, G. L. and A. M. Aertsen (Dec. 1, 1985). Representation of Cooperative Firing Activity among Simultaneously Recorded Neurons. *Journal of Neurophysiology* 54, 6, pp. 1513–1528. https://doi.org/10.1152/jn.1985.54.6.1513(cit. on p. 33)

Geschwind, N. (June 1965). Disconnexion Syndromes in Animals and Man. I. *Brain: A Journal of Neurology* 88, 2, pp. 237–294. https://doi.org/10.1093/brain/88.2.237(cit. on p. 31)

Geva-Sagiv, M., E. A. Mankin, D. Eliashiv, S. Epstein, N. Cherry, G. Kalender, N. Tchemodanov, Y. Nir, and I. Fried (June 2023). Augmenting Hippocampal–Prefrontal Neuronal Synchrony during Sleep Enhances Memory Consolidation in Humans. *Nature Neuroscience* 26, 6, pp. 1100–1110. https://doi.org/10.1038/s41593-023-01324-5(cit. on p. 46)

Ghosh, V. E. and A. Gilboa (Jan. 2014). What Is a Memory Schema? A Historical Perspective on Current Neuroscience Literature. *Neuropsychologia* 53, pp. 104–114. https://doi.org/10.1016/j.neuropsychologia.2013.11.010(cit. on pp. 25, 26)

Ghuman, A. S., N. M. Brunet, Y. Li, R. O. Konecky, J. A. Pyles, S. A. Walls, V. Destefino, W. Wang, and R. M. Richardson (Dec. 8, 2014). Dynamic Encoding of Face Information in the Human Fusiform Gyrus. *Nature Communications* 5, 1, p. 5672. https://doi.org/10.1038/ncomms6672(cit. on p. 176)

Giaquinto, S. (1973). Sleep Recordings from Limbic Structures in Man. *Confinia Neurologica* 35, 5, pp. 285–303. https://doi.org/10.1159/000102849(cit. on pp. 43, 144, 163)

Gilboa, A. and H. Marlatte (2017). Neurobiology of Schemas and Schema-Mediated Memory. *Trends in Cognitive Sciences* 21, 8, pp. 618–631. https://doi.org/10.1016/j.tics.2017.04.013(cit. on pp. 25, 26)

Girardeau, G., K. Benchenane, S. I. Wiener, G. Buzsáki, and M. B. Zugaro (Oct. 2009). Selective Suppression of Hippocampal Ripples Impairs Spatial Memory. *Nature Neuroscience* 12, 10, pp. 1222–1223. https://doi.org/10.1038/nn.2384(cit. on pp. 40, 141)

Girardeau, G. and V. Lopes-dos-Santos (Oct. 29, 2021). Brain Neural Patterns and the Memory Function of Sleep. *Science*. https://doi.org/10.1126/science.abi8370(cit. on pp. 40, 79, 159)

Giri, B., N. Kinsky, U. Kaya, K. Maboudi, T. Abel, and K. Diba (June 2024). Sleep Loss Diminishes Hippocampal Reactivation and Replay. *Nature* 630, 8018, pp. 935–942. https://doi.org/10.1038/s41586-024-07538-2(cit. on p. 154)

Givens, B. S. and D. S. Olton (Dec. 1990). Cholinergic and GABAergic Modulation of Medial Septal Area: Effect on Working Memory. *Behavioral Neuroscience* 104, 6, pp. 849–855. https://doi.org/10.1037//0735-7044.104.6.849(cit. on pp. 36, 37)

Glees, P. and H. B. Griffith (1952). Bilateral Destruction of the Hippocampus (Cornu Ammonis) in a Case of Dementia. *Monatsschrift Fur Psychiatrie Und Neurologie* 123, 4–5, pp. 193–204. https://doi.org/10.1159/000140010(cit. on p. 29)

Gonzalez, K. C., S. Terada, A. Noguchi, G. N. Zakka, C. O'Toole, G. Bilbao, L. Reynolds, A. Jász, B. Kertész, Z. Szadai, A. Shen, F. St-Pierre, F. Polleux, A. Losonczy, and B. Rózsa (May 20, 2026). Movement-Stabilized Three-Dimensional Optical Recordings of Membrane Potential Changes and Calcium Dynamics in Hippocampal CA1 Dendrites. *Neuron* 114, 10, 1818–1832.e9. https://doi.org/10.1016/j.neuron.2026.01.004(cit. on p. 35)

González-Arnay, E., I. Pérez-Santos, L. Jiménez-Sánchez, E. Cid, B. Gal, L. M. De La Prida, and C. Cavada (Jan. 5, 2024). Immunohistochemical Field Parcellation of the

Human Hippocampus along Its Antero-Posterior Axis. *Brain Structure and Function* 229, 2, pp. 359–385. https://doi.org/10.1007/s00429-023-02725-9(cit. on p. 123)
Gotman, J. and P. Gloor (Nov. 1976). Automatic Recognition and Quantification of Interictal Epileptic Activity in the Human Scalp EEG. *Electroencephalography and Clinical Neurophysiology* 41, 5, pp. 513–529. https://doi.org/10.1016/0013-4694(76)90063-8(cit. on p. 44)
Goyal, A., J. Miller, S. E. Qasim, A. J. Watrous, H. Zhang, J. M. Stein, C. S. Inman, R. E. Gross, J. T. Willie, B. Lega, J.-J. Lin, A. Sharan, C. Wu, M. R. Sperling, S. A. Sheth, G. M. McKhann, E. H. Smith, C. Schevon, and J. Jacobs (May 18, 2020). Functionally Distinct High and Low Theta Oscillations in the Human Hippocampus. *Nature Communications* 11, p. 2469. https://doi.org/10.1038/s41467-020-15670-6(cit. on p. 43)
Graff-Radford, N. R., D. Tranel, G. W. Van Hoesen, and J. P. Brandt (Feb. 1990). Diencephalic Amnesia. *Brain: A Journal of Neurology* 113 (Pt 1), pp. 1–25. https://doi.org/10.1093/brain/113.1.1(cit. on p. 32)
Gramfort, A., M. Luessi, E. Larson, D. Engemann, D. Strohmeier, C. Brodbeck, R. Goj, M. Jas, T. Brooks, L. Parkkonen, and M. Hämäläinen (2013). MEG and EEG Data Analysis with MNE-Python. *Frontiers in Neuroscience* 7. (Cit. on pp. 64, 76)
Grastyan, E., K. Lissak, I. Madarasz, and H. Donhoffer (Aug. 1959). Hippocampal Electrical Activity during the Development of Conditioned Reflexes. *Electroencephalography and Clinical Neurophysiology* 11, 3, pp. 409–430. https://doi.org/10.1016/0013-4694(59)90040-9(cit. on p. 36)
Gray, C. M., P. König, A. K. Engel, and W. Singer (Mar. 1989). Oscillatory Responses in Cat Visual Cortex Exhibit Inter-Columnar Synchronization Which Reflects Global Stimulus Properties. *Nature* 338, 6213, pp. 334–337. https://doi.org/10.1038/338334a0(cit. on p. 35)
Gray, C. M., P. E. Maldonado, M. Wilson, and B. McNaughton (Dec. 1, 1995). Tetrodes Markedly Improve the Reliability and Yield of Multiple Single-Unit Isolation from Multi-Unit Recordings in Cat Striate Cortex. *Journal of Neuroscience Methods* 63, 1, pp. 43–54. https://doi.org/10.1016/0165-0270(95)00085-2(cit. on p. 33)
Green, J. D. and A. A. Arduini (Nov. 1954). Hippocampal Electrical Activity in Arousal. *Journal of Neurophysiology* 17, 6, pp. 533–557. https://doi.org/10.1152/jn.1954.17.6.533(cit. on pp. 36, 37, 161)
Gridchyn, I., P. Schoenenberger, J. O'Neill, and J. Csicsvari (Apr. 22, 2020). Assembly-Specific Disruption of Hippocampal Replay Leads to Selective Memory Deficit. *Neuron* 106, 2, 291–300.e6. https://doi.org/10.1016/j.neuron.2020.01.021(cit. on p. 33)
Griffiths, T. L., C. Kemp, and J. B. Tenenbaum (2008). "Bayesian Models of Cognition". In: *The Cambridge Handbook of Computational Psychology*. Ed. by R. Sun. Cambridge Handbooks in Psychology. Cambridge: Cambridge University Press, pp. 59–100. https://doi.org/10.1017/CBO9780511816772.006 (cit. on p. 26).
Gross, C. G., C. E. Rocha-Miranda, and D. B. Bender (Jan. 1972). Visual Properties of Neurons in Inferotemporal Cortex of the Macaque. *Journal of Neurophysiology* 35, 1, pp. 96–111. https://doi.org/10.1152/jn.1972.35.1.96(cit. on pp. 32, 34)
Grunwald, T., K. Lehnertz, H. J. Heinze, C. Helmstaedter, and C. E. Elger (Mar. 17, 1998). Verbal Novelty Detection within the Human Hippocampus Proper. *Proceedings of the National Academy of Sciences of the United States of America* 95, 6, pp. 3193–3197. https://doi.org/10.1073/pnas.95.6.3193(cit. on p. 108)

Gueguen, M. C. M., A. Lopez-Persem, P. Billeke, J.-P. Lachaux, S. Rheims, P. Kahane, L. Minotti, O. David, M. Pessiglione, and J. Bastin (June 7, 2021). Anatomical Dissociation of Intracerebral Signals for Reward and Punishment Prediction Errors in Humans. *Nature Communications* 12, 1, p. 3344. https://doi.org/10.1038/s41467-021-23704-w(cit. on pp. 27, 176)

Guth, T. A., A. Brandt, P. C. Reinacher, A. Schulze-Bonhage, J. Jacobs, and L. Kunz (June 20, 2024). *Theta-Phase Locking of Single Neurons during Human Spatial Memory*. https://doi.org/10.1101/2024.06.20.599841. URL: https://www.biorxiv.org/content/10.1101/2024.06.20.599841v1 (visited on 06/25/2024). Pre-published (cit. on p. 44).

Guzowski, J. F., B. L. McNaughton, C. A. Barnes, and P. F. Worley (Dec. 1999). Environment-Specific Expression of the Immediate-Early Gene Arc in Hippocampal Neuronal Ensembles. *Nature Neuroscience* 2, 12, pp. 1120–1124. https://doi.org/10.1038/16046(cit. on p. 33)

Hafting, T., M. Fyhn, S. Molden, M.-B. Moser, and E. I. Moser (Aug. 11, 2005). Microstructure of a Spatial Map in the Entorhinal Cortex. *Nature* 436, 7052, pp. 801–806. https://doi.org/10.1038/nature03721(cit. on p. 33)

Halgren, E., T. L. Babb, and P. H. Crandall (June 1978). Human Hippocampal Formation EEG Desynchronizes during Attentiveness and Movement. *Electroencephalography and Clinical Neurophysiology* 44, 6, pp. 778–781. https://doi.org/10.1016/0013-4694(78)90212-2(cit. on pp. 42, 116)

Halgren, E., N. K. Squires, C. L. Wilson, J. W. Rohrbaugh, T. L. Babb, and P. H. Crandall (1980). Endogenous Potentials Generated in the Human Hippocampal Formation and Amygdala by Infrequent Events. *Science* 210, 4471, pp. 803–805. https://doi.org/10.1126/science.7434000(cit. on p. 108)

Halgren, M., I. Ulbert, H. Bastuji, D. Fabó, L. Erőss, M. Rey, O. Devinsky, W. K. Doyle, R. Mak-McCully, E. Halgren, L. Wittner, P. Chauvel, G. Heit, E. Eskandar, A. Mandell, and S. S. Cash (Nov. 19, 2019). The Generation and Propagation of the Human Alpha Rhythm. *Proceedings of the National Academy of Sciences of the United States of America* 116, 47, pp. 23772–23782. https://doi.org/10.1073/pnas.1913092116(cit. on p. 162)

Hangya, B., Z. Borhegyi, N. Szilágyi, T. F. Freund, and V. Varga (June 24, 2009). GABAergic Neurons of the Medial Septum Lead the Hippocampal Network during Theta Activity. *The Journal of Neuroscience: The Official Journal of the Society for Neuroscience* 29, 25, pp. 8094–8102. https://doi.org/10.1523/JNEUROSCI.5665-08.2009(cit. on pp. 38, 127)

Harper, R. M. (July 1, 1971). Frequency Changes in Hippocampal Electrical Activity during Movement and Tonic Immobility. *Physiology & Behavior* 7, 1, pp. 55–58. https://doi.org/10.1016/0031-9384(71)90235-6(cit. on p. 36)

Harris, C. R., K. J. Millman, S. J. van der Walt, R. Gommers, P. Virtanen, D. Cournapeau, E. Wieser, J. Taylor, S. Berg, N. J. Smith, R. Kern, M. Picus, S. Hoyer, M. H. van Kerkwijk, M. Brett, A. Haldane, J. F. del Río, M. Wiebe, P. Peterson, P. Gérard-Marchant, K. Sheppard, T. Reddy, W. Weckesser, H. Abbasi, C. Gohlke, and T. E. Oliphant (Sept. 2020). Array Programming with NumPy. *Nature* 585, 7825, pp. 357–362. https://doi.org/10.1038/s41586-020-2649-2(cit. on p. 76)

Harris, K. D., J. Csicsvari, H. Hirase, G. Dragoi, and G. Buzsáki (July 2003). Organization of Cell Assemblies in the Hippocampus. *Nature* 424, 6948, pp. 552–556. https://doi.org/10.1038/nature01834(cit. on p. 33)

Hartley, D. (1801). *Observations on Man, His Frame, His Duty and His Expectations*. London, Johnson. 544 pp. (cit. on p. 23).
Harvey, C. D., F. Collman, D. A. Dombeck, and D. W. Tank (Oct. 15, 2009). Intracellular Dynamics of Hippocampal Place Cells during Virtual Navigation. *Nature* 461, 7266, pp. 941–946. https://doi.org/10.1038/nature08499(cit. on p. 35)
Harvey, R. E., H. L. Robinson, C. Liu, A. Oliva, and A. Fernandez-Ruiz (July 2023). Hippocampo-Cortical Circuits for Selective Memory Encoding, Routing, and Replay. *Neuron* 111, 13, 2076–2090.e9. https://doi.org/10.1016/j.neuron.2023.04.015(cit. on p. 41)
Hasselmo, M. E. (Dec. 2006). The Role of Acetylcholine in Learning and Memory. *Current Opinion in Neurobiology* 16, 6, pp. 710–715. https://doi.org/10.1016/j.conb.2006.09.002(cit. on p. 38)
Hebb, D. O. (1949). *The Organization of Behavior*. 378 pp. (cit. on pp. 23, 33, 154).
Heit, G., M. E. Smith, and E. Halgren (June 1988). Neural Encoding of Individual Words and Faces by the Human Hippocampus and Amygdala. *Nature* 333, 6175, pp. 773–775. https://doi.org/10.1038/333773a0(cit. on p. 34)
Helfrich, R. F., J. D. Lendner, B. A. Mander, H. Guillen, M. Paff, L. Mnatsakanyan, S. Vadera, M. P. Walker, J. J. Lin, and R. T. Knight (Aug. 8, 2019). Bidirectional Prefrontal-Hippocampal Dynamics Organize Information Transfer during Sleep in Humans. *Nature Communications* 10, 1, p. 3572. https://doi.org/10.1038/s41467-019-11444-x(cit. on p. 46)
Henin, S., A. Shankar, H. Borges, A. Flinker, W. Doyle, D. Friedman, O. Devinsky, G. Buzsáki, and A. Liu (June 22, 2021). Spatiotemporal Dynamics between Interictal Epileptiform Discharges and Ripples during Associative Memory Processing. *Brain* 144, 5, pp. 1590–1602. https://doi.org/10.1093/brain/awab044(cit. on p. 44)
Henin, S., A. Shankar, N. Hasulak, D. Friedman, P. Dugan, L. Melloni, A. Flinker, C. Sarac, M. Fang, W. Doyle, T. Tcheng, O. Devinsky, L. Davachi, and A. Liu (Jan. 24, 2019). Hippocampal Gamma Predicts Associative Memory Performance as Measured by Acute and Chronic Intracranial EEG. *Scientific Reports* 9, 1, p. 593. https://doi.org/10.1038/s41598-018-37561-z(cit. on p. 45)
Hering, E. (1895). *On Memory and the Specific Energies of the Nervous System,* Chicago: Open court Pub. Co. (cit. on p. 28).
Herman, S., T. Walczak, and C. Bazil (June 12, 2001). Distribution of Partial Seizures during the Sleep–Wake Cycle. *Neurology* 56, 11, pp. 1453–1459. https://doi.org/10.1212/WNL.56.11.1453(cit. on p. 43)
Hirsh, R. (Dec. 1, 1974). The Hippocampus and Contextual Retrieval of Information from Memory: A Theory. *Behavioral Biology* 12, 4, pp. 421–444. https://doi.org/10.1016/S0091-6773(74)92231-7(cit. on p. 31)
Hirsh, R. (1980). The Hippocampus, Conditional Operations, and Cognition. *Physiological Psychology* 8, 2, pp. 175–182. https://doi.org/10.3758/BF03332848(cit. on p. 31)
Ho, J., T. Tumkaya, S. Aryal, H. Choi, and A. Claridge-Chang (July 2019). Moving beyond P Values: Data Analysis with Estimation Graphics. *Nature Methods* 16, 7, pp. 565–566. https://doi.org/10.1038/s41592-019-0470-3(cit. on p. 76)
Hodges, J. R. and K. S. Graham (Sept. 29, 2001). Episodic Memory: Insights from Semantic Dementia. *Philosophical Transactions of the Royal Society of London. Series B* 356, 1413, pp. 1423–1434. https://doi.org/10.1098/rstb.2001.0943(cit. on p. 30)

Hodges, J. R., K. Patterson, S. Oxbury, and E. Funnell (Dec. 1992). Semantic Dementia. Progressive Fluent Aphasia with Temporal Lobe Atrophy. *Brain: A Journal of Neurology* 115 (Pt 6), pp. 1783–1806. https://doi.org/10.1093/brain/115.6.1783(cit. on p. 30)

Hoffman, K. L., M. C. Dragan, T. K. Leonard, C. Micheli, R. Montefusco-Siegmund, and T. A. Valiante (2013). Saccades during Visual Exploration Align Hippocampal 3-8 Hz Rhythms in Human and Non-Human Primates. *Frontiers in Systems Neuroscience* 7, p. 43. https://doi.org/10.3389/fnsys.2013.00043(cit. on p. 167)

Hong, W., A. Kennedy, X. P. Burgos-Artizzu, M. Zelikowsky, S. G. Navonne, P. Perona, and D. J. Anderson (Sept. 22, 2015). Automated Measurement of Mouse Social Behaviors Using Depth Sensing, Video Tracking, and Machine Learning. *Proceedings of the National Academy of Sciences* 112, 38, E5351–E5360. https://doi.org/10.1073/pnas.1515982112(cit. on p. 28)

Horel, J. A. (Sept. 1978). The Neuroanatomy of Amnesia. A Critique of the Hippocampal Memory Hypothesis. *Brain: A Journal of Neurology* 101, 3, pp. 403–445. https://doi.org/10.1093/brain/101.3.403(cit. on p. 31)

Horel, J. A. and L. J. Misantone (July 23, 1976). Visual Discrimination Impaired by Cutting Temporal Lobe Connections. *Science* 193, 4250, pp. 336–338. https://doi.org/10.1126/science.819992(cit. on p. 31)

Huang, N. E., K. Hu, A. C. C. Yang, H.-C. Chang, D. Jia, W.-K. Liang, J. R. Yeh, C.-L. Kao, C.-H. Juan, C. K. Peng, J. H. Meijer, Y.-H. Wang, S. R. Long, and Z. Wu (Apr. 13, 2016). On Holo-Hilbert Spectral Analysis: A Full Informational Spectral Representation for Nonlinear and Non-Stationary Data. *Philosophical Transactions of the Royal Society A: Mathematical, Physical and Engineering Sciences* 374, 2065, p. 20150206. https://doi.org/10.1098/rsta.2015.0206(cit. on pp. 67, 70)

Huang, N. E., Z. Shen, and S. R. Long (Jan. 1, 1999). A NEW VIEW OF NONLINEAR WATER WAVES: The Hilbert Spectrum1. *Annual Review of Fluid Mechanics* 31, pp. 417–457. https://doi.org/10.1146/annurev.fluid.31.1.417(cit. on p. 98)

Huang, N. E., Z. Shen, S. R. Long, M. C. Wu, H. H. Shih, Q. Zheng, N.-C. Yen, C. C. Tung, and H. H. Liu (1998). The Empirical Mode Decomposition and the Hilbert Spectrum for Nonlinear and Non-Stationary Time Series Analysis. *Proceedings: Mathematical, Physical and Engineering Sciences* 454, 1971, pp. 903–995. (Cit. on pp. 68, 98, 125)

Hubel, D. H. (Mar. 22, 1957). Tungsten Microelectrode for Recording from Single Units. *Science* 125, 3247, pp. 549–550. https://doi.org/10.1126/science.125.3247.549(cit. on p. 32)

Hubel, D. H. and T. N. Wiesel (Oct. 1959). Receptive Fields of Single Neurones in the Cat's Striate Cortex. *The Journal of Physiology* 148, 3, pp. 574–591. https://doi.org/10.1113/jphysiol.1959.sp006308(cit. on pp. 32, 34)

Huh, K., K. J. Meador, G. P. Lee, D. W. Loring, A. M. Murro, D. W. King, B. B. Gallagher, J. R. Smith, and H. F. Flanigin (Aug. 1, 1990). Human Hippocampal EEG. *Neurology* 40, 8, pp. 1177–1177. https://doi.org/10.1212/WNL.40.8.1177(cit. on p. 42)

Hume, D. (1690). A Treatise of Human Nature. (Cit. on p. 23)

Hunter, J. D. (May 2007). Matplotlib: A 2D Graphics Environment. *Computing in Science & Engineering* 9, 3, pp. 90–95. https://doi.org/10.1109/MCSE.2007.55(cit. on p. 76)

Igata, H., Y. Ikegaya, and T. Sasaki (Jan. 5, 2021). Prioritized Experience Replays on a Hippocampal Predictive Map for Learning. *Proceedings of the National Academy of Sciences* 118, 1. https://doi.org/10.1073/pnas.2011266118(cit. on p. 41)

Ikegaya, Y., G. Aaron, R. Cossart, D. Aronov, I. Lampl, D. Ferster, and R. Yuste (Apr. 23, 2004). Synfire Chains and Cortical Songs: Temporal Modules of Cortical Activity. *Science* 304, 5670, pp. 559–564. https://doi.org/10.1126/science.1093173(cit. on p. 33)

Isaacson, R. L. and W. O. Wickelgren (Dec. 7, 1962). Hippocampal Ablation and Passive Avoidance. *Science* 138, 3545, pp. 1104–1106. https://doi.org/10.1126/science.138.3545.1104(cit. on p. 31)

Jacobs, J. (Feb. 5, 2014). Hippocampal Theta Oscillations Are Slower in Humans than in Rodents: Implications for Models of Spatial Navigation and Memory. *Philosophical Transactions of the Royal Society of London. Series B, Biological Sciences* 369, 1635, p. 20130304. https://doi.org/10.1098/rstb.2013.0304(cit. on pp. 42, 162)

Jacobs, J., M. J. Kahana, A. D. Ekstrom, and I. Fried (Apr. 4, 2007). Brain Oscillations Control Timing of Single-Neuron Activity in Humans. *The Journal of Neuroscience: The Official Journal of the Society for Neuroscience* 27, 14, pp. 3839–3844. https://doi.org/10.1523/JNEUROSCI.4636-06.2007(cit. on p. 44)

Jacobs, J., I. O. Korolev, J. B. Caplan, A. D. Ekstrom, B. Litt, G. Baltuch, I. Fried, A. Schulze-Bonhage, J. R. Madsen, and M. J. Kahana (May 2010). Right-Lateralized Brain Oscillations in Human Spatial Navigation. *Journal of cognitive neuroscience* 22, 5, pp. 824–836. https://doi.org/10.1162/jocn.2009.21240(cit. on p. 42)

Jacobs, J., J. Miller, S. A. Lee, T. Coffey, A. J. Watrous, M. R. Sperling, A. Sharan, G. Worrell, B. Berry, B. Lega, B. C. Jobst, K. Davis, R. E. Gross, S. A. Sheth, Y. Ezzyat, S. R. Das, J. Stein, R. Gorniak, M. J. Kahana, and D. S. Rizzuto (Dec. 7, 2016). Direct Electrical Stimulation of the Human Entorhinal Region and Hippocampus Impairs Memory. *Neuron* 92, 5, pp. 983–990. https://doi.org/10.1016/j.neuron.2016.10.062(cit. on p. 167)

Jamali, M., B. Grannan, J. Cai, A. R. Khanna, W. Muñoz, I. Caprara, A. C. Paulk, S. S. Cash, E. Fedorenko, and Z. M. Williams (July 2024). Semantic Encoding during Language Comprehension at Single-Cell Resolution. *Nature* 631, 8021, pp. 610–616. https://doi.org/10.1038/s41586-024-07643-2(cit. on p. 34)

James, W. (1890). *The Principles of Psychology, Vol I.* The Principles of Psychology, Vol I. New York, NY, US: Henry Holt and Co, pp. xii, 697. xii, 697. https://doi.org/10.1037/10538-000 (cit. on p. 23).

Janca, R., P. Jezdik, R. Cmejla, M. Tomasek, G. A. Worrell, M. Stead, J. Wagenaar, J. G. R. Jefferys, P. Krsek, V. Komarek, P. Jiruska, and P. Marusic (Jan. 2015). Detection of Interictal Epileptiform Discharges Using Signal Envelope Distribution Modelling: Application to Epileptic and Non-Epileptic Intracranial Recordings. *Brain Topography* 28, 1, pp. 172–183. https://doi.org/10.1007/s10548-014-0379-1(cit. on pp. 60, 104)

Jang, A. I., J. H. Wittig, S. K. Inati, and K. A. Zaghloul (June 5, 2017). Human Cortical Neurons in the Anterior Temporal Lobe Reinstate Spiking Activity during Verbal Memory Retrieval. *Current biology : CB* 27, 11, 1700–1705.e5. https://doi.org/10.1016/j.cub.2017.05.014(cit. on p. 45)

Jenkins, J. G. and K. M. Dallenbach (1924). Obliviscence During Sleep and Waking. *The American Journal of Psychology* 35, pp. 605–612. https://doi.org/10.2307/1414040(cit. on p. 40)

Ji, D. and M. A. Wilson (Jan. 2007). Coordinated Memory Replay in the Visual Cortex and Hippocampus during Sleep. *Nature Neuroscience* 10, 1, pp. 100–107. https://doi.org/10.1038/nn1825(cit. on p. 41)

Jiang, X., I. Shamie, W. K Doyle, D. Friedman, P. Dugan, O. Devinsky, E. Eskandar, S. S. Cash, T. Thesen, and E. Halgren (Dec. 12, 2017). Replay of Large-Scale Spatio-Temporal Patterns from Waking during Subsequent NREM Sleep in Human Cortex. *Scientific Reports* 7, 1, p. 17380. https://doi.org/10.1038/s41598-017-17469-w(cit. on p. 46)

Joensen, B. H., D. Bush, U. Vivekananda, A. J. Horner, J. A. Bisby, B. Diehl, A. Miserocchi, A. W. McEvoy, M. C. Walker, and N. Burgess (June 20, 2023). Hippocampal Theta Activity during Encoding Promotes Subsequent Associative Memory in Humans. *Cerebral Cortex (New York, N.Y.: 1991)* 33, 13, pp. 8792–8802. https://doi.org/10.1093/cercor/bhad162(cit. on p. 43)

Jones, E. G. and T. P. Powell (1970). An Anatomical Study of Converging Sensory Pathways within the Cerebral Cortex of the Monkey. *Brain: A Journal of Neurology* 93, 4, pp. 793–820. https://doi.org/10.1093/brain/93.4.793(cit. on p. 34)

Jones, M. W. and M. A. Wilson (Nov. 15, 2005). Theta Rhythms Coordinate Hippocampal–Prefrontal Interactions in a Spatial Memory Task. *PLOS Biology* 3, 12, e402. https://doi.org/10.1371/journal.pbio.0030402(cit. on p. 41)

Jouvet, M. (Jan. 3, 1969). Biogenic Amines and the States of Sleep. *Science* 163, 3862, pp. 32–41. https://doi.org/10.1126/science.163.3862.32(cit. on pp. 37, 38, 141)

Jouvet, M., F. Michel, and J. Courjon (1959). [On a stage of rapid cerebral electrical activity in the course of physiological sleep]. *Comptes Rendus Des Seances De La Societe De Biologie Et De Ses Filiales* 153, pp. 1024–1028. (Cit. on pp. 37, 141)

Juan, C.-H., K. T. Nguyen, W.-K. Liang, A. J. Quinn, Y.-H. Chen, N. G. Muggleton, J.-R. Yeh, M. W. Woolrich, A. C. Nobre, and N. E. Huang (2021). Revealing the Dynamic Nature of Amplitude Modulated Neural Entrainment With Holo-Hilbert Spectral Analysis. *Frontiers in Neuroscience* 15. (Cit. on pp. 68, 101, 123, 125)

Jung, R. and A. E. Kornmüller (Nov. 1, 1938). Eine Methodik der Ableitung Iokalisierter Potentialschwankungen aus subcorticalen Hirngebieten. *Archiv für Psychiatrie und Nervenkrankheiten* 109, 1, pp. 1–30. https://doi.org/10.1007/BF02157817(cit. on pp. 36, 163)

Jutras, M. J., P. Fries, and E. A. Buffalo (Oct. 7, 2009). Gamma-Band Synchronization in the Macaque Hippocampus and Memory Formation. *The Journal of Neuroscience: The Official Journal of the Society for Neuroscience* 29, 40, pp. 12521–12531. https://doi.org/10.1523/JNEUROSCI.0640-09.2009(cit. on p. 167)

Jutras, M. J., P. Fries, and E. A. Buffalo (Aug. 6, 2013). Oscillatory Activity in the Monkey Hippocampus during Visual Exploration and Memory Formation. *Proceedings of the National Academy of Sciences* 110, 32, pp. 13144–13149. https://doi.org/10.1073/pnas.1302351110(cit. on pp. 36, 161)

Kahana, M. J., D. Seelig, and J. R. Madsen (Dec. 1, 2001). Theta Returns. *Current Opinion in Neurobiology* 11, 6, pp. 739–744. https://doi.org/10.1016/S0959-4388(01)00278-1(cit. on p. 42)

Kahana, M. J., R. Sekuler, J. B. Caplan, M. Kirschen, and J. R. Madsen (June 1999). Human Theta Oscillations Exhibit Task Dependence during Virtual Maze Navigation. *Nature* 399, 6738, pp. 781–784. https://doi.org/10.1038/21645(cit. on p. 42)

Kanari, L., Y. Shi, A. Arnaudon, N. Barros-Zulaica, R. Benavides-Piccione, J. S. Coggan, J. DeFelipe, K. Hess, H. D. Mansvelder, E. J. Mertens, J. Meystre, R. d. C. Perin, M. Pezzoli, R. T. Daniel, R. Stoop, I. Segev, H. Markram, and C. P. J. de Kock (July 18, 2025). Of Mice and Men: Dendritic Architecture Differentiates Human from

Mouse Neuronal Networks. *iScience* 28, 7. https://doi.org/10.1016/j.isci.2025.112928(cit. on pp. 163, 164)
Kant, I. (1781). *Critique Of Pure Reason* (cit. on p. 24).
Karlsson, M. P. and L. M. Frank (July 2009). Awake Replay of Remote Experiences in the Hippocampus. *Nature Neuroscience* 12, 7, pp. 913–918. https://doi.org/10.1038/nn.2344(cit. on p. 45)
Karni, A., D. Tanne, B. S. Rubenstein, J. J. Askenasy, and D. Sagi (July 29, 1994). Dependence on REM Sleep of Overnight Improvement of a Perceptual Skill. *Science* 265, 5172, pp. 679–682. https://doi.org/10.1126/science.8036518(cit. on p. 40)
Katz, C. N., K. Patel, O. Talakoub, D. Groppe, K. Hoffman, and T. A. Valiante (Sept. 3, 2020). Differential Generation of Saccade, Fixation, and Image-Onset Event-Related Potentials in the Human Mesial Temporal Lobe. *Cerebral Cortex (New York, N.Y.: 1991)* 30, 10, pp. 5502–5516. https://doi.org/10.1093/cercor/bhaa132(cit. on p. 167)
Katz, C. N., A. G. P. Schjetnan, K. Patel, V. Barkley, K. L. Hoffman, S. K. Kalia, K. D. Duncan, and T. A. Valiante (July 25, 2022). A Corollary Discharge Mediates Saccade-Related Inhibition of Single Units in Mnemonic Structures of the Human Brain. *Current biology: CB* 32, 14, 3082–3094.e4. https://doi.org/10.1016/j.cub.2022.06.015(cit. on p. 167)
Katzner, S., I. Nauhaus, A. Benucci, V. Bonin, D. L. Ringach, and M. Carandini (Jan. 15, 2009). Local Origin of Field Potentials in Visual Cortex. *Neuron* 61, 1, pp. 35–41. https://doi.org/10.1016/j.neuron.2008.11.016(cit. on p. 35)
Kemp, I. R. and B. R. Kaada (Sept. 23, 1975). The Relation of Hippocampal Theta Activity to Arousal, Attentive Behaviour and Somato-Motor Movements in Unrestrained Cats. *Brain Research* 95, 2–3, pp. 323–342. https://doi.org/10.1016/0006-8993(75)90110-9(cit. on p. 36)
Kempadoo, K. A., E. V. Mosharov, S. J. Choi, D. Sulzer, and E. R. Kandel (Dec. 20, 2016). Dopamine Release from the Locus Coeruleus to the Dorsal Hippocampus Promotes Spatial Learning and Memory. *Proceedings of the National Academy of Sciences of the United States of America* 113, 51, pp. 14835–14840. https://doi.org/10.1073/pnas.1616515114(cit. on p. 41)
Kimble, D. P. (1963). The Effects of Bilateral Hippocampal Lesions in Rats. *Journal of Comparative and Physiological Psychology* 56, 2, pp. 273–283. https://doi.org/10.1037/h0048903(cit. on p. 31)
Király, B., A. Domonkos, M. Jelitai, V. Lopes-dos-Santos, S. Martínez-Bellver, B. Kocsis, D. Schlingloff, A. Joshi, M. Salib, R. Fiáth, P. Barthó, I. Ulbert, T. F. Freund, T. J. Viney, D. Dupret, V. Varga, and B. Hangya (Oct. 10, 2023). The Medial Septum Controls Hippocampal Supra-Theta Oscillations. *Nature Communications* 14, 1, p. 6159. https://doi.org/10.1038/s41467-023-41746-0(cit. on pp. 38, 127)
Klausberger, T., L. F. Márton, A. Baude, J. D. B. Roberts, P. J. Magill, and P. Somogyi (Jan. 1, 2004). Spike Timing of Dendrite-Targeting Bistratified Cells during Hippocampal Network Oscillations in Vivo. *Nature Neuroscience* 7, 1, pp. 41–47. https://doi.org/10.1038/nn1159(cit. on p. 38)
Klausberger, T. and P. Somogyi (July 4, 2008). Neuronal Diversity and Temporal Dynamics: The Unity of Hippocampal Circuit Operations. *Science* 321, 5885, pp. 53–57. https://doi.org/10.1126/science.1149381(cit. on pp. 38, 116, 119)
Kleen, J. K., J. E. Chung, K. K. Sellers, J. Zhou, M. Triplett, K. Lee, A. Tooker, R. Haque, and E. F. Chang (May 12, 2021). Bidirectional Propagation of Low Frequency

Oscillations over the Human Hippocampal Surface. *Nature Communications* 12, p. 2764. https://doi.org/10.1038/s41467-021-22850-5(cit. on p. 174)
Klemm, W. R. (Sept. 1971). EEG and Multiple-Unit Activity in Limbic and Motor Systems during Movement and Immobility. *Physiology & Behavior* 7, 3, pp. 337–343. https://doi.org/10.1016/0031-9384(71)90311-8(cit. on p. 36)
Klüver, H. and P. C. Bucy (1937). "Psychic Blindness" and Other Symptoms Following Bilateral Temporal Lobectomy in Rhesus Monkeys. *American Journal of Physiology* 119, pp. 352–353. (Cit. on p. 30)
Klüver, H. and P. C. Bucy (Jan. 1, 1938). An Analysis of Certain Effects of Bilateral Temporal Lobectomy in the Rhesus Monkey, with Special Reference to "Psychic Blindness". *The Journal of Psychology* 5, 1, pp. 33–54. https://doi.org/10.1080/00223980.1938.9917551(cit. on p. 30)
Kolibius, L. D., F. Roux, G. Parish, M. Ter Wal, M. Van Der Plas, R. Chelvarajah, V. Sawlani, D. T. Rollings, J. D. Lang, S. Gollwitzer, K. Walther, R. Hopfengärtner, G. Kreiselmeyer, H. Hamer, B. P. Staresina, M. Wimber, H. Bowman, and S. Hanslmayr (Oct. 5, 2023). Hippocampal Neurons Code Individual Episodic Memories in Humans. *Nature Human Behaviour*. https://doi.org/10.1038/s41562-023-01706-6(cit. on p. 34)
Kolodny, O. and S. Edelman (Sept. 2015). The Problem of Multimodal Concurrent Serial Order in Behavior. *Neuroscience & Biobehavioral Reviews* 56, pp. 252–265. https://doi.org/10.1016/j.neubiorev.2015.07.009(cit. on p. 24)
Konkel, A. and N. J. Cohen (Sept. 15, 2009). Relational Memory and the Hippocampus: Representations and Methods. *Frontiers in Neuroscience* 3. https://doi.org/10.3389/neuro.01.023.2009(cit. on pp. 26, 78, 79)
Konkel, A., D. E. Warren, M. C. Duff, D. Tranel, and N. J. Cohen (Oct. 29, 2008). Hippocampal Amnesia Impairs All Manner of Relational Memory. *Frontiers in Human Neuroscience* 2. https://doi.org/10.3389/neuro.09.015.2008(cit. on pp. 26, 79)
Kopell, N., G. B. Ermentrout, M. A. Whittington, and R. D. Traub (Feb. 15, 2000). Gamma Rhythms and Beta Rhythms Have Different Synchronization Properties. *Proceedings of the National Academy of Sciences of the United States of America* 97, 4, pp. 1867–1872. https://doi.org/10.1073/pnas.97.4.1867(cit. on p. 39)
Kota, S., M. D. Rugg, and B. C. Lega (Dec. 2, 2020). Hippocampal Theta Oscillations Support Successful Associative Memory Formation. *The Journal of Neuroscience: The Official Journal of the Society for Neuroscience* 40, 49, pp. 9507–9518. https://doi.org/10.1523/JNEUROSCI.0767-20.2020(cit. on p. 43)
Kragel, J. E., S. VanHaerents, J. W. Templer, S. Schuele, J. M. Rosenow, A. S. Nilakantan, and D. J. Bridge (Mar. 13, 2020). Hippocampal Theta Coordinates Memory Processing during Visual Exploration. *eLife* 9, e52108. https://doi.org/10.7554/eLife.52108(cit. on p. 43)
Kramis, R., C. H. Vanderwolf, and B. H. Bland (Oct. 1, 1975). Two Types of Hippocampal Rhythmical Slow Activity in Both the Rabbit and the Rat: Relations to Behavior and Effects of Atropine, Diethyl Ether, Urethane, and Pentobarbital. *Experimental Neurology* 49, 1, pp. 58–85. https://doi.org/10.1016/0014-4886(75)90195-8(cit. on pp. 36, 38, 161, 162)
Kreiman, G., C. Koch, and I. Fried (Sept. 2000). Category-Specific Visual Responses of Single Neurons in the Human Medial Temporal Lobe. *Nature Neuroscience* 3, 9, pp. 946–953. https://doi.org/10.1038/78868(cit. on p. 34)

Kremen, V., V. Sladky, F. Mivalt, N. M. Gregg, B. H. Brinkmann, I. Balzekas, V. Marks, M. Kucewicz, B. N. Lundstrom, J. Cui, E. K. St Louis, P. Croarkin, E. C. Alden, B. Joseph, J. Fields, K. Crockett, J. Adolf, J. Bilderbeek, D. Hermes, S. Messina, K. J. Miller, J. Van Gompel, T. Denison, and G. A. Worrell (Apr. 1, 2025). Modulating Limbic Circuits in Temporal Lobe Epilepsy: Impacts on Seizures, Memory, Mood and Sleep. *Brain Communications* 7, 2, fcaf106. https://doi.org/10.1093/braincomms/fcaf106(cit. on p. 169)

Kuhn, H. W. (1955). The Hungarian Method for the Assignment Problem. *Naval Research Logistics Quarterly* 2, 1–2, pp. 83–97. https://doi.org/10.1002/nav.3800020109(cit. on pp. 50, 81)

Kunz, L., B. P. Staresina, P. C. Reinacher, A. Brandt, T. A. Guth, A. Schulze-Bonhage, and J. Jacobs (Feb. 16, 2024). Ripple-Locked Coactivity of Stimulus-Specific Neurons and Human Associative Memory. *Nature Neuroscience*, pp. 1–13. https://doi.org/10.1038/s41593-023-01550-x(cit. on p. 45)

Kunz, L., L. Wang, D. Lachner-Piza, H. Zhang, A. Brandt, M. Dümpelmann, P. C. Reinacher, V. A. Coenen, D. Chen, W.-X. Wang, W. Zhou, S. Liang, P. Grewe, C. G. Bien, A. Bierbrauer, T. Navarro Schröder, A. Schulze-Bonhage, and N. Axmacher (July 2019). Hippocampal Theta Phases Organize the Reactivation of Large-Scale Electrophysiological Representations during Goal-Directed Navigation. *Science Advances* 5, 7, eaav8192. https://doi.org/10.1126/sciadv.aav8192(cit. on p. 44)

Lashley, K. S. (1950). "In Search of the Engram". In: *Physiological Mechanisms in Animal Behavior. (Society's Symposium IV.)* Oxford, England: Academic Press, pp. 454–482 (cit. on p. 31).

— (1951). "The Problem of Serial Order in Behavior". In: *Cerebral Mechanisms in Behavior; the Hixon Symposium*. Oxford, England: Wiley, pp. 112–146 (cit. on p. 24).

Lasztóczi, B. and T. Klausberger (Mar. 5, 2014). Layer-Specific GABAergic Control of Distinct Gamma Oscillations in the CA1 Hippocampus. *Neuron* 81, 5, pp. 1126–1139. https://doi.org/10.1016/j.neuron.2014.01.021(cit. on pp. 35, 38)

Lasztóczi, B. and T. Klausberger (July 6, 2016). Hippocampal Place Cells Couple to Three Different Gamma Oscillations during Place Field Traversal. *Neuron* 91, 1, pp. 34–40. https://doi.org/10.1016/j.neuron.2016.05.036(cit. on p. 35)

Laurent, G. (Aug. 2020). On the Value of Model Diversity in Neuroscience. *Nature Reviews. Neuroscience* 21, 8, pp. 395–396. https://doi.org/10.1038/s41583-020-0323-1(cit. on p. 28)

Lavenex, P. and D. G. Amaral (2000). Hippocampal-Neocortical Interaction: A Hierarchy of Associativity. *Hippocampus* 10, 4, pp. 420–430. https://doi.org/10.1002/1098-1063(2000)10:4<420::AID-HIPO8>3.0.CO;2-5(cit. on p. 127)

Lee, K., A. C. Paulk, Y. G. Ro, D. R. Cleary, K. J. Tonsfeldt, Y. Kfir, J. S. Pezaris, Y. Tchoe, J. Lee, A. M. Bourhis, R. Vatsyayan, J. R. Martin, S. M. Russman, J. C. Yang, A. Baohan, R. M. Richardson, Z. M. Williams, S. I. Fried, U. Hoi Sang, A. M. Raslan, S. Ben-Haim, E. Halgren, S. S. Cash, and S. A. Dayeh (Jan. 17, 2024). Flexible, Scalable, High Channel Count Stereo-Electrode for Recording in the Human Brain. *Nature Communications* 15, 1, p. 218. https://doi.org/10.1038/s41467-023-43727-9(cit. on pp. 166, 169)

Lee, M. G., J. J. Chrobak, A. Sik, R. G. Wiley, and G. Buzsáki (Oct. 1994). Hippocampal Theta Activity Following Selective Lesion of the Septal Cholinergic System. *Neuroscience* 62, 4, pp. 1033–1047. https://doi.org/10.1016/0306-4522(94)90341-7(cit. on p. 38)

Lega, B., J. Burke, J. Jacobs, and M. J. Kahana (Jan. 2016). Slow-Theta-to-Gamma Phase–Amplitude Coupling in Human Hippocampus Supports the Formation of New Episodic Memories. *Cerebral Cortex (New York, NY)* 26, 1, pp. 268–278. https://doi.org/10.1093/cercor/bhu232(cit. on p. 44)

Lega, B. C., J. Jacobs, and M. Kahana (Apr. 2012). Human Hippocampal Theta Oscillations and the Formation of Episodic Memories. *Hippocampus* 22, 4, pp. 748–761. https://doi.org/10.1002/hipo.20937(cit. on p. 42)

Lehongre, K., V. Lambrecq, S. Whitmarsh, V. Frazzini, L. Cousyn, D. Soleil, S. Fernandez-Vidal, B. Mathon, M. Houot, J.-D. Lemaréchal, S. Clemenceau, D. Hasboun, C. Adam, and V. Navarro (July 2022). Long-Term Deep Intracerebral Microelectrode Recordings in Patients with Drug-Resistant Epilepsy: Proposed Guidelines Based on 10-Year Experience. *NeuroImage* 254, p. 119116. https://doi.org/10.1016/j.neuroimage.2022.119116(cit. on p. 53)

Leksell, L. (Dec. 13, 1951). The Stereotaxic Method and Radiosurgery of the Brain. *Acta Chirurgica Scandinavica* 102, 4, pp. 316–319. (Cit. on p. 34)

Łęski, S., H. Lindén, T. Tetzlaff, K. H. Pettersen, and G. T. Einevoll (July 2013). Frequency Dependence of Signal Power and Spatial Reach of the Local Field Potential. *PLOS Computational Biology* 9, 7, e1003137. https://doi.org/10.1371/journal.pcbi.1003137(cit. on pp. 35, 39)

Lesting, J., R. T. Narayanan, C. Kluge, S. Sangha, T. Seidenbecher, and H.-C. Pape (June 28, 2011). Patterns of Coupled Theta Activity in Amygdala-Hippocampal-Prefrontal Cortical Circuits during Fear Extinction. *PLOS ONE* 6, 6, e21714. https://doi.org/10.1371/journal.pone.0021714(cit. on p. 127)

Li, J., D. Cao, V. Dimakopoulos, W. Shi, S. Yu, L. Fan, L. Stieglitz, L. Imbach, J. Sarnthein, and T. Jiang (Jan. 19, 2022). Anterior-Posterior Hippocampal Dynamics Support Working Memory Processing. *The Journal of Neuroscience: The Official Journal of the Society for Neuroscience* 42, 3, pp. 443–453. https://doi.org/10.1523/JNEUROSCI.1287-21.2021(cit. on p. 43)

Liao, Z., K. C. Gonzalez, D. M. Li, C. M. Yang, D. Holder, N. E. McClain, G. Zhang, S. W. Evans, M. Chavarha, J. Simko, C. D. Makinson, M. Z. Lin, A. Losonczy, and A. Negrean (July 26, 2024). Functional Architecture of Intracellular Oscillations in Hippocampal Dendrites. *Nature Communications* 15, 1, p. 6295. https://doi.org/10.1038/s41467-024-50546-z(cit. on p. 35)

Liberson, W. T. and K. Akert (May 1955). Hippocampal Seizure States in Guinea Pig. *Electroencephalography and Clinical Neurophysiology* 7, 2, pp. 211–222. https://doi.org/10.1016/0013-4694(55)90036-5(cit. on p. 36)

Liberson, W. T. and J. G. Cadilhac (1953). Electroshock and Rhinencephalic Seizure States. *Confinia Neurologica* 13, 5–6, pp. 278–286. https://doi.org/10.1159/000105425(cit. on pp. 36, 163)

Lin, J.-J., M. D. Rugg, S. Das, J. Stein, D. S. Rizzuto, M. J. Kahana, and B. C. Lega (Oct. 2017). Theta Band Power Increases in the Posterior Hippocampus Predict Successful Episodic Memory Encoding in Humans. *Hippocampus* 27, 10, pp. 1040–1053. https://doi.org/10.1002/hipo.22751(cit. on p. 43)

Lin, J.-J., G. Umbach, M. D. Rugg, and B. Lega (Feb. 2019). Gamma Oscillations during Episodic Memory Processing Provide Evidence for Functional Specialization in the Longitudinal Axis of the Human Hippocampus. *Hippocampus* 29, 2, pp. 68–72. https://doi.org/10.1002/hipo.23016(cit. on p. 45)

Lindén, H., T. Tetzlaff, T. C. Potjans, K. H. Pettersen, S. Grün, M. Diesmann, and G. T. Einevoll (Dec. 8, 2011). Modeling the Spatial Reach of the LFP. *Neuron* 72, 5, pp. 859–872. https://doi.org/10.1016/j.neuron.2011.11.006(cit. on p. 35)

Lisman, J., G. Buzsáki, H. Eichenbaum, L. Nadel, C. Ranganath, and A. D. Redish (Oct. 26, 2017). Viewpoints: How the Hippocampus Contributes to Memory, Navigation and Cognition. *Nature Neuroscience* 20, 11, pp. 1434–1447. https://doi.org/10.1038/nn.4661(cit. on p. 26)

Lisman, J. E. and A. A. Grace (June 2, 2005). The Hippocampal-VTA Loop: Controlling the Entry of Information into Long-Term Memory. *Neuron* 46, 5, pp. 703–713. https://doi.org/10.1016/j.neuron.2005.05.002(cit. on p. 41)

Lisman, J. E. and O. Jensen (Mar. 20, 2013). The Theta-Gamma Neural Code. *Neuron* 77, 6, pp. 1002–1016. https://doi.org/10.1016/j.neuron.2013.03.007(cit. on pp. 39, 41, 96, 122)

Liu, A. A., S. Henin, S. Abbaspoor, A. Bragin, E. A. Buffalo, J. S. Farrell, D. J. Foster, L. M. Frank, T. Gedankien, J. Gotman, J. A. Guidera, K. L. Hoffman, J. Jacobs, M. J. Kahana, L. Li, Z. Liao, J. J. Lin, A. Losonczy, R. Malach, M. A. van der Meer, K. McClain, B. L. McNaughton, Y. Norman, A. Navas-Olive, L. M. de la Prida, J. W. Rueckemann, J. J. Sakon, I. Skelin, I. Soltesz, B. P. Staresina, S. A. Weiss, M. A. Wilson, K. A. Zaghloul, M. Zugaro, and G. Buzsáki (Oct. 12, 2022). A Consensus Statement on Detection of Hippocampal Sharp Wave Ripples and Differentiation from Other Fast Oscillations. *Nature Communications* 13, 1, p. 6000. https://doi.org/10.1038/s41467-022-33536-x(cit. on pp. 44, 45, 147, 148, 164)

Liu, X., C. Ren, Y. Lu, Y. Liu, J.-H. Kim, S. Leutgeb, T. Komiyama, and D. Kuzum (June 2021). Multimodal Neural Recordings with Neuro-FITM Uncover Diverse Patterns of Cortical–Hippocampal Interactions. *Nature Neuroscience* 24, 6, pp. 886–896. https://doi.org/10.1038/s41593-021-00841-5(cit. on p. 41)

Liu, X., S. Ramirez, P. T. Pang, C. B. Puryear, A. Govindarajan, K. Deisseroth, and S. Tonegawa (Mar. 22, 2012). Optogenetic Stimulation of a Hippocampal Engram Activates Fear Memory Recall. *Nature* 484, 7394, pp. 381–385. https://doi.org/10.1038/nature11028(cit. on p. 33)

Locke, J. (1740). AN ESSAY CONCERNING HUMAN UNDERSTANDING. (Cit. on p. 23)

Long, N. M., J. F. Burke, and M. J. Kahana (Jan. 1, 2014). Subsequent Memory Effect in Intracranial and Scalp EEG. *NeuroImage* 84, pp. 488–494. https://doi.org/10.1016/j.neuroimage.2013.08.052(cit. on p. 42)

Lopes-Dos-Santos, V., D. Brizee, and D. Dupret (June 24, 2025). Spatio-Temporal Organization of Network Activity Patterns in the Hippocampus. *Cell Reports* 44, 6, p. 115808. https://doi.org/10.1016/j.celrep.2025.115808(cit. on pp. 36, 38, 53, 148)

Lopes-dos-Santos, V., S. Ribeiro, and A. B. L. Tort (Nov. 15, 2013). Detecting Cell Assemblies in Large Neuronal Populations. *Journal of Neuroscience Methods* 220, 2, pp. 149–166. https://doi.org/10.1016/j.jneumeth.2013.04.010(cit. on p. 169)

Lopes-dos-Santos, V., G. M. van de Ven, A. Morley, S. Trouche, N. Campo-Urriza, and D. Dupret (Nov. 2018). Parsing Hippocampal Theta Oscillations by Nested Spectral Components during Spatial Exploration and Memory-Guided Behavior. *Neuron* 100, 4, 940–952.e7. https://doi.org/10.1016/j.neuron.2018.09.031(cit. on pp. 33, 36, 39, 45, 154)

Lu, L., Y. Ren, T. Yu, Z. Liu, S. Wang, L. Tan, J. Zeng, Q. Feng, R. Lin, Y. Liu, Q. Guo, and M. Luo (Jan. 14, 2020). Control of Locomotor Speed, Arousal, and

Hippocampal Theta Rhythms by the Nucleus Incertus. *Nature Communications* 11, 1, p. 262. https://doi.org/10.1038/s41467-019-14116-y(cit. on p. 127)
Lyford, G. L., K. Yamagata, W. E. Kaufmann, L. K. Sanders, N. G. Copeland, D. J. Gilbert, I. N. A. Jenkins, A. A. Lanahan, and P. F. Worley (1995). Arc, a Growth Factor and Activity-Regulated Gene, Encodes a Novel Cytoskeleton-Associated Protein That Is Enriched in Neuronal Dendrites. *Neuron*. (Cit. on p. 33)
Macadar, A. W., L. M. Chalupa, and D. B. Lindsley (June 1, 1974). Differentiation of Brain Stem Loci Which Affect Hippocampal and Neocortical Electrical Activity. *Experimental Neurology* 43, 3, pp. 499–514. https://doi.org/10.1016/0014-4886(74)90190-3(cit. on p. 37)
Maclean, P. D., S. Flanigan, J. P. Flynn, C. Kim, and J. R. Stevens (Dec. 1955). Hippocampal Function: Tentative Correlations of Conditioning, EEG, Drug, and Radioautographic Studies. *The Yale Journal of Biology and Medicine* 28, 3–4, pp. 380–395. (Cit. on pp. 36, 163)
Magland, J., J. J. Jun, E. Lovero, A. J. Morley, C. L. Hurwitz, A. P. Buccino, S. Garcia, and A. H. Barnett (May 19, 2020). SpikeForest, Reproducible Web-Facing Ground-Truth Validation of Automated Neural Spike Sorters. *eLife* 9, e55167. https://doi.org/10.7554/eLife.55167(cit. on p. 53)
Maidenbaum, S., J. Miller, J. M. Stein, and J. Jacobs (Oct. 16, 2018). Grid-like Hexadirectional Modulation of Human Entorhinal Theta Oscillations. *Proceedings of the National Academy of Sciences* 115, 42, pp. 10798–10803. https://doi.org/10.1073/pnas.1805007115(cit. on p. 43)
Maingret, N., G. Girardeau, R. Todorova, M. Goutierre, and M. Zugaro (July 2016). Hippocampo-Cortical Coupling Mediates Memory Consolidation during Sleep. *Nature Neuroscience* 19, 7, pp. 959–964. https://doi.org/10.1038/nn.4304(cit. on p. 41)
Manning, J. R., J. Jacobs, I. Fried, and M. J. Kahana (Oct. 28, 2009). Broadband Shifts in Local Field Potential Power Spectra Are Correlated with Single-Neuron Spiking in Humans. *The Journal of Neuroscience: The Official Journal of the Society for Neuroscience* 29, 43, pp. 13613–13620. https://doi.org/10.1523/JNEUROSCI.2041-09.2009(cit. on pp. 56, 122)
Manning, J. R., S. M. Polyn, G. H. Baltuch, B. Litt, and M. J. Kahana (Aug. 2, 2011). Oscillatory Patterns in Temporal Lobe Reveal Context Reinstatement during Memory Search. *Proceedings of the National Academy of Sciences* 108, 31, pp. 12893–12897. https://doi.org/10.1073/pnas.1015174108(cit. on p. 45)
Mao, D., E. Avila, B. Caziot, J. Laurens, J. D. Dickman, and D. E. Angelaki (Nov. 3, 2021). Spatial Modulation of Hippocampal Activity in Freely Moving Macaques. *Neuron* 109, 21, 3521–3534.e6. https://doi.org/10.1016/j.neuron.2021.09.032(cit. on pp. 36, 163)
Maoz, S. L. L., M. Stangl, U. Topalovic, D. Batista, S. Hiller, Z. M. Aghajan, B. Knowlton, J. Stern, J.-P. Langevin, I. Fried, D. Eliashiv, and N. Suthana (Oct. 20, 2023). Dynamic Neural Representations of Memory and Space during Human Ambulatory Navigation. *Nature Communications* 14, 1, p. 6643. https://doi.org/10.1038/s41467-023-42231-4(cit. on pp. 43, 162, 168)
Markram, H., J. Lübke, M. Frotscher, and B. Sakmann (Jan. 10, 1997). Regulation of Synaptic Efficacy by Coincidence of Postsynaptic APs and EPSPs. *Science* 275, 5297, pp. 213–215. https://doi.org/10.1126/science.275.5297.213(cit. on p. 39)
Marshall, J. D., D. E. Aldarondo, T. W. Dunn, W. L. Wang, G. J. Berman, and B. P. Ölveczky (Feb. 3, 2021). Continuous Whole-Body 3D Kinematic Recordings across

the Rodent Behavioral Repertoire. *Neuron* 109, 3, 420–437.e8. https://doi.org/10.1016/j.neuron.2020.11.016(cit. on p. 28)

Maslarova, A., J. N. Shin, A. Navas-Olive, M. Vöröslakos, H. Hamer, A. Doerfler, S. Henin, G. Buzsáki, and A. Liu (Nov. 26, 2025). Spatiotemporal Patterns Differentiate Hippocampal Sharp-Wave Ripples from Interictal Epileptiform Discharges in Mice and Humans. *Nature Communications* 16, 1, p. 11636. https://doi.org/10.1038/s41467-025-66562-6(cit. on pp. 44, 71, 147, 148, 151)

Masurkar, A. V., K. V. Srinivas, D. H. Brann, R. Warren, D. C. Lowes, and S. A. Siegelbaum (Jan. 3, 2017). Medial and Lateral Entorhinal Cortex Differentially Excite Deep versus Superficial CA1 Pyramidal Neurons. *Cell Reports* 18, 1, pp. 148–160. https://doi.org/10.1016/j.celrep.2016.12.012(cit. on p. 38)

Masurkar, A. V., C. Tian, R. Warren, I. Reyes, D. C. Lowes, D. H. Brann, and S. A. Siegelbaum (Mar. 1, 2020). Postsynaptic Integrative Properties of Dorsal CA1 Pyramidal Neuron Subpopulations. *Journal of Neurophysiology* 123, 3, pp. 980–992. https://doi.org/10.1152/jn.00397.2019(cit. on p. 38)

Mathis, A., P. Mamidanna, K. M. Cury, T. Abe, V. N. Murthy, M. W. Mathis, and M. Bethge (Sept. 2018). DeepLabCut: Markerless Pose Estimation of User-Defined Body Parts with Deep Learning. *Nature Neuroscience* 21, 9, pp. 1281–1289. https://doi.org/10.1038/s41593-018-0209-y(cit. on p. 28)

Maudsley, H. (1877). *The Physiology of Mind*. Appleton & Company (cit. on p. 23).

McClelland, J. L., B. L. McNaughton, and R. C. O'Reilly (July 1995). Why There Are Complementary Learning Systems in the Hippocampus and Neocortex: Insights from the Successes and Failures of Connectionist Models of Learning and Memory. *Psychological Review* 102, 3, pp. 419–457. https://doi.org/10.1037/0033-295X.102.3.419(cit. on pp. 40, 79, 141)

McHugh, S. B., V. Lopes-Dos-Santos, M. Castelli, G. P. Gava, S. E. Thompson, S. K. E. Tam, K. Hartwich, B. Perry, R. Toth, T. Denison, A. Sharott, and D. Dupret (Nov. 20, 2024). Offline Hippocampal Reactivation during Dentate Spikes Supports Flexible Memory. *Neuron* 112, 22, 3768–3781.e8. https://doi.org/10.1016/j.neuron.2024.08.022(cit. on p. 41)

McKenzie, S., A. J. Frank, N. R. Kinsky, B. Porter, P. D. Rivière, and H. Eichenbaum (July 2, 2014). Hippocampal Representation of Related and Opposing Memories Develop within Distinct, Hierarchically Organized Neural Schemas. *Neuron* 83, 1, pp. 202–215. https://doi.org/10.1016/j.neuron.2014.05.019(cit. on p. 25)

McKinney, W. (May 1, 2010). Data Structures for Statistical Computing in Python. *SciPy 2010*. https://doi.org/10.25080/Majora-92bf1922-00a(cit. on p. 76)

McLelland, D. and R. VanRullen (Oct. 14, 2016). Theta-Gamma Coding Meets Communication-through-Coherence: Neuronal Oscillatory Multiplexing Theories Reconciled. *PLoS Computational Biology* 12, 10, e1005162. https://doi.org/10.1371/journal.pcbi.1005162(cit. on p. 39)

McNamara, C. G., Á. Tejero-Cantero, S. Trouche, N. Campo-Urriza, and D. Dupret (Dec. 2014). Dopaminergic Neurons Promote Hippocampal Reactivation and Spatial Memory Persistence. *Nature Neuroscience* 17, 12, pp. 1658–1660. https://doi.org/10.1038/nn.3843(cit. on p. 41)

McNaughton, B. L., J. O'Keefe, and C. A. Barnes (1983). The Stereotrode: A New Technique for Simultaneous Isolation of Several Single Units in the Central Nervous System from Multiple Unit Records. *Journal of Neuroscience Methods*, p. 7. (Cit. on p. 33)

Meador, K. J., J. L. Thompson, D. W. Loring, A. M. Murro, D. W. King, B. B. Gallagher, G. P. Lee, J. R. Smith, and H. F. Flanigin (June 1991). Behavioral State-Specific Changes in Human Hippocampal Theta Activity. *Neurology* 41, 6, pp. 869–872. https://doi.org/10.1212/wnl.41.6.869(cit. on p. 42)

Mertens, E. J., Y. Leibner, J. Pie, A. A. Galakhova, F. Waleboer, J. Meijer, T. S. Heistek, R. Wilbers, D. Heyer, N. A. Goriounova, S. Idema, M. B. Verhoog, B. E. Kalmbach, B. R. Lee, R. P. Gwinn, E. S. Lein, E. Aronica, J. Ting, H. D. Mansvelder, I. Segev, and C. P. J. de Kock (Apr. 23, 2024). Morpho-Electric Diversity of Human Hippocampal CA1 Pyramidal Neurons. *Cell Reports* 43, 4. https://doi.org/10.1016/j.celrep.2024.114100(cit. on p. 163)

Mill, J. (1829). *Analysis Of The Phenomena Of The Human Mind* (cit. on p. 23).

Mill, J. S. (1843). *A System of Logic, Ratiocinative and Inductive : Being a Connected View of the Principles of Evidence, and Methods of Scientific Investigation*. London : J. W. Parker. 608 pp. (cit. on pp. 23, 27).

Miller, A. (Apr. 15, 1967). The Lobotomy Patient—A Decade Later. *Canadian Medical Association Journal* 96, 15, pp. 1095–1103. (Cit. on p. 29)

Miller, A. M. P., A. D. Jacob, A. I. Ramsaran, M. L. De Snoo, S. A. Josselyn, and P. W. Frankland (June 21, 2023). Emergence of a Predictive Model in the Hippocampus. *Neuron* 111, 12, 1952–1965.e5. https://doi.org/10.1016/j.neuron.2023.03.011(cit. on p. 27)

Miller, J., A. J. Watrous, M. Tsitsiklis, S. A. Lee, S. A. Sheth, C. A. Schevon, E. H. Smith, M. R. Sperling, A. Sharan, A. A. Asadi-Pooya, G. A. Worrell, S. Meisenhelter, C. S. Inman, K. A. Davis, B. Lega, P. A. Wanda, S. R. Das, J. M. Stein, R. Gorniak, and J. Jacobs (June 21, 2018). Lateralized Hippocampal Oscillations Underlie Distinct Aspects of Human Spatial Memory and Navigation. *Nature Communications* 9, 1, p. 2423. https://doi.org/10.1038/s41467-018-04847-9(cit. on p. 43)

Miller, K. J., S. Zanos, E. E. Fetz, M. den Nijs, and J. G. Ojemann (Mar. 11, 2009). Decoupling the Cortical Power Spectrum Reveals Real-Time Representation of Individual Finger Movements in Humans. *Journal of Neuroscience* 29, 10, pp. 3132–3137. https://doi.org/10.1523/JNEUROSCI.5506-08.2009(cit. on p. 176)

Miller, K. J., C. J. Honey, D. Hermes, R. P. Rao, M. denNijs, and J. G. Ojemann (Jan. 15, 2014). Broadband Changes in the Cortical Surface Potential Track Activation of Functionally Diverse Neuronal Populations. *NeuroImage* 85, pp. 711–720. https://doi.org/10.1016/j.neuroimage.2013.08.070(cit. on p. 176)

Miller, K. J. (May 12, 2010). Broadband Spectral Change: Evidence for a Macroscale Correlate of Population Firing Rate? *The Journal of Neuroscience* 30, 19, p. 6477. https://doi.org/10.1523/JNEUROSCI.6401-09.2010(cit. on pp. 56, 122)

Miller, K. J., G. Schalk, D. Hermes, J. G. Ojemann, and R. P. N. Rao (Jan. 28, 2016). Spontaneous Decoding of the Timing and Content of Human Object Perception from Cortical Surface Recordings Reveals Complementary Information in the Event-Related Potential and Broadband Spectral Change. *PLOS Computational Biology* 12, 1, e1004660. https://doi.org/10.1371/journal.pcbi.1004660(cit. on p. 176)

Miller, K. J., L. B. Sorensen, J. G. Ojemann, and M. den Nijs (Dec. 18, 2009). Power-Law Scaling in the Brain Surface Electric Potential. *PLOS Computational Biology* 5, 12, e1000609. https://doi.org/10.1371/journal.pcbi.1000609(cit. on pp. 180, 183)

Miller, T. D., T. T.-J. Chong, A. M. Aimola Davies, M. R. Johnson, S. R. Irani, M. Husain, T. W. Ng, S. Jacob, P. Maddison, C. Kennard, P. A. Gowland, and C. R. Rosenthal (Jan. 24, 2020). Human Hippocampal CA3 Damage Disrupts Both Recent and Remote

Episodic Memories. *eLife* 9, e41836. https://doi.org/10.7554/eLife.41836(cit. on p. 29)
Miller, T. D., T. T.-J. Chong, A. M. Aimola Davies, T. W. Ng, M. R. Johnson, S. R. Irani, A. Vincent, M. Husain, S. Jacob, P. Maddison, C. Kennard, P. A. Gowland, and C. R. Rosenthal (May 1, 2017). Focal CA3 Hippocampal Subfield Atrophy Following LGI1 VGKC-complex Antibody Limbic Encephalitis. *Brain* 140, 5, pp. 1212–1219. https://doi.org/10.1093/brain/awx070(cit. on p. 29)
Milner, B. and W. Penfield (1955–1956). The Effect of Hippocampal Lesions on Recent Memory. *Transactions of the American Neurological Association*, pp. 42–48. (Cit. on p. 29)
Milner, B., S. Corkin, and H. .-. Teuber (Sept. 1, 1968). Further Analysis of the Hippocampal Amnesic Syndrome: 14-Year Follow-up Study of H.M. *Neuropsychologia* 6, 3, pp. 215–234. https://doi.org/10.1016/0028-3932(68)90021-3(cit. on pp. 29, 30)
Mishkin, M. (May 1978). Memory in Monkeys Severely Impaired by Combined but Not by Separate Removal of Amygdala and Hippocampus. *Nature* 273, 5660, pp. 297–298. https://doi.org/10.1038/273297a0(cit. on p. 30)
Mitchell, S. J. and J. B. Ranck (1980). Generation of Theta Rhythm in Medial Entorhinal Cortex of Freely Moving Rats. *Brain Research* 189, 1, pp. 49–66. https://doi.org/10.1016/0006-8993(80)90006-2(cit. on p. 37)
Miyawaki, H. and K. Mizuseki (Dec. 2022). De Novo Inter-Regional Coactivations of Preconfigured Local Ensembles Support Memory. *Nature Communications* 13, 1, p. 1272. https://doi.org/10.1038/s41467-022-28929-x(cit. on p. 41)
Mizumori, S. J., G. M. Perez, M. C. Alvarado, C. A. Barnes, and B. L. McNaughton (Sept. 24, 1990). Reversible Inactivation of the Medial Septum Differentially Affects Two Forms of Learning in Rats. *Brain Research* 528, 1, pp. 12–20. https://doi.org/10.1016/0006-8993(90)90188-h(cit. on pp. 36, 37)
Mizuseki, K., K. Diba, E. Pastalkova, and G. Buzsáki (Sept. 2011). Hippocampal CA1 Pyramidal Cells Form Functionally Distinct Sublayers. *Nature Neuroscience* 14, 9, pp. 1174–1181. https://doi.org/10.1038/nn.2894(cit. on p. 38)
Mizuseki, K., A. Sirota, E. Pastalkova, and G. Buzsáki (Oct. 29, 2009). Theta Oscillations Provide Temporal Windows for Local Circuit Computation in the Entorhinal-Hippocampal Loop. *Neuron* 64, 2, p. 267. https://doi.org/10.1016/j.neuron.2009.08.037(cit. on pp. 39, 127)
Montgomery, S. M., A. Sirota, and G. Buzsáki (June 25, 2008). Theta and Gamma Coordination of Hippocampal Networks during Waking and Rapid Eye Movement Sleep. *The Journal of Neuroscience* 28, 26, pp. 6731–6741. https://doi.org/10.1523/JNEUROSCI.1227-08.2008(cit. on p. 38)
Monti, G. and S. Meletti (Aug. 2015). Emotion Recognition in Temporal Lobe Epilepsy: A Systematic Review. *Neuroscience and Biobehavioral Reviews* 55, pp. 280–293. https://doi.org/10.1016/j.neubiorev.2015.05.009(cit. on p. 166)
Morgan, J. I., D. R. Cohen, J. L. Hempstead, and T. Curran (July 10, 1987). Mapping Patterns of C-Fos Expression in the Central Nervous System after Seizure. *Science* 237, 4811, pp. 192–197. https://doi.org/10.1126/science.3037702(cit. on p. 33)
Morgan, L. H. (1843). *Mind or Instinct: An Inquiry Concerning the Manifestation of Mind by the Lower Orders of Animals* (cit. on p. 27).
Mormann, F., J. Fell, N. Axmacher, B. Weber, K. Lehnertz, C. E. Elger, and G. Fernández (2005). Phase/Amplitude Reset and Theta–Gamma Interaction in the Human Medial

Temporal Lobe during a Continuous Word Recognition Memory Task. *Hippocampus* 15, 7, pp. 890–900. https://doi.org/10.1002/hipo.20117(cit. on p. 43)
Moroni, F., L. Nobili, G. Curcio, F. D. Carli, F. Fratello, C. Marzano, L. D. Gennaro, F. Ferrillo, M. Cossu, S. Francione, G. L. Russo, M. Bertini, and M. Ferrara (Sept. 12, 2007). Sleep in the Human Hippocampus: A Stereo-EEG Study. *PLOS ONE* 2, 9, e867. https://doi.org/10.1371/journal.pone.0000867(cit. on p. 43)
Morris, R. G. M., P. Garrud, J. N. P. Rawlins, and J. O'Keefe (June 1982). Place Navigation Impaired in Rats with Hippocampal Lesions. *Nature* 297, 5868, pp. 681–683. https://doi.org/10.1038/297681a0(cit. on p. 31)
Moser, M. B. and E. I. Moser (1998). Functional Differentiation in the Hippocampus. *Hippocampus* 8, 6, pp. 608–619. https://doi.org/10.1002/(SICI)1098-1063(1998)8:6<608::AID-HIPO3>3.0.CO;2-7(cit. on p. 123)
Mountcastle, V. B. (July 1957). Modality and Topographic Properties of Single Neurons of Cat's Somatic Sensory Cortex. *Journal of Neurophysiology* 20, 4, pp. 408–434. https://doi.org/10.1152/jn.1957.20.4.408(cit. on pp. 32, 34)
Muir, G. M., J. E. Brown, J. P. Carey, T. P. Hirvonen, C. C. Della Santina, L. B. Minor, and J. S. Taube (Nov. 18, 2009). Disruption of the Head Direction Cell Signal after Occlusion of the Semicircular Canals in the Freely Moving Chinchilla. *The Journal of Neuroscience* 29, 46, pp. 14521–14533. https://doi.org/10.1523/JNEUROSCI.3450-09.2009(cit. on p. 28)
Müller, M. and R. Wehner (July 1988). Path Integration in Desert Ants, Cataglyphis Fortis. *Proceedings of the National Academy of Sciences of the United States of America* 85, 14, pp. 5287–5290. https://doi.org/10.1073/pnas.85.14.5287(cit. on p. 26)
Murray, E. A., S. P. Wise, and K. S. Graham (2017). *The Evolution of Memory Systems: Ancestors, Anatomy, and Adaptations*. Oxford University Press. 529 pp. (cit. on pp. 27, 28).
Nauta, W. J. and D. G. Whitlock (Nov. 1956). Subcortical Projections from the Temporal Neocortex in Macaca Mulatta. *The Journal of Comparative Neurology* 106, 1, pp. 183–212. https://doi.org/10.1002/cne.901060107(cit. on p. 34)
Navas-Olive, A., M. Valero, T. Jurado-Parras, A. de Salas-Quiroga, R. G. Averkin, G. Gambino, E. Cid, and L. M. de la Prida (May 5, 2020). Multimodal Determinants of Phase-Locked Dynamics across Deep-Superficial Hippocampal Sublayers during Theta Oscillations. *Nature Communications* 11, 1, p. 2217. https://doi.org/10.1038/s41467-020-15840-6(cit. on p. 38)
Neckelmann, D. and R. Ursin (Aug. 1993). Sleep Stages and EEG Power Spectrum in Relation to Acoustical Stimulus Arousal Threshold in the Rat. *Sleep* 16, 5, pp. 467–477. (Cit. on p. 37)
Ng, M. and M. Pavlova (2013). Why Are Seizures Rare in Rapid Eye Movement Sleep? Review of the Frequency of Seizures in Different Sleep Stages. *Epilepsy Research and Treatment* 2013, p. 932790. https://doi.org/10.1155/2013/932790(cit. on p. 43)
Ngo, H.-V., J. Fell, and B. Staresina (July 13, 2020). Sleep Spindles Mediate Hippocampal-Neocortical Coupling during Long-Duration Ripples. *eLife* 9, e57011. https://doi.org/10.7554/eLife.57011(cit. on p. 46)
Norman, Y., O. Raccah, S. Liu, J. Parvizi, and R. Malach (Sept. 1, 2021). Hippocampal Ripples and Their Coordinated Dialogue with the Default Mode Network during Recent and Remote Recollection. *Neuron* 109, 17, 2767–2780.e5. https://doi.org/10.1016/j.neuron.2021.06.020(cit. on p. 45)

Norman, Y., E. M. Yeagle, S. Khuvis, M. Harel, A. D. Mehta, and R. Malach (Aug. 16, 2019). Hippocampal Sharp-Wave Ripples Linked to Visual Episodic Recollection in Humans. *Science* 365, 6454, eaax1030. https://doi.org/10.1126/science.aax1030(cit. on p. 45)

O'Keefe, J. (Apr. 1976). Place Units in the Hippocampus of the Freely Moving Rat. *Experimental Neurology* 51, 1, pp. 78–109. https://doi.org/10.1016/0014-4886(76)90055-8(cit. on pp. 25, 32)

O'Keefe, J. and J. Dostrovsky (Nov. 1971). The Hippocampus as a Spatial Map. Preliminary Evidence from Unit Activity in the Freely-Moving Rat. *Brain Research* 34, 1, pp. 171–175. https://doi.org/10.1016/0006-8993(71)90358-1(cit. on p. 32)

O'Keefe, J. and L. Nadel (1978). *The Hippocampus as a Cognitive Map*. Oxford: Clarendon Press (cit. on pp. 25–27, 31, 32, 79).

O'Keefe, J. and M. L. Recce (1993). Phase Relationship between Hippocampal Place Units and the EEG Theta Rhythm. *Hippocampus* 3, 3, pp. 317–330. https://doi.org/10.1002/hipo.450030307(cit. on pp. 38, 96, 116, 119)

O'Neill, J., T. J. Senior, K. Allen, J. R. Huxter, and J. Csicsvari (Feb. 2008). Reactivation of Experience-Dependent Cell Assembly Patterns in the Hippocampus. *Nature Neuroscience* 11, 2, pp. 209–215. https://doi.org/10.1038/nn2037(cit. on pp. 40, 154)

O'Reilly, R. C. and J. L. McClelland (Dec. 1994). Hippocampal Conjunctive Encoding, Storage, and Recall: Avoiding a Trade-Off. *Hippocampus* 4, 6, pp. 661–682. https://doi.org/10.1002/hipo.450040605(cit. on p. 40)

O'Reilly, R. C., R. Bhattacharyya, M. D. Howard, and N. Ketz (Aug. 2014). Complementary Learning Systems. *Cognitive Science* 38, 6, pp. 1229–1248. https://doi.org/10.1111/j.1551-6709.2011.01214.x(cit. on p. 40)

Olton, D. S., J. A. Walker, and F. H. Gage (Jan. 13, 1978). Hippocampal Connections and Spatial Discrimination. *Brain Research* 139, 2, pp. 295–308. https://doi.org/10.1016/0006-8993(78)90930-7(cit. on p. 32)

Pacheco Estefan, D., M. Sánchez-Fibla, A. Duff, A. Principe, R. Rocamora, H. Zhang, N. Axmacher, and P. F. M. J. Verschure (May 21, 2019). Coordinated Representational Reinstatement in the Human Hippocampus and Lateral Temporal Cortex during Episodic Memory Retrieval. *Nature Communications* 10, 1, p. 2255. https://doi.org/10.1038/s41467-019-09569-0(cit. on p. 45)

Papez, J. W. (1937). A Proposed Mechanism of Emotion. 1937. *The Journal of Neuropsychiatry and Clinical Neurosciences* 7, 1, pp. 103–112. https://doi.org/10.1176/jnp.7.1.103(cit. on p. 32)

Parish, G. M., S. Michelmann, and S. Hanslmayr (2023). "How Should I Re-reference My Intracranial EEG Data?" In: *Intracranial EEG: A Guide for Cognitive Neuroscientists*. Ed. by N. Axmacher. Cham: Springer International Publishing, pp. 451–473. https://doi.org/10.1007/978-3-031-20910-9_28 (cit. on p. 104).

Parker, A. and D. Gaffan (Aug. 1997). The Effect of Anterior Thalamic and Cingulate Cortex Lesions on Object-in-Place Memory in Monkeys. *Neuropsychologia* 35, 8, pp. 1093–1102. https://doi.org/10.1016/s0028-3932(97)00042-0(cit. on p. 32)

Parkin, A. J., J. E. Rees, N. M. Hunkin, and P. E. Rose (1994). Impairment of Memory Following Discrete Thalamic Infarction. *Neuropsychologia* 32, 1, pp. 39–51. https://doi.org/10.1016/0028-3932(94)90067-1(cit. on p. 32)

Paulk, A. C., Y. Kfir, A. R. Khanna, M. L. Mustroph, E. M. Trautmann, D. J. Soper, S. D. Stavisky, M. Welkenhuysen, B. Dutta, K. V. Shenoy, L. R. Hochberg, R. M. Richardson,

Z. M. Williams, and S. S. Cash (Feb. 2022). Large-Scale Neural Recordings with Single Neuron Resolution Using Neuropixels Probes in Human Cortex. *Nature Neuroscience* 25, 2, pp. 252–263. https://doi.org/10.1038/s41593-021-00997-0(cit. on pp. 166, 169)

Pavlov, I. P. (1927). *Conditioned Reflexes : An Investigation of the Physiological Activity of the Cerebral Cortex*. Oxford University Press (cit. on pp. 23, 28).

Payne, H. L., G. F. Lynch, and D. Aronov (July 16, 2021). Neural Representations of Space in the Hippocampus of a Food-Caching Bird. *Science (New York, N.Y.)* 373, 6552, pp. 343–348. https://doi.org/10.1126/science.abg2009(cit. on p. 28)

Pedregosa, F., G. Varoquaux, A. Gramfort, V. Michel, B. Thirion, O. Grisel, M. Blondel, P. Prettenhofer, R. Weiss, V. Dubourg, J. Vanderplas, A. Passos, D. Cournapeau, M. Brucher, M. Perrot, and É. Duchesnay (Nov. 1, 2011). Scikit-Learn: Machine Learning in Python. *The Journal of Machine Learning Research* 12, pp. 2825–2830. (Cit. on p. 76)

Penner, C., M. J, C. N, M. An, and R. U (May 2022). Properties and Hemispheric Differences of Theta Oscillations in the Human Hippocampus. *Hippocampus* 32, 5. https://doi.org/10.1002/hipo.23412(cit. on pp. 101, 123)

Perentos, N., M. Krstulovic, and A. J. Morton (Jan. 7, 2022). Deep Brain Electrophysiology in Freely Moving Sheep. *Current biology: CB*, S0960-9822(21)01722–X. https://doi.org/10.1016/j.cub.2021.12.035(cit. on pp. 36, 163)

Petit-Dutaillis, D., J. Christophe, B. Pertuiset, C. Dreyfus-Brisac, and C. Blanc (1954). [Temporal bilateral lobectomy in epilepsy; evolution of postoperative functional disorders]. *Revue Neurologique* 91, 2, pp. 129–133. (Cit. on p. 29)

Petsche, H., Ch. Stumpf, and G. Gogolak (Apr. 1, 1962). The Significance of the Rabbit's Septum as a Relay Station between the Midbrain and the Hippocampus I. The Control of Hippocampus Arousal Activity by the Septum Cells. *Electroencephalography and Clinical Neurophysiology* 14, 2, pp. 202–211. https://doi.org/10.1016/0013-4694(62)90030-5(cit. on pp. 37, 38)

Peyrache, A., M. Khamassi, K. Benchenane, S. I. Wiener, and F. P. Battaglia (July 2009). Replay of Rule-Learning Related Neural Patterns in the Prefrontal Cortex during Sleep. *Nature Neuroscience* 12, 7, pp. 919–926. https://doi.org/10.1038/nn.2337(cit. on p. 41)

Phuong, T. H., M. Houot, M. Méré, M. Denos, S. Samson, and S. Dupont (Apr. 2021). Cognitive Impairment in Temporal Lobe Epilepsy: Contributions of Lesion, Localization and Lateralization. *Journal of Neurology* 268, 4, pp. 1443–1452. https://doi.org/10.1007/s00415-020-10307-6(cit. on pp. 81, 84, 93, 94, 166)

Piaget, J. (1923). *Le Langage et la Pensée chez l'enfant*. Neuchatel: Delachaux & Niestlé. 213 pp. (cit. on p. 24).

— (1952). *The Origins of Intelligence in Children*. Red. by M. Cook. The Origins of Intelligence in Children. New York, NY, US: W. W. Norton & Company, p. 419. 419 pp. https://doi.org/10.1037/11494-000 (cit. on p. 24).

Piolino, P., S. Belliard, B. Desgranges, M. Perron, and F. Eustache (Oct. 1, 2003). Autobiographical Memory and Autoneotic Consciousness in a Case of Semantic Dementia. *Cognitive Neuropsychology* 20, 7, pp. 619–639. https://doi.org/10.1080/02643290242000899(cit. on p. 30)

Plihal, W. and J. Born (July 1997). Effects of Early and Late Nocturnal Sleep on Declarative and Procedural Memory. *Journal of Cognitive Neuroscience* 9, 4, pp. 534–547. https://doi.org/10.1162/jocn.1997.9.4.534(cit. on p. 40)

Preston, A. R. and H. Eichenbaum (Sept. 9, 2013). Interplay of Hippocampus and Prefrontal Cortex in Memory. *Current biology: CB* 23, 17, R764–773. https://doi.org/10.1016/j.cub.2013.05.041(cit. on p. 26)

Qu, Y., J. Ou, L. Pang, S. Wu, Y. Luo, T. Behrens, and Y. Liu (Mar. 25, 2026). Development of Non-Spatial Grid-like Neural Codes Tracks Inference and Intelligence. *Cell*. https://doi.org/10.1016/j.cell.2026.02.028(cit. on p. 25)

Quian Quiroga, R. (Nov. 14, 2019). Plugging in to Human Memory: Advantages, Challenges, and Insights from Human Single-Neuron Recordings. *Cell* 179, 5, pp. 1015–1032. https://doi.org/10.1016/j.cell.2019.10.016(cit. on p. 34)

Quian Quiroga, R. (Mar. 2026). 20 Years of Concept Cells: From Invariant Responses to a Unique Coding of Human Memory. *Neuron*, S0896627326000516. https://doi.org/10.1016/j.neuron.2026.01.026(cit. on p. 34)

Quirk, G. J., R. U. Muller, J. L. Kubie, and J. B. Ranck (May 1992). The Positional Firing Properties of Medial Entorhinal Neurons: Description and Comparison with Hippocampal Place Cells. *The Journal of Neuroscience: The Official Journal of the Society for Neuroscience* 12, 5, pp. 1945–1963. https://doi.org/10.1523/JNEUROSCI.12-05-01945.1992(cit. on p. 33)

Quiroga, R. Q., L. Reddy, G. Kreiman, C. Koch, and I. Fried (June 2005). Invariant Visual Representation by Single Neurons in the Human Brain. *Nature* 435, 7045, pp. 1102–1107. https://doi.org/10.1038/nature03687(cit. on pp. 34, 164)

Quiroga, R. Q. (Aug. 2012). Concept Cells: The Building Blocks of Declarative Memory Functions. *Nature Reviews Neuroscience* 13, 8, pp. 587–597. https://doi.org/10.1038/nrn3251(cit. on p. 34)

Quiroga, R. Q., A. Kraskov, C. Koch, and I. Fried (Aug. 11, 2009). Explicit Encoding of Multimodal Percepts by Single Neurons in the Human Brain. *Current Biology* 19, 15, pp. 1308–1313. https://doi.org/10.1016/j.cub.2009.06.060(cit. on p. 34)

Raghavachari, S., M. J. Kahana, D. S. Rizzuto, J. B. Caplan, M. P. Kirschen, B. Bourgeois, J. R. Madsen, and J. E. Lisman (May 1, 2001). Gating of Human Theta Oscillations by a Working Memory Task. *Journal of Neuroscience* 21, 9, pp. 3175–3183. https://doi.org/10.1523/JNEUROSCI.21-09-03175.2001(cit. on pp. 42, 162)

Ramirez, S., X. Liu, P.-A. Lin, J. Suh, M. Pignatelli, R. L. Redondo, T. J. Ryan, and S. Tonegawa (July 26, 2013). Creating a False Memory in the Hippocampus. *Science* 341, 6144, pp. 387–391. https://doi.org/10.1126/science.1239073(cit. on p. 33)

Rao, R. P. N. and D. H. Ballard (Jan. 1999). Predictive Coding in the Visual Cortex: A Functional Interpretation of Some Extra-Classical Receptive-Field Effects. *Nature Neuroscience* 2, 1, pp. 79–87. https://doi.org/10.1038/4580(cit. on p. 26)

Reber, T. P., M. Bausch, S. Mackay, J. Boström, C. E. Elger, and F. Mormann (June 3, 2019). Representation of Abstract Semantic Knowledge in Populations of Human Single Neurons in the Medial Temporal Lobe. *PLoS Biology* 17, 6, e3000290. https://doi.org/10.1371/journal.pbio.3000290(cit. on p. 34)

Reber, T. P., J. Faber, J. Niediek, J. Boström, C. E. Elger, and F. Mormann (Oct. 9, 2017). Single-Neuron Correlates of Conscious Perception in the Human Medial Temporal Lobe. *Current biology: CB* 27, 19, 2991–2998.e2. https://doi.org/10.1016/j.cub.2017.08.025(cit. on p. 34)

Rechtschaffen, A., P. Hauri, and M. Zeitlin (June 1966). Auditory Awakening Thresholds in REM and NREM Sleep Stages. *Perceptual and Motor Skills* 22, 3, pp. 927–942. https://doi.org/10.2466/pms.1966.22.3.927(cit. on p. 37)

Reddy, L., M. W. Self, B. Zoefel, M. Poncet, J. K. Possel, J. C. Peters, J. C. Baayen, S. Idema, R. VanRullen, and P. R. Roelfsema (Aug. 10, 2021). Theta-Phase Dependent Neuronal Coding during Sequence Learning in Human Single Neurons. *Nature Communications* 12, 1, p. 4839. https://doi.org/10.1038/s41467-021-25150-0(cit. on p. 44)

Redondo, R. L., J. Kim, A. L. Arons, S. Ramirez, X. Liu, and S. Tonegawa (Sept. 2014). Bidirectional Switch of the Valence Associated with a Hippocampal Contextual Memory Engram. *Nature* 513, 7518, pp. 426–430. https://doi.org/10.1038/nature13725(cit. on p. 33)

Reif, P. S., A. Strzelczyk, and F. Rosenow (Oct. 2016). The History of Invasive EEG Evaluation in Epilepsy Patients. *Seizure* 41, pp. 191–195. https://doi.org/10.1016/j.seizure.2016.04.006(cit. on p. 34)

Reijmers, L. G., B. L. Perkins, N. Matsuo, and M. Mayford (Aug. 31, 2007). Localization of a Stable Neural Correlate of Associative Memory. *Science* 317, 5842, pp. 1230–1233. https://doi.org/10.1126/science.1143839(cit. on p. 33)

Reimann, M. W., C. A. Anastassiou, R. Perin, S. L. Hill, H. Markram, and C. Koch (July 24, 2013). A Biophysically Detailed Model of Neocortical Local Field Potentials Predicts the Critical Role of Active Membrane Currents. *Neuron* 79, 2, pp. 375–390. https://doi.org/10.1016/j.neuron.2013.05.023(cit. on p. 35)

Rey, H. G., C. Pedreira, and R. Quian Quiroga (Oct. 1, 2015). Past, Present and Future of Spike Sorting Techniques. *Brain Research Bulletin* 119, pp. 106–117. https://doi.org/10.1016/j.brainresbull.2015.04.007(cit. on p. 38)

Ribot, T. (1888). *Les maladies de la mémoire*. Paris : Félix Alcan. 173 pp. (cit. on pp. 23, 28, 32).

Rizzuto, D. S., J. R. Madsen, E. B. Bromfield, A. Schulze-Bonhage, D. Seelig, R. Aschenbrenner-Scheibe, and M. J. Kahana (June 24, 2003). Reset of Human Neocortical Oscillations during a Working Memory Task. *Proceedings of the National Academy of Sciences* 100, 13, pp. 7931–7936. https://doi.org/10.1073/pnas.0732061100(cit. on p. 42)

Robinson, T. E. (May 1980). Hippocampal Rhythmic Slow Activity (RSA; Theta): A Critical Analysis of Selected Studies and Discussion of Possible Species-Differences. *Brain Research* 203, 1, pp. 69–101. https://doi.org/10.1016/0165-0173(80)90004-1(cit. on p. 36)

Rolls, E. T. (Oct. 30, 2013). The Mechanisms for Pattern Completion and Pattern Separation in the Hippocampus. *Frontiers in Systems Neuroscience* 7, p. 74. https://doi.org/10.3389/fnsys.2013.00074(cit. on p. 40)

Rosenbaum, D. A., R. G. Cohen, S. A. Jax, D. J. Weiss, and R. van der Wel (Aug. 2007). The Problem of Serial Order in Behavior: Lashley's Legacy. *Human Movement Science* 26, 4, pp. 525–554. https://doi.org/10.1016/j.humov.2007.04.001(cit. on p. 24)

Rosenbaum, R. S., S. Köhler, D. L. Schacter, M. Moscovitch, R. Westmacott, S. E. Black, F. Gao, and E. Tulving (Jan. 1, 2005). The Case of K.C.: Contributions of a Memory-Impaired Person to Memory Theory. *Neuropsychologia* 43, 7, pp. 989–1021. https://doi.org/10.1016/j.neuropsychologia.2004.10.007(cit. on p. 29)

Rosenbaum, R. S., S. Priselac, S. Köhler, S. E. Black, F. Gao, L. Nadel, and M. Moscovitch (Oct. 2000). Remote Spatial Memory in an Amnesic Person with Extensive Bilateral Hippocampal Lesions. *Nature Neuroscience* 3, 10, pp. 1044–1048. https://doi.org/10.1038/79867(cit. on p. 29)

Rothschild, G., E. Eban, and L. M. Frank (Feb. 2017). A Cortical-Hippocampal-Cortical Loop of Information Processing during Memory Consolidation. *Nature Neuroscience* 20, 2, pp. 251–259. https://doi.org/10.1038/nn.4457(cit. on p. 41)

Roux, L., B. Hu, R. Eichler, E. Stark, and G. Buzsáki (June 2017). Sharp Wave Ripples during Learning Stabilize the Hippocampal Spatial Map. *Nature Neuroscience* 20, 6, pp. 845–853. https://doi.org/10.1038/nn.4543(cit. on pp. 40, 141)

Rudoler, J. H., N. A. Herweg, and M. J. Kahana (Jan. 25, 2023). Hippocampal Theta and Episodic Memory. *Journal of Neuroscience* 43, 4, pp. 613–620. https://doi.org/10.1523/JNEUROSCI.1045-22.2022(cit. on p. 43)

Rutishauser, U., A. N. Mamelak, and E. M. Schuman (Mar. 16, 2006). Single-Trial Learning of Novel Stimuli by Individual Neurons of the Human Hippocampus-Amygdala Complex. *Neuron* 49, 6, pp. 805–813. https://doi.org/10.1016/j.neuron.2006.02.015(cit. on p. 34)

Rutishauser, U., L. Reddy, F. Mormann, and J. Sarnthein (Feb. 3, 2021). The Architecture of Human Memory: Insights from Human Single-Neuron Recordings. *The Journal of Neuroscience: The Official Journal of the Society for Neuroscience* 41, 5, pp. 883–890. https://doi.org/10.1523/JNEUROSCI.1648-20.2020(cit. on p. 34)

Rutishauser, U., I. B. Ross, A. N. Mamelak, and E. M. Schuman (Apr. 2010). Human Memory Strength Is Predicted by Theta-Frequency Phase-Locking of Single Neurons. *Nature* 464, 7290, pp. 903–907. https://doi.org/10.1038/nature08860(cit. on pp. 44, 79)

Rutishauser, U., E. M. Schuman, and A. N. Mamelak (Jan. 8, 2008). Activity of Human Hippocampal and Amygdala Neurons during Retrieval of Declarative Memories. *Proceedings of the National Academy of Sciences* 105, 1, pp. 329–334. https://doi.org/10.1073/pnas.0706015105(cit. on p. 34)

Rutishauser, U., S. Ye, M. Koroma, O. Tudusciuc, I. B. Ross, J. M. Chung, and A. N. Mamelak (July 2015). Representation of Retrieval Confidence by Single Neurons in the Human Medial Temporal Lobe. *Nature Neuroscience* 18, 7, pp. 1041–1050. https://doi.org/10.1038/nn.4041(cit. on p. 34)

Ryan, T. J., D. S. Roy, M. Pignatelli, A. Arons, and S. Tonegawa (May 29, 2015). Memory. Engram Cells Retain Memory under Retrograde Amnesia. *Science* 348, 6238, pp. 1007–1013. https://doi.org/10.1126/science.aaa5542(cit. on p. 33)

Sagar, S. M., F. R. Sharp, and T. Curran (June 3, 1988). Expression of C-Fos Protein in Brain: Metabolic Mapping at the Cellular Level. *Science* 240, 4857, pp. 1328–1331. https://doi.org/10.1126/science.3131879(cit. on p. 33)

Sainsbury, R. S. and C. P. Montoya (Oct. 1, 1984). The Relationship between Type 2 Theta and Behavior. *Physiology & Behavior* 33, 4, pp. 621–626. https://doi.org/10.1016/0031-9384(84)90381-0(cit. on pp. 36, 38, 162, 163)

Sainsbury, R. S., A. Heynen, and C. P. Montoya (Jan. 1, 1987). Behavioral Correlates of Hippocampal Type 2 Theta in the Rat. *Physiology & Behavior* 39, 4, pp. 513–519. https://doi.org/10.1016/0031-9384(87)90382-9(cit. on p. 38)

Saint Amour di Chanaz, L., A. Pérez-Bellido, X. Wu, D. Lozano-Soldevilla, D. Pacheco-Estefan, K. Lehongre, E. Conde-Blanco, P. Roldan, C. Adam, V. Lambrecq, V. Frazzini, A. Donaire, M. Carreño, V. Navarro, A. Valero-Cabré, and L. Fuentemilla (May 8, 2023). Gamma Amplitude Is Coupled to Opposed Hippocampal Theta-Phase States during the Encoding and Retrieval of Episodic Memories in Humans. *Current Biology* 33, 9, 1836–1843.e6. https://doi.org/10.1016/j.cub.2023.03.073(cit. on pp. 43, 44)

Sakai, K., K. Sano, and S. Iwahara (May 1973). Eye Movements and Hipocampal Theta Activity in Cats. *Electroencephalography and Clinical Neurophysiology* 34, 5, pp. 547–549. https://doi.org/10.1016/0013-4694(73)90072-2(cit. on pp. 36, 37)

Sakon, J. J. and M. J. Kahana (Oct. 4, 2022). Hippocampal Ripples Signal Contextually Mediated Episodic Recall. *Proceedings of the National Academy of Sciences* 119, 40, e2201657119. https://doi.org/10.1073/pnas.2201657119(cit. on p. 45)

Salmon, D. P., S. Zola-Morgan, and L. R. Squire (1987). Retrograde Amnesia Following Combined Hippocampus-Amygdala Lesions in Monkeys. *Psychobiology* 15, 1, pp. 37–47. (Cit. on p. 30)

Samborska, V., J. L. Butler, M. E. Walton, T. E. J. Behrens, and T. Akam (Oct. 2022). Complementary Task Representations in Hippocampus and Prefrontal Cortex for Generalizing the Structure of Problems. *Nature Neuroscience* 25, 10, pp. 1314–1326. https://doi.org/10.1038/s41593-022-01149-8(cit. on p. 25)

Sara, S. J. (Mar. 2009). The Locus Coeruleus and Noradrenergic Modulation of Cognition. *Nature Reviews Neuroscience* 10, 3, pp. 211–223. https://doi.org/10.1038/nrn2573(cit. on p. 41)

Schacter, D. L. and E. Tulving, red. (1994). *Memory Systems 1994*. Memory Systems 1994. Cambridge, MA, US: The MIT Press, pp. viii, 407. viii, 407 (cit. on p. 30).

Schmidt, R., J. Rose, and V. Muralidharan (Dec. 1, 2023). Transient Oscillations as Computations for Cognition: Analysis, Modeling and Function. *Current Opinion in Neurobiology* 83, p. 102796. https://doi.org/10.1016/j.conb.2023.102796(cit. on p. 162)

Schonhaut, D. R., A. M. Rao, A. G. Ramayya, E. A. Solomon, N. A. Herweg, I. Fried, and M. J. Kahana (Jan. 9, 2024). MTL Neurons Phase-Lock to Human Hippocampal Theta. *eLife* 13, e85753. https://doi.org/10.7554/eLife.85753(cit. on p. 44)

Schreiner, T., B. J. Griffiths, M. Kutlu, C. Vollmar, E. Kaufmann, S. Quach, J. Remi, S. Noachtar, and T. Staudigl (June 19, 2024). Spindle-Locked Ripples Mediate Memory Reactivation during Human NREM Sleep. *Nature Communications* 15, 1, p. 5249. https://doi.org/10.1038/s41467-024-49572-8(cit. on p. 46)

Schulman, A. I. (Jan. 1974). Memory for Words Recently Classified. *Memory & Cognition* 2, 1, pp. 47–52. https://doi.org/10.3758/BF03197491(cit. on p. 25)

Scoville, W. B. and B. Milner (Feb. 1957). LOSS OF RECENT MEMORY AFTER BILATERAL HIPPOCAMPAL LESIONS. *Journal of Neurology, Neurosurgery, and Psychiatry* 20, 1, pp. 11–21. (Cit. on pp. 25, 29, 31, 40, 79)

Seabold, S. and J. Perktold (May 1, 2010). Statsmodels: Econometric and Statistical Modeling with Python. *SciPy 2010*. https://doi.org/10.25080/Majora-92bf1922-011(cit. on p. 76)

Sebastian, E. R., J. P. Quintanilla, A. Sánchez-Aguilera, J. Esparza, E. Cid, and L. M. de la Prida (Dec. 2023). Topological Analysis of Sharp-Wave Ripple Waveforms Reveals Input Mechanisms behind Feature Variations. *Nature Neuroscience* 26, 12, pp. 2171–2181. https://doi.org/10.1038/s41593-023-01471-9(cit. on p. 38)

Sechenov, I. M. (M. (1863). *Reflexes of the Brain*. Cambridge, Mass., M.I.T. Press. 170 pp. (cit. on pp. 27, 28).

Sederberg, P. B., M. J. Kahana, M. W. Howard, E. J. Donner, and J. R. Madsen (Nov. 26, 2003). Theta and Gamma Oscillations during Encoding Predict Subsequent Recall. *Journal of Neuroscience* 23, 34, pp. 10809–10814. https://doi.org/10.1523/JNEUROSCI.23-34-10809.2003(cit. on p. 42)

Sederberg, P. B., A. Schulze-Bonhage, J. R. Madsen, E. B. Bromfield, D. C. McCarthy, A. Brandt, M. S. Tully, and M. J. Kahana (May 2007). Hippocampal and Neocortical Gamma Oscillations Predict Memory Formation in Humans. *Cerebral Cortex* 17, 5, pp. 1190–1196. https://doi.org/10.1093/cercor/bhl030(cit. on p. 42)

Seeber, M., M. Stangl, M. Vallejo Martelo, U. Topalovic, S. Hiller, C. H. Halpern, J.-P. Langevin, V. R. Rao, I. Fried, D. Eliashiv, and N. Suthana (Mar. 10, 2025). Human Neural Dynamics of Real-World and Imagined Navigation. *Nature Human Behaviour*, pp. 1–13. https://doi.org/10.1038/s41562-025-02119-3(cit. on pp. 43, 116, 162, 168)

Seger, S. E., J. L. S. Kriegel, B. C. Lega, and A. D. Ekstrom (July 18, 2023). Memory-Related Processing Is the Primary Driver of Human Hippocampal Theta Oscillations. *Neuron*. https://doi.org/10.1016/j.neuron.2023.06.015(cit. on p. 43)

Seidenbecher, T., T. R. Laxmi, O. Stork, and H.-C. Pape (Aug. 8, 2003). Amygdalar and Hippocampal Theta Rhythm Synchronization during Fear Memory Retrieval. *Science* 301, 5634, pp. 846–850. https://doi.org/10.1126/science.1085818(cit. on p. 127)

Semon, R. W. (1921). *The Mneme*. London, Allen & Unwin. 318 pp. (cit. on pp. 28, 32).

Sheintuch, L., N. Geva, D. Deitch, A. Rubin, and Y. Ziv (Feb. 28, 2023). Organization of Hippocampal CA3 into Correlated Cell Assemblies Supports a Stable Spatial Code. *Cell Reports* 42, 2. https://doi.org/10.1016/j.celrep.2023.112119(cit. on p. 33)

Sherrington, C. S. (1906). Observations on the Scratch-Reflex in the Spinal Dog. *The Journal of Physiology* 34, 1–2, pp. 1–50. https://doi.org/10.1113/jphysiol.1906.sp001139(cit. on p. 32)

Shimazono, Y., T. Horie, Y. Yanagisawa, N. Hori, S. Chikazawa, and K. Shozuka (1960). 6. the Correlation of the Rhyihmic Waves of the Hippocampus with the Behaviors of Dogs. *Neurologia medico-chirurgica* 2, 1–2, pp. 82–88. https://doi.org/10.2176/nmc.2.82(cit. on pp. 36, 37, 163)

Shouse, M. N., A. M. da Silva, and M. Sammaritano (Jan. 1996). Circadian Rhythm, Sleep, and Epilepsy. *Journal of Clinical Neurophysiology: Official Publication of the American Electroencephalographic Society* 13, 1, pp. 32–50. https://doi.org/10.1097/00004691-199601000-00004(cit. on p. 43)

Siapas, A. G., E. V. Lubenov, and M. A. Wilson (Apr. 7, 2005). Prefrontal Phase Locking to Hippocampal Theta Oscillations. *Neuron* 46, 1, pp. 141–151. https://doi.org/10.1016/j.neuron.2005.02.028(cit. on p. 41)

Silva, A. B., A. N. Khambhati, B. A. Speidel, E. F. Chang, and V. R. Rao (June 30, 2021). Effects of Anterior Thalamic Nuclei Stimulation on Hippocampal Activity: Chronic Recording in a Patient with Drug-Resistant Focal Epilepsy. *Epilepsy & Behavior Reports* 16, p. 100467. https://doi.org/10.1016/j.ebr.2021.100467(cit. on p. 168)

Singer, W. and C. M. Gray (Mar. 1, 1995). Visual Feature Integration and the Temporal Correlation Hypothesis. *Annual Review of Neuroscience* 18, pp. 555–586. https://doi.org/10.1146/annurev.ne.18.030195.003011(cit. on p. 39)

Skelin, I., H. Zhang, J. Zheng, S. Ma, B. A. Mander, O. Kim McManus, S. Vadera, R. T. Knight, B. L. McNaughton, and J. J. Lin (May 25, 2021). Coupling between Slow Waves and Sharp-Wave Ripples Engages Distributed Neural Activity during Sleep in Humans. *Proceedings of the National Academy of Sciences of the United States of America* 118, 21, e2012075118. https://doi.org/10.1073/pnas.2012075118(cit. on p. 46)

Skinner, B. F. (1938). *The Behavior Of Organisms An Experimental* (cit. on pp. 23, 27, 28).

Škoch, A., B. Rehák Bučková, J. Mareš, J. Tintěra, P. Sanda, L. Jajcay, J. Horáček, F. Španiel, and J. Hlinka (Aug. 9, 2022). Human Brain Structural Connectivity Matrices–Ready for Modelling. *Scientific Data* 9, 1, p. 486. https://doi.org/10.1038/s41597-022-01596-9(cit. on pp. 127, 129)

Snowden, J. S., P. J. Goulding, and D. Neary (1989). Semantic Dementia: A Form of Circumscribed Cerebral Atrophy. *Behavioural Neurology* 2, 3, pp. 167–182. https://doi.org/10.1155/1989/124043(cit. on p. 30)

Solomon, E. A., B. C. Lega, M. R. Sperling, and M. J. Kahana (Nov. 26, 2019). Hippocampal Theta Codes for Distances in Semantic and Temporal Spaces. *Proceedings of the National Academy of Sciences of the United States of America* 116, 48, pp. 24343–24352. https://doi.org/10.1073/pnas.1906729116(cit. on p. 43)

Solomon, E. A., J. M. Stein, S. Das, R. Gorniak, M. R. Sperling, G. Worrell, C. S. Inman, R. J. Tan, B. C. Jobst, D. S. Rizzuto, and M. J. Kahana (Apr. 2019). Dynamic Theta Networks in the Human Medial Temporal Lobe Support Episodic Memory. *Current Biology* 29, 7, 1100–1111.e4. https://doi.org/10.1016/j.cub.2019.02.020(cit. on pp. 43, 44)

Spencer, H. (1855). *The Principles of Psychology*. London : Longman, Brown, Green, and Longmans. 638 pp. (cit. on pp. 23, 27).

Spiegel, E. A., H. T. Wycis, M. Marks, and A. J. Lee (Oct. 10, 1947). Stereotaxic Apparatus for Operations on the Human Brain. *Science* 106, 2754, pp. 349–350. https://doi.org/10.1126/science.106.2754.349(cit. on p. 34)

Spiers, H. J., N. Burgess, E. A. Maguire, S. A. Baxendale, T. Hartley, P. J. Thompson, and J. O'Keefe (Dec. 2001). Unilateral Temporal Lobectomy Patients Show Lateralized Topographical and Episodic Memory Deficits in a Virtual Town. *Brain: A Journal of Neurology* 124, pp. 2476–2489. https://doi.org/10.1093/brain/124.12.2476(cit. on p. 29)

Squire, L. R. (Apr. 1992). Memory and the Hippocampus: A Synthesis from Findings with Rats, Monkeys, and Humans. *Psychological Review* 99, 2, pp. 195–231. https://doi.org/10.1037/0033-295x.99.2.195(cit. on pp. 30, 31, 79)

Squire, L. R. and P. Alvarez (Apr. 1995). Retrograde Amnesia and Memory Consolidation: A Neurobiological Perspective. *Current Opinion in Neurobiology* 5, 2, pp. 169–177. https://doi.org/10.1016/0959-4388(95)80023-9(cit. on p. 40)

Squire, L. R. and R. Y. Moore (Dec. 1979). Dorsal Thalamic Lesion in a Noted Case of Human Memory Dysfunction. *Annals of Neurology* 6, 6, pp. 503–506. https://doi.org/10.1002/ana.410060607(cit. on p. 32)

Squire, L. R. and S. Zola-Morgan (Sept. 20, 1991). The Medial Temporal Lobe Memory System. *Science* 253, 5026, pp. 1380–1386. https://doi.org/10.1126/science.1896849(cit. on p. 30)

Squire, L. R. (1987). *Memory and Brain*. Memory and Brain. New York, NY, US: Oxford University Press, pp. xiii, 315. xiii, 315 (cit. on p. 30).

Squire, L. R. (1992). Declarative and Nondeclarative Memory: Multiple Brain Systems Supporting Learning and Memory. *Journal of Cognitive Neuroscience* 4, 3, pp. 232–243. https://doi.org/10.1162/jocn.1992.4.3.232(cit. on p. 30)

Squire, L. R. (Nov. 2004). Memory Systems of the Brain: A Brief History and Current Perspective. *Neurobiology of Learning and Memory* 82, 3, pp. 171–177. https://doi.org/10.1016/j.nlm.2004.06.005(cit. on p. 30)

Squire, L. R. (Oct. 14, 2009). Memory and Brain Systems: 1969–2009. *Journal of Neuroscience* 29, 41, pp. 12711–12716. https://doi.org/10.1523/JNEUROSCI.3575-09.2009(cit. on p. 30)

Staba, R. J., C. L. Wilson, A. Bragin, I. Fried, and J. Engel (Oct. 2002). Quantitative Analysis of High-Frequency Oscillations (80–500 Hz) Recorded in Human Epileptic Hippocampus and Entorhinal Cortex. *Journal of Neurophysiology* 88, 4, pp. 1743–1752. https://doi.org/10.1152/jn.2002.88.4.1743(cit. on p. 44)

Stangl, M., U. Topalovic, C. S. Inman, S. Hiller, D. Villaroman, Z. M. Aghajan, L. Christov-Moore, N. R. Hasulak, V. R. Rao, C. H. Halpern, D. Eliashiv, I. Fried, and N. Suthana (Jan. 2021). Boundary-Anchored Neural Mechanisms of Location-Encoding for Self and Others. *Nature* 589, 7842, pp. 420–425. https://doi.org/10.1038/s41586-020-03073-y(cit. on pp. 43, 162, 168)

Staresina, B. P. (Apr. 1, 2024). Coupled Sleep Rhythms for Memory Consolidation. *Trends in Cognitive Sciences* 28, 4, pp. 339–351. https://doi.org/10.1016/j.tics.2024.02.002(cit. on p. 46)

Staresina, B. P., T. O. Bergmann, M. Bonnefond, R. van der Meij, O. Jensen, L. Deuker, C. E. Elger, N. Axmacher, and J. Fell (Nov. 2015). Hierarchical Nesting of Slow Oscillations, Spindles and Ripples in the Human Hippocampus during Sleep. *Nature Neuroscience* 18, 11, pp. 1679–1686. https://doi.org/10.1038/nn.4119(cit. on pp. 46, 144)

Staresina, B. P., J. C. Gray, and L. Davachi (May 2009). Event Congruency Enhances Episodic Memory Encoding through Semantic Elaboration and Relational Binding. *Cerebral Cortex* 19, 5, pp. 1198–1207. https://doi.org/10.1093/cercor/bhn165(cit. on p. 25)

Staresina, B. P., S. Michelmann, M. Bonnefond, O. Jensen, N. Axmacher, and J. Fell (Aug. 10, 2016). Hippocampal Pattern Completion Is Linked to Gamma Power Increases and Alpha Power Decreases during Recollection. *eLife* 5, e17397. https://doi.org/10.7554/eLife.17397(cit. on p. 45)

Staresina, B. P., J. Niediek, V. Borger, R. Surges, and F. Mormann (July 10, 2023). How Coupled Slow Oscillations, Spindles and Ripples Coordinate Neuronal Processing and Communication during Human Sleep. *Nature Neuroscience*, pp. 1–9. https://doi.org/10.1038/s41593-023-01381-w(cit. on pp. 46, 144)

Staresina, B. P., T. P. Reber, J. Niediek, J. Boström, C. E. Elger, and F. Mormann (Apr. 3, 2019). Recollection in the Human Hippocampal-Entorhinal Cell Circuitry. *Nature Communications* 10, 1, p. 1503. https://doi.org/10.1038/s41467-019-09558-3(cit. on p. 34)

Stevenson, R. F., J. Zheng, L. Mnatsakanyan, S. Vadera, R. T. Knight, J. J. Lin, and M. A. Yassa (Oct. 2, 2018). Hippocampal CA1 Gamma Power Predicts the Precision of Spatial Memory Judgments. *Proceedings of the National Academy of Sciences of the United States of America* 115, 40, pp. 10148–10153. https://doi.org/10.1073/pnas.1805724115(cit. on p. 45)

Stickgold, R., D. Whidbee, B. Schirmer, V. Patel, and J. A. Hobson (2000). Visual Discrimination Task Improvement: A Multi-Step Process Occurring during Sleep. *Journal of Cognitive Neuroscience* 12, 2, pp. 246–254. https://doi.org/10.1162/089892900562075(cit. on p. 40)

Strange, B. A., M. P. Witter, E. S. Lein, and E. I. Moser (Oct. 2014). Functional Organization of the Hippocampal Longitudinal Axis. *Nature Reviews Neuroscience* 15, 10, pp. 655–669. https://doi.org/10.1038/nrn3785(cit. on p. 123)

Suthana, N., Z. Haneef, J. Stern, R. Mukamel, E. Behnke, B. Knowlton, and I. Fried (Feb. 9, 2012). Memory Enhancement and Deep-Brain Stimulation of the Entorhinal Area. *New England Journal of Medicine* 366, 6, pp. 502–510. https://doi.org/10.1056/NEJMoa1107212(cit. on p. 167)

Sutherland, R. J. and R. J. McDonald (Feb. 12, 1990). Hippocampus, Amygdala, and Memory Deficits in Rats. *Behavioural Brain Research* 37, 1, pp. 57–79. https://doi.org/10.1016/0166-4328(90)90072-M(cit. on p. 31)

Tacikowski, P., G. Kalender, D. Ciliberti, and I. Fried (Sept. 25, 2024). Human Hippocampal and Entorhinal Neurons Encode the Temporal Structure of Experience. *Nature*, pp. 1–8. https://doi.org/10.1038/s41586-024-07973-1(cit. on p. 34)

Takeuchi, T., A. J. Duszkiewicz, A. Sonneborn, P. A. Spooner, M. Yamasaki, M. Watanabe, C. C. Smith, G. Fernández, K. Deisseroth, R. W. Greene, and R. G. M. Morris (Sept. 2016). Locus Coeruleus and Dopaminergic Consolidation of Everyday Memory. *Nature* 537, 7620, pp. 357–362. https://doi.org/10.1038/nature19325(cit. on p. 41)

Tal, I., S. Neymotin, S. Bickel, P. Lakatos, and C. E. Schroeder (Sept. 15, 2020). Oscillatory Bursting as a Mechanism for Temporal Coupling and Information Coding. *Frontiers in Computational Neuroscience* 14. https://doi.org/10.3389/fncom.2020.00082(cit. on p. 162)

Talairach, J., J. Bancaud, A. Bonis, G. Szikla, and P. Tournoux (1962). Functional Stereotaxic Exploration of Epilepsy. *Confinia Neurologica* 22, pp. 328–331. https://doi.org/10.1159/000104378(cit. on p. 34)

Tallman, C. W., P. N. Steinmetz, and J. T. Wixted (Nov. 18, 2025). Neuronal Allocation and Sparse Coding of Episodic Memories in the Human Hippocampus. *Scientific Reports* 15, 1, p. 40430. https://doi.org/10.1038/s41598-025-21967-7(cit. on pp. 34, 164)

Taube, J. S., R. U. Muller, and J. B. Ranck (Feb. 1990). Head-Direction Cells Recorded from the Postsubiculum in Freely Moving Rats. II. Effects of Environmental Manipulations. *The Journal of Neuroscience: The Official Journal of the Society for Neuroscience* 10, 2, pp. 436–447. https://doi.org/10.1523/JNEUROSCI.10-02-00436.1990(cit. on p. 33)

Teitelbaum, H. and P. Milner (1963). Activity Changes Following Partial Hippocampal Lesions in Rats. *Journal of Comparative and Physiological Psychology* 56, 2, pp. 284–289. https://doi.org/10.1037/h0047052(cit. on p. 31)

Tenenbaum, J. B., V. de Silva, and J. C. Langford (Dec. 22, 2000). A Global Geometric Framework for Nonlinear Dimensionality Reduction. *Science*. https://doi.org/10.1126/science.290.5500.2319(cit. on p. 71)

Terzian, H. and G. D. Ore (June 1955). Syndrome of Klüver and Bucy; Reproduced in Man by Bilateral Removal of the Temporal Lobes. *Neurology* 5, 6, pp. 373–380. https://doi.org/10.1212/wnl.5.6.373(cit. on p. 29)

Teyler, T. J. and P. DiScenna (1986). The Hippocampal Memory Indexing Theory. *Behavioral Neuroscience* 100, 2, pp. 147–154. https://doi.org/10.1037/0735-7044.100.2.147(cit. on p. 40)

Teyler, T. J. and J. W. Rudy (2007). The Hippocampal Indexing Theory and Episodic Memory: Updating the Index. *Hippocampus* 17, 12, pp. 1158–1169. https://doi.org/10.1002/hipo.20350(cit. on p. 40)

Thorndike, E. L. (1898). Animal Intelligence: An Experimental Study of the Associative Processes in Animals. *The Psychological Review: Monograph Supplements* 2, 4, pp. i–109. https://doi.org/10.1037/h0092987(cit. on pp. 23, 28)

Tingley, D. and A. Peyrache (Apr. 6, 2020). On the Methods for Reactivation and Replay Analysis. *Philosophical Transactions of the Royal Society B: Biological Sciences* 375, 1799, p. 20190231. https://doi.org/10.1098/rstb.2019.0231(cit. on p. 154)

Titiz, A. S., M. R. H. Hill, E. A. Mankin, Z. M Aghajan, D. Eliashiv, N. Tchemodanov, U. Maoz, J. Stern, M. E. Tran, P. Schuette, E. Behnke, N. A. Suthana, and I. Fried (Oct. 24, 2017). Theta-Burst Microstimulation in the Human Entorhinal Area Improves Memory Specificity. *eLife* 6, e29515. https://doi.org/10.7554/eLife.29515(cit. on p. 167)

Todorova, R. and M. Zugaro (Oct. 18, 2019). Isolated Cortical Computations during Delta Waves Support Memory Consolidation. *Science* 366, 6463, pp. 377–381. https://doi.org/10.1126/science.aay0616(cit. on p. 41)

Tolman, E. C. (1948). Cognitive Maps in Rats and Men. *Psychological Review* 55, 4, pp. 189–208. https://doi.org/10.1037/h0061626(cit. on p. 25)

Tomé, D. F., Y. Zhang, T. Aida, O. Mosto, Y. Lu, M. Chen, S. Sadeh, D. S. Roy, and C. Clopath (Mar. 2024). Dynamic and Selective Engrams Emerge with Memory Consolidation. *Nature Neuroscience* 27, 3, pp. 561–572. https://doi.org/10.1038/s41593-023-01551-w(cit. on p. 33)

Tong, A. P. S., A. P. Vaz, J. H. Wittig, S. K. Inati, and K. A. Zaghloul (Nov. 15, 2021). Ripples Reflect a Spectrum of Synchronous Spiking Activity in Human Anterior Temporal Lobe. *eLife* 10, e68401. https://doi.org/10.7554/eLife.68401(cit. on p. 45)

Topalovic, U., Z. M. Aghajan, D. Villaroman, S. Hiller, L. Christov-Moore, T. J. Wishard, M. Stangl, N. R. Hasulak, C. S. Inman, T. A. Fields, V. R. Rao, D. Eliashiv, I. Fried, and N. Suthana (Oct. 28, 2020). Wireless Programmable Recording and Stimulation of Deep Brain Activity in Freely Moving Humans. *Neuron* 108, 2, 322–334.e9. https://doi.org/10.1016/j.neuron.2020.08.021(cit. on p. 168)

Topalovic, U., S. Barclay, C. Ling, A. Alzuhair, W. Yu, V. Hokhikyan, H. Chandrakumar, D. Rozgic, W. Jiang, S. Basir-Kazeruni, S. L. Maoz, C. S. Inman, M. Stangl, J. Gill, A. Bari, A. Fallah, D. Eliashiv, N. Pouratian, I. Fried, N. Suthana, and D. Markovic (Feb. 20, 2023). A Wearable Platform for Closed-Loop Stimulation and Recording of Single-Neuron and Local Field Potential Activity in Freely Moving Humans. *Nature Neuroscience*, pp. 1–11. https://doi.org/10.1038/s41593-023-01260-4(cit. on p. 168)

Tort, A. B. L., R. Komorowski, H. Eichenbaum, and N. Kopell (Aug. 2010). Measuring Phase-Amplitude Coupling Between Neuronal Oscillations of Different Frequencies. *Journal of Neurophysiology* 104, 2, pp. 1195–1210. https://doi.org/10.1152/jn.00106.2010(cit. on p. 65)

Traub, R. D., R. Miles, and R. K. Wong (Mar. 10, 1989). Model of the Origin of Rhythmic Population Oscillations in the Hippocampal Slice. *Science* 243, 4896, pp. 1319–1325. https://doi.org/10.1126/science.2646715(cit. on p. 33)

Trautner, P., T. Dietl, M. Staedtgen, A. Mecklinger, T. Grunwald, C. E. Elger, and M. Kurthen (Oct. 12, 2004). Recognition of Famous Faces in the Medial Temporal Lobe: An Invasive ERP Study. *Neurology* 63, 7, pp. 1203–1208. https://doi.org/10.1212/01.wnl.0000140487.55973.d7(cit. on p. 108)

Troester, M. M., S. F. Quan, A. A. o. S. Medicine, and R. B. Berry (June 3, 2023). *The AASM Manual for the Scoring of Sleep and Associated Events, Version 3*. American Academy Of Sleep Medicine. 96 pp. (cit. on pp. 51, 53, 141).

Trouche, S., P. V. Perestenko, G. M. van de Ven, C. T. Bratley, C. G. McNamara, N. Campo-Urriza, S. L. Black, L. G. Reijmers, and D. Dupret (Apr. 2016). Recoding a Cocaine-Place Memory Engram to a Neutral Engram in the Hippocampus. *Nature neuroscience* 19, 4, pp. 564–567. https://doi.org/10.1038/nn.4250(cit. on p. 33)

Tse, D., R. F. Langston, M. Kakeyama, I. Bethus, P. A. Spooner, E. R. Wood, M. P. Witter, and R. G. M. Morris (Apr. 6, 2007). Schemas and Memory Consolidation. *Science* 316, 5821, pp. 76–82. https://doi.org/10.1126/science.1135935(cit. on p. 25)

Tse, D., T. Takeuchi, M. Kakeyama, Y. Kajii, H. Okuno, C. Tohyama, H. Bito, and R. G. M. Morris (Aug. 12, 2011). Schema-Dependent Gene Activation and Memory Encoding in Neocortex. *Science* 333, 6044, pp. 891–895. https://doi.org/10.1126/science.1205274(cit. on p. 25)

Tsetsenis, T., J. K. Badyna, J. A. Wilson, X. Zhang, E. N. Krizman, M. Subramaniyan, K. Yang, S. A. Thomas, and J. A. Dani (Oct. 5, 2021). Midbrain Dopaminergic Innervation of the Hippocampus Is Sufficient to Modulate Formation of Aversive Memories. *Proceedings of the National Academy of Sciences of the United States of America* 118, 40, e2111069118. https://doi.org/10.1073/pnas.2111069118(cit. on p. 41)

Tsetsenis, T., J. I. Broussard, and J. A. Dani (Jan. 27, 2023). Dopaminergic Regulation of Hippocampal Plasticity, Learning, and Memory. *Frontiers in Behavioral Neuroscience* 16. https://doi.org/10.3389/fnbeh.2022.1092420(cit. on p. 41)

Tulving, E. (1972). "Episodic and Semantic Memory". In: *Organization of Memory*. Oxford, England: Academic Press, pp. xiii, 423–xiii, 423 (cit. on p. 30).

— (1983). *Elements of Episodic Memory*. Oxford, GB: Oxford University Press (cit. on p. 30).

Tulving, E. (1985). Memory and Consciousness. *Canadian Psychology / Psychologie canadienne* 26, 1, pp. 1–12. https://doi.org/10.1037/h0080017(cit. on p. 30)

Tulving, E. and D. M. Thomson (1973). Encoding Specificity and Retrieval Processes in Episodic Memory. *Psychological Review* 80, 5, pp. 352–373. https://doi.org/10.1037/h0020071(cit. on p. 30)

Ulanovsky, N. and C. F. Moss (Feb. 2007). Hippocampal Cellular and Network Activity in Freely Moving Echolocating Bats. *Nature Neuroscience* 10, 2, pp. 224–233. https://doi.org/10.1038/nn1829(cit. on pp. 28, 33, 36, 161, 163)

Urgolites, Z. J., J. T. Wixted, S. D. Goldinger, M. H. Papesh, D. M. Treiman, L. R. Squire, and P. N. Steinmetz (May 10, 2022). Two Kinds of Memory Signals in Neurons of the Human Hippocampus. *Proceedings of the National Academy of Sciences* 119, 19, e2115128119. https://doi.org/10.1073/pnas.2115128119(cit. on pp. 34, 164)

Valero, M., R. G. Averkin, I. Fernandez-Lamo, J. Aguilar, D. Lopez-Pigozzi, J. R. Brotons-Mas, E. Cid, G. Tamas, and L. M. de la Prida (June 21, 2017). Mechanisms for Selective Single-Cell Reactivation during Offline Sharp-Wave Ripples and Their Distortion by Fast Ripples. *Neuron* 94, 6, 1234–1247.e7. https://doi.org/10.1016/j.neuron.2017.05.032(cit. on pp. 44, 148)

Valero, M., E. Cid, R. G. Averkin, J. Aguilar, A. Sanchez-Aguilera, T. J. Viney, D. Gomez-Dominguez, E. Bellistri, and L. M. De La Prida (Sept. 2015). Determinants of Different Deep and Superficial CA1 Pyramidal Cell Dynamics during Sharp-Wave Ripples. *Nature Neuroscience* 18, 9, pp. 1281–1290. https://doi.org/10.1038/nn.4074(cit. on p. 38)

Valero, M. and L. M. de la Prida (Oct. 1, 2018). The Hippocampus in Depth: A Sublayer-Specific Perspective of Entorhinal–Hippocampal Function. *Current Opinion in Neu-*

robiology 52, pp. 107–114. https://doi.org/10.1016/j.conb.2018.04.013(cit. on p. 38)

Van Beest, E. H., C. Bimbard, J. M. J. Fabre, S. W. Dodgson, F. Takács, P. Coen, A. Lebedeva, K. D. Harris, and M. Carandini (Apr. 2025). Tracking Neurons across Days with High-Density Probes. *Nature Methods* 22, 4, pp. 778–787. https://doi.org/10.1038/s41592-024-02440-1(cit. on p. 167)

Van Kesteren, M. T. R., D. J. Ruiter, G. Fernández, and R. N. Henson (Apr. 2012). How Schema and Novelty Augment Memory Formation. *Trends in Neurosciences* 35, 4, pp. 211–219. https://doi.org/10.1016/j.tins.2012.02.001(cit. on p. 25)

Van Rheede, J. J., L. K. Feldmann, J. L. Busch, J. E. Fleming, V. Mathiopoulou, T. Denison, A. Sharott, and A. A. Kühn (July 8, 2022). Diurnal Modulation of Subthalamic Beta Oscillatory Power in Parkinson's Disease Patients during Deep Brain Stimulation. *npj Parkinson's Disease* 8, 1, p. 88. https://doi.org/10.1038/s41531-022-00350-7(cit. on p. 168)

Van Vugt, M. K., A. Schulze-Bonhage, B. Litt, A. Brandt, and M. J. Kahana (Feb. 17, 2010). Hippocampal Gamma Oscillations Increase with Memory Load. *The Journal of Neuroscience* 30, 7, pp. 2694–2699. https://doi.org/10.1523/JNEUROSCI.0567-09.2010(cit. on p. 42)

Van de Ven, G. M., S. Trouche, C. G. McNamara, K. Allen, and D. Dupret (Dec. 7, 2016). Hippocampal Offline Reactivation Consolidates Recently Formed Cell Assembly Patterns during Sharp Wave-Ripples. *Neuron* 92, 5, pp. 968–974. https://doi.org/10.1016/j.neuron.2016.10.020(cit. on pp. 33, 154)

Van Hoesen, G. and D. N. Pandya (Sept. 12, 1975). Some Connections of the Entorhinal (Area 28) and Perirhinal (Area 35) Cortices of the Rhesus Monkey. I. Temporal Lobe Afferents. *Brain Research* 95, 1, pp. 1–24. https://doi.org/10.1016/0006-8993(75)90204-8(cit. on p. 34)

Vandecasteele, M., V. Varga, A. Berényi, E. Papp, P. Barthó, L. Venance, T. F. Freund, and G. Buzsáki (Sept. 16, 2014). Optogenetic Activation of Septal Cholinergic Neurons Suppresses Sharp Wave Ripples and Enhances Theta Oscillations in the Hippocampus. *Proceedings of the National Academy of Sciences of the United States of America* 111, 37, pp. 13535–13540. https://doi.org/10.1073/pnas.1411233111(cit. on p. 38)

Vanderwolf, C. H. (Apr. 1, 1969). Hippocampal Electrical Activity and Voluntary Movement in the Rat. *Electroencephalography and Clinical Neurophysiology* 26, 4, pp. 407–418. https://doi.org/10.1016/0013-4694(69)90092-3(cit. on pp. 37, 38, 96, 161, 163)

Vanderwolf, C. H. (Jan. 1975). Neocortical and Hippocampal Activation Relation to Behavior: Effects of Atropine, Eserine, Phenothiazines, and Amphetamine. *Journal of Comparative and Physiological Psychology* 88, 1, pp. 300–323. https://doi.org/10.1037/h0076211(cit. on pp. 36, 38, 161, 162)

Vanderwolf, C. H. and D. P. Cain (Aug. 1994). The Behavioral Neurobiology of Learning and Memory: A Conceptual Reorientation. *Brain Research. Brain Research Reviews* 19, 3, pp. 264–297. https://doi.org/10.1016/0165-0173(94)90015-9(cit. on pp. 28, 31)

Vasconcelos, M. (July 2008). Transitive Inference in Non-Human Animals: An Empirical and Theoretical Analysis. *Behavioural Processes* 78, 3, pp. 313–334. https://doi.org/10.1016/j.beproc.2008.02.017(cit. on p. 26)

Vass, L. K., M. S. Copara, M. Seyal, K. Shahlaie, S. T. Farias, P. Y. Shen, and A. D. Ekstrom (Mar. 16, 2016). Oscillations Go the Distance: Low-Frequency Human Hip-

pocampal Oscillations Code Spatial Distance in the Absence of Sensory Cues during Teleportation. *Neuron* 89, 6, pp. 1180–1186. https://doi.org/10.1016/j.neuron.2016.01.045(cit. on p. 43)

Vaz, A. P., S. K. Inati, N. Brunel, and K. A. Zaghloul (Mar. 2019). Coupled Ripple Oscillations between the Medial Temporal Lobe and Neocortex Retrieve Human Memory. *Science* 363, 6430, pp. 975–978. https://doi.org/10.1126/science.aau8956(cit. on p. 45)

Vaz, A. P., J. H. Wittig, S. K. Inati, and K. A. Zaghloul (Mar. 6, 2020). Replay of Cortical Spiking Sequences during Human Memory Retrieval. *Science* 367, 6482, pp. 1131–1134. https://doi.org/10.1126/science.aba0672(cit. on p. 45)

Vertes, R. P. (1982). Brain Stem Generation of the Hippocampal EEG. *Progress in Neurobiology* 19, 3, pp. 159–186. https://doi.org/10.1016/0301-0082(82)90005-3(cit. on p. 37)

Vertes, R. P. and B. Kocsis (Dec. 1997). Brainstem-Diencephalo-Septohippocampal Systems Controlling the Theta Rhythm of the Hippocampus. *Neuroscience* 81, 4, pp. 893–926. https://doi.org/10.1016/s0306-4522(97)00239-x(cit. on pp. 37, 127)

Victor, M. and D. Agamanolis (1990). Amnesia Due to Lesions Confined to the Hippocampus: A Clinical-Pathologic Study. *Journal of Cognitive Neuroscience* 2, 3, pp. 246–257. https://doi.org/10.1162/jocn.1990.2.3.246(cit. on p. 29)

Villette, V., M. Chavarha, I. K. Dimov, J. Bradley, L. Pradhan, B. Mathieu, S. W. Evans, S. Chamberland, D. Shi, R. Yang, B. B. Kim, A. Ayon, A. Jalil, F. St-Pierre, M. J. Schnitzer, G. Bi, K. Toth, J. Ding, S. Dieudonné, and M. Z. Lin (Dec. 12, 2019). Ultrafast Two-Photon Imaging of a High-Gain Voltage Indicator in Awake Behaving Mice. *Cell* 179, 7, 1590–1608.e23. https://doi.org/10.1016/j.cell.2019.11.004(cit. on p. 35)

Vinck, M., M. van Wingerden, T. Womelsdorf, P. Fries, and C. M. A. Pennartz (May 15, 2010). The Pairwise Phase Consistency: A Bias-Free Measure of Rhythmic Neuronal Synchronization. *NeuroImage* 51, 1, pp. 112–122. https://doi.org/10.1016/j.neuroimage.2010.01.073(cit. on p. 55)

Vinogradova, O. S., E. S. Brazhnik, V. F. Kichigina, and V. S. Stafekhina (May 1993). Theta Modulation of Neurons of the Hippocampus of the Rabbit and Its Interrelationship with Other Parameters of Spontaneous and Evoked Activity. *Neuroscience and Behavioral Physiology* 23, 3, pp. 226–239. https://doi.org/10.1007/BF01182921(cit. on p. 37)

Virtanen, P., R. Gommers, T. E. Oliphant, M. Haberland, T. Reddy, D. Cournapeau, E. Burovski, P. Peterson, W. Weckesser, J. Bright, S. J. van der Walt, M. Brett, J. Wilson, K. J. Millman, N. Mayorov, A. R. J. Nelson, E. Jones, R. Kern, E. Larson, C. J. Carey, İ. Polat, Y. Feng, E. W. Moore, J. VanderPlas, D. Laxalde, J. Perktold, R. Cimrman, I. Henriksen, E. A. Quintero, C. R. Harris, A. M. Archibald, A. H. Ribeiro, F. Pedregosa, and P. van Mulbregt (Mar. 2020). SciPy 1.0: Fundamental Algorithms for Scientific Computing in Python. *Nature Methods* 17, 3, pp. 261–272. https://doi.org/10.1038/s41592-019-0686-2(cit. on p. 76)

Vivekananda, U., D. Bush, J. A. Bisby, S. Baxendale, R. Rodionov, B. Diehl, F. A. Chowdhury, A. W. McEvoy, A. Miserocchi, M. C. Walker, and N. Burgess (Feb. 2021). Theta Power and Theta-gamma Coupling Support Long-term Spatial Memory Retrieval. *Hippocampus* 31, 2, pp. 213–220. https://doi.org/10.1002/hipo.23284(cit. on pp. 43, 44)

Von Cramon, D. Y., N. Hebel, and U. Schuri (Dec. 1, 1985). A CONTRIBUTION TO THE ANATOMICAL BASIS OF THALAMIC AMNESIA. *Brain* 108, 4, pp. 993–1008. https://doi.org/10.1093/brain/108.4.993(cit. on p. 32)

Wagner, A. D., D. L. Schacter, M. Rotte, W. Koutstaal, A. Maril, A. M. Dale, B. R. Rosen, and R. L. Buckner (Aug. 21, 1998). Building Memories: Remembering and Forgetting of Verbal Experiences as Predicted by Brain Activity. *Science* 281, 5380, pp. 1188–1191. https://doi.org/10.1126/science.281.5380.1188(cit. on p. 110)

Wang, L., S. Chen, C. Liu, W. Lin, and H. Huang (Jan. 2020). Factors for Cognitive Impairment in Adult Epileptic Patients. *Brain and Behavior* 10, 1, e01475. https://doi.org/10.1002/brb3.1475(cit. on pp. 81, 84, 93, 94, 166)

Ward, A. A. and L. B. Thomas (Feb. 1955). The Electrical Activity of Single Units in the Cerebral Cortex of Man. *Electroencephalography and Clinical Neurophysiology* 7, 1, pp. 135–136. https://doi.org/10.1016/0013-4694(55)90067-5(cit. on p. 34)

Warrington, E. K. and L. Weiskrantz (1982). Amnesia: A Disconnection Syndrome? *Neuropsychologia* 20, 3, pp. 233–248. https://doi.org/10.1016/0028-3932(82)90099-9(cit. on p. 32)

Waskom, M. L. (Apr. 6, 2021). Seaborn: Statistical Data Visualization. *Journal of Open Source Software* 6, 60, p. 3021. https://doi.org/10.21105/joss.03021(cit. on p. 76)

Watrous, A. J., J. Miller, S. E. Qasim, I. Fried, and J. Jacobs (June 22, 2018). Phase-Tuned Neuronal Firing Encodes Human Contextual Representations for Navigational Goals. *eLife* 7, e32554. https://doi.org/10.7554/eLife.32554(cit. on p. 44)

Watrous, A. J., I. Fried, and A. D. Ekstrom (Apr. 2011). Behavioral Correlates of Human Hippocampal Delta and Theta Oscillations during Navigation. *Journal of Neurophysiology* 105, 4, pp. 1747–1755. https://doi.org/10.1152/jn.00921.2010(cit. on pp. 42, 168)

Watrous, A. J., D. J. Lee, A. Izadi, G. G. Gurkoff, K. Shahlaie, and A. D. Ekstrom (2013). A Comparative Study of Human and Rat Hippocampal Low-Frequency Oscillations during Spatial Navigation. *Hippocampus* 23, 8, pp. 656–661. https://doi.org/10.1002/hipo.22124(cit. on pp. 42, 168)

Watson, B. O., M. Ding, and G. Buzsáki (Oct. 2018). Temporal Coupling of Field Potentials and Action Potentials in the Neocortex. *The European Journal of Neuroscience* 48, 7, pp. 2482–2497. https://doi.org/10.1111/ejn.13807(cit. on pp. 56, 122)

Watson, J. F., V. Vargas-Barroso, R. J. Morse-Mora, A. Navas-Olive, M. R. Tavakoli, J. G. Danzl, M. Tomschik, K. Rössler, and P. Jonas (Dec. 11, 2024). Human Hippocampal CA3 Uses Specific Functional Connectivity Rules for Efficient Associative Memory. *Cell* 0, 0. https://doi.org/10.1016/j.cell.2024.11.022(cit. on p. 163)

Watson, J. B. (B. (1919). *Psychology from the Standpoint of a Behaviorist*. Philadelphia Lippincott. 460 pp. (cit. on p. 28).

Waydo, S., A. Kraskov, R. Quian Quiroga, I. Fried, and C. Koch (Oct. 4, 2006). Sparse Representation in the Human Medial Temporal Lobe. *The Journal of Neuroscience: The Official Journal of the Society for Neuroscience* 26, 40, pp. 10232–10234. https://doi.org/10.1523/JNEUROSCI.2101-06.2006(cit. on pp. 34, 164)

Wehner, R. and S. Wehner (May 1, 1990). Insect Navigation: Use of Maps or Ariadne's Thread? *Ethology Ecology & Evolution* 2, 1, pp. 27–48. https://doi.org/10.1080/08927014.1990.9525492(cit. on p. 26)

West, T. O., B. Duchet, S. F. Farmer, K. J. Friston, and H. Cagnan (Feb. 1, 2023). When Do Bursts Matter in the Primary Motor Cortex? Investigating Changes in

the Intermittencies of Beta Rhythms Associated with Movement States. *Progress in Neurobiology* 221, p. 102397. https://doi.org/10.1016/j.pneurobio.2022.102397(cit. on p. 162)

Whishaw, I. Q. and C. H. Vanderwolf (Apr. 1, 1973). Hippocampal EEG and Behavior: Change in Amplitude and Frequency of RSA (Theta Rhythm) Associated with Spontaneous and Learned Movement Patterns in Rats and Cats. *Behavioral Biology* 8, 4, pp. 461–484. https://doi.org/10.1016/S0091-6773(73)80041-0(cit. on p. 36)

Wierzynski, C. M., E. V. Lubenov, M. Gu, and A. G. Siapas (Feb. 26, 2009). State-Dependent Spike-Timing Relationships between Hippocampal and Prefrontal Circuits during Sleep. *Neuron* 61, 4, pp. 587–596. https://doi.org/10.1016/j.neuron.2009.01.011(cit. on p. 41)

Wilson, C. L., T. L. Babb, E. Halgren, and P. H. Crandall (June 1983). Visual Receptive Fields and Response Properties of Neurons in Human Temporal Lobe and Visual Pathways. *Brain: A Journal of Neurology* 106 (Pt 2), pp. 473–502. https://doi.org/10.1093/brain/106.2.473(cit. on p. 34)

Wilson, M. A. and B. L. McNaughton (Aug. 20, 1993). Dynamics of the Hippocampal Ensemble Code for Space. *Science* 261, 5124, pp. 1055–1058. https://doi.org/10.1126/science.8351520(cit. on p. 33)

Wilson, M. A. and B. L. McNaughton (July 29, 1994). Reactivation of Hippocampal Ensemble Memories During Sleep. *Science* 265, 5172, pp. 676–679. https://doi.org/10.1126/science.8036517(cit. on pp. 37, 40, 141, 144, 154)

Wiltschko, A. B., M. J. Johnson, G. Iurilli, R. E. Peterson, J. M. Katon, S. L. Pashkovski, V. E. Abraira, R. P. Adams, and S. R. Datta (Dec. 16, 2015). Mapping Sub-Second Structure in Mouse Behavior. *Neuron* 88, 6, pp. 1121–1135. https://doi.org/10.1016/j.neuron.2015.11.031(cit. on p. 28)

Winson, J. (July 14, 1978). Loss of Hippocampal Theta Rhythm Results in Spatial Memory Deficit in the Rat. *Science* 201, 4351, pp. 160–163. https://doi.org/10.1126/science.663646(cit. on pp. 36, 37, 96)

Winson, J. (Aug. 1, 1972). Interspecies Differences in the Occurrence of Theta. *Behavioral Biology* 7, 4, pp. 479–487. https://doi.org/10.1016/S0091-6773(72)80210-4(cit. on pp. 37, 38, 96, 141)

Winson, J. (Jan. 1, 1974). Patterns of Hippocampal Theta Rhythm in the Freely Moving Rat. *Electroencephalography and Clinical Neurophysiology* 36, pp. 291–301. https://doi.org/10.1016/0013-4694(74)90171-0(cit. on pp. 36, 163)

Wixted, J. T., L. R. Squire, Y. Jang, M. H. Papesh, S. D. Goldinger, J. R. Kuhn, K. A. Smith, D. M. Treiman, and P. N. Steinmetz (July 2014). Sparse and Distributed Coding of Episodic Memory in Neurons of the Human Hippocampus. *Proceedings of the National Academy of Sciences* 111, 26, pp. 9621–9626. https://doi.org/10.1073/pnas.1408365111(cit. on pp. 34, 164)

Wundt, W. M. (1910). *Principles of Physiological Psychology*. London : Swan, Sonnenschein. 376 pp. (cit. on p. 23).

Yaffe, R. B., M. S. D. Kerr, S. Damera, S. V. Sarma, S. K. Inati, and K. A. Zaghloul (Dec. 30, 2014). Reinstatement of Distributed Cortical Oscillations Occurs with Precise Spatiotemporal Dynamics during Successful Memory Retrieval. *Proceedings of the National Academy of Sciences* 111, 52, pp. 18727–18732. https://doi.org/10.1073/pnas.1417017112(cit. on p. 45)

Ylinen, A., A. Bragin, Z. Nadasdy, G. Jando, I. Szabo, A. Sik, and G. Buzsaki (Jan. 1, 1995). Sharp Wave-Associated High-Frequency Oscillation (200 Hz) in the Intact

Hippocampus: Network and Intracellular Mechanisms. *The Journal of Neuroscience* 15, 1, pp. 30–46. https://doi.org/10.1523/JNEUROSCI.15-01-00030.1995(cit. on pp. 37, 38)

Yuste, R. (Aug. 2015). From the Neuron Doctrine to Neural Networks. *Nature Reviews Neuroscience* 16, 8, pp. 487–497. https://doi.org/10.1038/nrn3962(cit. on pp. 32, 33)

Yuste, R., R. Cossart, and E. Yaksi (Mar. 20, 2024). Neuronal Ensembles: Building Blocks of Neural Circuits. *Neuron* 112, 6, pp. 875–892. https://doi.org/10.1016/j.neuron.2023.12.008(cit. on p. 33)

Zaki, Y., Z. T. Pennington, D. Morales-Rodriguez, M. E. Bacon, B. Ko, T. R. Francisco, A. R. LaBanca, P. Sompolpong, Z. Dong, S. Lamsifer, H.-T. Chen, S. Carrillo Segura, Z. Christenson Wick, A. J. Silva, K. Rajan, M. van der Meer, A. Fenton, T. Shuman, and D. J. Cai (Jan. 2025). Offline Ensemble Co-Reactivation Links Memories across Days. *Nature* 637, 8044, pp. 145–155. https://doi.org/10.1038/s41586-024-08168-4(cit. on p. 33)

Zanello, M., P. Duriez, A.-S. Savoureux, F. Vinckier, F. Chretien, M. Gavaret, P. Gorwood, R. Gaillard, and J. Pallud (July 2022). Jean Talairach (1911-2007). An Untold Story of the Pioneer of Stereotactic and Functional Neurosurgery. *Neuro-Chirurgie* 68, 4, pp. 398–408. https://doi.org/10.1016/j.neuchi.2021.12.008(cit. on p. 34)

Zeithamova, D., M. L. Schlichting, and A. R. Preston (Mar. 26, 2012). The Hippocampus and Inferential Reasoning: Building Memories to Navigate Future Decisions. *Frontiers in Human Neuroscience* 6, p. 70. https://doi.org/10.3389/fnhum.2012.00070(cit. on pp. 26, 79)

Zentall, T. R., E. A. Wasserman, O. F. Lazareva, R. K. R. Thompson, and M. J. Rattermann (2008). Concept Learning in Animals. *Comparative Cognition & Behavior Reviews* 3. https://doi.org/10.3819/ccbr.2008.30002(cit. on p. 26)

Zhang, H. and J. Jacobs (Sept. 9, 2015). Traveling Theta Waves in the Human Hippocampus. *Journal of Neuroscience* 35, 36, pp. 12477–12487. https://doi.org/10.1523/JNEUROSCI.5102-14.2015(cit. on p. 174)

Zhang, H., A. J. Watrous, A. Patel, and J. Jacobs (June 27, 2018). Theta and Alpha Oscillations Are Traveling Waves in the Human Neocortex. *Neuron* 98, 6, 1269–1281.e4. https://doi.org/10.1016/j.neuron.2018.05.019(cit. on pp. 162, 174)

Zhang, H., J. Fell, and N. Axmacher (Oct. 5, 2018). Electrophysiological Mechanisms of Human Memory Consolidation. *Nature Communications* 9, 1, p. 4103. https://doi.org/10.1038/s41467-018-06553-y(cit. on p. 46)

Zheng, J., M. Yebra, A. G. P. Schjetnan, K. Patel, C. N. Katz, M. Kyzar, C. P. Mosher, S. K. Kalia, J. M. Chung, C. M. Reed, T. A. Valiante, A. N. Mamelak, G. Kreiman, and U. Rutishauser (Dec. 2024). Theta Phase Precession Supports Memory Formation and Retrieval of Naturalistic Experience in Humans. *Nature Human Behaviour* 8, 12, pp. 2423–2436. https://doi.org/10.1038/s41562-024-01983-9(cit. on p. 43)

Zhou, J., C. Jia, M. Montesinos-Cartagena, M. P. H. Gardner, W. Zong, and G. Schoenbaum (Feb. 2021). Evolving Schema Representations in Orbitofrontal Ensembles during Learning. *Nature* 590, 7847, pp. 606–611. https://doi.org/10.1038/s41586-020-03061-2(cit. on p. 25)

Ziaei, M., C. Arnold, K. Thompson, and D. C. Reutens (Feb. 2023). Social Cognition in Temporal and Frontal Lobe Epilepsy: Systematic Review, Meta-analysis, and Clinical Recommendations. *Journal of the International Neuropsychological Society: JINS* 29, 2, pp. 205–229. https://doi.org/10.1017/S1355617722000066(cit. on p. 166)

Zola-Morgan, S., L. R. Squire, and D. G. Amaral (Oct. 1, 1986). Human Amnesia and the Medial Temporal Region: Enduring Memory Impairment Following a Bilateral Lesion Limited to Field CA1 of the Hippocampus. *Journal of Neuroscience* 6, 10, pp. 2950–2967. https://doi.org/10.1523/JNEUROSCI.06-10-02950.1986(cit. on p. 29)

Zola-Morgan, S., L. R. Squire, and D. G. Amaral (Mar. 1, 1989). Lesions of the Hippocampal Formation but Not Lesions of the Fornix or the Mammillary Nuclei Produce Long-Lasting Memory Impairment in Monkeys. *Journal of Neuroscience* 9, 3, pp. 898–913. https://doi.org/10.1523/JNEUROSCI.09-03-00898.1989(cit. on p. 30)

Zola-Morgan, S., L. R. Squire, N. L. Rempel, R. P. Clower, and D. G. Amaral (July 1992). Enduring Memory Impairment in Monkeys after Ischemic Damage to the Hippocampus. *The Journal of Neuroscience: The Official Journal of the Society for Neuroscience* 12, 7, pp. 2582–2596. https://doi.org/10.1523/JNEUROSCI.12-07-02582.1992(cit. on p. 30)

Zola-Morgan, S. M. and L. R. Squire (Oct. 12, 1990). The Primate Hippocampal Formation: Evidence for a Time-Limited Role in Memory Storage. *Science* 250, 4978, pp. 288–290. https://doi.org/10.1126/science.2218534(cit. on p. 30)

Zong, W., J. Zhou, M. P. H. Gardner, Z. Zhang, K. M. Costa, and G. Schoenbaum (May 2025). Hippocampal Output Suppresses Orbitofrontal Cortex Schema Cell Formation. *Nature Neuroscience* 28, 5, pp. 1048–1060. https://doi.org/10.1038/s41593-025-01928-z(cit. on p. 26)